

PETROGRAPHY AND DIAGENESIS OF THE
CARBONIFEROUS DEER LAKE GROUP AND
HOWLEY FORMATION, DEER LAKE
SUBBASIN, WESTERN NEWFOUNDLAND

CENTRE FOR NEWFOUNDLAND STUDIES

**TOTAL OF 10 PAGES ONLY
MAY BE XEROXED**

(Without Author's Permission)

QUENTIN GALL

0101

CENTRE FOR NFLD. STUDIES
NOV 8 1986
MEMORIAL UNIVERSITY
OF NEWFOUNDLAND

MEMORIAL UNIVERSITY
PERIODICALS
NOV 6 1986
DIVISION
OF NEWFOUNDLAND

0103

CENTRE FOR NFLD. STUDIES
NOV 8 1986
MEMORIAL UNIVERSITY
OF NEWFOUNDLAND

MEMORIAL UNIVERSITY
PERIODICALS
NOV 6 1986
DIVISION
OF NEWFOUNDLAND



National Library
of Canada

Bibliothèque nationale
du Canada

Canadian Theses Service

Services des thèses canadiennes

Ottawa, Canada
K1A 0N4

CANADIAN THESES

THÈSES CANADIENNES

NOTICE

The quality of this microfiche is heavily dependent upon the quality of the original thesis submitted for microfilming. Every effort has been made to ensure the highest quality of reproduction possible.

If pages are missing, contact the university which granted the degree.

Some pages may have indistinct print especially if the original pages were typed with a poor typewriter ribbon or if the university sent us an inferior photocopy.

Previously copyrighted materials (journal articles, published tests, etc.) are not filmed.

Reproduction in full or in part of this film is governed by the Canadian Copyright Act, R.S.C. 1970, c. C-30. Please read the authorization forms which accompany this thesis.

**THIS DISSERTATION
HAS BEEN MICROFILMED
EXACTLY AS RECEIVED**

AVIS

La qualité de cette microfiche dépend grandement de la qualité de la thèse soumise au microfilmage. Nous avons tout fait pour assurer une qualité supérieure de reproduction.

S'il manque des pages, veuillez communiquer avec l'université qui a conféré le grade.

La qualité d'impression de certaines pages peut laisser à désirer, surtout si les pages originales ont été dactylographiées à l'aide d'un ruban usé ou si l'université nous a fait parvenir une photocopie de qualité inférieure.

Les documents qui font déjà l'objet d'un droit d'auteur (articles de revue, examens publiés, etc.) ne sont pas microfilmés.

La reproduction, même partielle, de ce microfilm est soumise à la Loi canadienne sur le droit d'auteur, SRC 1970, c. C-30. Veuillez prendre connaissance des formules d'autorisation qui accompagnent cette thèse.

**LA THÈSE A ÉTÉ
MICROFILMÉE TELLE QUE
NOUS L'AVONS REÇUE**

PETROGRAPHY AND DIAGENESIS OF THE CARBONIFEROUS,
DEER LAKE GROUP AND HOWLEY FORMATION,
DEER LAKE SUBBASIN, WESTERN NEWFOUNDLAND

by



Quentin Gall, B.Sc.

A thesis submitted in partial fulfillment
of the requirements for the degree of
Master of Science

Department of Earth Sciences
Memorial University of Newfoundland

1984

ABSTRACT

The Deer Lake subbasin is one of two northeast-trending, mainly Carboniferous, subbasins in western Newfoundland. Within the subbasin the Deer Lake Group and Howley Formation consist entirely of non-marine sediments deposited in a half-graben which was extensively faulted along its eastern side. Petrographic investigation of nine drill cores has shown that coarse grained alluvial fan and fluvial sediments from the North Brook, Humber Falls, and Howley Formations, and high-grade uranium-mineralized sandstone boulder samples found in Pleistocene tills above the northern body of the Humber Falls Formation, have essentially the same detrital and diagenetic mineral assemblage and display the same paragenetic sequence. The dominantly lacustrine siliciclastic and carbonate sediment samples from the Rocky Brook Formation have a mineral assemblage and paragenetic sequence different from the coarser grained formations. Basic mineralogic differences are the absence of diagenetic kaolinite and illite-montmorillonite, and the presence of "analcime" in the Rocky Brook Formation sediments. The paragenetic sequence for the North Brook, Humber Falls, and Howley Formations and the mineralized samples reflects an acidic to alkaline geochemical environment. The paragenetic sequence for the Rocky Brook Formation on the other hand appears to have developed within a more stable alkaline geochemical environment. Correlating paleomagnetic data with

the derived paragenetic sequence for the three coarse grained formations suggests that the sequence took more than 40 Ma to completely develop. A postmineralization episode of hematite cementation may mean that economic quantities of uranium no longer exist in the sandstones.

High-volatile bituminous B and C coaly material and diagenetic clay mineral assemblages extracted from the drill core samples suggest that the sediments remained within the diagenetic realm after deposition, and that maximum temperatures between about 125° C and 135° C were attained during coalification and authigenic clay growth.

ACKNOWLEDGEMENTS

The writer gratefully acknowledges Shell Resources (Calgary), Shell Explorer (Houston), and Westfield Minerals Limited (Toronto) who financially supported this thesis as part of the Deer Lake Basin Project. The help given by Mr. R. Wilkinson (Westfield Minerals Ltd., Deer Lake) in obtaining company publications and drill core samples is also appreciated.

The writer would like to thank in particular his advisor Dr. R. Hiscott for guidance and support, as well as Dr. R. Hyde whose extensive knowledge of the Deer Lake subbasin and constructive suggestions helped to develop many parts of the thesis, and Dr. H. Kodama (Agriculture Canada, Ottawa) for enlightening the writer on certain aspects of clay mineral identification and illite crystallinity measurements. Appreciation is also expressed to Ms. C. Emerson for her technical assistance during the use of the scanning electron microscope and to Mr. W. Marsh for his guidance during photomicrograph preparation.

CONTENTS

	Page
LIST OF TABLES.....	ix
LIST OF FIGURES.....	ix
CHAPTER ONE- INTRODUCTION	
1.1 Location and access.....	1
1.2 Physiography.....	1
1.3 Previous work.....	3
1.4 Scope of present thesis study.....	5
CHAPTER TWO- PART 1 REGIONAL GEOLOGY	
2.1.1 Introduction.....	6
2.1.2 Pre-Devonian geology of the Humber and Dunnage Zones in Newfoundland and) Labrador.....	8
2.1.3 Upper Devonian to Permian geology in Atlantic Canada.....	11
PART 2 GEOLOGY OF THE DEER LAKE SUBBASIN	
2.2.1 Introduction.....	16
2.2.2 Anguille Group.....	19
2.2.3 Wetstone Point and Wigwam Brook Formations.....	20
2.2.4 Deer Lake Group.....	21
2.2.5 Howley Formation.....	25

	Page
2.2.6 Summary of the depositional environments and trends in the Deer Lake subbasin.....	27
2.2.7 Carboniferous deformation within the Deer Lake subbasin.....	29
 CHAPTER THREE- DRILL HOLE STRATIGRAPHY AND PETROGRAPHY	
3.1 Analytical methods.....	32
3.1.1 Stratigraphy.....	32
3.1.2 Colouration.....	33
3.1.3 Porosity.....	34
3.1.4 Mineralogy.....	34
3.1.5 X-ray diffractometry.....	36
3.1.6 Scanning electron microscopy.....	38
3.1.7 Cathodoluminescence.....	39
3.2 North Brook Formation.....	39
3.2.1 Introduction.....	39
3.2.2 Drill hole 79A-007 (A7).....	40
3.2.3 Drill hole 79B-003 (B3).....	51
3.3 Rocky Brook Formation.....	62
3.3.1 Introduction.....	62
3.3.2 Drill hole 79A-003 (A3).....	63
3.3.3 Drill hole 79A-005 (A5).....	77
3.4 Humber Falls Formation.....	86
3.4.1 Introduction.....	86

	Page
3.4.2 Drill hole DDH 79-69 (79-69).....	86
3.4.3 Drill hole DDH 79-29 (79-29).....	101
3.4.4 Drill hole DDH 80-70 (80-70).....	108
3.5 Howley Formation.....	120
3.5.1 Introduction.....	120
3.5.2 Drill hole 79D-004 (D4).....	123
3.5.3 Drill hole 79D-005 (D5).....	134
3.6 General discussion.....	143
CHAPTER FOUR- ECONOMIC GEOLOGY	
4.1 Introduction.....	148
4.2 Uranium mineralization.....	149
4.2.1 Mineralized sandstone boulders.....	149
4.2.2 Uranium-mineralized drill core.....	159
4.2.3 Discussion.....	160
4.3 Coal.....	167
4.3.1 Coal petrology.....	167
4.3.2 Vitrinite reflectance.....	175
4.3.3 Discussion.....	179
CHAPTER FIVE- DIAGENESIS	
5.1 General introduction.....	181
5.2 Paragenetic sequences in the Deer Lake Group and Howley Formation.....	182
5.2.1 Introduction.....	182
5.2.2 The "sandstone" sequence.....	184

	Page
5.2.3 The "shale" sequence.....	189
5.2.4 Discussion.....	193
5.3 Thermal maturation indicators.....	196
5.3.1 Introduction.....	196
5.3.2 Vitrinite reflectance.....	197
5.3.3 Diagenetic clay mineral assemblages....	198
5.3.4 Illite crystallinity.....	201
5.3.5 Discussion.....	206
CHAPTER SIX- SUMMARY AND CONCLUSIONS.....	208
REFERENCES.....	218
APPENDICES	
I Modal composition for each drill hole described in chapter three and mineralized boulder samples	236
II Microprobe analyses of Rocky Brook ¹ Formation "analcime".....	242
Trace element analyses of mineralized and unmineralized Rocky Brook Formation samples	242

LIST OF TABLES

	Page
Table	
4.1 Summary of trench and drill core sample properties.....	169

LIST OF FIGURES

Figures	
1.1 Location map of the Deer Lake subbasin ..	2
2.1 Distribution of the tectono-stratigraphic zones and the Maritimes Basin in the northern Appalachians	7
2.2 Upper Paleozoic stratigraphy of Atlantic Canada	15
2.3 Geological map of the Deer Lake subbasin	17
2.4 Stratigraphy, thickness, and dated fossils of the Deer Lake subbasin	18
3.1 Details of drill hole 79A-007	42
3.2 Representative 79A-007 drill core	44
3.3 Illitized feldspar grain	44
3.4 QRF diagram of North Brook Fm. sandstone samples	45
3.5 Clay-fraction diffractogram of North Brook Fm. samples	47

x

	Page
3.6 Laths of diagenetic illite	49
3.7 Late-stage hematite cement	49
3.8 Details of drill hole 79B-003	52
3.9 Representative 79B-003 drill core	54
3.10 Plagioclase grain dissolution	54
3.11 Authigenic calcite within a plagioclase grain	57
3.12 Quartz overgrowths and montmorillonite .	57
3.13 Diagenetic vermicular kaolinite	59
3.14 Poikilotopic, twinned calcite cement ...	59
3.15 Two generations of zoned calcite cement	61
3.16 Two generations of zoned calcite cement	61
3.17 Details of drill hole 79A-003	64
3.18 Classification diagram of Rocky Brook Fm. samples	65
3.19 Representative 79A-003 drill core	67
3.20 "Analcime" crystals in late-stage calcite cement	67
3.21 Calcite stockwork cut by an 'open' microfracture	70
3.22 Rhizolith cross-section	70
3.23 Clay-fraction diffractogram of Rocky Brook Fm. samples	71
3.24 Rhizolith cross-section	75

	Page
3.25 Mesovug porosity	75
3.26 Details of drill hole 79A-005	79
3.27 Representative 79A-005 drill core	81
3.28 Pyrite crystal aggregates	81
3.29 Pyrite and calcite in late-stage microfractures	85
3.30 Representative DDH 79-69 drill core	85
3.31 Details of drill hole DDH 79-69	89
3.32 QRF diagram of Humber Falls Fm. sandstone samples	90
3.33 Clay-fraction diffractogram of Humber Falls Fm. samples	91
3.34 Sheaves of diagenetic illite	94
3.35 Poikilotopic calcite cement	94
3.36 Grain disruption by calcite cement	96
3.37 Authigenic vermicular kaolinite	96
3.38 Proof of an early stage of porosity development	98
3.39 Hematite cement corroding calcite cement	98
3.40 Dissolution pits in calcite cement	100
3.41 Representative DDH 79-29 drill core	100
3.42 Details of drill hole DDH 79-29	103
3.43 Late-stage corrosive hematite cement	107

	Page
3.44 Pervasive late-stage porosity	
development	107
3.45 Details of drill hole DDH 80-70	110
3.46 Representative DDH 80-70 drill core	112
3.47 Diagenetic edge-to-face and rosette	
chlorite	112
3.48 Diagenetic chlorite rosettes	115
3.49 Pyrite cement	115
3.50 Diagenetic framboidal pyrite	117
3.51 Diagenetic pyrite cubes	117
3.52 Diagenetic siderite rhombs	119
3.53 Representative 79D-004 drill core	119
3.54 Details of drill hole 79D-004	121
3.55 QRF diagram of Howley Fm. sandstone	
samples	122
3.56 Chlorite platelets on quartz overgrowths	125
3.57 Diagenetic vermicular chlorite	127
3.58 Diagenetic vermicular chlorite	127
3.59 Diagenetic chlorite rosettes	129
3.60 Diagenetic chlorite rosettes	129
3.61 Diagenetic montmorillonite	131
3.62 Diagenetic montmorillonite	131
3.63 Clay-fraction diffractogram of Howley	
Fm. samples	132

	Page
3.64 Details of drill hole 79D-005	135
3.65 Representative 79D-005 drill core	137
3.66 Concavo-convex grain boundaries and quartz overgrowths	137
3.67 Diagenetic vermicular macrokaolinite ...	139
3.68 Macrokaolinite dissolution	139
3.69 Corrosive calcite cement	141
3.70 Calcite cement masking vermicular kaolinite	141
4.1 Details of uranium-mineralized boulder samples	151
4.2 QRF diagram and comparative plot of uranium-mineralized boulder samples	152
4.3 Clay-fraction diffractogram of uranium-mineralized boulder samples	153
4.4 Hematization after uranophane development	157
4.5 Uraninite cement	157
4.6 Hematization after uraninite cementation	158
4.7 Cellular vitrinite maceral	171
4.8 Cellular inertinite maceral	171
4.9 Pyritiferous cellular inertinite and vitrinite macerals	173
4.10 Structureless vitrinite maceral	173

	Page
4.11 Reflectogram for coal samples	177
5.1 Paragenetic sequences in the Deer Lake Group and Howley Fm.	183
5.2 Illite crystallinity measurements of the Deer Lake Group and Howley Fm.	204, 205

CHAPTER ONE
INTRODUCTION

1.1 Location and access

The Deer Lake subbasin of western Newfoundland is approximately 4000 km² in area, and exhibits an overall elliptical shape with a northeast-trending long axis. It is bounded by latitudes 49° 45' and 48° 45' north, and longitudes 57° 45' and 56° 45' west.

The towns of Deer Lake and Pasadena are the main communities in the area (Fig. 1.1). They are located beside the Trans-Canada Highway which follows the trend of the basin as it passes through the area. Smaller communities in the area are linked by paved and unpaved secondary roads to the Trans-Canada Highway. Regularly scheduled commercial aircraft fly from the Deer Lake airport to other cities in eastern Canada. Those parts of the Deer Lake subbasin that are inaccessible by road can be reached using (1) helicopter or float plane from Pasadena, or (2) boat along the Humber and Adies Rivers or through one of the major lakes (Fig. 1.1).

1.2 Physiography

The Deer Lake subbasin is also a physiographic basin, except for two fault-bounded highland areas: the Fisher Hills block between Grand Lake and Deer Lake and the Birchy

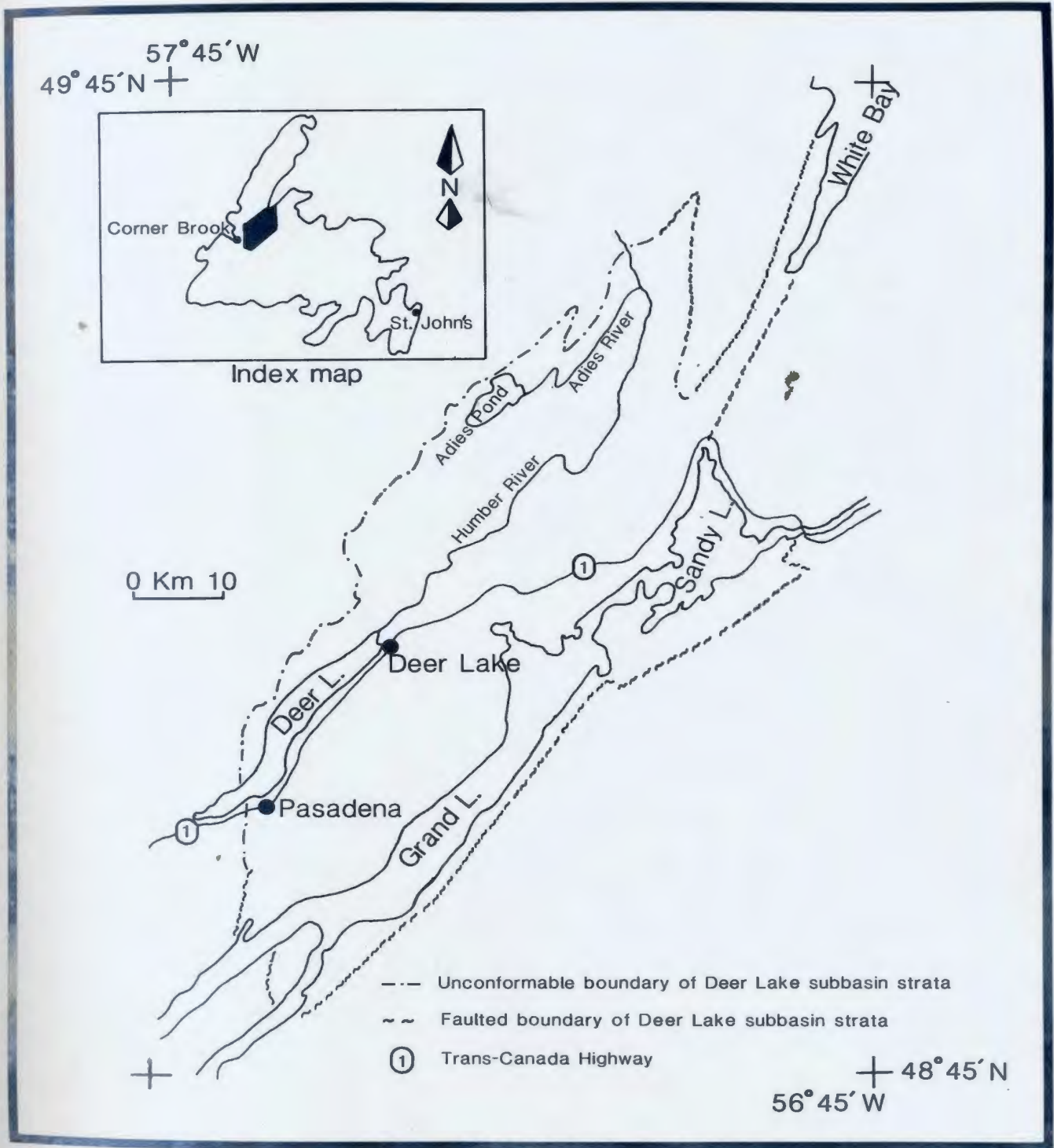


Figure 1.1 Location map of the Deer Lake subbasin

Ridge - White Bay block extending from the north side of Grand Lake northeast to White Bay. The subbasin is almost completely surrounded by highlands underlain by pre-Upper Devonian rocks.

The surrounding highlands and intra-basinal blocks control the drainage pattern in the modern basin, producing northeast-trending lakes and the southwesterly-flowing Humber River. Glacial till and recent alluvium and soil overlie much of the bedrock, the best exposures being along road and brook cuts and lakeshores. The lowlands are dotted by swamps, lakes, and cultivated fields. Otherwise, the area is dominated by commercial coniferous forests which continue onto the surrounding highlands.

1.3 Previous work

Early work in the Deer Lake subbasin focused on mapping and describing the oil shales (Hatch, 1919; Landell-Mills, 1922, 1954; Baird, 1950) and coal (Hayes, 1949). After detailed mapping for Claybar Uranium and Oil Ltd. and Newkirk Mining Co., and as part of his doctoral thesis on the geology of the Humber-Valley, Werner (1955, 1956) named, subdivided and described the Deer Lake Group. Baird (1959), while mapping the Sandy Lake area, adopted the term Anguille Group (Hayes and Johnson, 1938) for the oldest sediments in the basin and correlated the overlying Deer Lake Group with the Windsor Group of the Maritime Provinces. Spores from the basin (Hacquebard et al, 1960) led to the dating and informal

naming of the youngest sediments in the basin, the Howley Beds, later to become the Howley Formation (Hyde, 1978).

A series of regional studies by Belt (1968a, 1968b, 1969) incorporated the Deer Lake subbasin sediments in discussions of Carboniferous sedimentation patterns and Late Paleozoic tectonics in the northern Appalachian-Caledonide trend. Popper (1970) completed a doctoral thesis on the stratigraphy and structure of the Anguille Group. The same year Fleming (1970) published a summary of past petroleum exploration in Newfoundland and Labrador in which he showed some drill hole logs from the Deer Lake subbasin and summarized the significant hydrocarbon showings in the area.

The Newfoundland Department of Mines and Energy began a mapping project of the Carboniferous Deer Lake subbasin in 1975. The sedimentary sequence has since been mapped and formally described by Fong (1976), Hyde (1978, 1979a, b), and Hyde and Ware (1980, 1981). Hyde (1979b, 1981, in press) has described and discussed the various types of mineralization found in the basin. The completion of the mapping project has resulted in a 1:100,000 map of the Deer Lake Basin (Hyde, 1983). The most significant recent economic activity in the basin began in 1978 with discovery of high-grade uranium-bearing sandstone boulders at Wigwam Brook off the Humber River.

1.4 Scope of present thesis study

This thesis is part of the Deer Lake Basin Project, a composite study conceived in 1981 to investigate the geophysical, sedimentological, thermal, and tectonic characteristics of the Carboniferous Deer Lake subbasin sediments of western Newfoundland. The project is jointly sponsored by Westfield Minerals Ltd. (Toronto), Shell Resources (Calgary) and Shell Explorer (Houston).

The aim of this thesis is to describe the petrography and diagenesis of the sediments of the Deer Lake Group and Howley Formation. This is done through complete petrographic analyses of drill core, and the measurement of organic and inorganic thermal indicators contained within the sediments. As well, coaly material and uraniferous sediments found in the drill core, and uraniferous sandstone boulders found above the Humber Falls Formation, are also described. The thesis helps to define some of the sedimentological and diagenetic characteristics of the basin fill, and petrological characteristics and significance of the local uranium mineralization. It is hoped the thesis may also be useful as a comparative base for future offshore Carboniferous studies.

CHAPTER TWO

PART 1 REGIONAL GEOLOGY

2.1.1 Introduction

The five major northern Appalachian zones (Fig. 2.1A), as defined by Williams (1976), form a pre-Upper Devonian basement on which the Maritimes Basin (Williams, 1974) formed during the Alleghanian disturbance. One of the subbasins to form was the Deer Lake subbasin of western Newfoundland (Fig. 2.1B).

The Deer Lake subbasin unconformably overlies the two most westerly tectono-stratigraphic zones of the northern Appalachian orogen; namely, the Humber Zone to the west and the Dunnage Zone to the east. Seismic surveys (Miller and Wright, 1984) indicate that the Humber Zone basement rocks extend eastward to a position below the axis of the Humber syncline in the centre of the Deer Lake subbasin. The subbasin sediments also overlie the Baie Verte - Brompton Line, a narrow, polydeformed and metamorphosed zone defined by ophiolite complexes, along which the Humber and Dunnage Zones were structurally juxtaposed (St-Julien et al., 1976; Williams and St-Julien, 1982). The distribution of these tectono-stratigraphic elements is shown in Figure 2.1A.

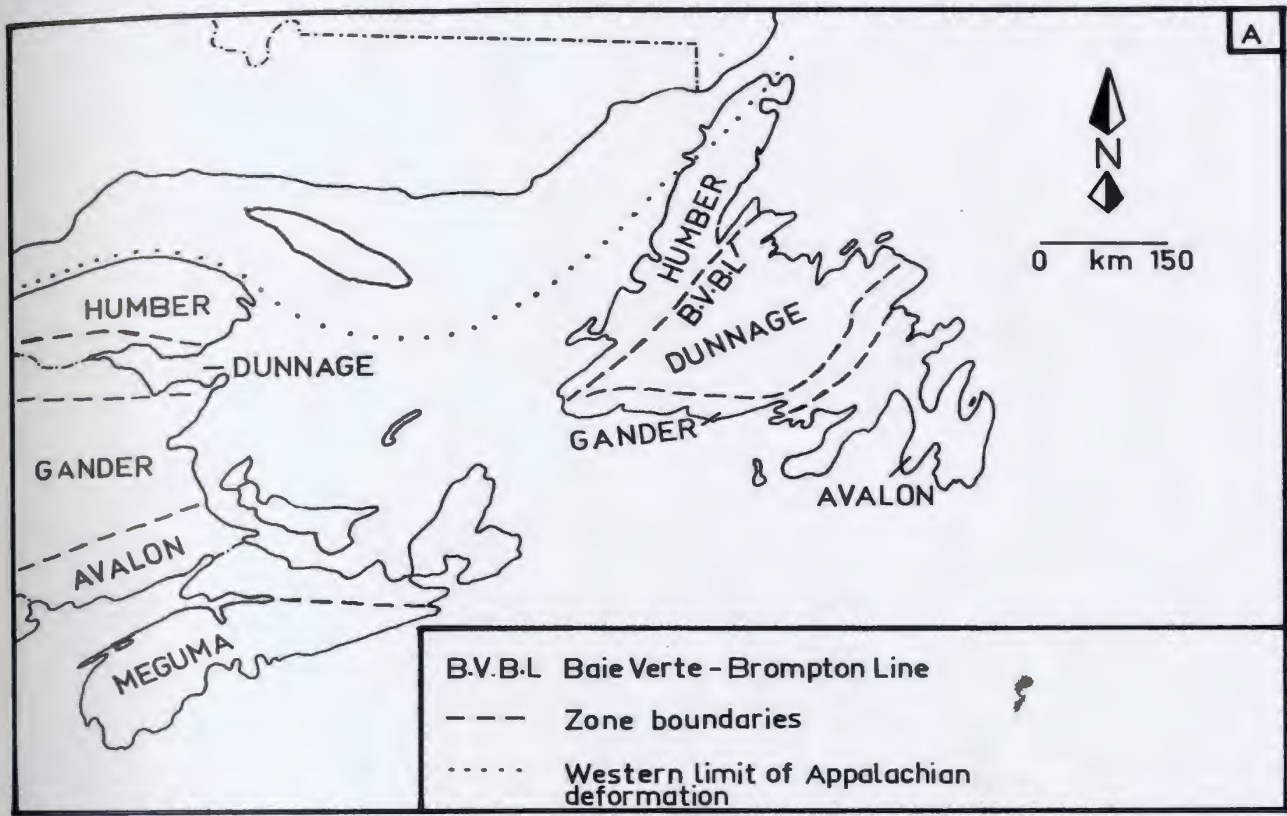
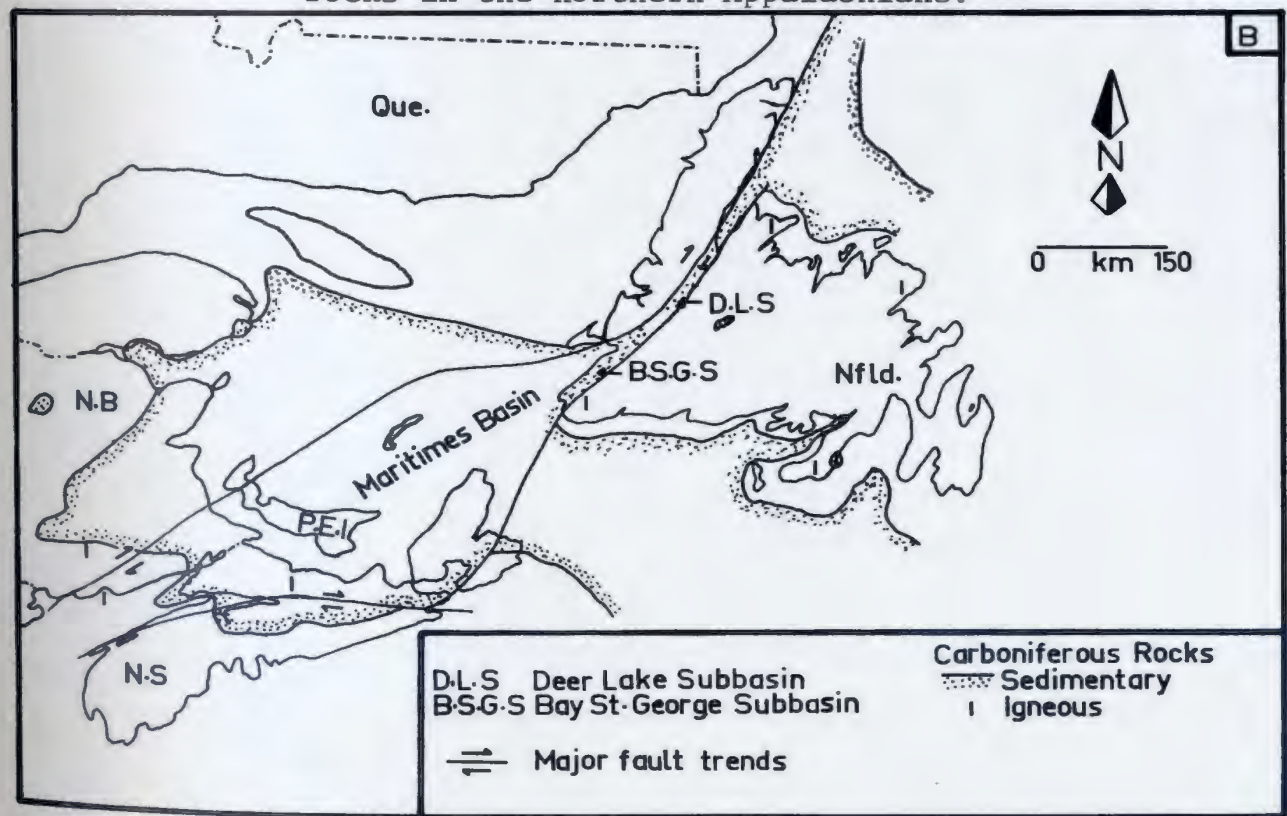


Figure 2.1 (A) The distribution of tectono-stratigraphic zones in the northern Appalachians.
 (B) Extent of the Upper Paleozoic Maritimes Basin and the distribution of Carboniferous sediments and igneous rocks in the northern Appalachians.



2.1.2 Pre-Upper Devonian geology of the Humber and Dunnage Zones in Newfoundland and Labrador

The stratigraphy of the Humber Zone records a Late Hadrynian to Early Ordovician constructive phase of a passive continental margin, followed by a destructive phase which continued into the Late Ordovician. The constructive and destructive phases respectively reflect the generation and destruction of the Cambro-Ordovician Iapetus Ocean (Wilson, 1966; Dewey, 1969; Church and Stevens, 1971; Williams, 1971; Williams and Stevens, 1974). Remnants of Iapetus are represented in the transported siliciclastic sequences, ophiolite and ophiolitic melange of the Humber Arm and Hare Bay allochthons along the western margin of the Humber Zone, and along the Baie Verte - Brompton Line which defines the eastern edge of the zone.

Grenvillian schists and gneisses of predominantly sedimentary origin, cut by granitic to anorthositic and minor mafic intrusives, constitute the basement of the autochthonous stratigraphy of the Humber Zone (Clifford and Baird, 1962; Williams, 1964). In the late Precambrian, rifting of the Grenvillian basement resulted in mafic dike intrusions, mafic volcanism, and deposition of siliciclastic sediments in the rift zone (Williams and Stevens, 1974; Strong, 1975). Along the eastern margin of the Humber Zone, more highly metamorphosed and deformed rift zone sediments are included in the Fleur de Lys Supergroup (Williams, 1964).

After the inundation of the rift zone by the Iapetus Ocean, a Lower Cambrian to Middle Ordovician siliciclastic and carbonate passive margin sequence of sediments developed along the ancient continental margin of North America (Rodgers, 1968). This eastward thickening sequence is comprised of two siliciclastic to carbonate megacycles (Swett and Smit, 1972).

The oldest (Early Cambrian) megacycle consists of terrestrial basal conglomerates and sandstones, and overlying shallow-water sandstones of the Bradore Formation (Hiscott et al., in press), overlain by shallow marine, shaly, siliciclastic sediments and limestones of the Forteau Formation (Schuchert and Dunbar, 1934). The younger (Early Cambrian to Middle Ordovician) megacycle begins with basal, regressive sandstones of the Hawk Bay Formation (Palmer and James, 1980), overlain by tidal to shallow subtidal argillaceous siliciclastic and carbonate sediments of the March Point and Petit Jardin Formations (Swett and Smit, 1972). The carbonate section of the upper megacycle continues with the subtidal and peritidal biohermal limestones and dolostones of the Lower Ordovician St. George Group (Pratt and James, 1982). Above the St. George Group, subtidal, bioturbated limestones of the Middle Ordovician Table Head Group pass upward into argillaceous siliciclastics, limestones and minor calcarenites (Klappa et al., 1980). The two megacycles are overlain by easterly-derived flysch sediments of the Mainland sandstone

(Schillereff and Williams, 1979).

Overlying the autochthonous strata are easterly-derived allochthonous thrust slices. The structurally lowest slices contain continental margin and slope sediments including the Cow Head Group (Williams and Stevens, 1974). In this group, breccias with shallow-water limestone clasts are interbedded with deeper-water argillaceous limestones and siliciclastic sediments (James, 1981). The structurally highest allochthonous slices are the Humber Arm and Hare Bay ophiolite suites (Williams, 1975).

The Dunnage Zone is bound by the Baie Verte - Brompton Line to the west and by a poorly defined belt of ophiolites and ophiolitic melange along its southeastern boundary, the Gander River Ultramafic Belt of Jenness (1958). The zone has been considered both allochthonous and autochthonous (Pajari and Currie, 1978; Hibbard and Williams, 1979; Williams, 1980; Williams and St-Julien, 1982; Karlstrom, 1983).

A generalized stratigraphy for the complex Dunnage Zone would show the following sequence. Oceanic crust and upper mantle of Ordovician age, now exposed in steeply dipping, east-facing ophiolite complexes and as melange blocks, forms the base of a subaqueous to subaerial island arc sequence (Upadhyay et al., 1971; Williams and Talkington, 1977). Subaqueous, mafic, pillowed volcanic flows, pelagic cherts and volcanoclastic turbidites pass upward into shallow water and subaerial volcanoclastic sediments, in part calcareous,

and felsic volcanic flows and pyroclastic rocks (Kean and Strong, 1975; Strong, 1977). Black Caradocian shales then blanketed most of the earlier Ordovician stratigraphy, indicating a quiescent period in the development of the Dunnage Zone island arc sequence. This correlates with the final emplacement of allochthonous rocks onto the Humber Zone (Williams, 1979) but may be related to an episode of global sea-level rise (Leggett, 1978). Rejuvenation of more localized centres of igneous activity and successor basin sedimentation during the Silurian and Devonian produced subaqueous and subaerial sequences of more felsic volcanic flows and pyroclastic rocks intercalated with fluvial gray- and red-beds (Strong, 1977; Chandler, 1982; Arnott, 1983). Punctuating the Ordovician to Devonian sequence are Devonian and Carboniferous dioritic to granitic intrusions, with lesser amounts of quartz-poor intrusives (Bell and Blenkinsop, 1977; Strong, 1980; Wilton, 1983).

2.1.3 Upper Devonian to Permian geology in Atlantic Canada

Between Late Devonian and Permian time, the Alleghanian disturbance developed the fault-controlled northeast-trending complex of basins, intrabasinal horsts, and bordering highlands which cut across every zone in the northern Appalachians (Fig. 2.1A and B). The entire complex is referred to here as the Maritimes Basin (Williams, 1974). The Late Devonian to Permian Alleghanian disturbance and the formation of the Maritimes Basin has been attributed to

wrench faulting and folding (Belt, 1968a; Lock, 1969; Webb, 1969; Hyde, 1979b; Fralick and Schenk, 1981; McMaster et al., 1980; Bradley, 1982). In the Maritimes Basin, up to 250 km of dextral Alleghanian movement has been postulated along the major faults (Belt, 1968a; Webb, 1969).

Paleomagnetic data for the Late Paleozoic (Irving, 1977, 1979; Kent and Opdyke, 1979; Diehl and Shive, 1981; Lefort and van der Voo, 1981; Kent, 1982) suggest that, during the Carboniferous, Newfoundland was between 17° and 20° south of the paleoequator.

As the Maritimes Basin developed, terrestrial siliciclastic sediments were quickly shed into low-lying areas, developing thick sequences of alluvial fan, fluvial, and lacustrine sediment (Belt, 1968a, b; Howie and Barss, 1974; Rust, 1981). These sequences typically display rapid facies changes from alluvial fans nearest the faulted basin margins to fluvial, and then basin-centre lacustrine facies and in places a lake-margin deltaic facies. In areas of extension, Devonian and Carboniferous basaltic lava flowed from faults and interfingered with the terrestrial sediments (Keppie et al., 1978; Rast et al., in press). Granitoid intrusives of similar age were focussed along zones of tension or crustal thickening (Clarke et al., 1980; Strong, 1980). Some of the Carboniferous igneous rocks are indicated on Figure 2.1B.

A Late Mississippian marine incursion penetrated the tortuously interconnected subbasins of the Maritimes Basin, locally covering earlier terrestrial sediments with thick marine sandstone-shale sequences and thinner argillite-carbonate-sulphate/chloride evaporite cyclothems. This transgression did not reach the Deer Lake subbasin. In marine areas, biohermal communities eventually developed on topographic highs (Schenk, 1969, 1975; Geldsetzer, 1977, 1978; Giles et al., 1979; Howie, 1979; Knight, 1983). These marine deposits laterally interfingered with various terrestrial red-bed sediments.

A final marine regression occurred toward the end of Viséan time allowed the system to return to terrestrial sedimentation. Mixed alluvial fan - fluvial deposits gave way to only fluvial deposits as first the subbasins filled and then their faulted margins were overstepped (Fig. 2, 1B). During the Late Carboniferous a "sagging platform" stage (Belt, 1968b), or "thermal subsidence" stage (Bradley, 1982) of the Alleghanian disturbance, allowed a low relief blanket of more mature sediment to spread out over pre-Upper Devonian basement rocks. Organic material was then able to accumulate in topographically low floodplain regions (Legun and Rust, 1982) and in paralic environments along the northern margin of a regressed Hercynian Ocean (Duff et al., 1982).

In Newfoundland, onland exposures of Upper Devonian to Upper Carboniferous marine and non-marine sediments crop out in two major northeast-trending, fault-controlled subbasins, the Bay St. George and Deer Lake subbasins (Belt, 1969; Hyde, 1979b; Knight, 1983), and in smaller isolated exposures in central Newfoundland (Belt, 1969) and on the Burin Peninsula (Strong et al., 1978; Laracy and Hiscott, 1982). Similar Devonian to Carboniferous sediments form an extensive offshore apron around much of Newfoundland (Howie and Barrs, 1974; Sanford et al., 1979). The stratigraphic ages, subdivisions and regional correlations for the sedimentary rocks of the Maritimes Basin are given in Figure 2.2.

The two western Newfoundland subbasins formed along the narrow northeastern extension of the Maritimes Basin (Fig. 2.1B). A topographic high near present-day Corner Brook probably separated the two subbasins. Granitic to tonalitic plutonism, east of both White Bay and the Bay St. George subbasin, coincided with Late Devonian - Early Carboniferous sedimentation in the subbasins (Bell and Blenkinsop, 1977; Wilton, 1983).

AGE		STRATIGRAPHY				
		MARITIME PROVINCES	BAY ST-GEORGE BASIN	DEER LAKE BASIN		
Carboniferous	Permian	E	Pictou Gp.			
	Stephanian	D				
	Westphalian	C	Cumberland Gp.			
		B				
		A				
	Namurian		Riversdale Gp.		Barachois Gp.	
			Canso Gp.			
			Windsor Gp.			
	Viséan				Codroy Gp.	Deer Lake Gp.
	Tournasian		Horton Gp.		Anguille Gp.	Wigwam Brook Fm.
		Wetstone Point Fm.				
Devonian	L			Anguille Gp.		
	M					

Figure 2.2 Stratigraphic age, subdivisions; and correlation for the Upper Paleozoic rocks of Atlantic Canada (after Howie and Barss, 1974; Hyde, 1983; and Knight, 1983).

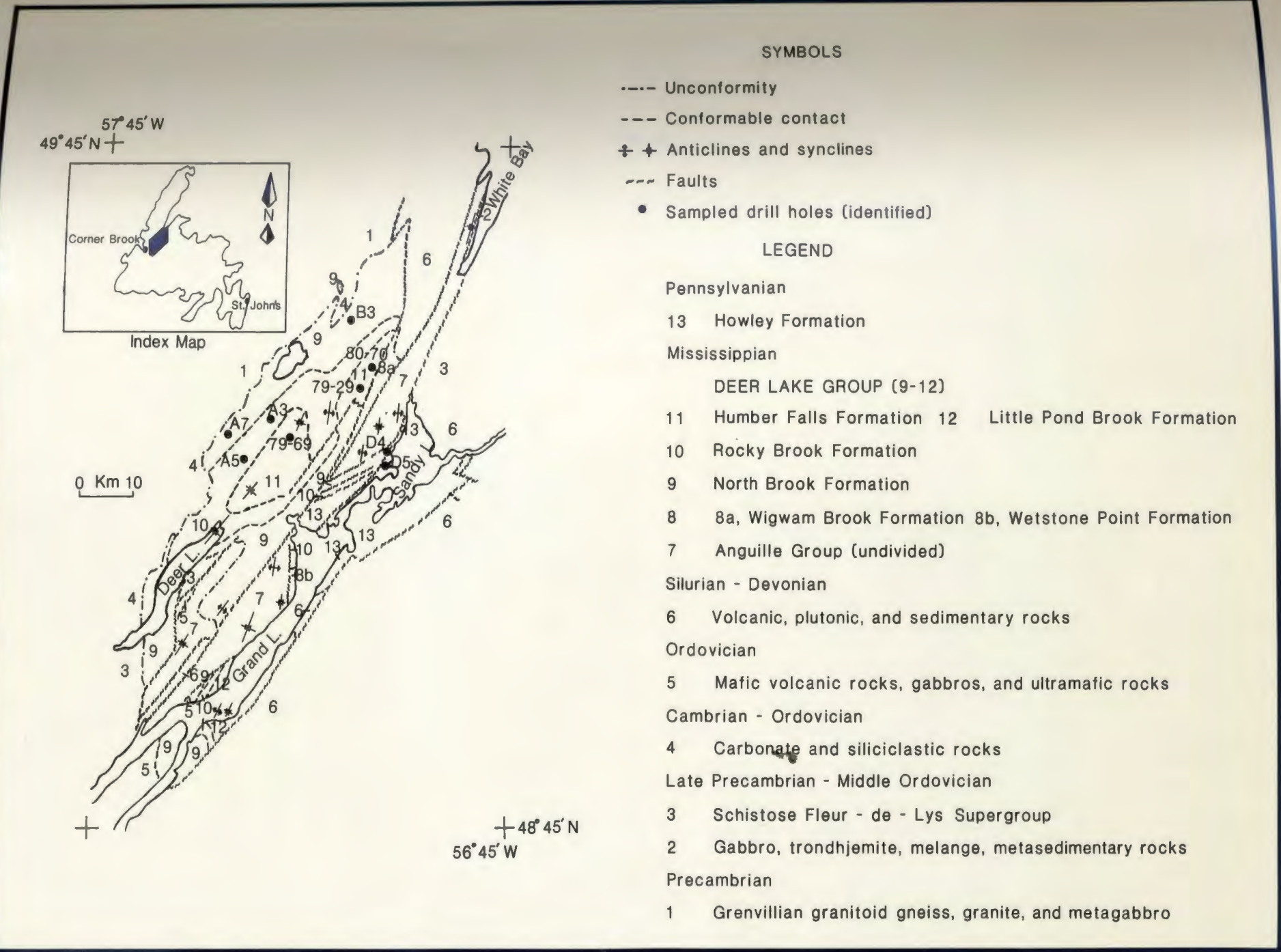
PART 2 GEOLOGY OF THE DEER LAKE SUBBASIN

2.2.1 Introduction

The dominantly Carboniferous Deer Lake subbasin and the larger Bay St. George subbasin of western Newfoundland are the two largest in Newfoundland. In the past, the Deer Lake subbasin has also been called the Hampden Basin (Belt, 1968b), the North-Central Basin (Belt, 1968a, 1969), and the Deer Lake - White Bay Basin (Fong, 1976); the White Bay area is considered here to be part of the Deer Lake subbasin.

The stratigraphy of the subbasin consists of alluvial fan, fluvial, and lacustrine lithologies. These sediments are now disposed in elongate northeast-trending units (Fig. 2.3), in part fault-bounded, from Glover Island on Grand Lake to White Bay, where they continue offshore (Haworth et al., 1976; Hyde, 1983). The age of these sediments has been obtained from spore assemblages, and fish and plant remains found within the sediments. Figure 2.4 shows the stratigraphy, estimated thickness, and dated fossils of the Deer Lake subbasin sediments.

Cross sections by Hyde (1983) indicate that the Anguille Group (Fig. 2.4) alone might reach a thickness of 1.2 km below the Thirty-ninth Brook syncline west of Grand Lake. Gravity measurements by Miller and Wright (1984) show comparable basement depth estimates of 1.5 km for the Howley Formation in the Howley area, and 1.2 km for the Deer Lake



Simplified after Hyde 1979a, In press .

Figure 2.3 DEER LAKE SUBBASIN WESTERN NEWFOUNDLAND

Carboniferous	Westphalian A	Howley Fm. (3100m.) s		
	Namurian			
	Viséan	Deer Lake Group	Humber Falls Fm. (250m.) s	Little Pond Brook Fm. (750m.) s
			Rocky Brook Fm. (1000m.) s	
			North Brook Fm. (2000m.)	
	Tournaisian		Wigwam Brook Fm. (300m.) s	Wetstone Point Fm. (300m.) s
			Thirty-Fifth Brook Fm. (1000m.)	Cape Rouge Fm. (1200m.) s
		Anguille Group	Saltwater Cove Fm. (2700m.)  	
			Forty-Five Brook Fm. (500m.)	Gold Cove Fm. (500m.)
			Blue Gulch Brook Fm. (400m.)	

Figure 2.4 Stratigraphy, thickness, and dated fossils of the Carboniferous Deer Lake subbasin. Age dates obtained by: s= spore assemblages,  = fish remains,  = plant remains.

Group along the Humber syncline.

2.2.2 Anguille Group

The Anguille Group (Hayes and Johnson, 1938; Baird, 1959) is confined to two largely fault-bounded, northeast-trending highland blocks in the Deer Lake subbasin: the Fisher Hills block between Deer Lake and Grand Lake, and the Birchy Ridge-White Bay block extending from Sandy Lake northeast to at least the town of Conche on the Northern Peninsula. Lithologic correlation, and dating of spore assemblages, and plant and fish remains (Heyl, 1937; Baird and Cote, 1964; Baird, 1966; Belt, 1969) suggest a Tournaisian age for the Anguille Group. In the Bay St. George subbasin the base of the Anguille Group is interpreted as Famennian age (Belt, 1969; Knight, 1983). In the Deer Lake subbasin the lowermost units of the Anguille Group, the Blue Gulch and Gold Cove Formations, are undated. It is possible therefore that the stratigraphy of the Deer Lake subbasin also ranges into the Upper Devonian. The unconformable contact with the pre-Anguille Group basement can only be seen on Groais Island near Conche (Belt, 1969).

The Anguille Group is dominated by gray indurated sandstone, siltstone, and mudstone lithologies, arranged in both fining- and coarsening-upward sequences that contain some turbidites. The sequences were deposited in lake or lake-margin deltaic environments. Lesser amounts of conglomerate representing delta distributary channel and

basin-margin alluvial fan deposits, and micritic lacustrine carbonate rocks are also present in the Anguille Group (Popper, 1970; Hyde, 1978, 1979b). The Anguille Group sediments also show varying amounts of carbonate nodules, organic material including fossil trees (Popper, 1970), and detrital flakes of mica. Paleocurrent measurements by Popper (1970) and Hyde (1979b) generally indicate a transport direction away from peripheral highlands, into a large central lake, and then northeast and southwest along the basin axis. Informal subdivisions of the Anguille Group by Popper (1970) and Hyde (1979b) are now replaced by the formal subdivisions of Hyde (1983).

2.2.3 Wetstone Point and Wigwam Brook Formations

Both of these Tournaisian-age formations have only recently been delineated by Hyde (1983). They lie above the Anguille Group and below the Deer Lake Group. The two formations are only seen in fault-contact with other lithologies except where the Wigwam Brook Formation unconformably onlaps granitic basement rocks along its northeastern margin (Fig. 2.3). The Wigwam Brook Formation consists of coarse to medium grained sandstones and pebble conglomerate containing lenses of micritic limestone. Dr. R. Hyde (pers. comm. 1983) considers the limestones to have been inorganically precipitated in pools on floodplain surfaces. This formation is placed stratigraphically above the Anguille Group as it contains sedimentary clasts of the

Saltwater Cove Formation (Dr. R. Hyde, pers. comm. 1982); it probably was developed due to upfaulting and erosion of the Saltwater Cove Formation, which is now east of and in fault-contact with the Wigwan Brook Formation.

The Wetstone Point Formation contains interlayered gray pebble conglomerates and pebbly sandstones; and gray, red, and green sandstones, siltstones, and shaly claystones. These show a northward paleoflow direction and are interpreted as fluvial deposits. This formation is placed stratigraphically above the Anguille Group because, unlike the Anguille Group, it is semi-lithified and has a well preserved spore assemblage (Dr. R. Hyde, pers. comm. 1983).

2.2.4 Deer Lake Group

North Brook Formation

The North Brook Formation (Werner, 1955) is the basal red-bed formation of the Deer Lake Group, and is the most widespread stratigraphic unit in the Deer Lake subbasin (Fig. 2.3). The North Brook Formation is undated, but has been correlated stratigraphically with Viséan rocks of the Maritime Provinces by Belt (1968b). Although the lower contact is never observed, it is considered by Hyde (1979b) to unconformably overlie the Anguille Group. The formation is either in fault contact with various basement lithologies or unconformably onlaps them along the western margin of the

subbasin.

The North Brook Formation consists mainly of red to gray, interbedded, polymict pebble to boulder conglomerates, and cross-stratified sandstones, with lesser amounts of siltstone, mudstone, and micritic limestone. These lithologies form a fining-upward megasequence comprised of smaller, fining-upward sequences of metre-scale conglomerate or pebbly sandstone to siltstone. The coarsest sediments are found above the basement unconformity.

Finer grained sandstone and siltstone units often exhibit calcareous nodules and caliche beds. Silicified wood fragments and rhizoliths locally occur, respectively, in conglomerate beds and in finer-grained sandstone and siltstone layers. On Lanes Brook just east of Deer Lake, a few calcareous layers resembling hemispherical stromatolites occur within thicker conglomerate debris flows. These possibly formed in organic-rich pools on alluvial-fan surfaces (Hyde, 1979b). Another feature of the subbasin stratigraphy, particularly well demonstrated in the North Brook Formation, is the direct correlation between the dominant rock fragment type in the conglomerates and the most proximal basement lithology. For example, north of Deer Lake where the North Brook Formation overlies Ordovician carbonate rocks, limestone and limestone breccia rock fragments are dominant; near Adies Pond, where the formation overlies Grenville basement, granitoid rock fragments are dominant (Dr. R. Hyde, pers. comm. 1982). Paleocurrent indicators

show sediment movement away from highland basement terrains surrounding the basin toward the basin centre (Werner, 1956; Hyde, 1979b).

The North Brook Formation has been interpreted by Belt (1968b), Hyde (1979b), and Hyde and Ware (1981) as basin-margin alluvial-fan deposits, changing to fluvial sediments and possibly ephemeral lake deposits toward the centre of the basin.

Rocky Brook Formation

The Rocky Brook Formation (Werner, 1955) gradationally overlies the North Brook Formation, and locally onlaps carbonate basement rocks northwest of Deer Lake. It too is widely distributed within the Deer Lake subbasin, but to a lesser extent than the North Brook Formation (Fig. 2.3). Based on spore assemblage identification by S. Barss (Dr. R. Hyde, pers. comm. 1982), a Viséan age has been assigned to it. Its base is defined as the first appearance of green or gray siltstones or mudstones (Hyde and Ware, 1981).

The formation has been divided by Hyde (1983) into the lower Spillway Member, and the upper Squires Park Member. The Spillway Member is dominated by calcareous red siltstones and minor sandstones, green and gray siltstones and mudstones, and micritic carbonate rocks. These fine grained sediments are found as intercalated thin beds and laminae, commonly with desiccation cracks. In this member, generally

gradational cycles are developed on a metre scale, showing gray limestone passing upward into gray to green mudstone, which in turn is overlain by red siltstone. The Squires Park Member contains similar lithologies and structures, but is dominantly green, gray or black in colour with no red strata. More common in the upper member are various orthochemical and allochemical carbonate rocks containing fish remains, ostracods, branchiopods, plant remains, and carbonate nodules which coalesce in places into continuous layers.

Belt (1968b) included the Rocky Brook Formation in his lacustrine and mixed fluvial-lacustrine facies categories. The presence of lacustrine facies sequences (Hyde, 1979b; Hyde and Ware, 1981), typical lacustrine stromatolites (Dr. R. Hyde, pers. comm. 1983), and "analcime", and the lack of marine fossils, suggest that the Rocky Brook Formation developed within a restricted alkaline lake environment which was fringed by low gradient delta complexes and alluvial plains.

Humber Falls and Little Pond Brook Formations

The Humber Falls Formation (Hayes, 1949) and Little Pond Brook Formation (Hyde, 1983) are the highest stratigraphic units of the Deer Lake Group. Viséan spores have been identified in both by S. Barss (Dr. R. Hyde, pers. comm., 1982). The Little Pond Brook Formation gradationally overlies the Rocky Brook Formation and onlaps volcanic basement rocks at Grand Lake (Fig. 2.3). Varicoloured

pebble conglomerates, cross-stratified sandstones and organic-rich siltstones arranged in crude fining-upward sequences are the main rock types. Paleocurrent indicators suggest westward fluvial transport of sediment.

The Humber Falls Formation outcrops in two areas about the geographical centre of the subbasin (Fig. 2.3). It has a sharper, possibly unconformable contact with the underlying Rocky Brook Formation, but essentially contains lithologies similar to the Little Pond Brook Formation. It does appear to contain more carbonate nodules, coalified wood fragments, and fining-upward fluvial sequences (Hiscott, 1979). Coarse sediment was deposited by rivers flowing from highlands to the north and northeast (Werner, 1956; Belt, 1968b; Hyde, 1979b).

2.2.5 Howley Formation

The youngest sediments in the Deer Lake subbasin belong to the Howley Formation (Hyde, 1978). Spore assemblages from the Howley Formation have been dated as Westphalian A (Hacquebard et al., 1960). The formation crops out along the eastern margin of the subbasin near the shores of Sandy Lake and north of Grand Lake (Fig. 2.3), and has a total thickness of approximately 3.1 km (Hyde, 1979b; Fig. 2.4). The depth to basement below the Howley Formation east of Sandy Lake is about 1.5 km (Miller and Wright, 1984). It is only seen in fault contact with older units.

The Howley Formation consists of interbedded gray to red polymict pebble conglomerates, cross-stratified sandstones, siltstones, and mudstones. These often contain carbonate and ironstone nodules and coalified wood debris. Rock fragments in the formation indicate highland basement sources to the east and northeast. Coal seams, interbedded with pyritiferous and carbonaceous gray sandstones and siltstones, are also found within this formation.

Hyde (1979b) proposed an informal three-fold subdivision of the formation: (1) a basal, red, sandstone-dominated unit; (2) a middle, gray, sandstone-conglomerate unit; and (3) an upper coal-bearing unit. In places, metre-thick fining-upward sequences are developed within these units. The formation has been interpreted as dominantly fluvial (Belt, 1968b; Hyde, 1979b), with the coal probably developing in swamps on alluvial plains during a late stage of peneplanation.

2.2.6 Summary of the depositional environments and trends in the Deer Lake subbasin

Sedimentation patterns within the Deer Lake subbasin varied throughout its development. During initiation of the northeast-trending western Newfoundland wrench zone (the rift stage of Belt, 1968b; and Bradley, 1982), the Upper Devonian (?) to Lower Mississippian Anguille Group was rapidly deposited into a newly created subbasin, as suggested by both east and west paleoflow indicators from opposite sides of the inferred subbasin. The Anguille Group changes upward from alluvial fan conglomerate and braided fluvial conglomerate and sandstone sedimentation, to finer grained, dominantly lacustrine sediments, possibly reflecting a deepening basin forming under humid conditions. In places, contemporaneous fining- and coarsening-upward trends are evident (Hyde, 1979b).

Contrasting attitudes of the Anguille Group and the overlying North Brook Formation in the Fisher Hills block suggests an unconformity between them. As well, the Anguille Group is generally darker gray, more indurated, and is more deformed than the overlying Deer Lake Group and Howley Formation (Popper, 1970).

The Deer Lake Group is an arkosic red-bed sequence that shows major shifts in the prevailing depositional environment. A scarcity of Anguille Group clasts in the basal sediments of the North Brook Formation (Hyde, 1979b)

suggests that the Anguille Group was deformed but not substantially uplifted before alluvial fans and braided streams of the North Brook Formation spread out over previously deposited sediments and exposed basement lithologies. A tectonically quiescent period allowed a large restricted lake to develop in the subbasin, fed by low gradient streams via fringing deltas. Reactivation of local faults appears to have caused a sharp sedimentary discontinuity in the central basin area, where coarse fluvial sediments of the Humber Falls Formation overlie fine grained Rocky Brook Formation sediments.

The position of the Howley Formation and its Westphalian A age, suggest that it may have been deposited in a low-lying region along the eastern margin of the Deer Lake subbasin, and may represent a local manifestation of the "sagging platform" stage (Belt, 1968b), or "thermal subsidence" stage (Bradley, 1982) of the Alleghanian disturbance.

There seems to have been a climatic shift from semi-arid to humid conditions during the development of the Deer Lake subbasin. Red-bed sequences may form under humid or arid conditions (Krynine, 1950; Van Houten, 1961; Walker, 1974; Hubert and Reed, 1978), but their abundance and association with rhizoliths, caliche beds, and, on a regional scale, with evaporites, points to an arid to semi-arid climate (Folk, 1976; Schenk, 1969; Glennie, 1970; Leeder, 1975; Collinson, 1978). Such conditions prevailed during the Viséan in the Deer Lake subbasin and in the rest of the

Maritimes Basin. The coal-bearing Howley Formation, and equivalent Pennsylvanian sediments throughout the Maritimes Basin, indicate a change to humid conditions with the widespread development of fluvial systems and peat bogs.

2.2.7 Carboniferous deformation within the Deer Lake subbasin

As mentioned earlier, the Anguille and Deer Lake Groups display contrasting degrees of deformation. The Anguille Group rocks show tight to open, upright to west-verging folds. These are generally arranged as shallow doubly-plunging en echelon folds (Popper, 1970; Hyde, 1979b) with axial-surface traces oriented at a low angle to the main northeast trend of the subbasin (Fig. 2.3). Tensional faults are developed perpendicular to the axial surface trace of the en echelon folds (Phair, 1949; Belt, 1969; Lock, 1969). The en echelon folds and tensional faults are typical features developed during early stages of strike-slip motion (Cloos, 1955; Moody and Hill, 1956; Wilcox et al., 1973). The en echelon folds in the Anguille Group are the strongest evidence for dextral strike-slip faulting in the Deer Lake subbasin.

The Deer Lake Group and Howley Formation rocks show open, shallowly-plunging folds except adjacent to faults where they become tightly folded and cataclastic. The folds have a long wavelength, parasitic folds, and an axial surface trace nearly parallel to the subbasin (wrench zone) trend. This is particularly evident in the Humber syncline, the

major structural feature along the western side of the subbasin (Fig. 2.3).

From the above the Deer Lake subbasin seems to have developed in two stages. The first stage resulted in deposition of the Anguille Group adjacent to steeply-dipping, active, strike-slip faults (en echelon folds, tensional faults perpendicular to the folds, subhorizontal slickensides, Hyde, 1979b), whereas the second stage resulted in the development of the Deer Lake Group during normal and reverse faulting (folds parallel to faults, fining-upward megasequences, vertical slickensides, Hyde, 1979b).

Development as pull-apart basins has been proposed for some of the subbasins within the Maritimes Basin (McCabe et al., 1980; McMaster et al., 1980; Frählick and Schenk, 1981) including the Deer Lake (Bradley, 1982). Pull-apart basins imply that specific geologic features are present. Horsts and grabens in and around a major pull-apart basin are rhombic in plan geometry (Aydin and Nur, 1982). Pull-apart basins are extensional features which commonly form when the through-going wrench fault has a double bend, or a major structural offset, allowing a gap, and therefore a pull-apart basin to form (Burchfiel and Stewart, 1966; Crowell, 1974). Sedimentologically, overall coarsening- and then fining-upward, large-scale cycles in pull-apart basins show the respective effects of vertical and then lateral movement on the basin margin faults (Steel and Gloppen, 1980). The progressive imbrication of large-scale sequences along the

basin floor as the basin grows is another feature of some pull-apart basins (Crowell, 1975; Steel and Aasheim, 1978).

In the Deer Lake subbasin the evidence for pull-apart origin is not compelling. Rather, differential subsidence along sinuous strike-slip faults may be sufficient to explain the history of sedimentation in the Anguille Group. The present disposition of the Deer Lake Group sediments suggests that they may have been deposited in a half-graben, downthrown along its highly faulted eastern margin.

CHAPTER THREE

DRILL HOLE STRATIGRAPHY AND PETROGRAPHY

3.1 Analytical methods

3.1.1 Stratigraphy

Between 1978 and 1980 numerous one-inch diameter cored holes were drilled into the stratigraphic units of the Deer Lake subbasin by Northgate Exploration Co. and Westfield Minerals Ltd. Nine of these drill holes were systematically sampled and studied. Two holes were sampled from each of the North Brook, Rocky Brook, and Howley Formations, and three holes from the Humber Falls Formation. The Humber Falls Formation was sampled more thoroughly, not only due to its location in two geographically distinct areas (Fig. 2.3, p. 17), but also to investigate any relationship with the anomalous uranium-bearing sandstone boulders found above the northern body of the formation. Figure 2.3 shows the disposition of the drill holes in the Deer Lake subbasin and their abbreviated drill hole number.

Representative drill holes through the four formations met the following criteria: they contained the spectrum of lithologies typically found in the formation; they were from widely spaced, essentially undeformed areas; the cores were the longest and most complete available. All the holes that were chosen had been drilled vertically. Each drill hole was sampled every ten metres starting at the top of the drill

hole; in places, samples of particularly unusual features (e.g., calcareous nodules, uranium anomalies) were also taken between the ten metre intervals. Most of the drill core used in this study had been stored out-of-doors for approximately three years. However, the only change which may be attributed to recent weathering is the increase of late secondary porosity. The stratigraphic columns presented in this chapter are derived both from personal field notes and from drill hole logs prepared by employees of Westfield Minerals Ltd. and Northgate Exploration Co.

3.1.2 Colouration

The fresh surface colour of the core was recorded using names and colour codes of the Munsell colour system. The code has four components: hue, colour, value, and chroma; these are recorded in similar order. The hue designations zero and ten indicate the boundary between one colour and the next. The basic rock colours of the sampled core were: green (G), red (R), black (N), and yellow (Y). The value, or lightness number, increases from two to eight with increasing lightness. The chroma number indicates the degree of colour saturation from dark (one) to vivid (six). Where a rock sample displayed more than one colour due to redox effects, weathering, or large proportions of conglomerate clasts, the dominant fresh sandstone or conglomerate matrix colour was recorded.

3.1.3 Porosity

Estimations of total porosity were made on every possible sample. The poor consolidation of some samples prevented porosity measurements. Total porosity was estimated during systematic point counting of thin sections. This was facilitated by the impregnation of the heated sample with blue-tinted epoxy resin before thin sectioning. The effective porosity was obtained using a Beckman 930 air comparison pycnometer and premeasured cylinders of core approximately one centimetre high.

All the porosity measurements are included with modal compositions in Appendix I. In this chapter, the total and effective porosities will be presented as line graphs. Total porosity is also included in modal composition graphs within the 'others' category. The porosity measured is referred to as 'present' because it is almost impossible to identify and quantify any primary porosity, or the amount of porosity present at any point during diagenesis, because of the ensuing stages of dissolution and precipitation.

The criteria and terminology of Schmidt et al. (1977) are used to describe the secondary porosity seen in the sandstones. Choquette and Pray's (1970) porosity classification has been used for the carbonate-rich sediments of the Rocky Brook Formation.

3.1.4 Mineralogy

The modal composition of the samples was obtained by counting 250 points in thin sections cut perpendicular to the drill-hole axis. Due to the friability of the fine grained sediments and grain size of the conglomerates, thin sectioning, and therefore petrographic description, was only possible with the sandstones and a few of the more indurated finer grained samples. Mineral identification was made using conventional petrographic microscopy on thin sections stained with alizarin red S and sodium cobaltinitrite (Friedman, 1971) for carbonate and potassium feldspar identification respectively.

QRF ternary plots (Q = monocrystalline and polycrystalline quartz, R = all rock fragments including chert, F = all feldspars) were made for the North Brook, Humber Falls, and Howley Formations. Due to the fine grained nature of the Rocky Brook Formation sediments, classification of these sediments was based on Picard's (1971) scheme.

The identification of clay minerals was not always possible through petrographic microscopy alone. Therefore, characteristic basal X-ray diffraction peaks, and mineral morphology revealed by scanning electron microscopy, were used to help identify the clay minerals. Unless otherwise stated, the word clay is used to describe detrital and diagenetic minerals less than two microns in size. Illite is used for clay size minerals belonging to the mica group (Grim et al., 1937; Brown, 1955; Yoder and Eugster, 1955; Hower and Mowatt, 1966). In some cases, mineral identification was

aided by electron microprobe analyses using a JEOL JXA-50A electron probe microanalyser with Krisel Control, interfaced to a PDP-11 microcomputer.

3.1.5 X-ray diffractometry

X-ray diffraction analyses assisted in the identification of the clay minerals, and in estimating the relative percentages of kaolinite, chlorite, illite, and montmorillonite. The analyses were carried out in three stages.

(1) Separation of the $< 2 \mu$ fraction from each core sample; removal of amorphous iron (Mehra and Jackson, 1960); and mounting of three, .02 gm, oriented clay aliquots from each sample onto glass slides. One aliquot was spiked with a talc internal standard; the second was treated with acid to remove the chlorite diffraction peaks that overlap the kaolinite peaks, and then spiked with talc; the third was expanded with ethylene glycol vapours. Montmorillonite and montmorillonite-bearing mixed-layer clays undergo a peak shift to lower 2θ angles after exposure to ethylene glycol. Flocculation of the clay suspension using magnesium chloride resulted in magnesium-saturated samples.

(2) Each Mg-saturated oriented aliquot was selectively scanned using a Philips X-ray diffractometer with a graphite monochromator and the following operating conditions: Cu K_{α} radiation, 40 kv, 20 ma, $1/4^{\circ} 2\theta$ per minute goniometer rate, 1

cm per minute chart speed, rate meter of 2000 cps, time constant of 4, 1° divergent slit, 1° receiving slit. Teletapes recording total counts for each 10 second increment were simultaneously made.

(3) Teletype data was entered into a HP9845B desktop computer. After editing, specific peaks were digitized (including the standard talc peak) to find their relative peak areas and eventually their relative percentages through the weighting method of Biscaye (1965) as corrected by Heath and Piasias (1979).

Diagrams of relative clay percentages and of representative diffractograms of the minerals typically found in the clay fraction were produced for each drill hole and formation respectively. The identification of the diffractogram peaks is based on mineral X-ray powder data presented in Bayliss et al. (1980), Brindley and Brown (1980), Carroll (1970), and standard mineral diffractograms belonging to the Department of Earth Sciences at Memorial University.

Researchers have found that the methods of clay mineral quantification are in fact only semi-quantitative estimates, and that, even when the analytical techniques are consistent and carried out with as much precision as possible, the results may only be accurate to \pm ten percent of the amount present (Johns et al., 1954; Pierce and Siegel, 1969; Carroll, 1970). Errors in measuring the relative abundance

of clay minerals may be due to different mounting techniques (Gibbs, 1968), different sample weights (Stokke and Carson, 1973; Kodama et al., 1977), or different mineral mass absorption coefficients (Carroll, 1970). Problems also arise when choosing the particular method for determining the relative amounts of clay minerals, particularly when attempts are made to compare data which have used dissimilar methods (Pierce and Siegel, 1969; Kodama et al., 1977). For example, Biscaye (1965) questioned the validity of the peak height method. Scafe and Kunze (1971) on the other hand found that, for their purposes, the peak height method gave better results than the peak area method. A third view was taken by Harlan (1966, cited in Scafe and Kunze, 1971) who suggested that both methods supply comparable results. Pierce and Siegel (1969) stated that "It must be noted that although calculation methods differ and give significantly different results if used with the same diffractograms, each method is internally consistent for a given study and can give results that suggest meaningful geologic trends". This is perhaps the safest and most realistic statement on clay mineral quantification methods.

3.1.6 Scanning electron microscopy

The inspection of small pieces of sandstone using scanning electron microscopy (SEM) permitted the morphological identification of various minerals, and also allowed some of their physical interrelationships to be

determined. Small fragments of sandstone containing both framework grains and pore material were mounted on aluminum stubs with silver paint and then gold coated in an Edwards S150A sputter coater. The specimens were then viewed in a Cambridge Stereoscan Mark 2A scanning electron microscope, operating at 5 or 10 kv and various aperture settings. Records of any interesting features were made on Polaroid Type 665 film.

3.1.7 Cathodoluminescence

A few thin sections from the four formations were examined under cathodoluminescence so that petrographic features not seen by conventional microscopy or SEM could be revealed. A Nuclide luminoscope was linked to a Wild M400 Photomat microphotometry system. Uncovered, unstained thin sections were illuminated by a 60 ma electron beam achieved by using a vacuum of 50 millitorr and a voltage of approximately 12 kv. Photomicrographs were taken using Kodak ASA 1000 film; exposure times were between one half and ten minutes. Detrital feldspars and carbonate cement were the most fluorescent minerals. The only new information revealed by cathodoluminescence pertained to carbonate cements.

3.2 North Brook Formation

3.2.1 Introduction

Two representative drill holes were selected from the North Brook Formation; 79A-007 (abbr. A7) and 79B-003 (abbr. B3). The location of each drill hole is shown in Figure 2.3, p. 17. Originally A7 was drilled to locate the Carboniferous-basement unconformity, which it failed to reach; B3 was drilled to sample the North Brook Formation stratigraphy. Drill hole A7 has also been sampled for paleomagnetic studies (Irving and Strong, in press).

3.2.2 Drill hole 79A-007 (A7)

Stratigraphy

This drill core is comprised of interlayered conglomerates, sandstones, siltstones, and mudstones, with sandstones being the dominant lithology (Fig. 3.1). Fining-upward conglomerate to siltstone fluvial sequences, up to 15 m thick, are present. In Figure 3.2, conglomerates tend to be pale red or light gray, sandstones are predominantly red, and siltstones and mudstones are more friable and a deeper brownish-red colour. The red colouration and light gray to green bands and spots are diagenetic redox features.

Conglomerates are dominated by lithologically immature, pebble-size framework clasts, derived from plutonic, metamorphic and carbonate sedimentary sources, and supported by a calcareous granule- to sand-size matrix. Very coarse to very fine grained sandstone units are crudely

cross-stratified and display sharp or gradational contacts with the conglomerate and siltstone-mudstone layers.

Siltstones and mudstones are poorly preserved, but do exhibit some laminations. Both the fine grained sediments and sandstones contain calcareous nodules.

Petrography

The arkosic sandstones have a relatively uniform mineralogy (Figs. 3.1 and 3.4 and Appendix I). The dominant detrital minerals, in order of abundance, are as follows: feldspars (plagioclase = orthoclase > microcline > perthites), quartz (monocrystalline > polycrystalline), rock fragments (plutonic > metamorphic > sedimentary = volcanic), with minor amounts of muscovite, biotite, chlorite, magnetite, and epidote. The detrital minerals are generally well sorted, subangular to subrounded grains, bound together by minor amounts of diagenetic clay, carbonate and hematite cements. The diagenetic mineral assemblage consists of calcite, hematite, kaolinite, chlorite, illite, montmorillonite, and lesser amounts of mixed-layer illite-montmorillonite, pyrite, quartz overgrowths, and limonite.

Plagioclase and microcline have been generally altered more than orthoclase, so that they now exhibit extensive dissolution features and illitization (Fig. 3.3). Feldspar in rock fragments, especially in granitoid fragments, may show progressive dissolution and illitization as well.

NORTH BROOK FM. 79A-007

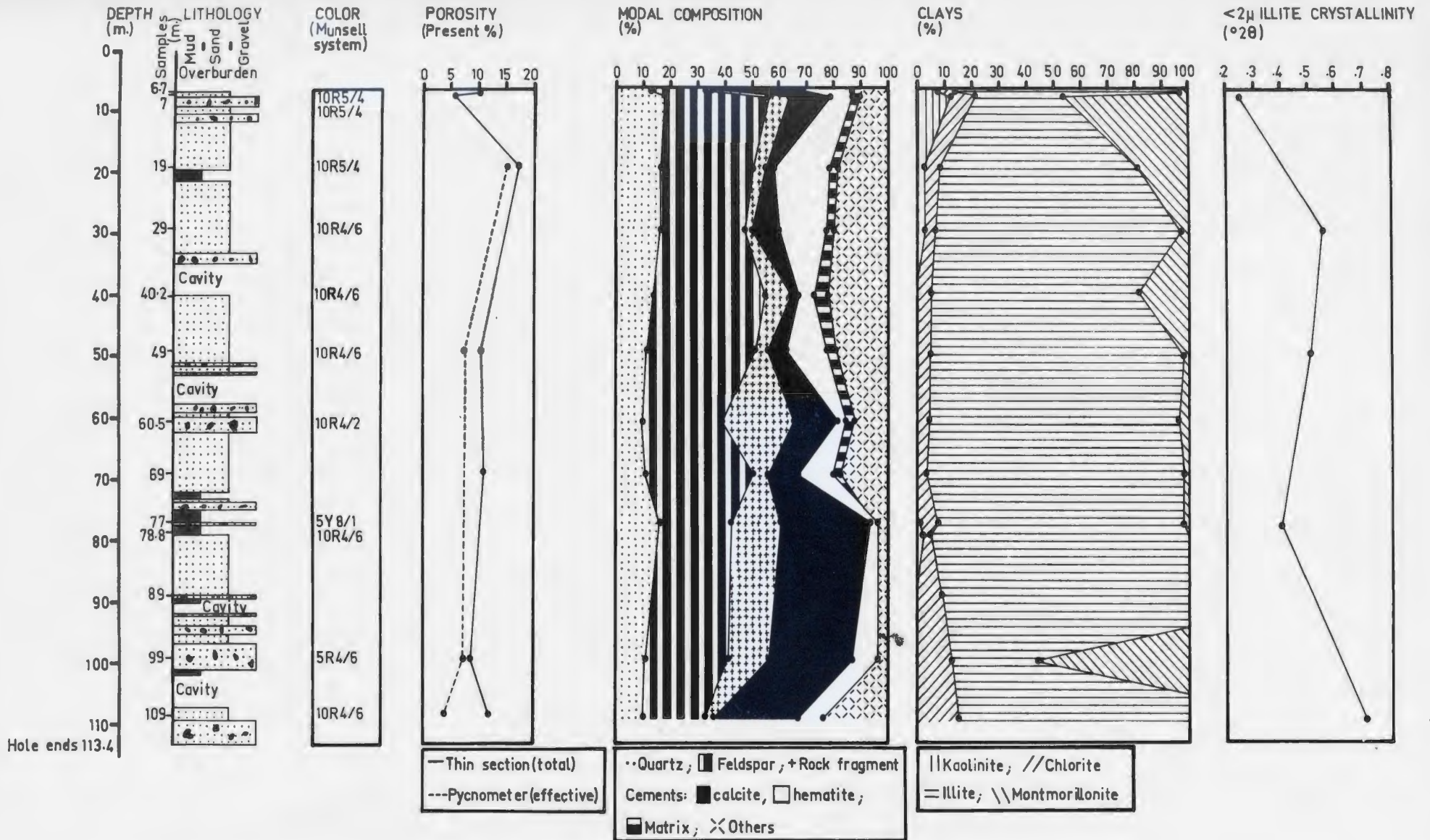
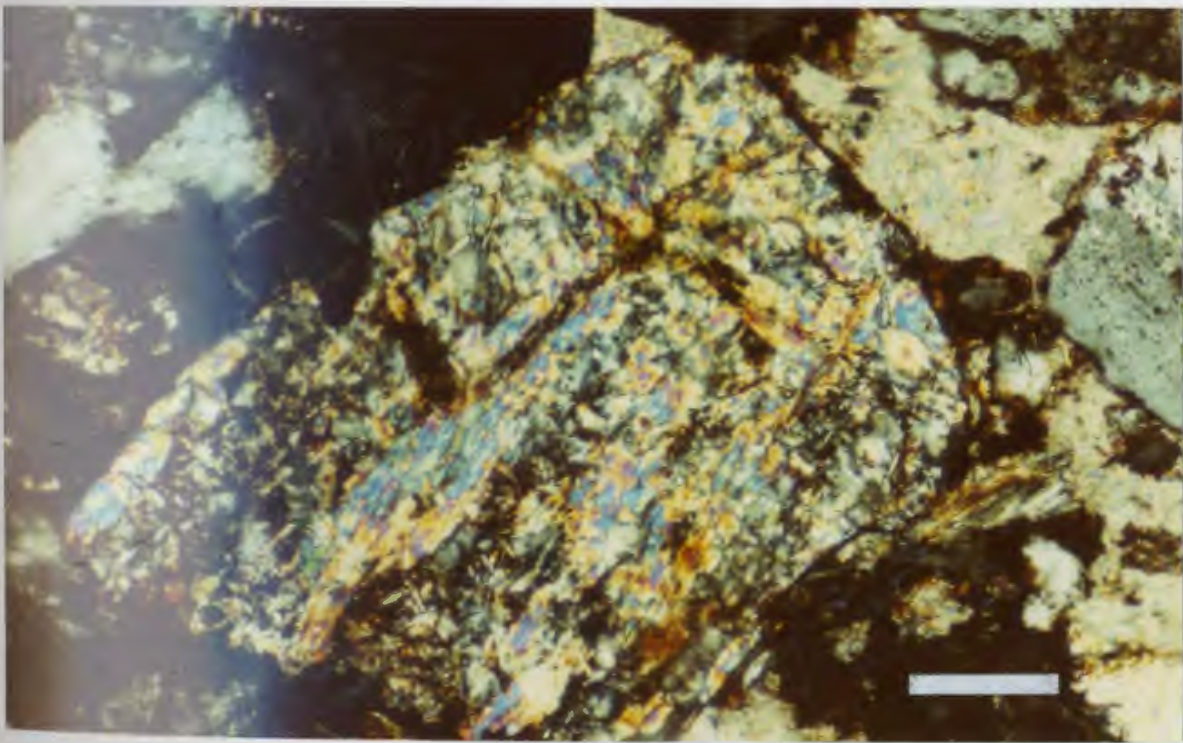


Figure 3.1 Stratigraphic and petrographic details for drill hole 79A-007.

Figure 3.2. Representative drill core from hole A7 (61.5-87.2 m). The transition from dark brownish-red to light gray follows a change in grain size from silt to conglomerate respectively.

Figure 3.3. Illitized feldspar grain partly masked by late-stage hematite cement. Bar scale 0.25 mm.



NORTH BROOK FM.

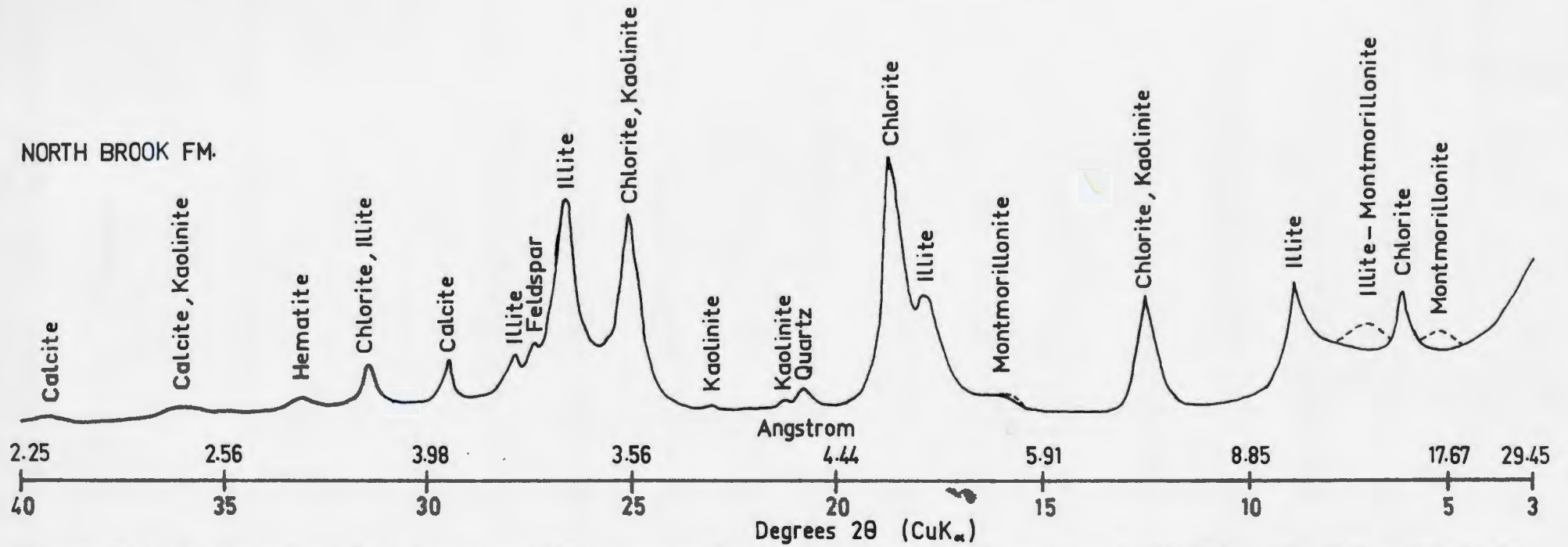


Figure 3.5 A composite clay-fraction diffractogram for the North Brook Formation drill holes 79A-007 and 79B-003 (dashed line is peak position after glycolation).

Detrital mica grains are mechanically bent around larger silicate grains, with biotite often being heavily oxidized and chloritized, particularly along cleavage planes. Monocrystalline and polycrystalline quartz grains exhibit both straight and undulose extinction. Quartz overgrowths are suggested by vague oxidized dust rims within quartz crystals.

The large amounts of illite (Figs. 3.1 and 3.5) are a combination of both clay-sized detrital mica grains and diagenetic illite. Recognition of diagenetic illite is based on the criteria of Wilson and Pittman (1977). The main criteria are (and this applies to diagenetic illite in the other drill holes as well): (1) the illite is seen at all stages of growth, partly replacing feldspars; (2) some crystals bridge grains near points of grain contact (Fig. 3.6); (3) detrital micas are generally larger and show signs of alteration (oxidation, chloritization, bending, and frayed or corroded grain edges). Illite crystallinity measurements (chapter five, section 5.3.4) also suggest the presence of detrital and diagenetic micas. The only mixed-layer clay mineral identified in the diffractograms for this drill hole is a mixed-layer illite-montmorillonite mineral. Diffractogram inspection indicates that illite-montmorillonite is only present in a few of the sandstone samples. Very few grains of detrital chlorite were observed in thin section.

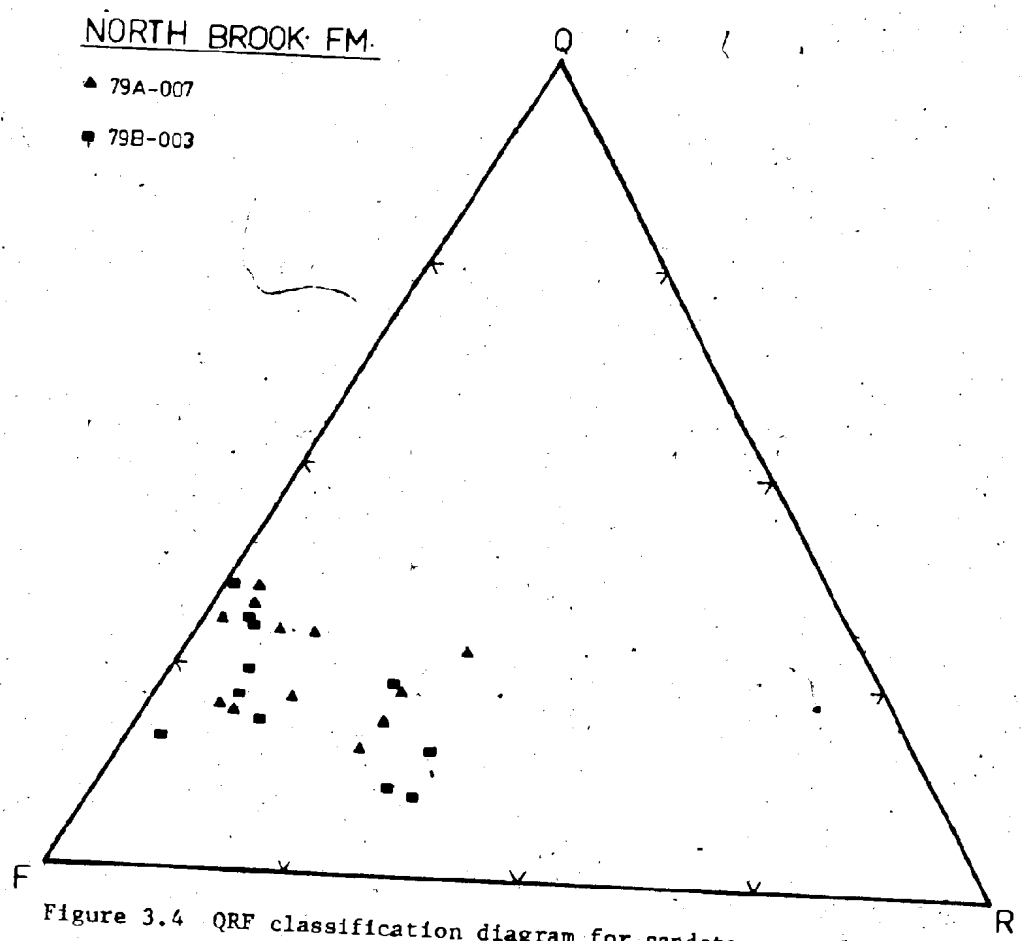
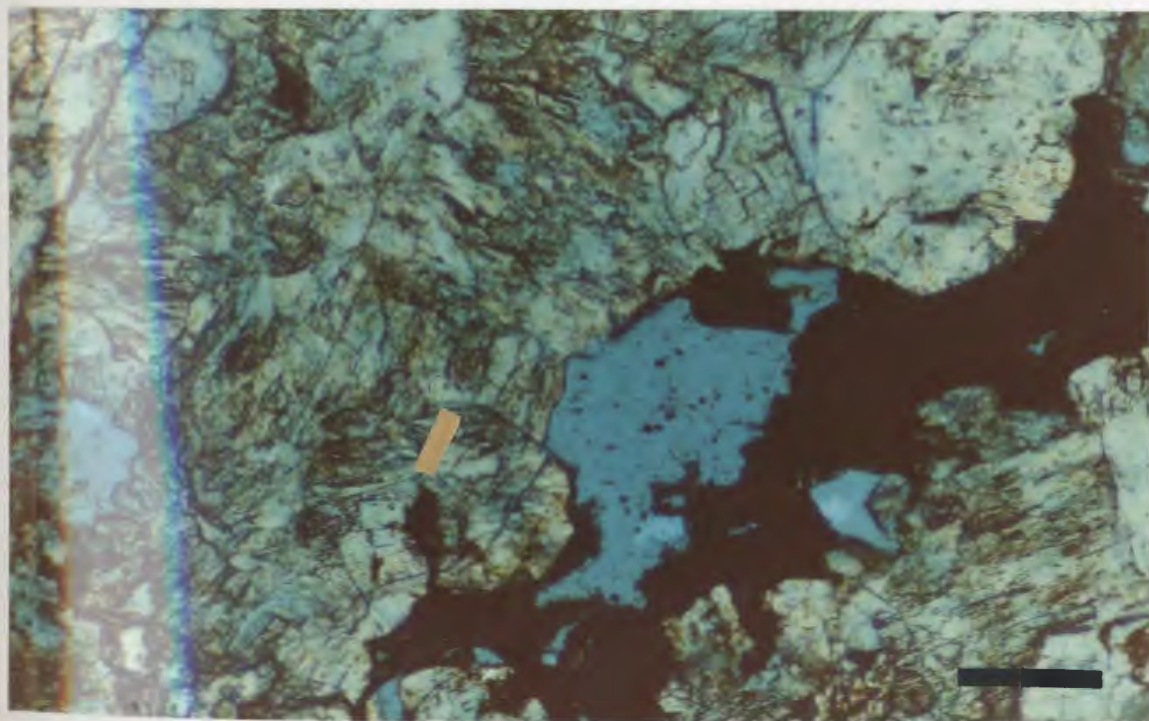
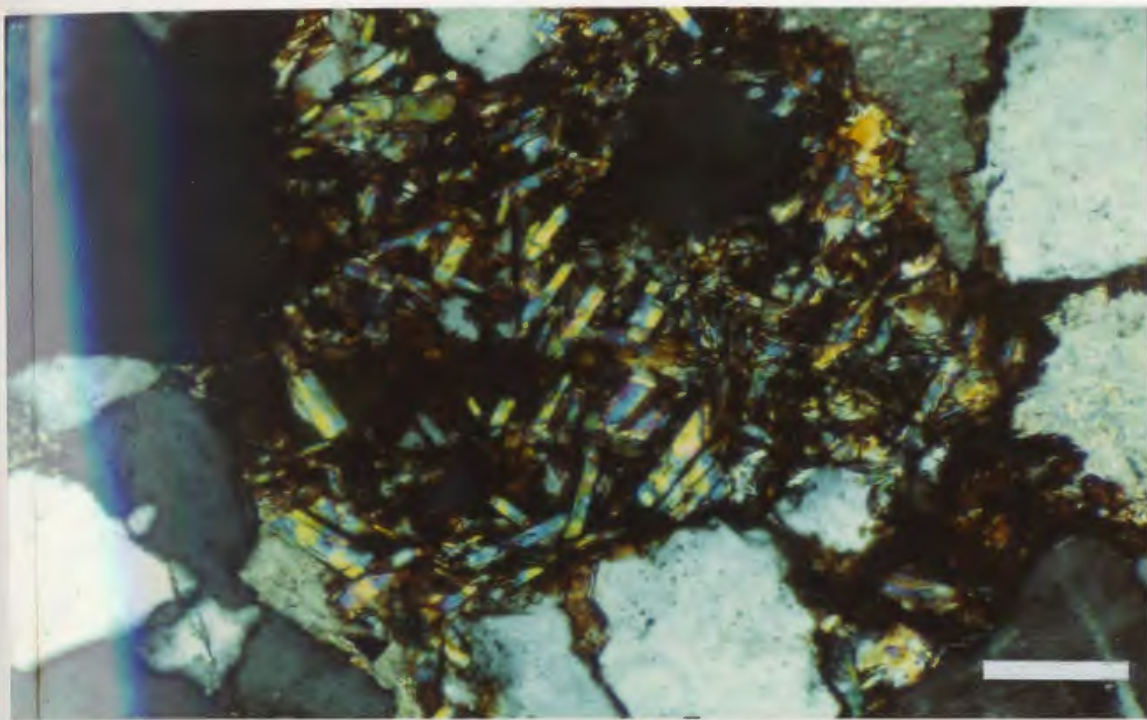


Figure 3.4 QRF classification diagram for sandstone samples from the North Brook Formation drill holes 79A-007 and 79B-003.

Figure 3.6. Laths of diagenetic illite have grown across detrital grain boundaries prior to a late stage of hematite cementation. Bar scale 0.25 mm.

Figure 3.7. Late-stage hematite cement (opaque) corrodes and impregnates detrital grains and partly fills pore space (blue). Bar scale 0.25 mm.



Calcite cement partly masks earlier matrix material and appears to change from coarser to finely crystalline cement with a decrease in detrital grain size. Late-stage hematite cement penetrates, and rims all previously deposited or developed minerals and pore space, including the calcite cement (Figs. 3.6 and 3.7). Minor limonite is also developed on opaque minerals.

The total porosity ranges from 5-7 %, with most of it being effective porosity (Fig. 3.1). Dissolution has created enlarged intergranular and intragranular secondary porosity. No strong correlations can be made between porosity, lithology and mineralogy. However, in the upper 20 m of the drill hole, total porosity varies inversely with the relative amount of kaolinite.

3.2.3 Drill hole 79B-003 (B3)

Stratigraphy

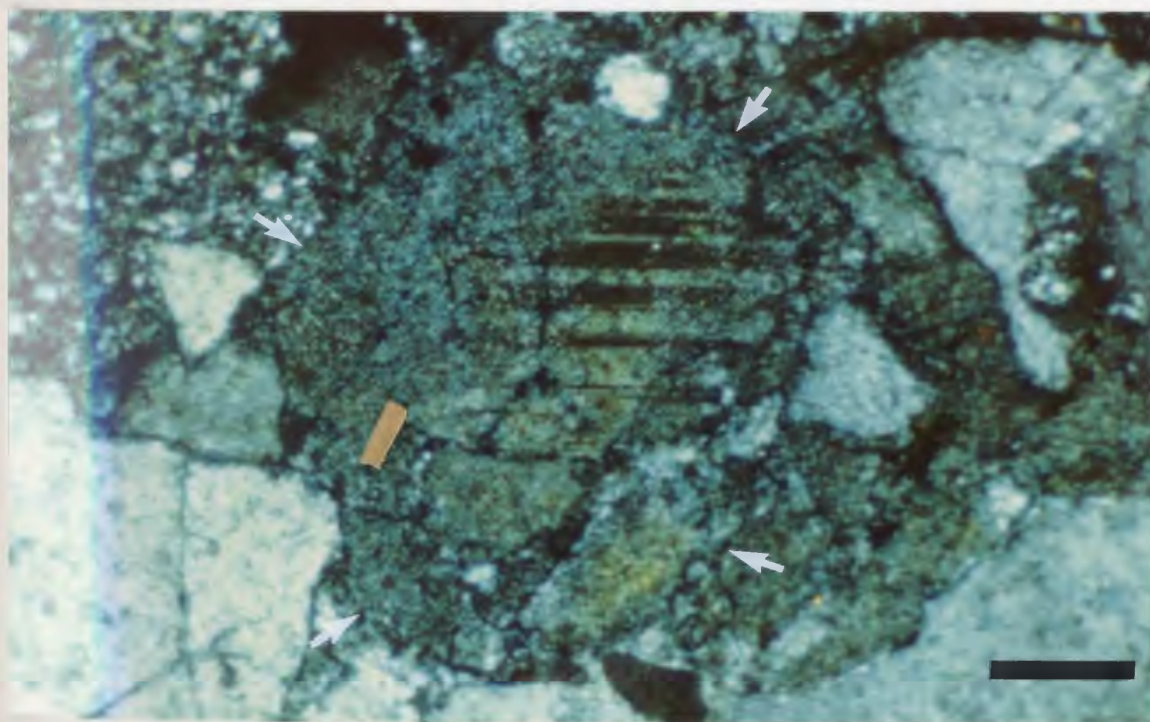
With the exception of the top and bottom 40 m, which are dominated by sandstones, this drill hole is comprised of subequal amounts of interlayered gray to pale red conglomerates, and light gray to brownish-red sandstones, with minor thin layers of brownish-red siltstone and mudstone (Figs. 3.8 and 3.9).

The conglomerate contains poorly to well sorted, subrounded, granitic, felsic volcanic, schistose carbonate, quartz, and chert pebbles, within an arkosic sandstone matrix. The submature to mature, very coarse to fine grained sandstones are arkosic in composition (Fig. 3.4), and contain variable amounts of hematite and carbonate cements (as does the conglomerate matrix). Redox fronts sometimes follow cross-bed foresets developed in the sandstones. The sandstone units are usually in gradational contact with the finer and coarser grained sediments. Siltstones and mudstones are usually poorly indurated, less calcareous and micaceous, and contain a few mud chips and calcareous nodules.

Petrography

Figure 3.9. Representative drill core from hole B3 (76.5-94.1 m). Note the friable nature of the brownish-red siltstones and mudstones and the unoxidized gray spots in the coherent sandstones.

Figure 3.10. Partial dissolution of a plagioclase grain. Arrows indicate original grain boundaries. Blue epoxy fills voids. Bar scale 0.25 mm.



Drill hole B3 has identical detrital and diagenetic mineral assemblages to drill hole A7 (Fig. 3.8 and Appendix I). Relative mineral abundances, their interrelationships, and the textural maturity of the sandstones are very similar to A7 as well, except that B3 is generally less oxidized and micaceous, and contains more kaolinite and mixed-layer illite-montmorillonite.

Detrital quartz and feldspar are again corroded. Microcline and plagioclase in particular have undergone extensive dissolution, facilitating the development of secondary intragranular porosity (Figs. 3.10). Plagioclase was locally partly replaced by calcite rhombs (Fig. 3.11). Euhedral quartz overgrowths on detrital silicate grains (commonly quartz) are visible outside oxidized dust rims, and appear in SEM photographs to predate montmorillonite and calcite (Fig. 3.12). Intergranular kaolinite booklets clearly display a vermiform morphology (Fig. 3.13).

All the corrosive calcite cements appeared coarsely crystalline and twinned (Fig. 3.14). Cathodoluminescence reveals the presence of two zoned generations of calcite cementation (Figs. 3.15 and 3.16). The calcite cements display a dark brown and a bright reddish-orange fluorescence colour. The darker colour is developed in the coarsely crystalline poikilotopic cement, which is typically located in the centre of the interstitial space. The more brightly coloured calcite cement is locally zoned and occurs around the margins of the coarsely crystalline calcite and in

Figure 3.11. Calcite rhombs (arrows) have grown into small, interconnected dissolution pores (blue) within a plagioclase grain. Bar scale 0.05 mm.

Figure 3.12. SEM photo of quartz overgrowths (Q) which appear to predate 'cornflake' montmorillonite (M) (c.f., Sachdev, 1980, p.165). Bar scale 10 μ .

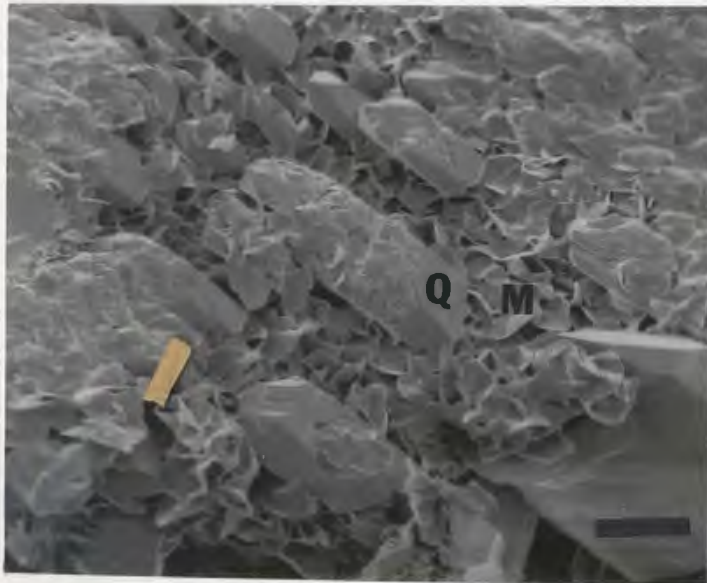
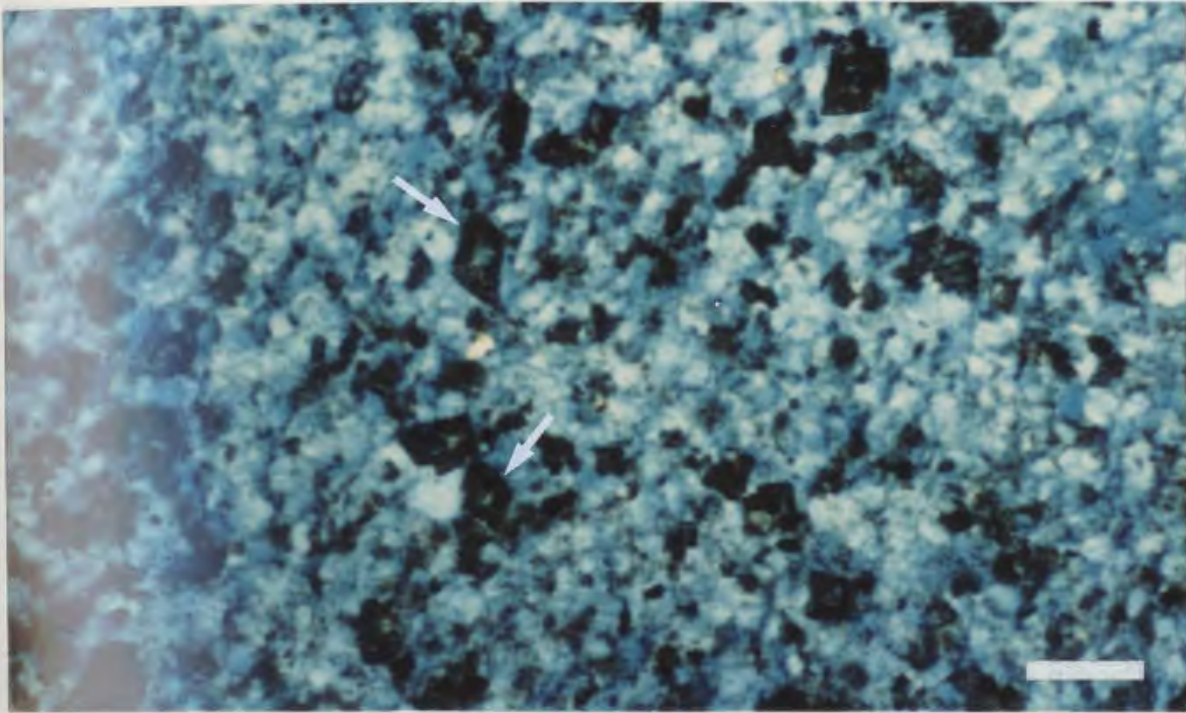


Figure 3.13. SEM photo of tightly bunched interstitial vermicular kaolinite (c.f. Keller, 1978, p.7). Bar scale 10 μ .

Figure 3.14. Twinned calcite cement (Cc) has partly corroded detrital grains (G). Bar scale 0.25 mm.

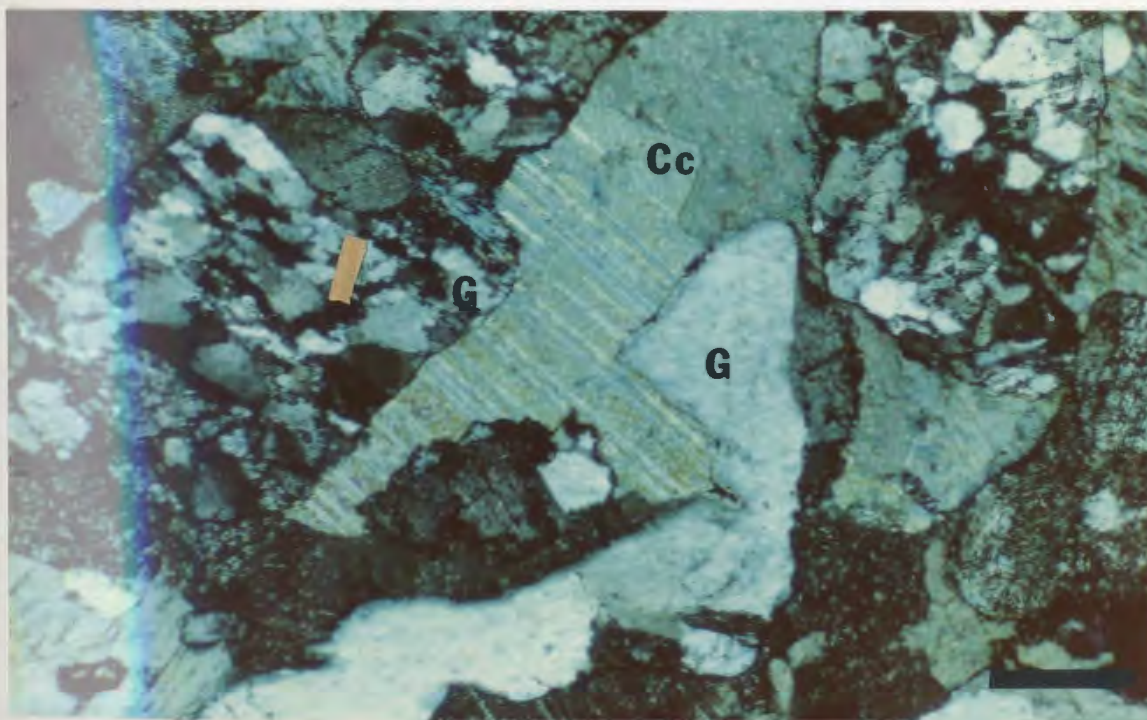
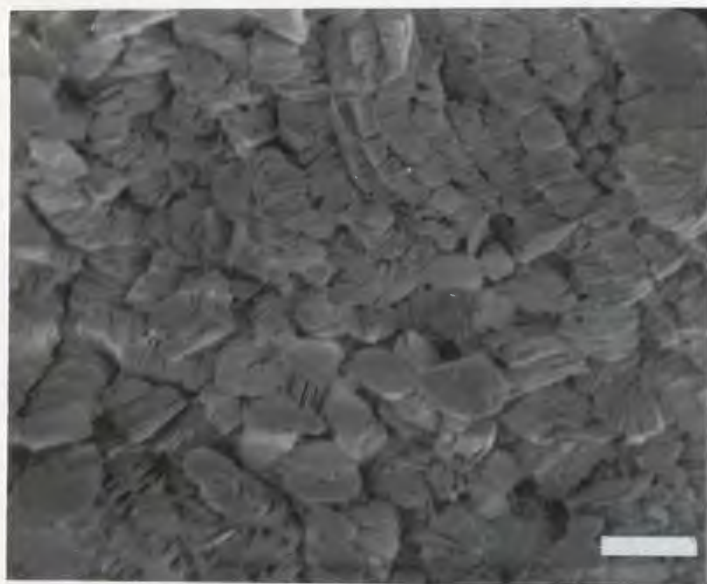
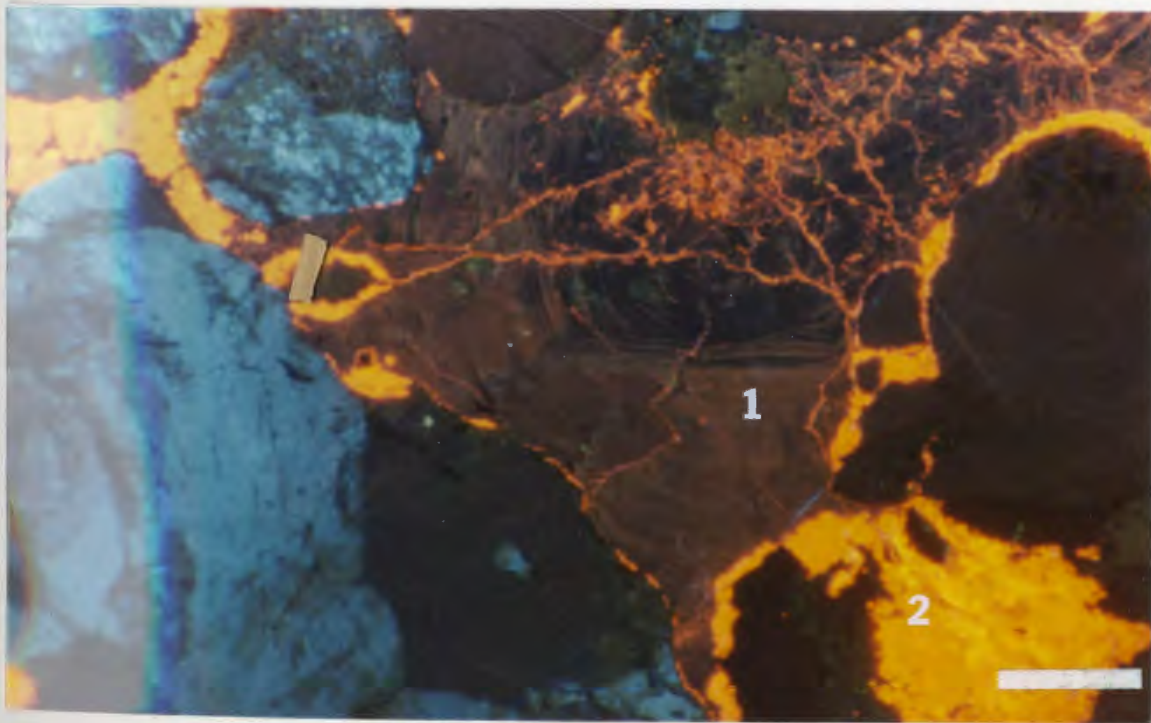
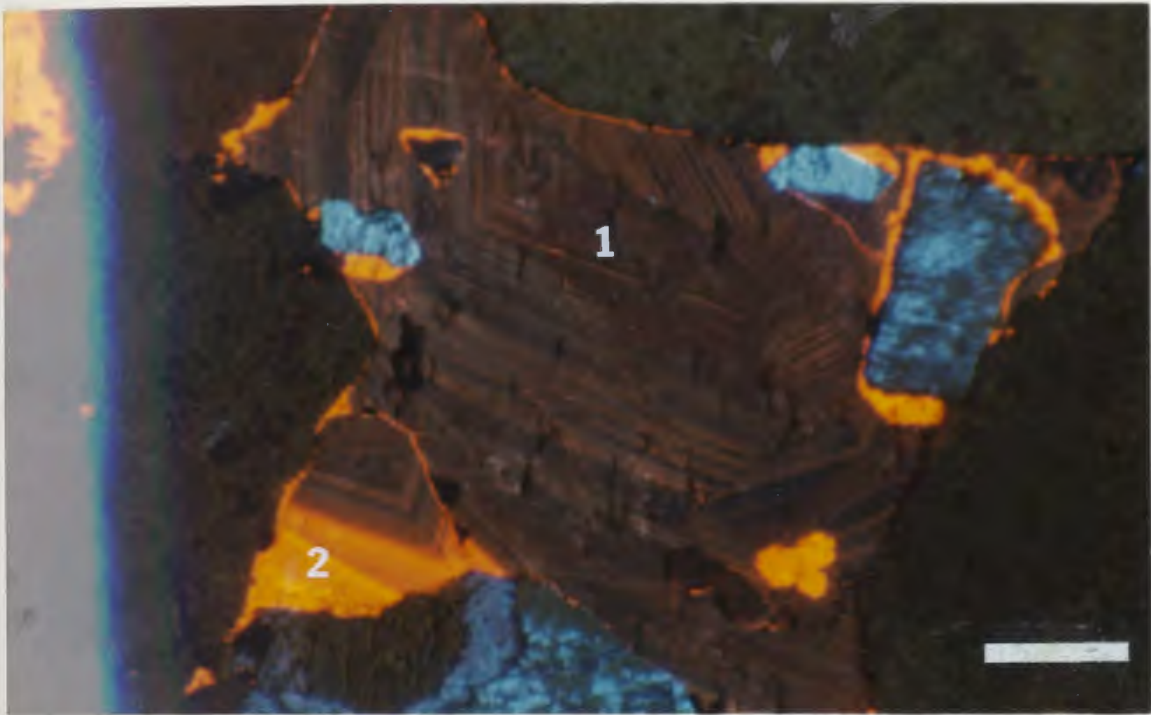


Figure 3.15. First (1) and second (2) generation zoned calcite cement revealed by cathodoluminescence. Bar scale 0.25 mm.

Figure 3.16. Cathodoluminescence reveals dark brown calcite (1) cut by microfractures containing a second generation of reddish-orange calcite (2). Bar scale 0.25 mm.



microfractures developed within the coarser calcite. Both phases of calcite are twinned. The sharp contrast in fluorescence colour, and the revelation of calcite-filled microfractures within the coarsely crystalline calcite, suggest that there were two consecutive stages of calcite cementation, an iron-rich stage (dark brown) followed by an iron-poor stage (reddish-orange). The most reasonable tentative explanation for the colour difference is the quenching of activator ions (usually divalent manganese) by trivalent iron in the darker, coarsely crystalline calcite (Sippel and Glover, 1965). Hematite cement cuts into and rims both detrital grains and calcite cement, and heavily oxidizes any ferro-silicate minerals.

Total porosity occupies 9-19 % of the total rock volume; where measured, most of the porosity again appears to be effective (Fig. 3.8). Much of the porosity appears to be due to extensive feldspar dissolution prior to carbonate cementation.

3.3 Rocky Brook Formation

3.3.1 Introduction

The two representative Rocky Brook Formation drill holes, 79A-003 (abbr. A3) and 79A-005 (abbr. A5), were chosen primarily because they were the least weathered and because they sampled the Spillway Member (A3) and the Squires Park Member (A5) of the Rocky Brook Formation. A3 also penetrates red siltstones from the upper part of the North

Brook Formation. Figure 2.3 (p. 17) shows the location of these drill holes along the relatively undisturbed west side of the Deer Lake subbasin. Apart from the plethora of allochemical carbonate rocks (Hyde, 1979b; Hyde and Ware, 1980, 1981), all important Rocky Brook Formation lithologies were sampled.

Due to the fine grained nature of these sediments, their modal composition, ternary classification plot, and point count results (Appendix I) use clay, silt, and carbonate as the main components. Furthermore, due to the lack of sand-size grains and the abundance of carbonates in the Rocky Brook Formation, carbonate is substituted for sand in Picard's (1971) classification for fine grained sediments (Fig. 3.18), and Folk's (1962) classification for carbonate rocks is adopted when there is a dominant carbonate component.

3.3.2 Drill hole 79A-Q03 (A3)

Stratigraphy

The majority of the A3 drill core (Fig. 3.17) is comprised of interlayered and laminated gray, green, and brown mudstones and claystones, and various micritic carbonate rocks from the lower Spillway Member. Those examined in thin section and plotted in Figure 3.18 were classified as calcareous claystones, clayey and silty mudstones, and an intramicrudite. White, and less commonly

ROCKY BROOK FM. 79A-003

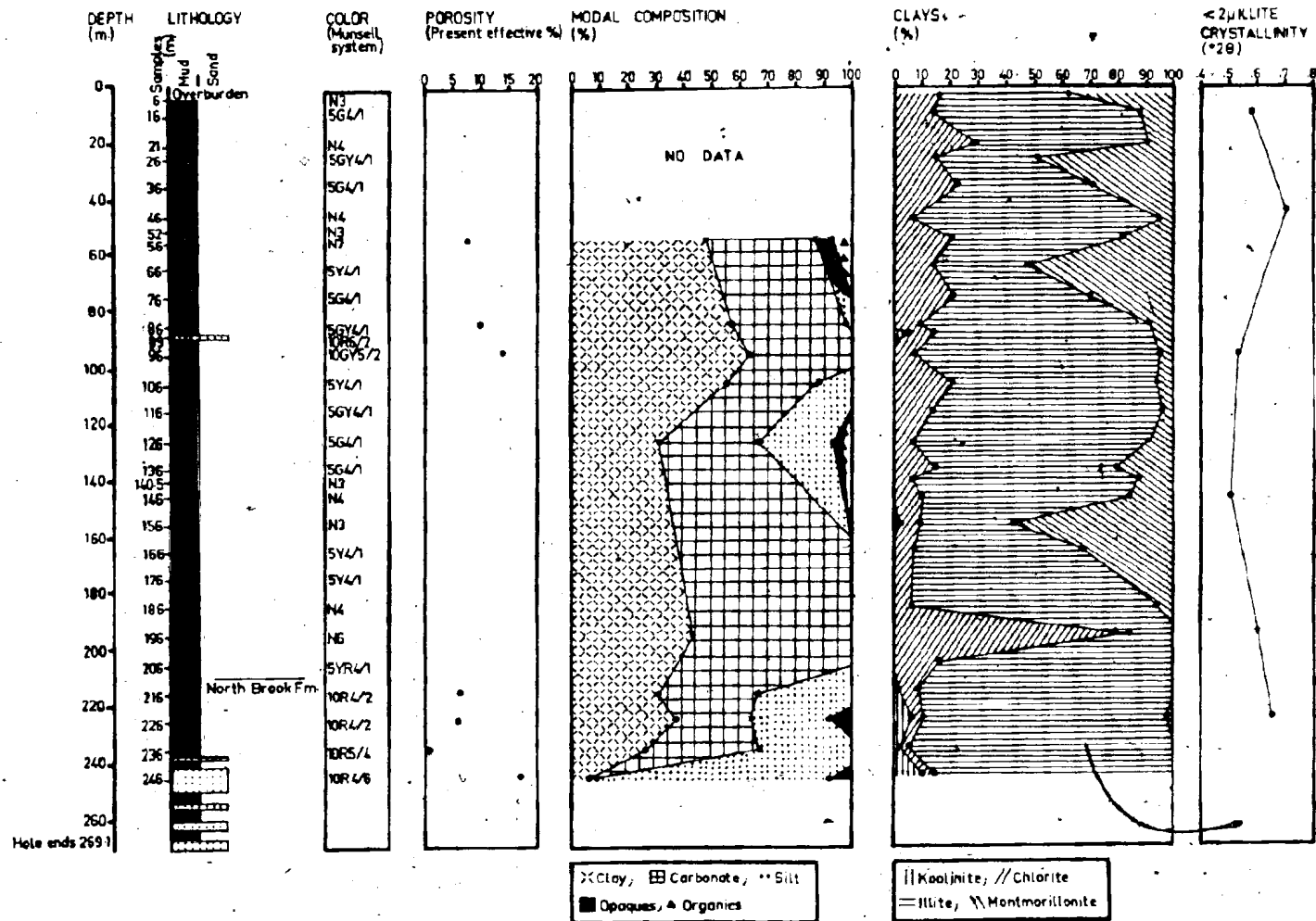


Figure 3.17 Stratigraphic and petrographic details for drill hole 79A-003.

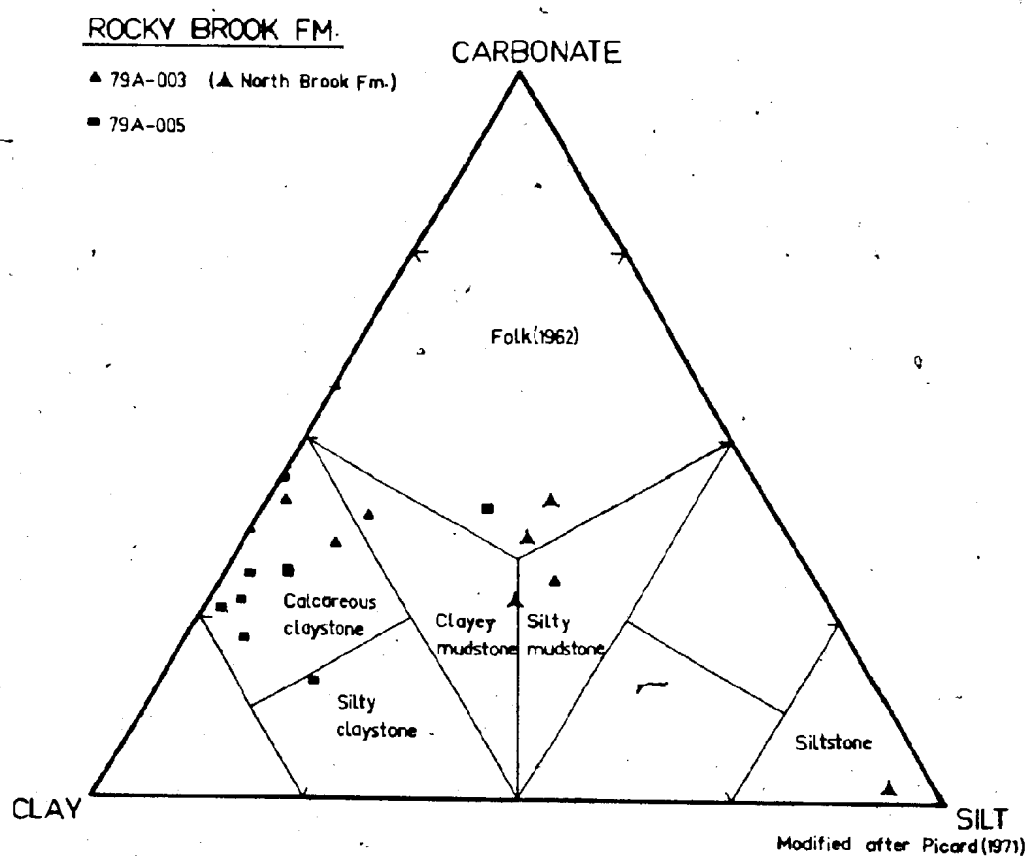
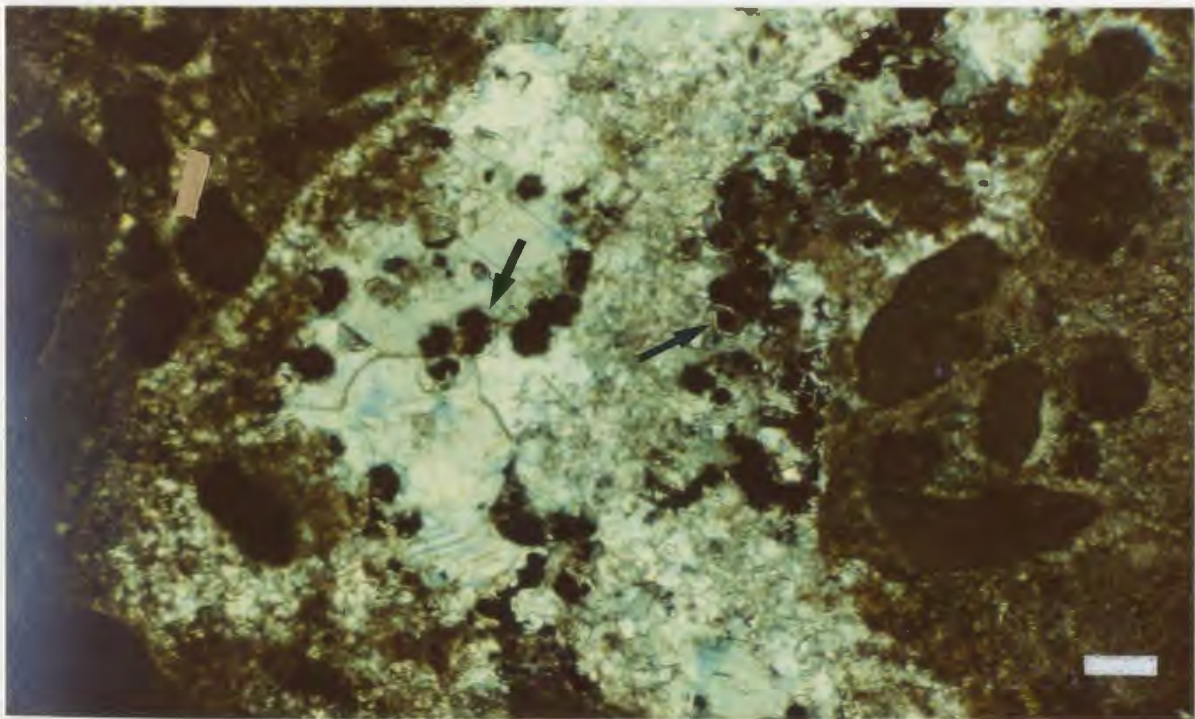


Figure 3.18 Carbonate-silt-clay classification diagram for the fine grained sediment samples from the Rocky Brook Formation drill holes 79A-003 and 79A-005.

Figure 3.19. Representative drill core from hole A3 (48.7-73.1 m). Note the fissility of the interlayered mudstones, claystones, and carbonates.

Figure 3.20. Late-stage coarsely crystalline calcite cement within an intramicrudite. Note the small "analcime" crystals (arrows) and the corrosion of some of the crystals by calcite. Bar scale 0.25 mm.



purple, calcite stockwork is found throughout the A3 drill core, as are calcareous nodules and rhizoliths. Figure 3.19 shows a representative drill core section of the shaly, varicoloured lacustrine sediments from drill hole A3.

Toward the bottom of the hole, there is a gradational contact between reddish-brown mudstones of the Rocky Brook Formation and red and brown siltstones of the North Brook Formation. Company drill core logs show the contact between the two formations was placed at the top of the sandstone bed seen in Figure 3.17. On the suggestion of Dr. R. Hyde (pers. comm. 1983), the conformable contact has been placed higher up in the drill hole at the top of a red and brown silty sequence.

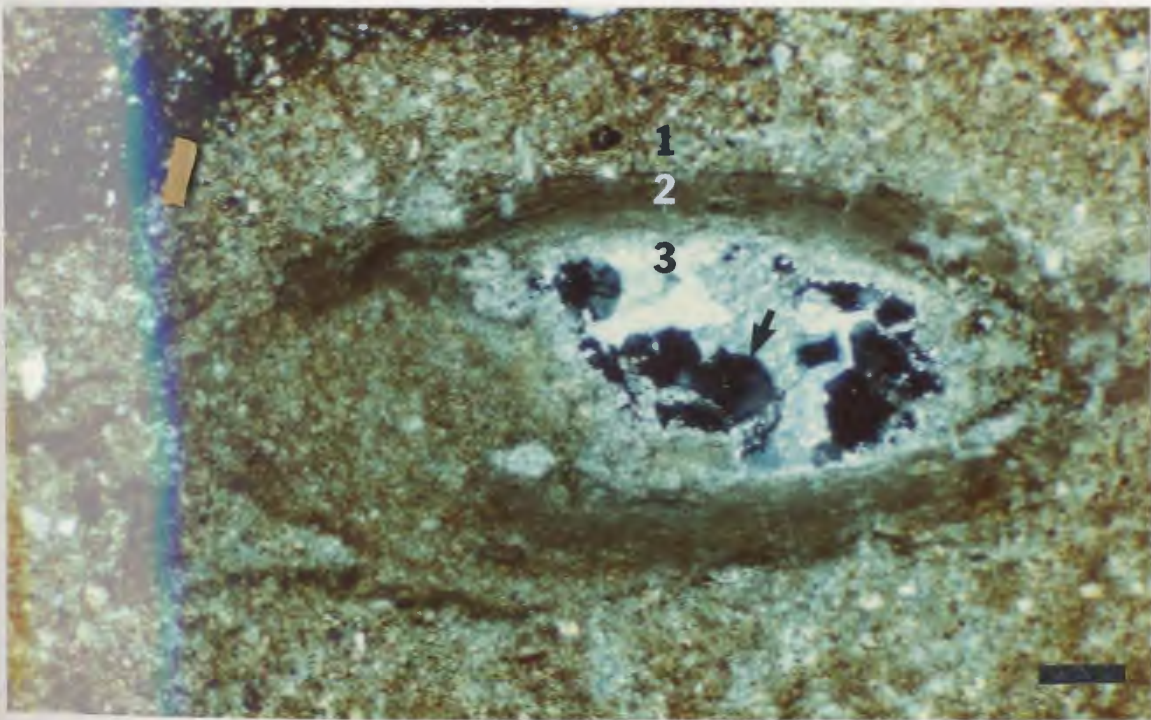
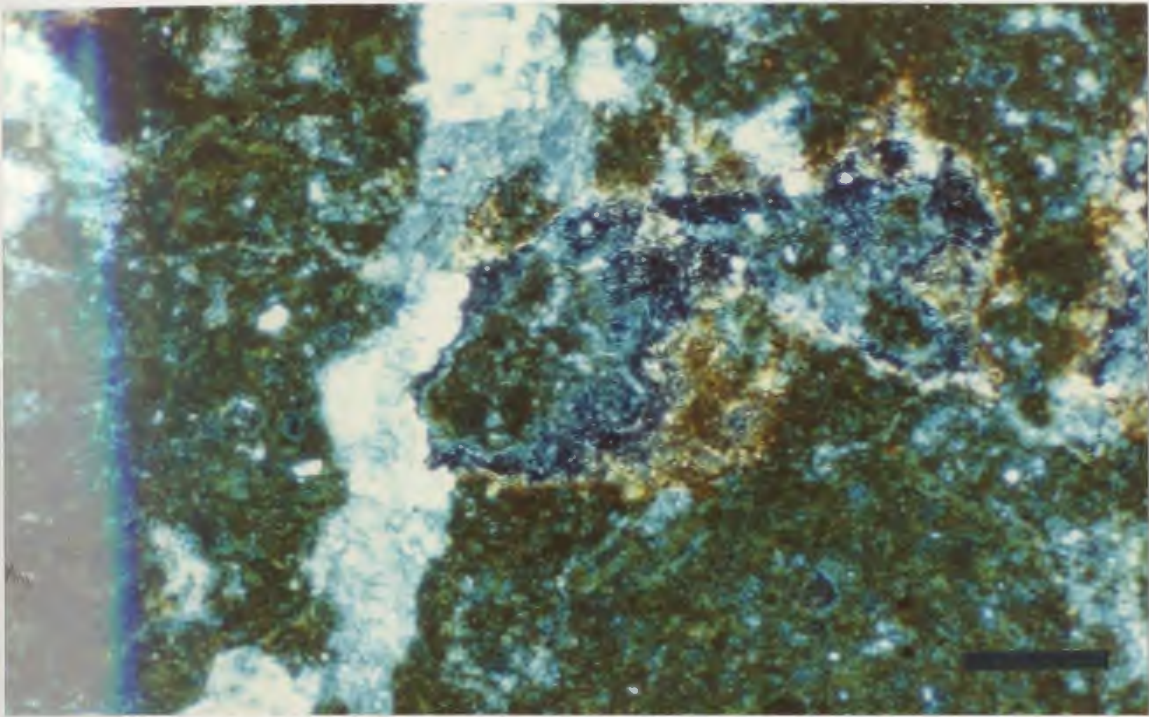
Gamma-ray drill-hole logging by Westfield Minerals revealed thin anomalous uraniferous horizons in dark mudstones and carbonates (see chapter four section 4.2.2).

Petrography

Thin section inspection (Fig. 3.17 and Appendix I) and X-ray diffractometry (Fig. 3.23) reveal that the two main groups of minerals in the core samples are carbonates and clays. The rest of the samples contain variable amounts of silt size clasts, "analcime", pyrite and organic material. These components are usually homogeneously distributed, but silt- and carbonate-rich patches, or contorted laminae, are also present.

Figure 3.21. A microfracture filled with late coarse calcite is cross-cut by later 'open' microfracture porosity. Note the oxidized margins of the 'open' microfracture. Bar scale 0.25 mm.

Figure 3.22. Cross-section of a rhizolith showing three concentric zones (numbered): (1) outer hematized silty calcite envelope; (2) clay- and organic-rich ring; (3) inner coarsely crystalline calcite-"analcime" (arrow) core. Bar scale 0.5 mm.



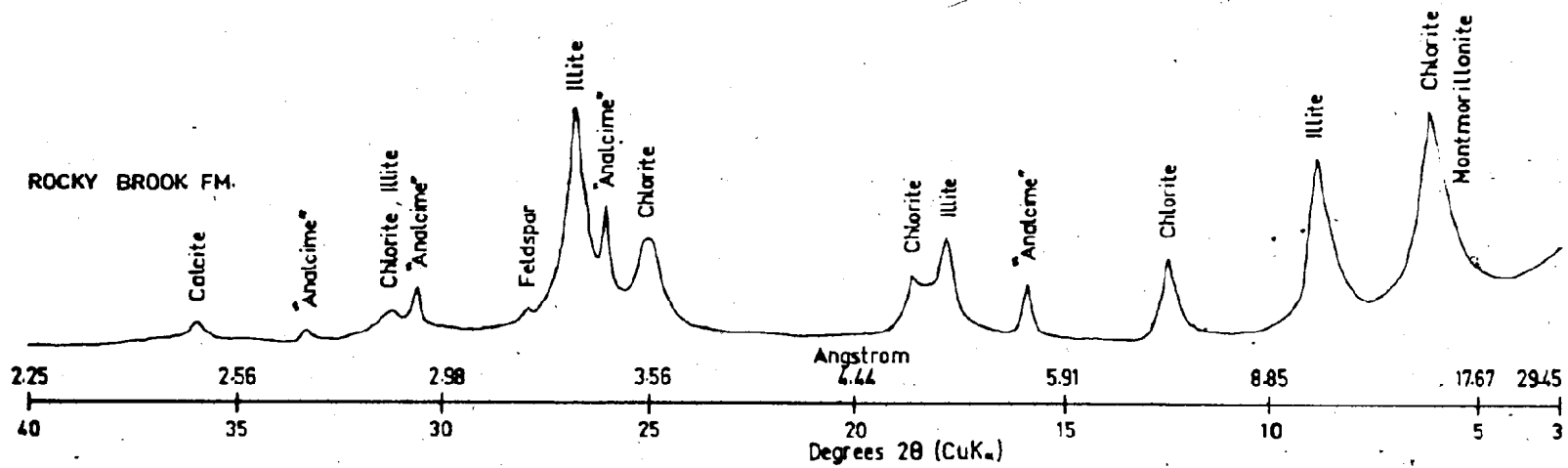


Figure 3.23 A composite clay-fraction diffractogram for the Rocky Brook Formation drill holes 79A-003 and 79A-005 (dashed line is peak position after glycolation).

Fine to medium crystalline calcite and dolomite are the two carbonate minerals. In places, dolomite crystals appear slightly larger than the crystalline calcite. No dissolution or replacement features were apparent between the two. A later stage of calcite precipitation is also present as medium to coarsely crystalline irregular patches and microfracture fillings (Figs. 3.20 and 3.21). The euhedral crystal form, 'clear' nature of the patches of calcite crystals, their connection to calcite-filled microfractures, and an occasional decrease in crystal size away from the centre of the patches suggest that the medium to coarsely crystalline patches of calcite are solution-cavity fillings (Folk, 1965) rather than being neomorphic in origin. Cathodoluminescence did not reveal any zoning of the calcite. In places, the calcite-filled microfractures are cross-cut by 'open' microfractures with hematized margins (Fig. 3.21).

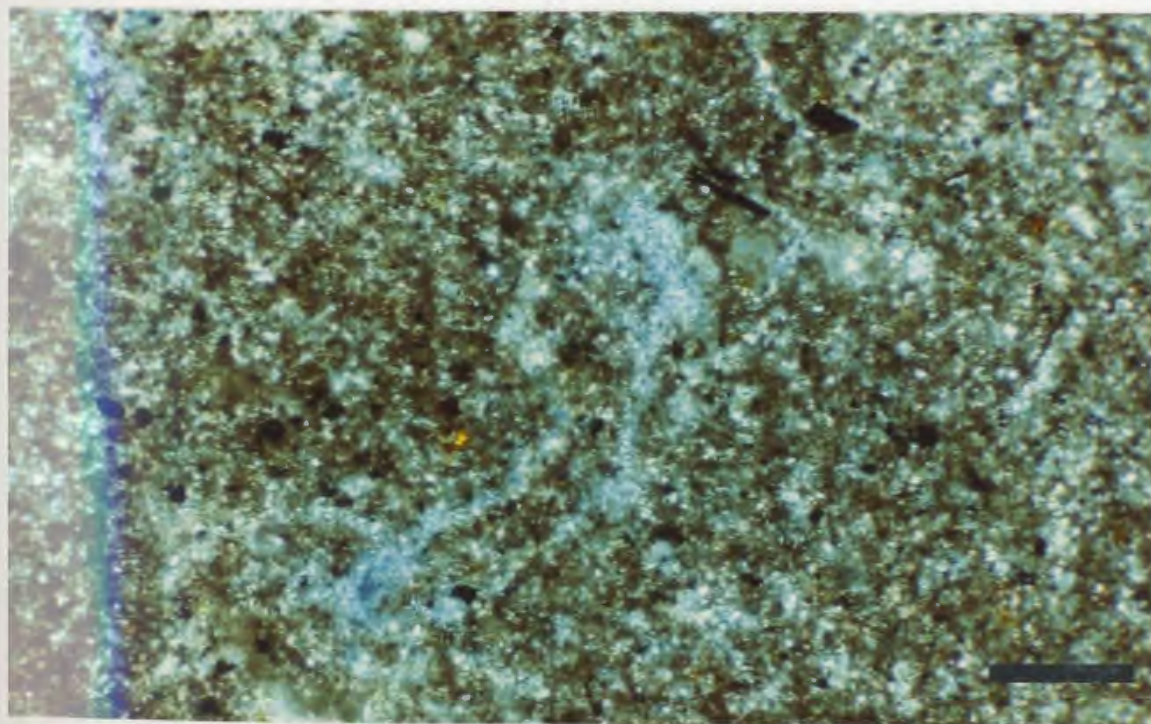
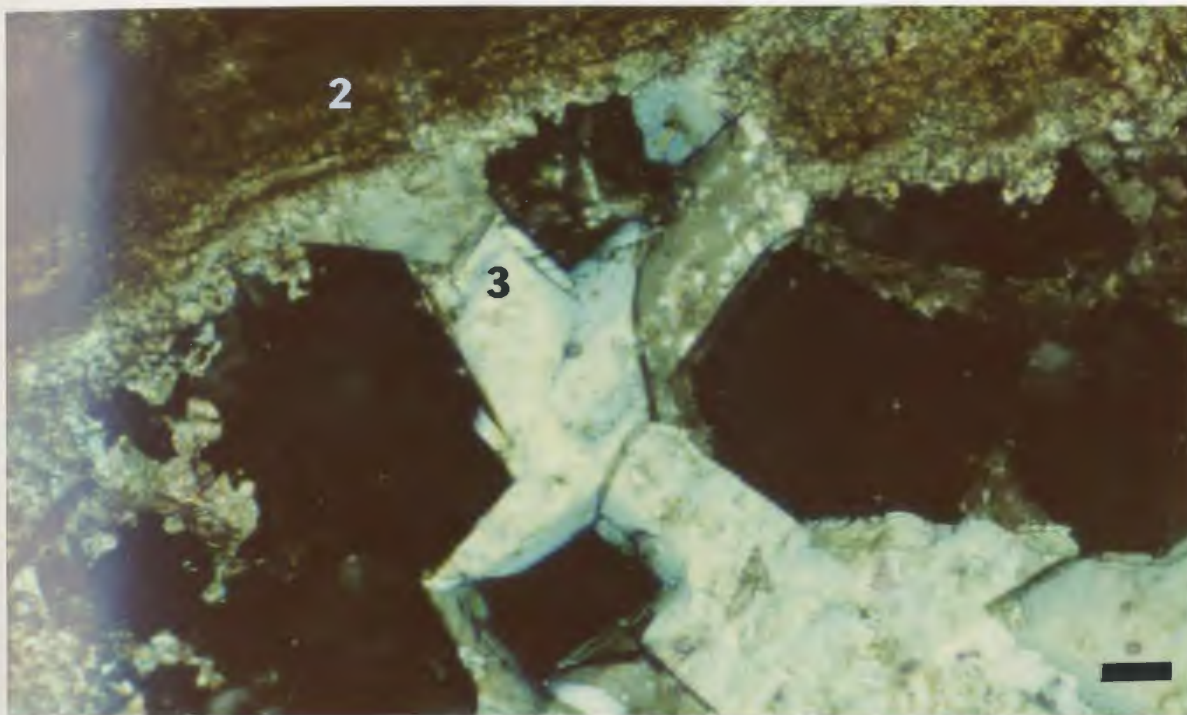
Clay minerals occur in three settings: (1) as clay-rich laminae; (2) as diffuse, connected and unconnected clots; and (3) as intraclasts and peloids. Figures 3.17 and 3.23 show that illite, chlorite, and montmorillonite are the major clay minerals, and that kaolinite is absent, or only present within the coarser North Brook Formation sediments. The visual identification of detrital mica and the presence of clay-rich intraclasts and peloids, suggests that some of the clay-size minerals are detrital.

The silt component is made up of quartz, plagioclase, orthoclase, microcline and muscovite grains. The silt grains are usually rounded to subrounded, and are heavily rimmed by hematite cement. This is particularly so in the calcareous siltstones at the top of the North Brook Formation. Silt-size dark brown to opaque organic material occurs as dispersed rod-shaped or equant grains. Diagenetic pyrite occurs as both euhedral crystals and small crystal aggregates.

"Analcime" was identified in thin section and by X-ray diffraction (Fig. 3.23), by characteristic peak positions and by its absence in the acid-treated clay samples. Microscopic examination found the "analcime" developed in the coarsely crystalline cores of rhizoliths, and in the medium to coarsely crystalline patches of calcite. In both cases, the crystals are hexagonal and weakly anisotropic. The crystals typically occur singly; they are engulfed in, and locally corroded by, the calcite, or form border phases both in the rhizolith cores (Figs. 3.22 and 3.24) and in the coarsely crystalline patches. In both situations the "analcime" has retained most of its euhedral nature. These relationships suggest formation before the coarsely crystalline calcite. The crystals are referred to as "analcime" as they produce X-ray diffraction peaks very similar to analcime (Fig. 3.23) which characteristically disappear from diffractograms upon acid treatment (Brindley and Brown, 1980). The petrographic properties of these

Figure 3.24. Zones 2 and 3 (numbered) of the same rhizolith cross-section. Bar scale 0.25 mm.

Figure 3.25. Late mesovug porosity (blue) developed in a calcareous claystone. Opaques are both organic matter and authigenic pyrite. Bar scale 0.25 mm.



7

crystals are also very similar to analcime (Deer et al., 1966; Dr. S. Papezik, pers. comm. 1983; Dr. R. Hay, pers. comm. 1984). Microprobe analyses of a few "analcime" crystals are tabulated in Appendix II. The analyses are anomalous (but consistent), in that they display a composition between analcime and albite. Unfortunately no mineral has been found which satisfies the X-ray, petrographic and microprobe results, therefore the mineral is referred to as "analcime".

In thin section the rhizoliths display partial replacement of, and cementation within, what appears to be a cross-section through a plant root. They look very similar to the rhizoliths defined and described by Klappa (1980). A complete cross-section of one of the Rocky Brook Formation rhizoliths shows three main, crudely concentric zones (Figs. 3.22 and 3.24): (1) an outer envelope of hematized, micrite-cemented silt grains; (2) an organic-rich ring, in places very finely laminated, that may represent the original epithelial root walls; and (3) an inner core of coarsely crystalline "analcime" and calcite. "Analcime" and the micritic zone 1 calcite appear to have crystallized before the coarsely crystalline zone 3 calcite. The core minerals have irregular outer crystal boundaries and long euhedral interior boundaries.

A claystone sample from drill hole A3 contains a rhizolith, approximately 3 cm in diameter, exhibiting concentric calcite laminae around a coarser core. Adjacent claystone laminae draped over the rhizolith. This is similar to the type 1 concretions of Raiswell (1971), which suggest an early pre-lithification growth of the rhizoliths. The outer calcite-rich envelope may develop due to the release of HCO_3^- ions or organic acids from living or decaying organic matter, the combination of the HCO_3^- ions with calcium, and the subsequent precipitation of calcite (Johnson, 1967; Gray and Williams, 1971). Theoretically, further decay of internal organic material could increase the alkalinity of the microenvironment (Klappa, 1980), thus possibly encouraging the precipitation of "analcime" in the core zone.

Three types of porosity can be identified in these sediments: microintercrystal and mesovug porosity (Fig. 3.25) (Choquette and Pray, 1970), and microfracture porosity (Fig. 3.21). Figure 3.17 indicates an increase in effective porosity in the silt- and sand-rich lithologies. The total porosity measurements that could be made were not recorded, as they often showed values below the effective porosity measurements, and therefore were not considered reliable. One reason for this may be the inability to easily detect microporosity in thin section.

3.3.3 Drill hole 79A-005 (A5)

Stratigraphy

Drill hole A5 sampled only the upper Squires Park Member of the Rocky Brook Formation. The lithologies are uniformly fine grained, with a paucity of sand-size material (Fig. 3.26). Weathering and the fissility of the fine grained sediments, made it impossible to study some sections of the drill core in detail. Drill core inspection and thin-section point counting (Fig. 3.18 and Appendix I), showed that the main lithologies are interlayered, massive to laminated, calcareous to silty claystones and micritic limestones. The sediments range from dark gray, to dark greenish- and brownish-gray in colour; unlike drill hole A3, there is a definite lack of red strata (Fig. 3.27).

Mottled, subrounded nodules and rhizoliths, and pyrite crystals can easily be seen in hand sample. Calcite stockwork is also developed but not to the extent seen in drill hole A3. A few dark shaly samples produced a slight oily odour when rubbed, and also gave a brown streak. These features are characteristic of oil shale samples found in outcrop (Dr. R. Hyde, pers. comm. 1982). Company gamma ray logs and sludge assays indicate slight uranium anomalies from dark calcareous claystones and mudstones.

Petrography

ROCKY BROOK FM 79A-005

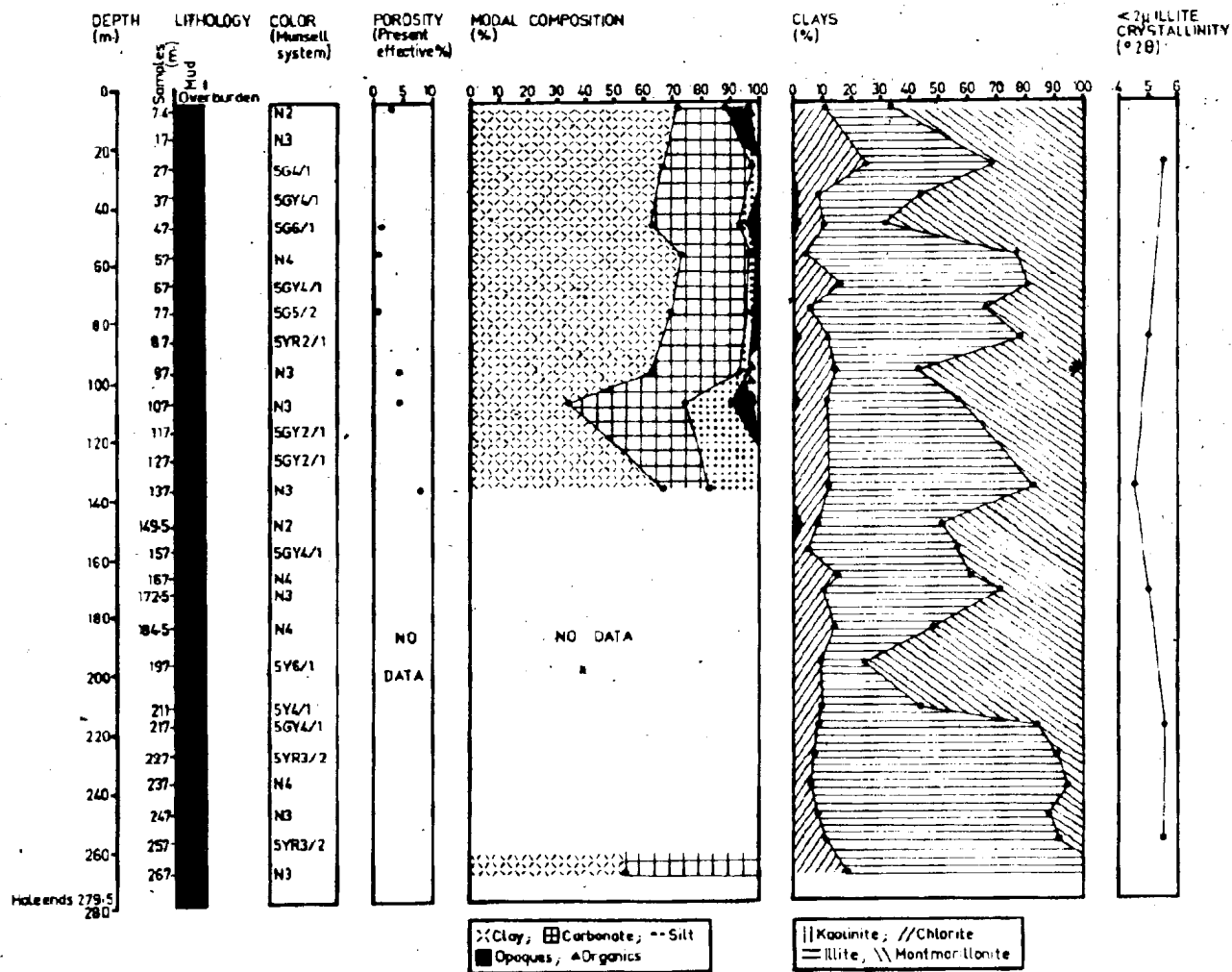
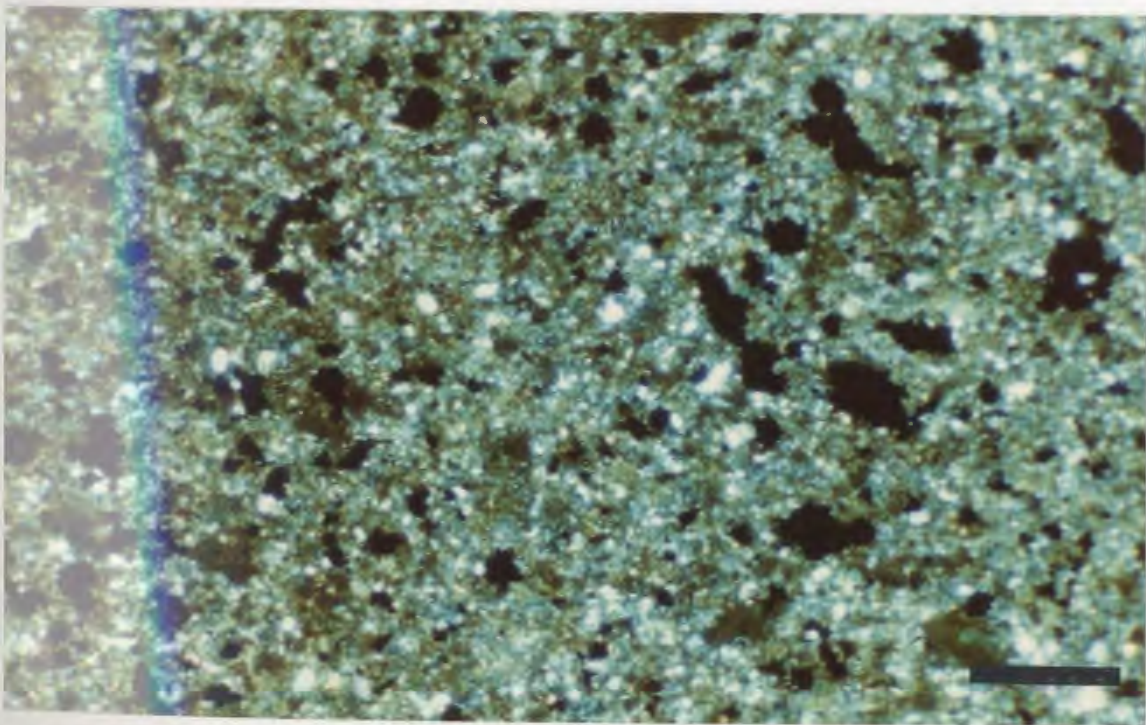


Figure 3.26 Stratigraphic and petrographic details for drill hole 79A-005.

Figure 3.27. Representative drill core from hole A5 (51.3-74.8 m). Note the lack of red strata.

Figure 3.28. Opaque pyrite crystal aggregates seem to have encroached on neighbouring minerals and pore space (blue) within a calcareous claystone. Bar scale 0.25 mm.



In thin section there is a fairly uniform distribution of clay and carbonate minerals, with lesser, variable amounts of silt-size quartz, feldspar, and mica grains, pyrite, and organic material (Fig. 3.26 and Appendix I). A few "analcime" crystals were seen in patches of coarsely crystalline calcite; the calcite had partly corroded and engulfed the "analcime". X-ray diffractograms show that "analcime" is present in most samples.

Clay minerals appear as either evenly distributed dark material, locally disrupted by late-stage calcite-filled microfractures, or as irregularly shaped clots mixed with, and separated by, carbonate minerals. X-ray analyses show that there are subequal amounts of illite and montmorillonite, less chlorite and negligible amounts of kaolinite.

Calcite and dolomite are present as fine- to medium-size crystals intermixed with the clay minerals; calcite is also found in a few coarsely crystalline patches and ramifying microfractures. This distribution of carbonate minerals is therefore essentially the same as that found in the samples from drill hole A3. As in drill hole A3, the calcite-filled microfractures are in turn cross-cut by 'open' microfractures.

Silt-sized, subrounded to subangular grains of quartz, potassic feldspars, micas, and organic material are dispersed or form thin arkosic laminae. Diagenetic euhedral to

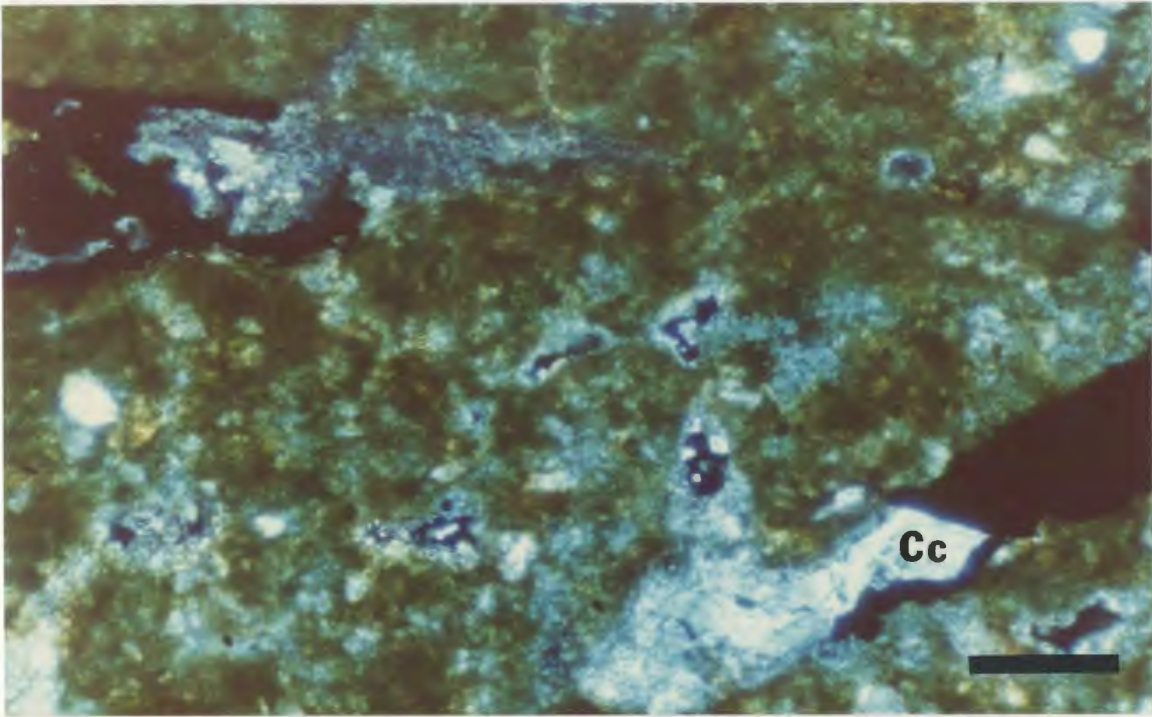
subhedral pyrite crystals or crystal aggregates have encroached on neighbouring minerals (Fig. 3.28). Pyrite, in minor amounts, is also associated with calcite in the late-stage microfractures (Fig. 3.29).

Barite, chalcedony and chert have also been found within the Squires Park Member. The barite was found in a claystone sample from Sir Richard Squires Memorial Park. Fractures in the calcareous claystone sample were lined with purple calcite (possible reflecting contamination by the claystone host rock), followed by white calcite and then white barite toward the centre of the fracture, where some void space was preserved. Both calcite and barite were identified by X-ray diffraction smear mounts. Hyde and Ware (1981) describe these fractures as shrinkage cracks. Even though not found in any drill hole samples, discussions with Dr. R. Hyde and inspection of surface samples supplied by him, reveal that chalcedony and chert can also be found within the Squires Park Member. Thin sections showed that chert usually rimmed the length-fast chalcedony, which appeared to be a pore-closing phase. The chalcedony and chert were cut by the late-stage, coarsely crystalline calcite- and dolomite-filled microfractures.

Microinterparticle, mesovug, and microfracture porosity are again evident. Effective porosity measurements indicate a slight increase in porosity with increased amounts of silt (Fig. 3.26).

Figure 3.29. Opaque pyrite and calcite cement (Cc) filling late-stage microfractures. Bar scale 0.25 mm.

Figure 3.30. Representative drill core from hole 79-69 (14-37 m). Note the brownish-red friable siltstones compared to the coherent coarser sediments.



3.4 Humber Falls Formation

3.4.1 Introduction

Three drill holes were sampled and studied from the two large bodies of the Humber Falls Formation: DDH 79-69 (abbr. 79-69), DDH 79-29 (abbr. 79-29) and DDH 80-70 (abbr. 80-70). Their exact locations are shown in Figure 2.3 (p. 17). The discovery of uranium-rich boulders in the northern body of the formation led to a concentrated drilling program there. Two drill holes from this area were sampled primarily to see if petrographic similarities existed between the sediments of the Humber Falls Formation and the mineralized sandstone boulders, and to see if signs of mineralization could be seen in subsurface. Drill holes 79-29 and 80-70 were also chosen because they penetrated the Humber Falls Formation - Rocky Brook Formation unconformity.

Further data on these drill holes, not included in this chapter, include modal point-count percentages (Appendix I), and coal maceral reflectograms for coaly material found in holes 80-70 and 79-29, and for similar coaly material collected from surface trenches in the area by Dr. D. F. Strong (chapter four, section 4.3).

3.4.2 Drill hole DDH 79-69 (79-69)

Stratigraphy

Drill hole 79-69 (Fig. 3.30) consists of interlayered gravelly sandstones, sandstones, siltstones and mudstones, and a single nine-metre-thick conglomerate unit. The top half of the drill hole is dominated by sandstones and the conglomerate unit, while the bottom half is dominated by the fine grained sediments (Fig. 3.31).

The conglomerate and gravelly patches within the sandstones consist of subrounded to rounded, granule- to pebble-size clasts in an arkosic sandstone matrix. Granitoid plutonic, felsic volcanic, and chert rock fragments form the gravel component, with the granitoid clasts being the largest and most abundant. The sandstones are generally submature to immature, medium to coarse grained arkoses (Fig. 3.32). They are light gray to pale red in colour. Large flakes of detrital white mica, and large crystals of authigenic kaolinite, can easily be seen in drill core. Some cross-stratification and mud rip-ups are also present. Arkosic siltstones and mudstones are also micaceous and, depending on the state of oxidation, they are red to gray in colour. Calcareous nodules are sometimes developed in these finer grained sediments.

Petrography

The distribution of the minerals and mineral groups in the drill hole sediments are shown in Figure 3.31. Detrital feldspars, quartz and rock fragments comprise the largest volume of material in these sediments, with feldspar being

most abundant (Fig. 3.32). Clay cement, and lesser amounts of calcite and hematite cement, comprise the bulk of the intergranular material. Secondary porosity, developed from two stages of mineral dissolution, accounts for the remaining volume of rock.

Original subrounded to subangular clasts of feldspars, quartz and rock fragments have been extensively altered by diagenetic mineral development, and secondary dissolution. Monocrystalline and polycrystalline quartz grains with straight and undulose extinction locally exhibit quartz overgrowths delineated by oxidized dust rims.

Figure 3.33 is a composite, representative diffractogram, which shows the typical clay-fraction mineral assemblages from the Humber Falls Formation drill holes. The clay minerals are predominantly authigenic kaolinite and both detrital and diagenetic illite (Fig. 3.31). The presence of diagenetic illite is suggested by illite crystallinity measurements (chapter five, section 5.3.4). Highly birefringent, interstitial, fibrous material which is colourless in plane light (Fig. 3.34) may be diagenetic illite. Montmorillonite and mixed-layer illite-montmorillonite are also minor constituents in both sandstone and finer grained samples.

In situ dissolution of detrital quartz and feldspar grains probably contributed the elements necessary to develop diagenetic kaolinite and possibly other diagenetic minerals,

HUMBER FALLS FM. DDH 79-69

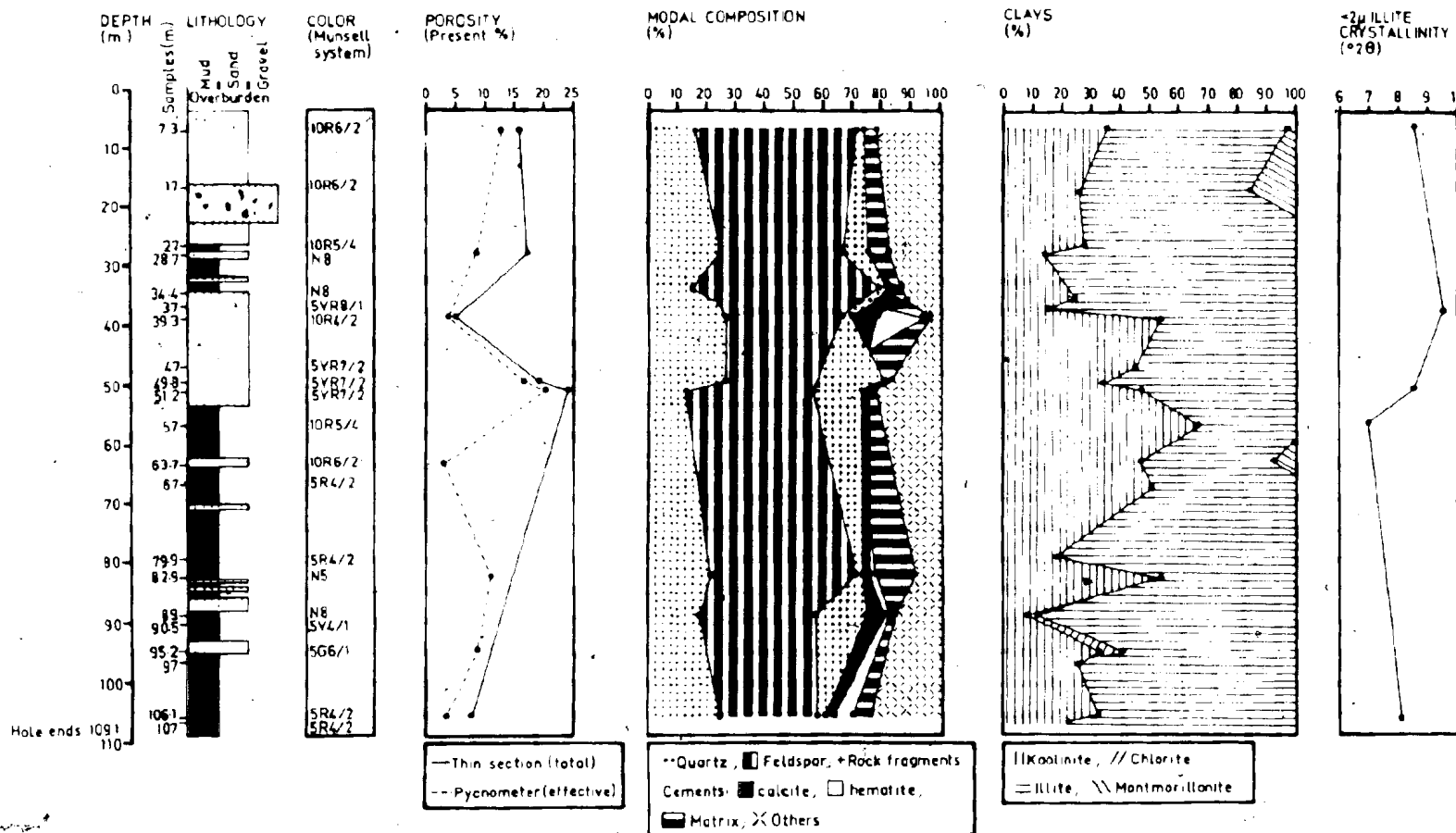


Figure 3.31 Stratigraphic and petrographic details for drill hole DDH 79-69.

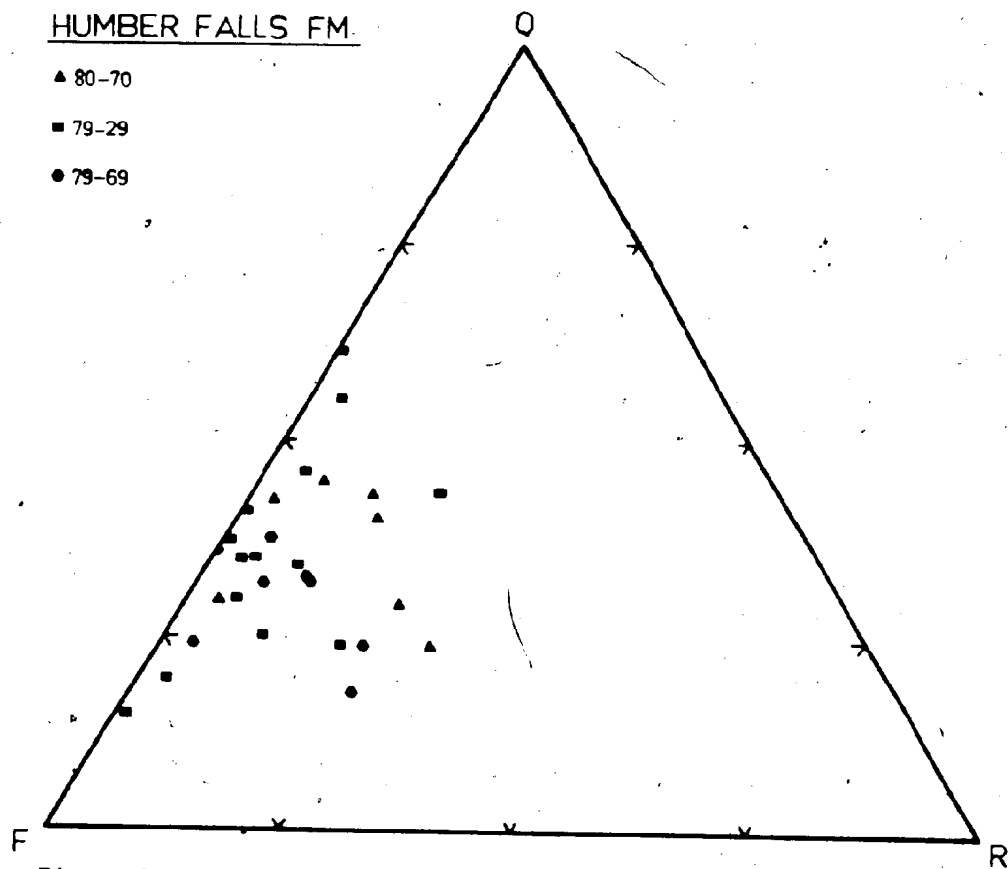


Figure 3.32 QRF classification diagram for sandstone samples from the Humber Falls Formation drill holes DDH 80-70, DDH 79-29, and DDH 79-69.

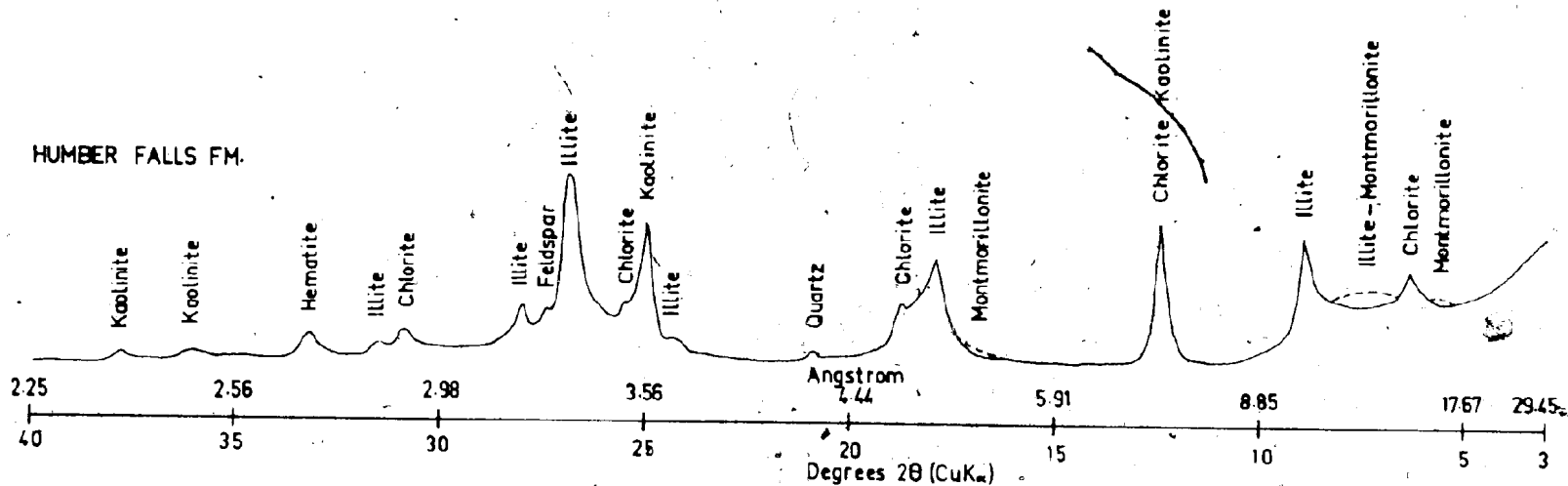


Figure 3.33 A composite clay-fraction diffractogram for the Humber Falls Formation drill holes DDH 80-70, DDH 79-29, and DDH 79-69 (dashed line is peak position after glycolation).

before an influx of coarsely crystalline calcite cement corroded the clay minerals and grain edges and locally fractured and infilled the detrital grains (Figs. 3.35 and 3.36).

It appears that diagenesis proceeded in the following order: (1) early development of secondary porosity from silicate grain dissolution, (2) diagenetic growth of kaolinite, illite, chlorite, and lesser amounts of montmorillonite and mixed-layer illite-montmorillonite, and (3) calcite cementation. This sequence is suggested by the following observations: (a) the diagenetic clay minerals are consistently adjacent to detrital grains and in places appear to blend into them (Fig. 3.37) and are in turn partly or wholly masked by calcite cement; (b) in one example (Fig. 3.38) kaolinite grew in an intragranular dissolution pore within a plagioclase grain, and then calcite cement precipitated and masked parts of both the plagioclase and kaolinite.

A late stage of hematite cement generally penetrates all other primary and secondary (diagenetic) minerals. The calcite cement in particular has been corroded and hematized. Interestingly, the hematite cement has attacked the interior of calcite crystals rather than the crystal edges. Figures 3.39 and 3.40 show how dissolution and the hematite cement preferentially followed the internal lattice structure of the calcite crystals. Cathodoluminescence of a few thin sections failed to detect any calcite zoning.

Figure 3.34. Radiating sheaves of highly birefringent illite cement. Bar scale 0.05 mm.

Figure 3.35. Calcite (Cc) has engulfed and corroded an orthoclase grain (G). Bar scale 0.25 mm.

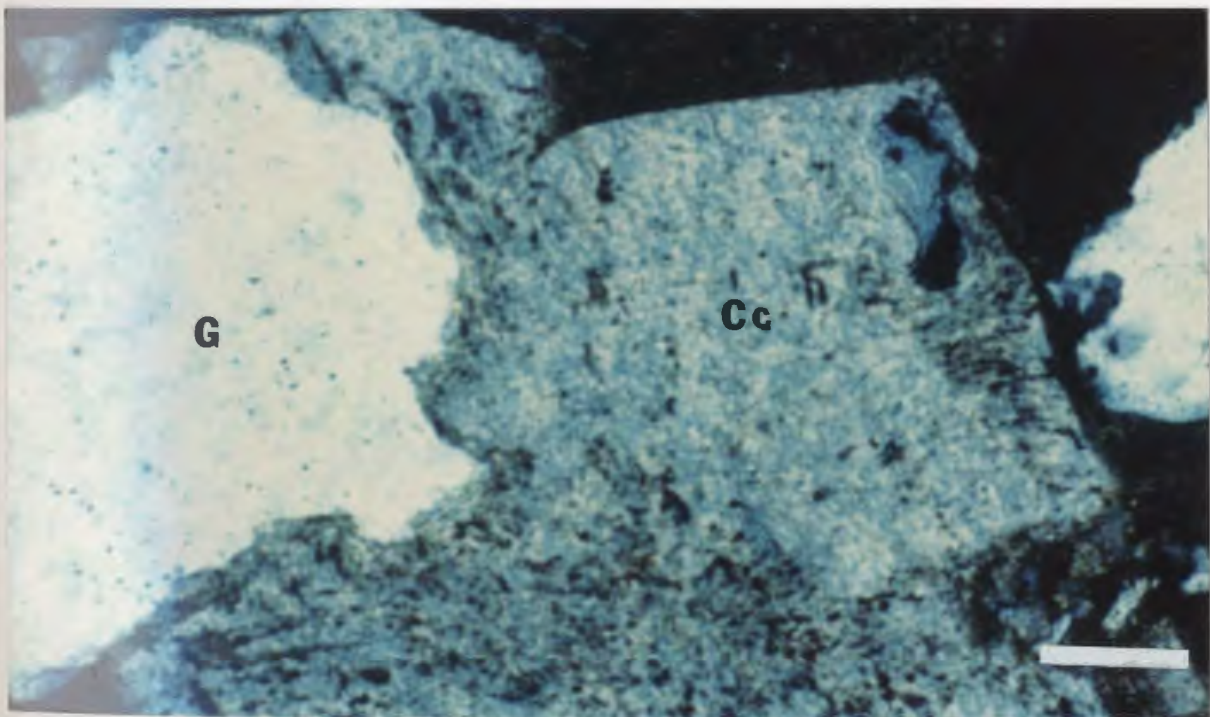
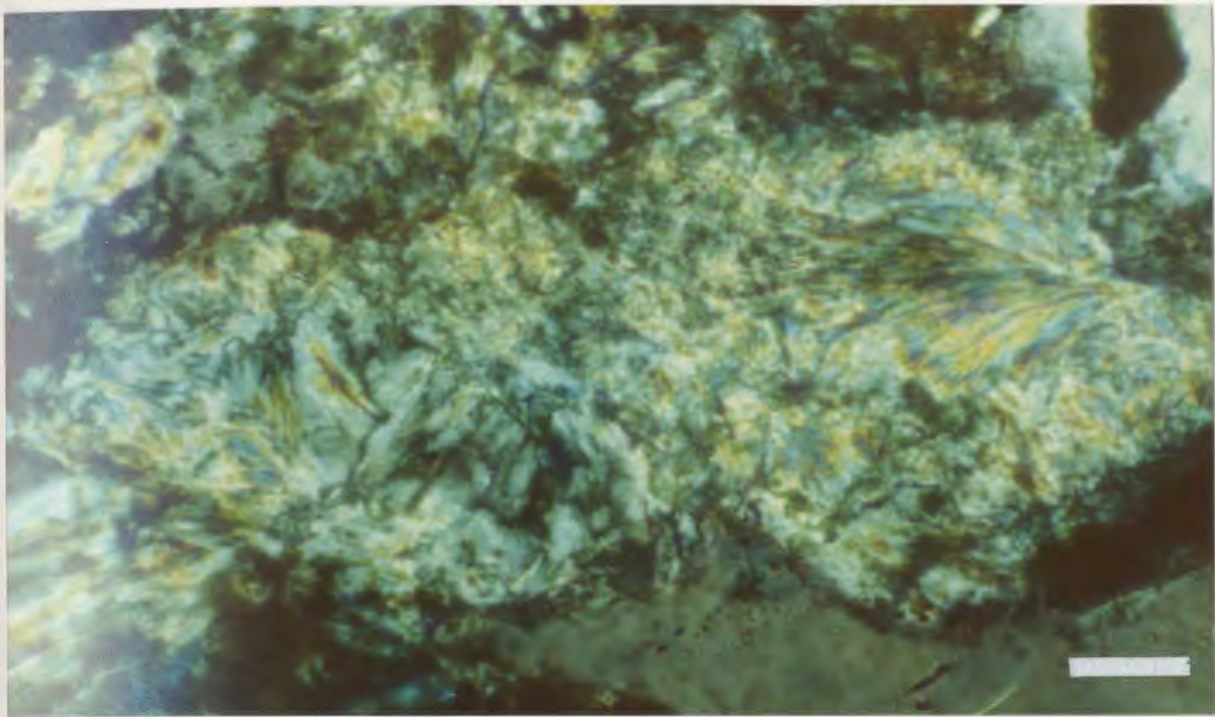


Figure 3.36. A piece of a detrital grain (G) has been detached by the later stage of calcite cementation (Cc). Bar scale 0.05 mm.

Figure 3.37. Authigenic vermicular kaolinite (K) blends into the neighbouring feldspar grains (G) and fills adjacent interstitial pore space. Bar scale 0.05 mm.

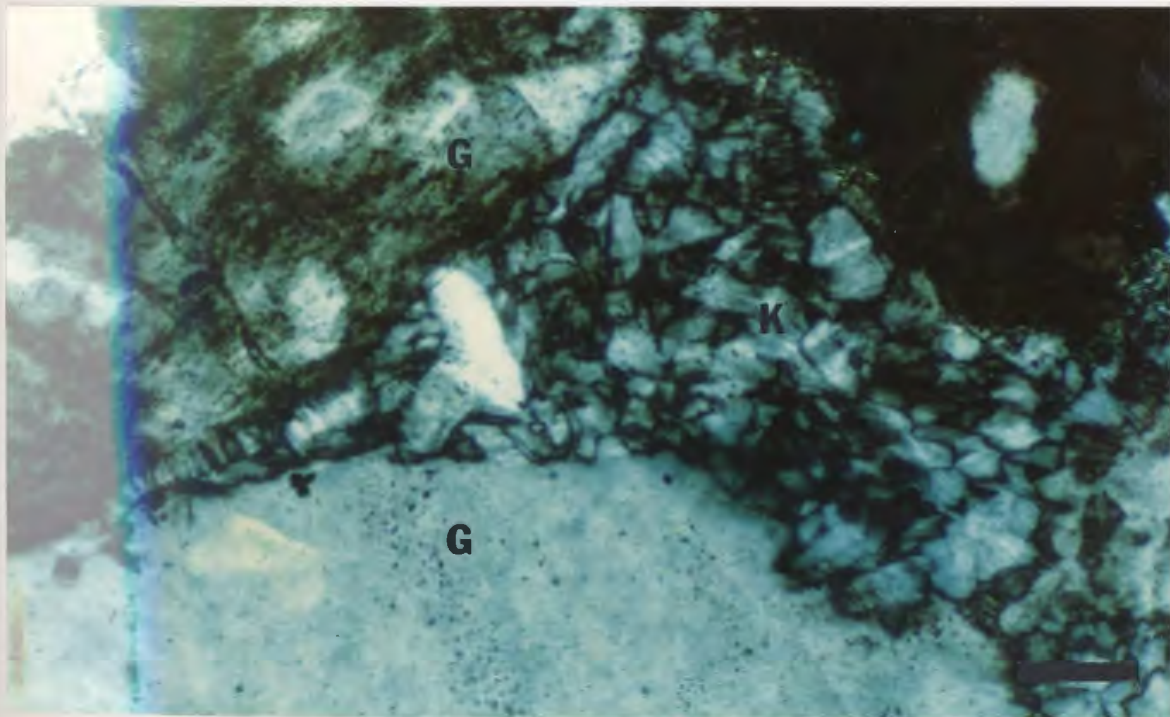
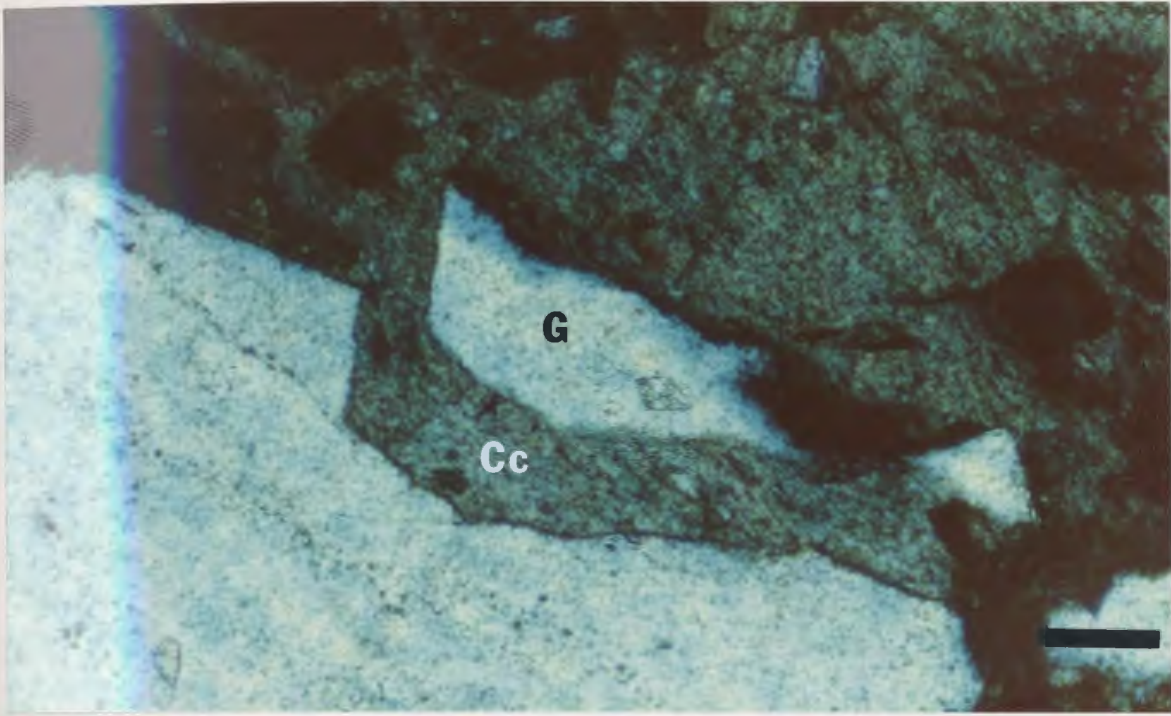
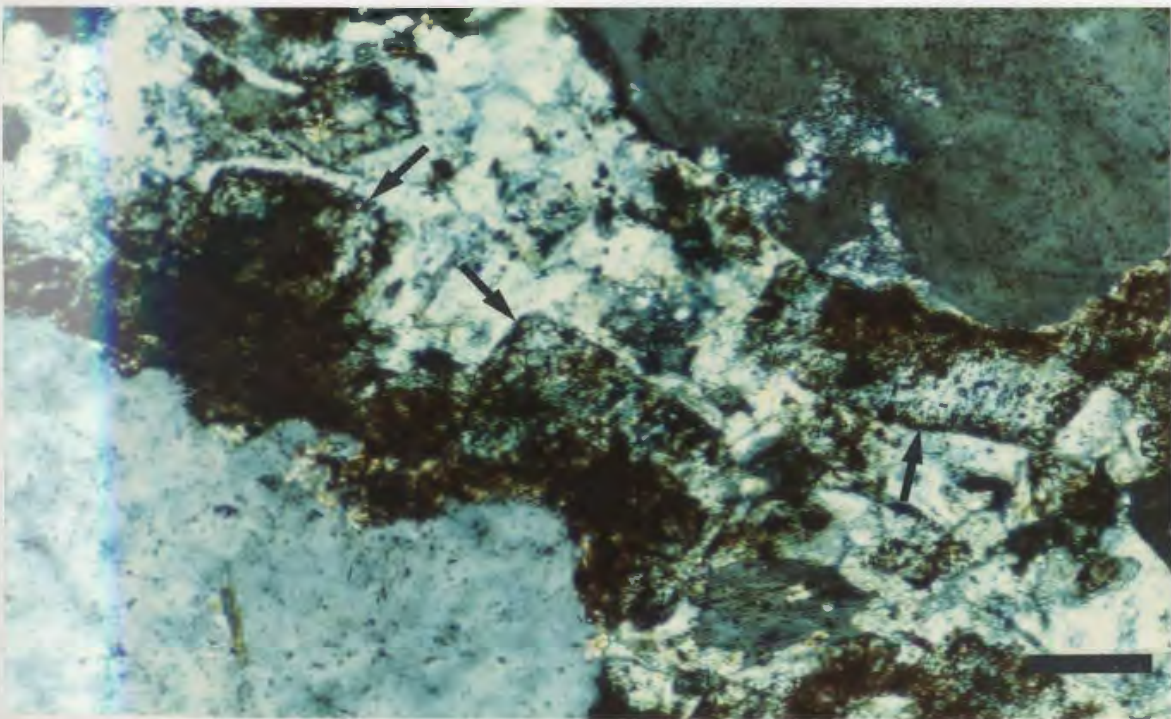
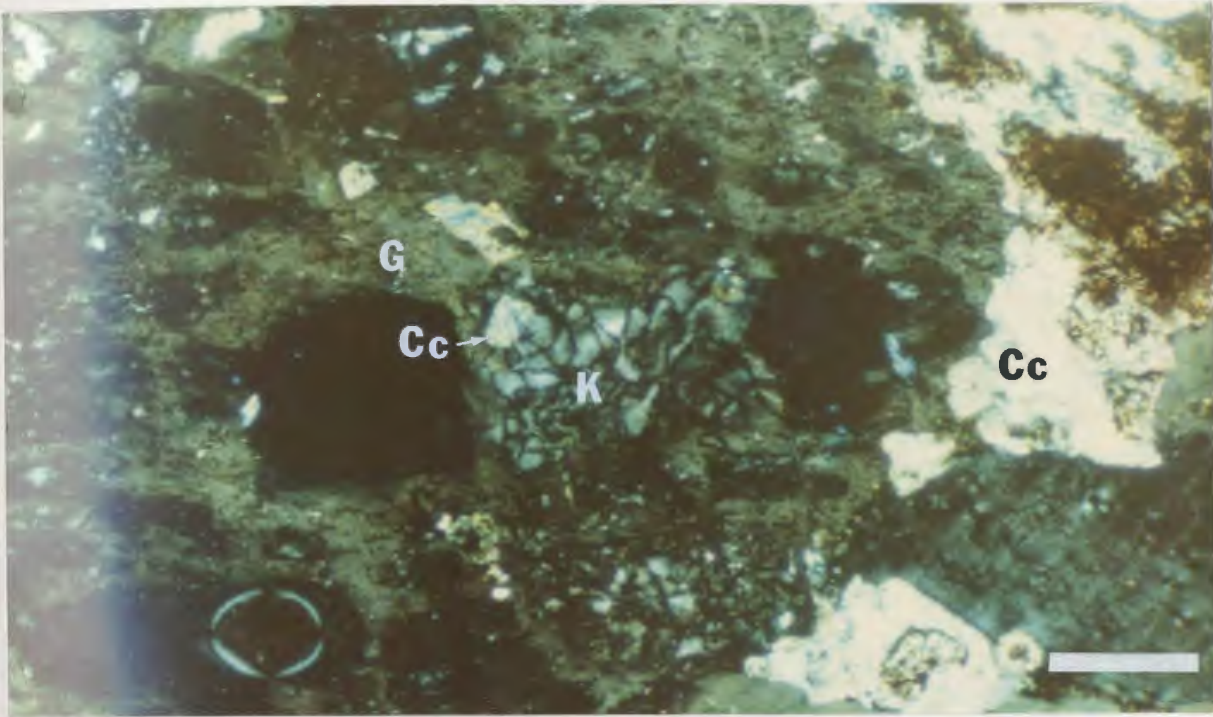


Figure 3.38. Proof for an early stage of porosity development. Kaolinite (K) has grown within an intragranular dissolution pore in a plagioclase grain (G) and has in turn been partly masked by calcite cement (Cc). Bar scale 0.25 mm.

Figure 3.39. Late-stage hematite cement (opaque) has preferentially followed the internal lattice structure of the calcite cement crystals (arrow) and has attacked the central areas of the crystals rather than the exteriors. Bar scale 0.25 mm.



The image is a scanning electron microscope (SEM) photograph showing the surface of calcite cement. It displays a regular, grid-like internal structure. Several small, dark, irregular pits are visible, with one specifically pointed out by a small black arrow. The overall appearance is that of a crystalline material with some surface erosion or dissolution.

Figure 3.40. SEM photo showing that dissolution pits (arrow) in calcite cement follow the regular internal structure of the calcite. Bar scale 5 μ .

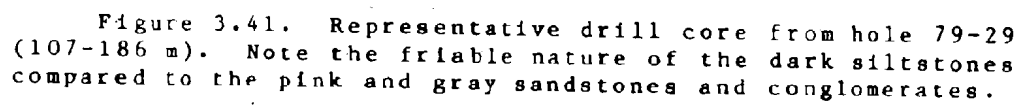
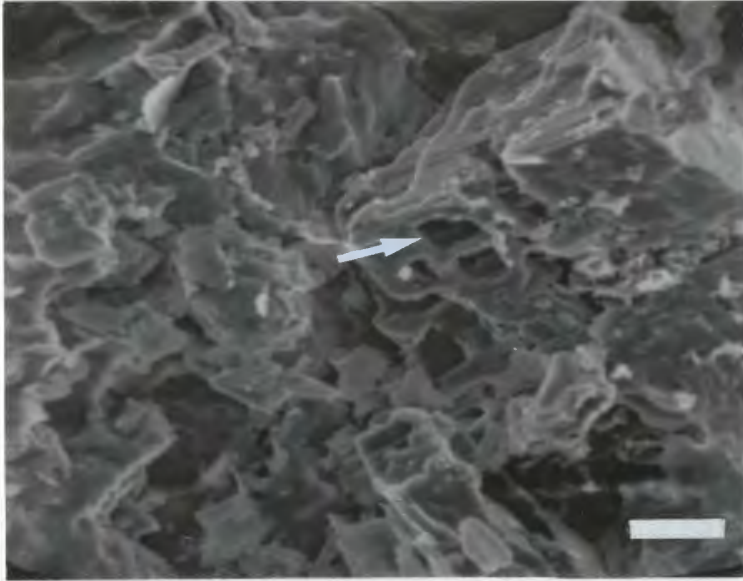
The image shows a representative drill core from hole 79-29, located at depths of 107-186 meters. The core consists of several distinct layers of sedimentary rock. From top to bottom, there are layers of pink sandstone, dark siltstone, and gray sandstone and conglomerates. The dark siltstone layer is notably friable, appearing more fragmented and less cohesive than the surrounding sandstone layers.

Figure 3.41. Representative drill core from hole 79-29 (107-186 m). Note the friable nature of the dark siltstones compared to the pink and gray sandstones and conglomerates.



Total porosity measurements range from 4-25 % of the rock volume, with at least half of that being effective porosity (Fig. 3.31). The highest porosities occur in the coarse grained top half of the drill hole. The low porosities recorded at approximately 39 m and 64 m may reflect relative increases in diagenetic clay and hematite cements.

3.4.3 Drill hole DDH 79-29 (79-29)

Stratigraphy

In this drill hole, interlayered conglomerates, gravelly sandstones and sandstones, and siltstones and mudstones of the Humber Falls Formation overlie mixed siltstones and mudstones of the Rocky Brook Formation (Fig. 3.42). At the erosional unconformity, gray gravelly sandstones of the Humber Falls Formation sharply overlie patchy greenish-gray and red mudstones. In the Humber Falls Formation, gravelly sandstones and sandstones dominate the section. Metre-scale units contribute to a single, approximately 24 m thick conglomerate to siltstone fining-upward sequence near the top of the sequence. Figure 3.41 shows pinkish-gray sandstones and conglomerate and greenish-gray siltstones from the middle of drill hole 79-29.

The conglomerates are light gray to grayish-red, with irregular red oxidation patches. The pebble- to granule-size framework clasts are subangular to subrounded, and both poorly and moderately sorted. The most common framework clast types are granitoid plutonic (some clasts are granophytic), followed by felsic volcanic, schistose metamorphic, and chert rock fragments. Grains of feldspar and quartz also reach granule size. The matrix component is a carbonate-cemented quartz-feldspar sand.

The medium to coarse grained sandstone and gravelly sandstone units are generally gray to dark red in colour, and display submature to immature textures. Commonly, large pink potassic feldspar, white feldspar and macrokaolinite (sand-size kaolinite, Isphording and Lodding, 1973), and frosted quartz grains give the sandstone a very granitic appearance. QRF plots for some of the sandstones indicate both arkose and lithic arkose compositions (Fig. 3.32). These sandstones also show the widest range of composition compared with sandstones from the other two Humber Falls Formation drill holes. Large flakes of detrital white mica and calcite-filled vugs are easily seen in hand sample. Locally, faint cross-stratification is developed in medium grained sandstones, as are very thin laminae of coalified organic material.

HUMBER FALLS FM DDH 79-29

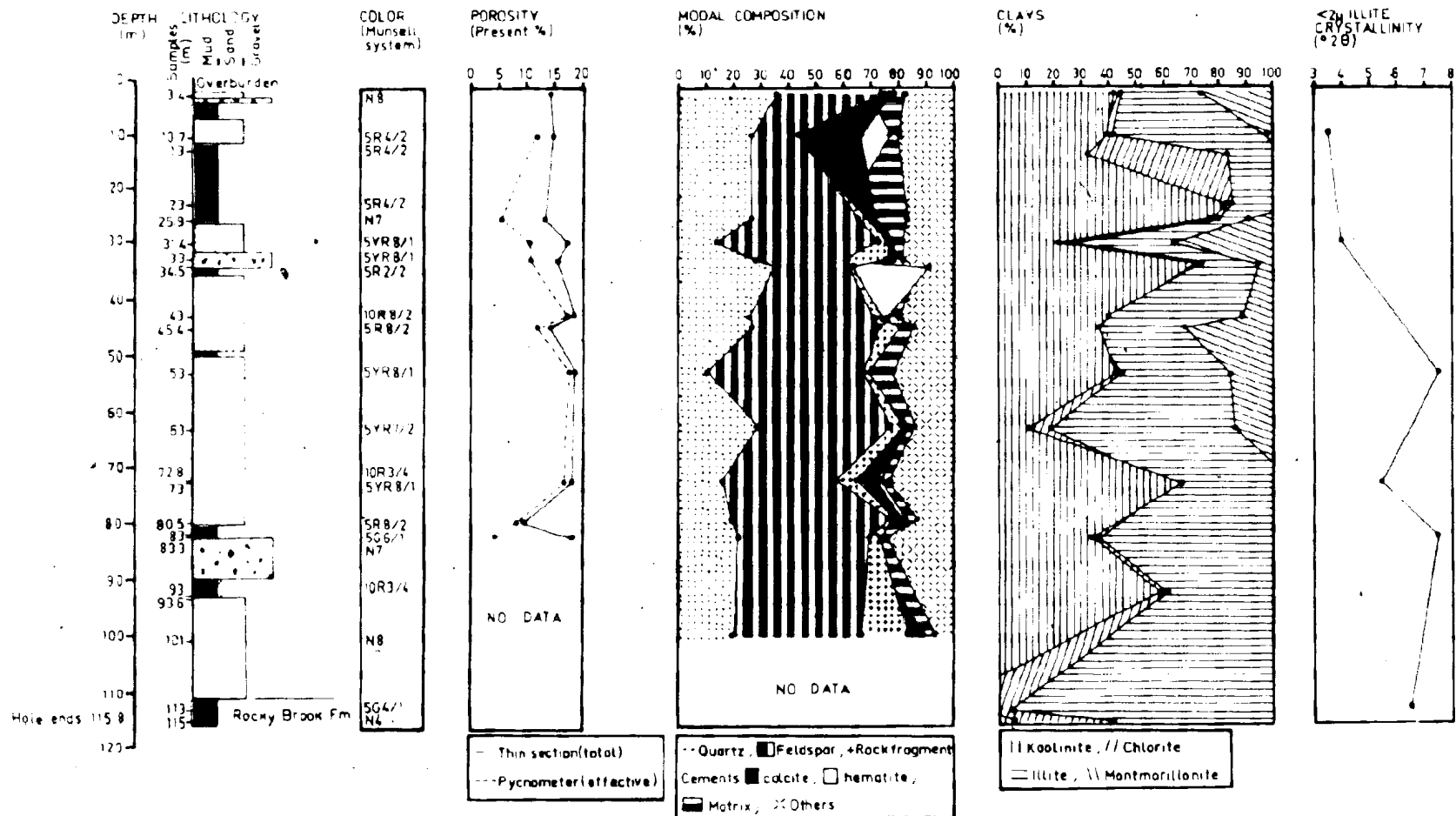


Figure 3.42 Stratigraphic and petrographic details for drill hole DDH 79-29.

The finer grained siltstones and mudstones are similar to those from the underlying Rocky Brook Formation, in that they are reddish-brown and gray to dark greenish-gray in colour, and their silt fraction is arkosic in composition. The fine grained Humber Falls Formation sediments contain faint ripple laminae, calcareous nodules and rootlets. These primary features are not seen in the underlying fines of the Rocky Brook Formation.

Petrography

Subangular to subrounded monocrystalline quartz and subequal amounts of plagioclase and orthoclase comprise most of the detrital grains in the sandstones. The various lithic clasts are generally larger but less abundant than the quartz and feldspar grains. The margins and interior of feldspar grains, especially microcline and plagioclase, have been extensively leached.

The larger clasts are surrounded by detrital muscovite and biotite, diagenetic kaolinite, illite, montmorillonite, mixed-layer illite-montmorillonite, calcite and hematite; and accessory amounts of detrital organic material, magnetite, epidote, sphene, and zircon. The relative amounts of most of these minerals are shown in Figure 3.42 and Appendix I.

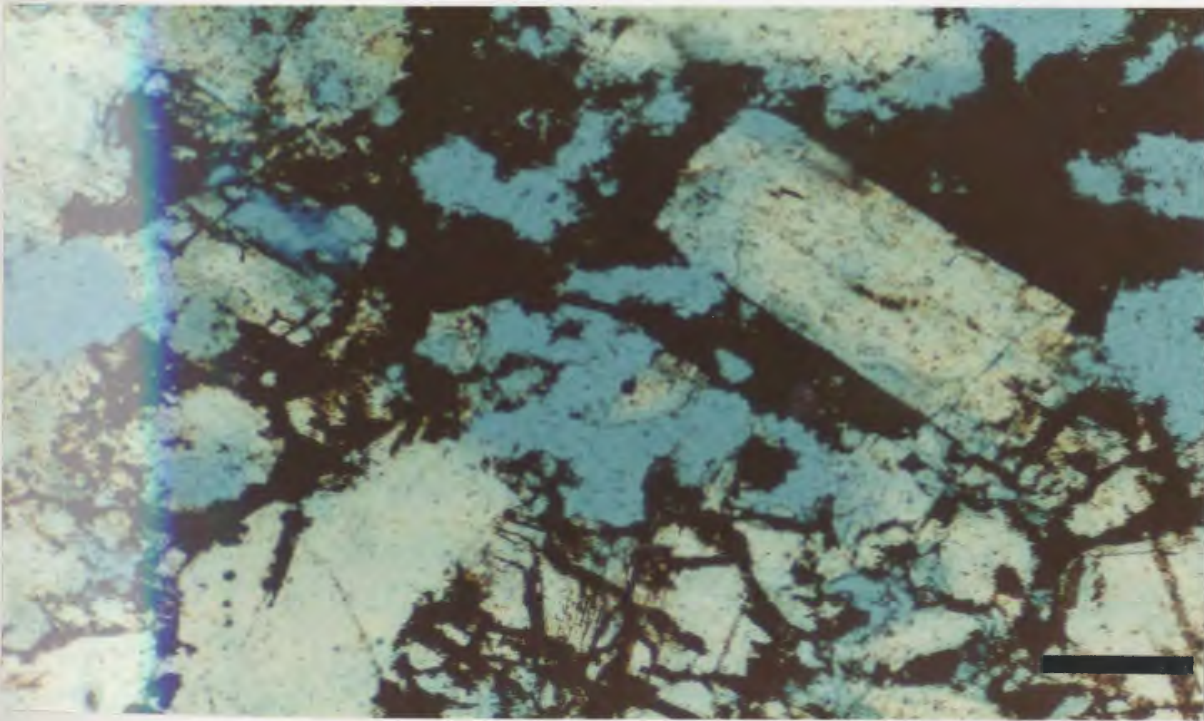
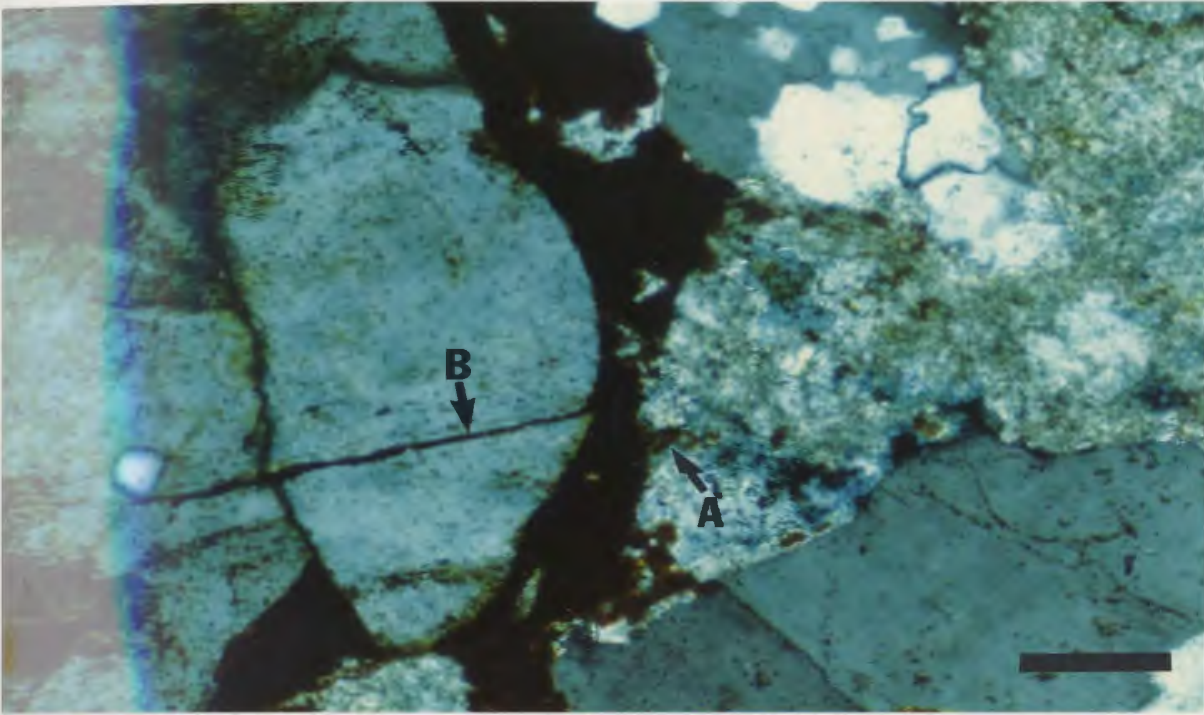
Diagenetic vermicular kaolinite composed of books of pseudo-hexagonal plates is typically developed along quartz and potassic feldspar grain boundaries, commonly completely filling the adjacent pore space. Kaolinite is the dominant clay mineral in the Humber Falls Formation section of this drill hole (Fig. 3.42), but quickly decreases to very minor amounts in the underlying Rocky Brook Formation. Diagenetic illite is found both as a fibrous interstitial clay mineral, and as larger lamellae on detrital feldspar or rock fragment grains. Montmorillonite and mixed-layer illite-montmorillonite were present in minor amounts in sandstone and siltstone samples. Interstitial material in the sandstones has been partly destroyed and masked by the later stages of calcite and hematite cementation.

Finely to coarsely crystalline carbonate cements both corroded and fractured grains. Dolomite has been identified in one sandstone sample. The carbonate cement is in turn affected by extensive hematite cementation. The hematite corroded and engulfed the carbonate cement, and penetrated along carbonate-grain boundaries (Fig. 3.43). In places, the hematite totally surrounds the detrital grains, occluding any intergranular porosity.

Total porosity ranges from approximately 9-18%. Most of the porosity is effective in the sandstones (Fig. 3.42), while the finer grained sediments show much less effective porosity. This may be due to the higher proportions of diagenetic and detrital clay minerals in the finer grained

Figure 3.43. Late-stage hematite (opaque) has precipitated within earlier calcite cement (arrow A), and along carbonate-grain boundaries and fractures within grains (arrow B). Bar scale 0.25 mm.

Figure 3.44. A late stage of pervasive dissolution and pore development (blue), has even destroyed the hematite cement (opaque). Bar scale 0.25 mm.



sediments. The porosity in the sandstones can be attributed to the dissolution of silicate grains, especially feldspars, and to a late stage of pervasive dissolution which has even affected the hematite cement (Fig. 3.44). It is difficult to tell how much porosity was developed prior to the influx of calcite and then hematite cement.

3.4.4 Drill hole DDH 80-70 (80-70)

Stratigraphy

Drill hole 80-70 penetrates into the top of the Rocky Brook Formation (Fig. 3.45). The contact may be an erosional unconformity, as it shows greenish-gray calcareous siltstones of the Rocky Brook Formation overlain by green pebbly conglomerate and sandstones of the Humber Falls Formation. The Humber Falls Formation in this drill hole consists of interlayered conglomerates, gravelly sandstones and sandstones, and siltstones (Figs. 3.45 and 3.46). They are all generally unoxidized and gray in colour, except for a few reddish-brown siltstone layers.

The pebble to granule conglomerate has a moderate to well sorted clast framework dominated by subrounded granitoid plutonic rock fragments. The matrix material is calcite-cemented sand-size quartz, feldspar, and a few rock-fragment grains. Gravelly sandstones and coarse to fine grained sandstones comprise most of drill hole 80-70. They are generally submature arkoses and lithic arkoses (Fig.

3.32) bound by calcite and clay cements.

Cross-stratification is more common in the coarser sandstones, while fine grained sandstones are commonly more micaceous. The brownish-red to greenish-gray arkosic siltstones are too friable to show any internal structures.

More coalified organic material was found in this drill hole than in any of the other drill holes studied. The material occurs as thin laminae and irregular pebble-size fragments in gray sandstones. The coaly material is discussed further in chapter four section 4.3. Large irregular masses of pyrite line and fill pores in the sandstones, particularly near the coaly material.

Petrography

Sandstones from drill hole 80-70 contain the following detrital grains, in order of abundance (Fig. 4.3.45 and Appendix I): feldspars (orthoclase > plagioclase > microcline > perthites), subequal amounts of monocrystalline and polycrystalline quartz, rock fragments (plutonic > metamorphic > chert > other sedimentary), mica, and biotite. Quartz- and feldspar-rich plutonic rock fragments are the largest clasts present. Microcline, perthites and plagioclase grains commonly display dissolution pits and illitization. These large detrital grains also show dentate or diffuse grain boundaries when in contact with one another. Muscovite and chloritized biotite grains are also present.

HUMBER FALLS FM DDH 80-70

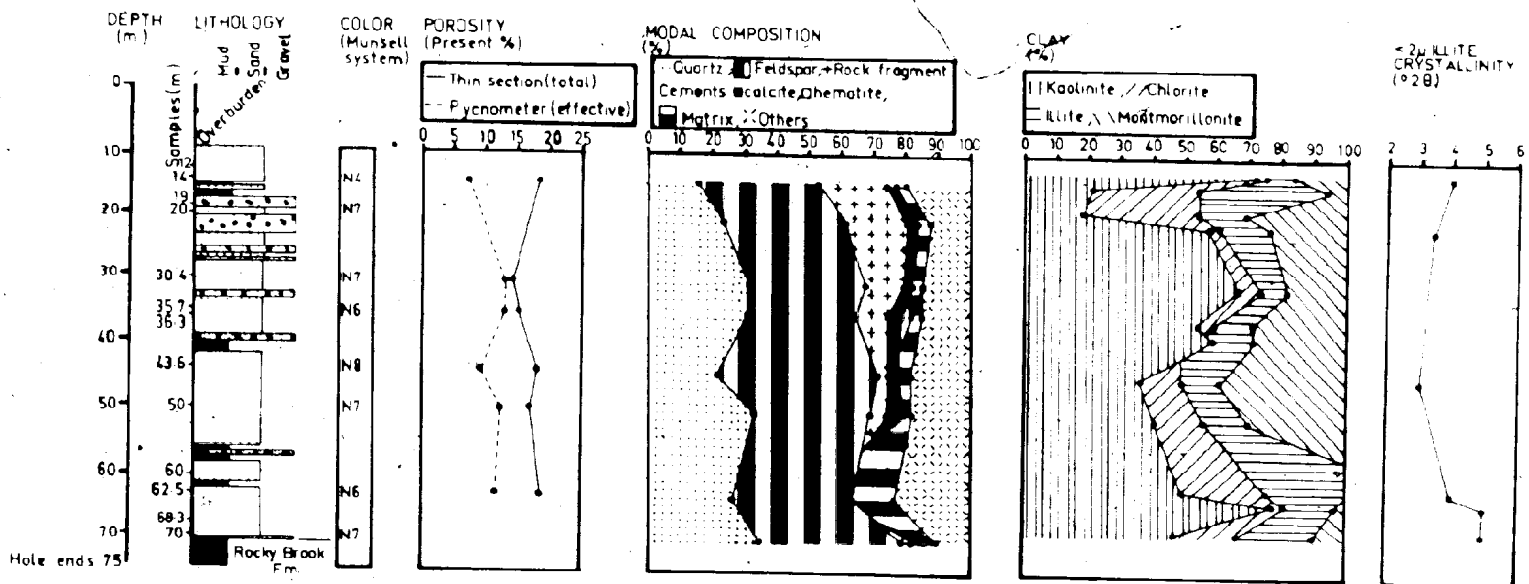
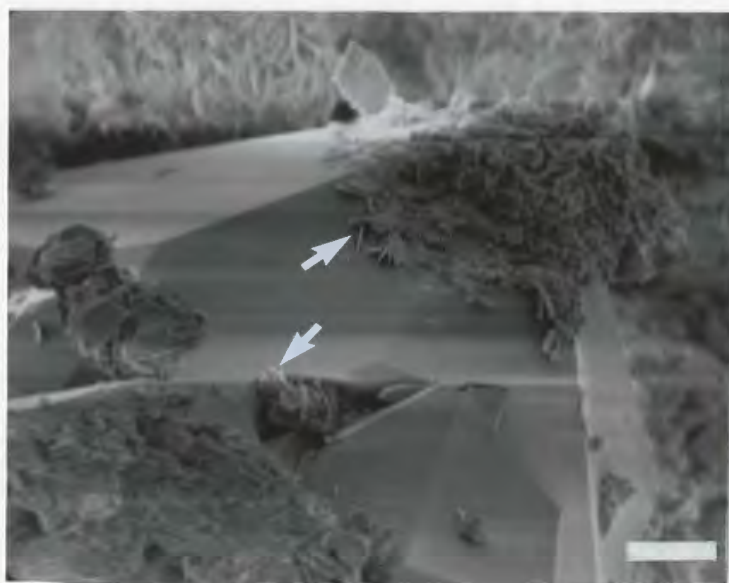


Figure 3.45 Stratigraphic and petrographic details for drill hole DDH 80-70.

Figure 3.46. Representative drill core from hole 80-70 (32-60 m) displaying gray arkosic sandstones and dark friable finer grained sediments.



Figure 3.47. SEM photo of edge-to-face and rosette chlorite (arrows) partly covering euhedral quartz overgrowths. Bar scale 10 μ .



Locally, quartz overgrowths partly envelop quartz grains, and in turn are masked by authigenic minerals such as chlorite (Fig. 3.47). The chlorite typically forms rosettes made up of individual chlorite platelets, which coalesce and cover grain surfaces (Fig. 3.48). Vermicular kaolinite and fine flakes of illite can also be seen in the interstitial material. Montmorillonite has been identified in most samples (Fig. 3.45). Mixed-layer illite-montmorillonite has only been identified in three sandstone and siltstone samples.

Medium to coarsely crystalline calcite cement corrodes detrital grain edges and locally engulfs smaller grains. In some samples, the calcite cement, and previously developed detrital or diagenetic minerals, are corroded and disrupted by irregular patches of pyrite cement. The pyrite rims or completely fills pores, indiscriminantly fracturing and corroding detrital grains and interstitial material (Fig. 3.49). SEM reveals two forms of pyrite in this drill hole: (1) framboidal pyrite (Fig. 3.50); and (2) large coalesced pyrite cubes (Fig. 3.51). Figure 3.51 also shows small disrupted clumps of matrix material caught up in the pyrite crystals. Locally, flattened rhombs of siderite are associated with areas of reduction (Fig. 3.52). Where developed, hematite cement corrodes and partly masks detrital grains and the calcite cement, and forms oxidized halos around the patches of pyrite cement.

Figure 3.48. SEM photo of chlorite rosettes (C) partly covering a feldspar grain (G) which has undergone dissolution (c.f. Hicks et al., 1980, p.211). Bar scale 10 μ .

Figure 3.49. Opaque pyrite fractures, engulfs, and partly corrodes detrital grains and interstitial material. Bar scale 0.25 mm,

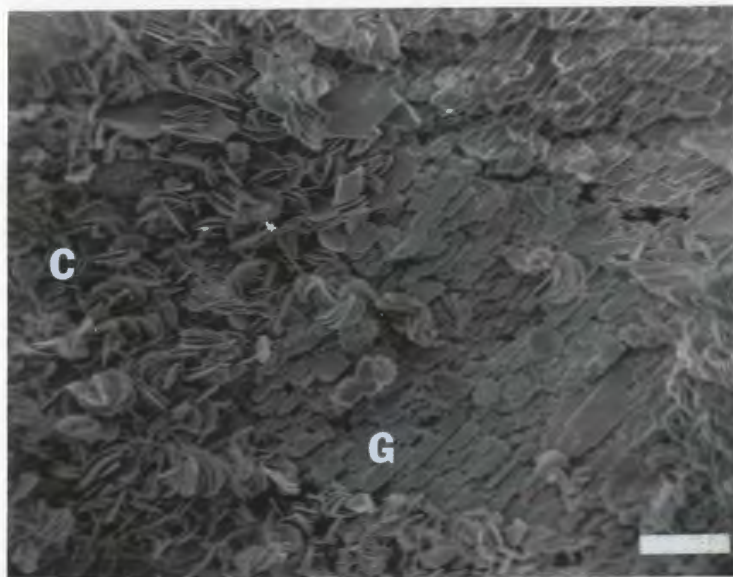


Figure 3.50. SEM photo of pyrite framboids lining part of the pore space (c.f., Scholle, 1979, p.153). Bar scale 10 μ .

Figure 3.51. SEM photo of coalesced, intergranular pyrite cubes. Bar scale 100 μ .

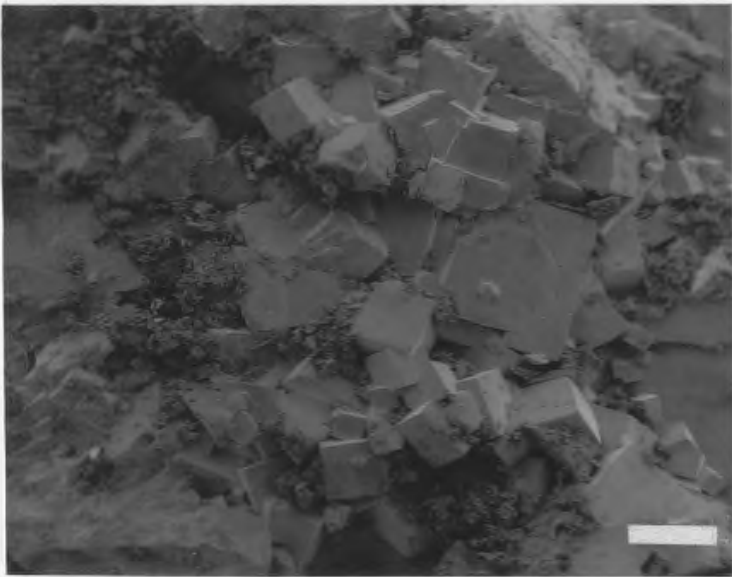
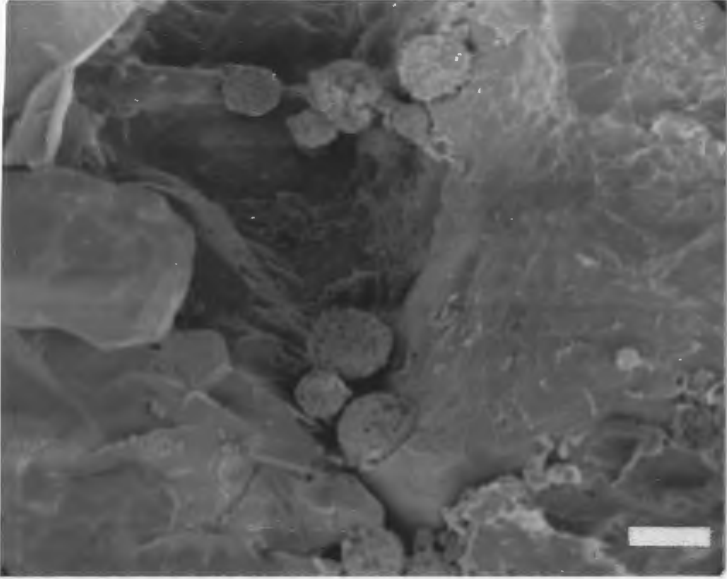
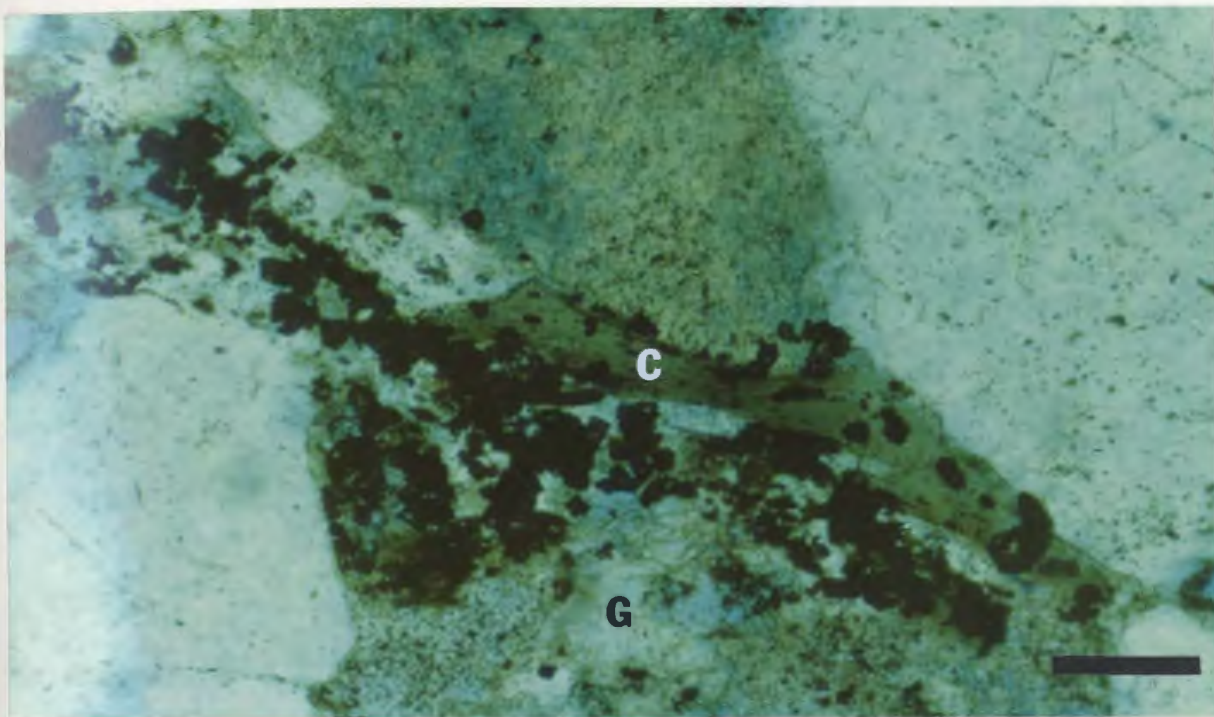


Figure 3.52. Siderite rhombs overgrowing chlorite after biotite (C) and altered plagioclase grains (C). Bar scale 0.25 mm.

Figure 3.53. Representative drill core from hole D4 (12.3-37.5 m) showing the down hole transition from gray sandstone into badly weathered reddish-brown siltstone.



Total porosity in these rocks is approximately 8-19 % (Fig. 3.45 and Appendix I). The effective porosity shows an inverse relationship with the total porosity. The reason for such variability is not obvious. Signs of detrital silicate grain dissolution prior to authigenic mineral growth and cementation indicates that at least part of the total porosity can be attributed to early diagenetic grain dissolution.

3.5 Howley Formation

3.5.1 Introduction

Two drill holes west of Sandy Lake (Fig. 2.3, p. 17) were chosen to represent the Howley Formation: 79D-004 (abbr. D4) and 79D-005 (abbr. D5). Unfortunately, there are two problems with these drill holes. Firstly, the friable nature of the rock led to poor core recovery. Recent weathering also accentuated the frailty of the core. Secondly, no age-diagnostic fossils were found in the vicinity of the two holes, nor did either hole reveal any of the coaly material typical of the Howley Formation. Nevertheless, the two drill holes were the best available for this study, and mapping by Hyde (1979a, 1983) and Hyde and Ware (1980, 1981) indicates that the two holes had been drilled into the Howley Formation.

HOWLEY FM. 79D-CC4

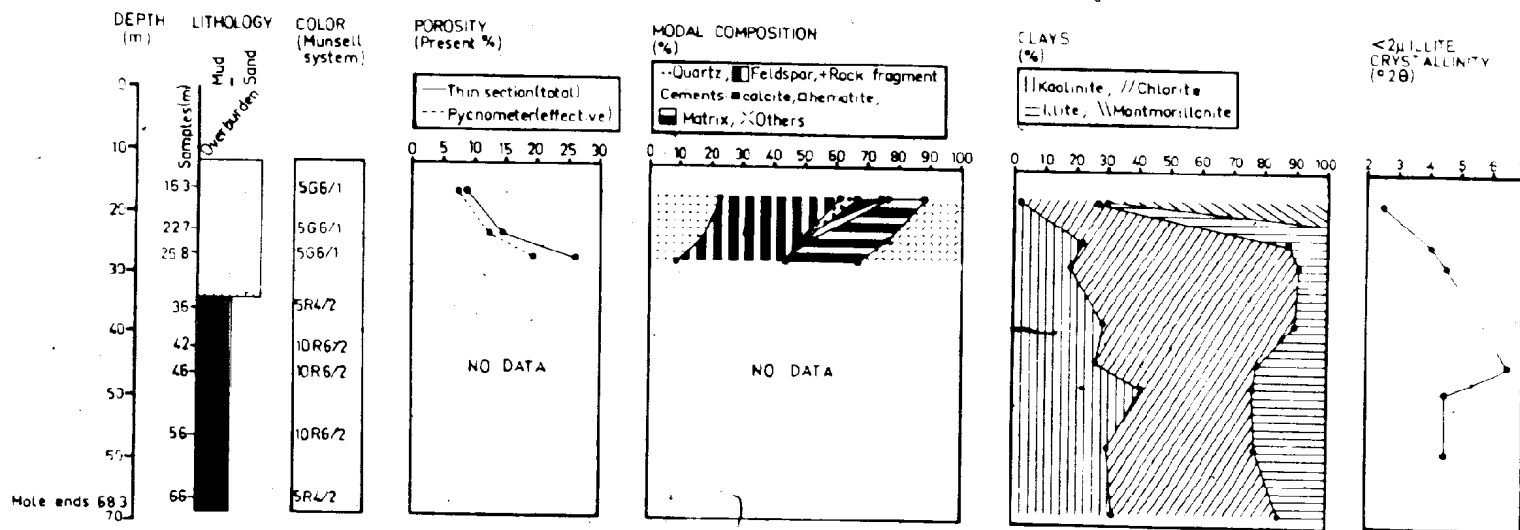


Figure 3.54 Stratigraphic and petrographic details for drill hole 79D-004.

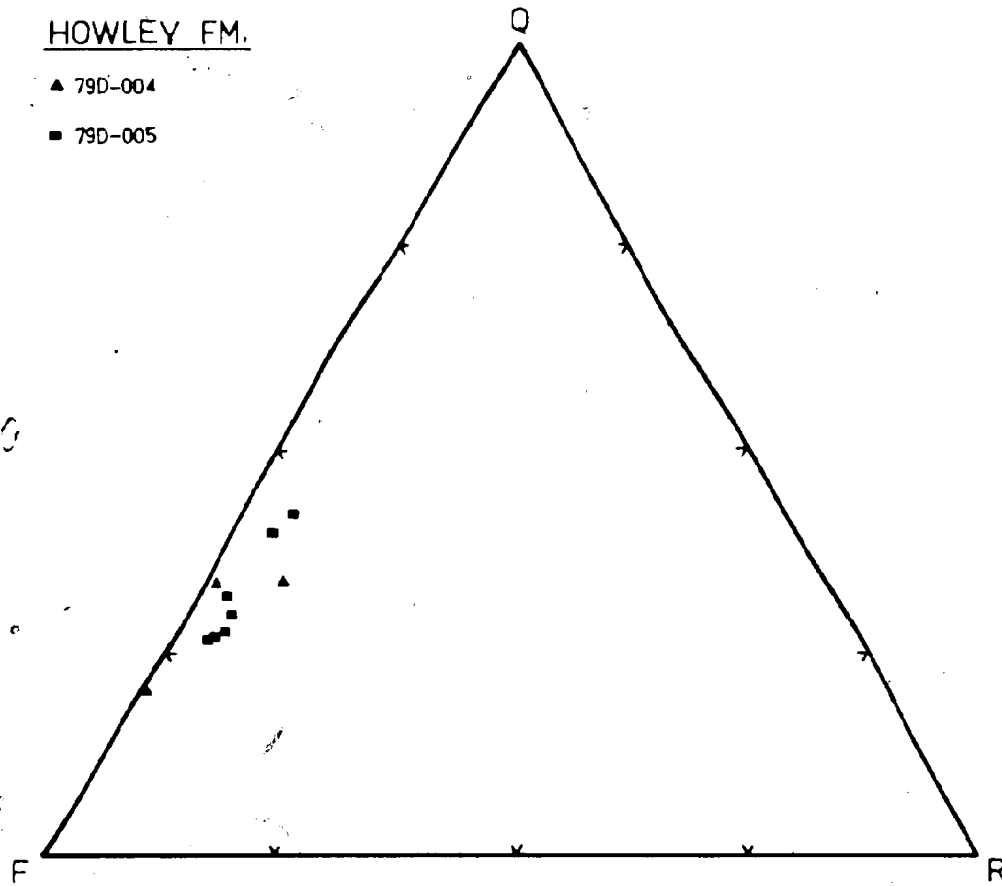


Figure 3.55 QRF classification diagram for sandstone samples from the Howley Formation drill holes 79D-004 and 79D-005.

Evidence in these holes of the informal three-fold subdivision of the Howley Formation (Hyde, 1979b) is uncertain. The lack of coarse basal siliciclastics and coaly material, and the abundance of finer grained material in the two drill holes, may permit a rough correlation with Hyde's middle, dominantly gray unit. A better local correlation can be made between the two drill holes themselves. In both D4 and D5, the top third is dominated by grayish sandstones, whereas the bottom two-thirds of the holes is dominated by brownish-red siltstones. Also, neither drill hole contains conglomerate.

3.5.2 Drill hole 79D-004 (D4)

Stratigraphy

Drill hole D4 consists of approximately 45 m of greenish-gray sandstones overlying a thicker unit of pale to grayish-red siltstones and mudstones (Fig. 3.54). Figure 3.53 shows the top half of the drill hole, the sandstone to siltstone transition, and the general state of the core.

The sandstones are homogeneous medium to fine grained arkoses (Fig. 3.55). They contain scattered flakes of detrital white mica, pin-prick oxidation spots, and a few red coloured mud chips. The intermixed siltstones and mudstones are also micaceous, but are generally dark brownish-red in colour with small greenish-gray unoxidized patches. The friable nature of the finer grained sediments precluded any

detailed descriptions.

Petrography

Sandstones from the top of the drill core have a detrital component consisting mostly of quartz and feldspars grains, with lesser amounts of rock fragments, muscovite, biotite, epidote, and sphene (Fig. 3.54 and Appendix I). The 'others' category in Figure 3.54 includes total porosity and accessory amounts of epidote and sphene. Subangular to subrounded clasts of monocrystalline quartz and orthoclase are by far the most abundant minerals. Metamorphic, chert, plutonic, and volcanic rock fragments are found in subequal amounts. Some compaction of these grains is suggested by intact concavo-convex grain boundaries, and bent muscovite and biotite grains. Quartz overgrowths (Fig. 3.56) may have received silica from nearby points of pressure solution.

Three types of diagenetic chlorite were identified: (1) vermicular chlorite, perhaps pseudomorphous after kaolinite (only found in one sample, Figures 3.57 and 3.58); (2) highly birefringent chlorite rosettes (Figs. 3.59, and 3.60); and (3) individual platelets of chlorite growing on grain surfaces and exhibiting rounded edges (Fig. 3.56). Montmorillonite was also identified with SEM by its interconnected 'cornflake' morphology (Figs. 3.61 and 3.62). Diagenetic kaolinite and illite are also present. Many of the above minerals were also identified by X-ray diffraction (Fig. 3.63).

Figure 3.56. SEM photo showing euhedral quartz overgrowth (Q) partly engulfed by individual platelets of chlorite (C). Chlorite may be growing at the expense of quartz (c.f., Tillman and Almon, 1979, p.368). Bar scale 5 μ .

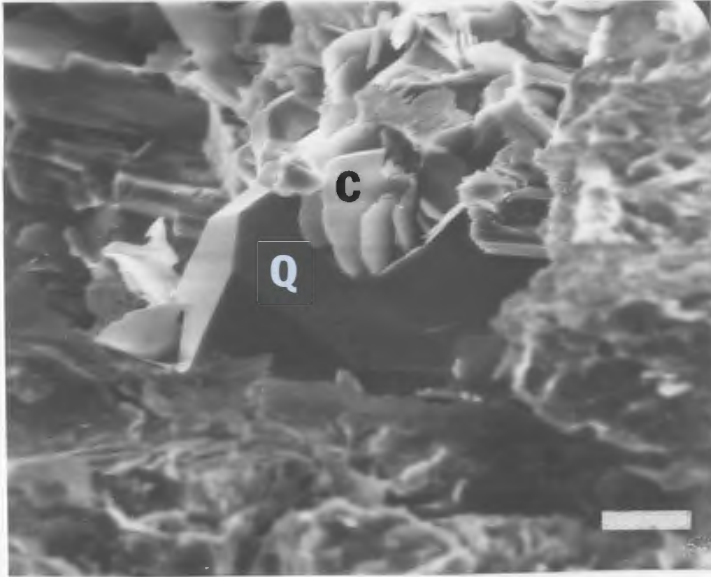


Figure 3.57. Vermicular chlorite (C). Bar scale 0.05 mm.

Figure 3.58. Same as figure 3.57 but in plane light.
Bar scale 0.05 mm.

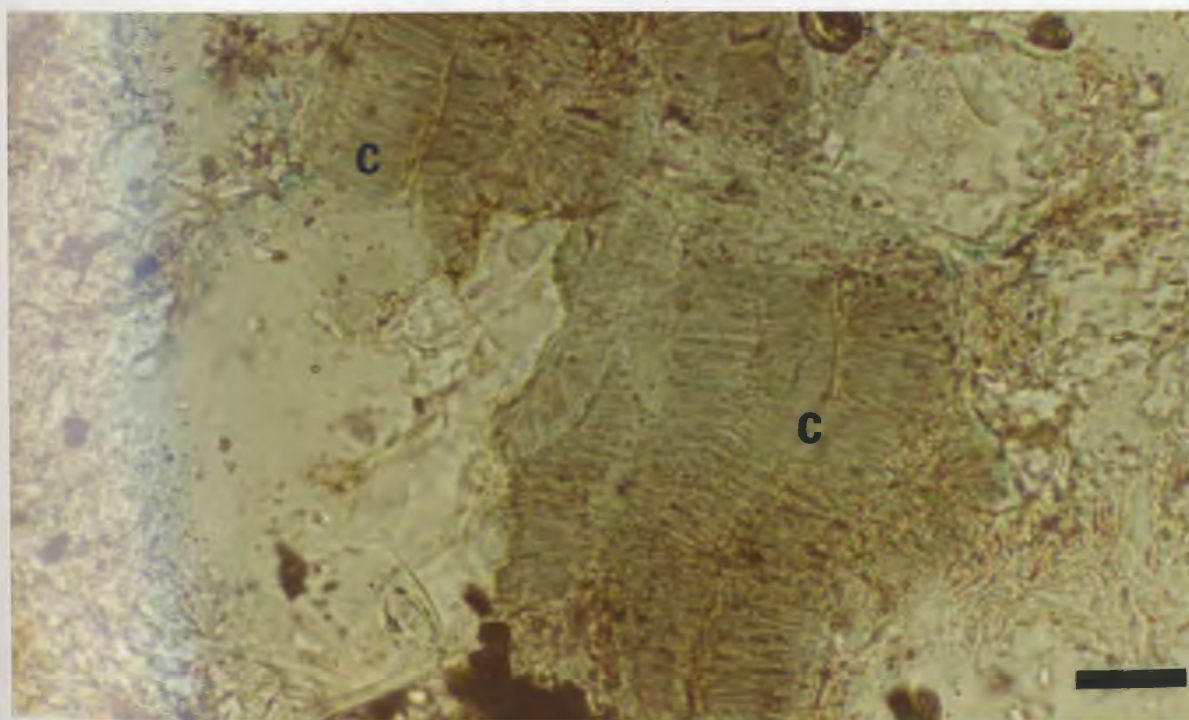
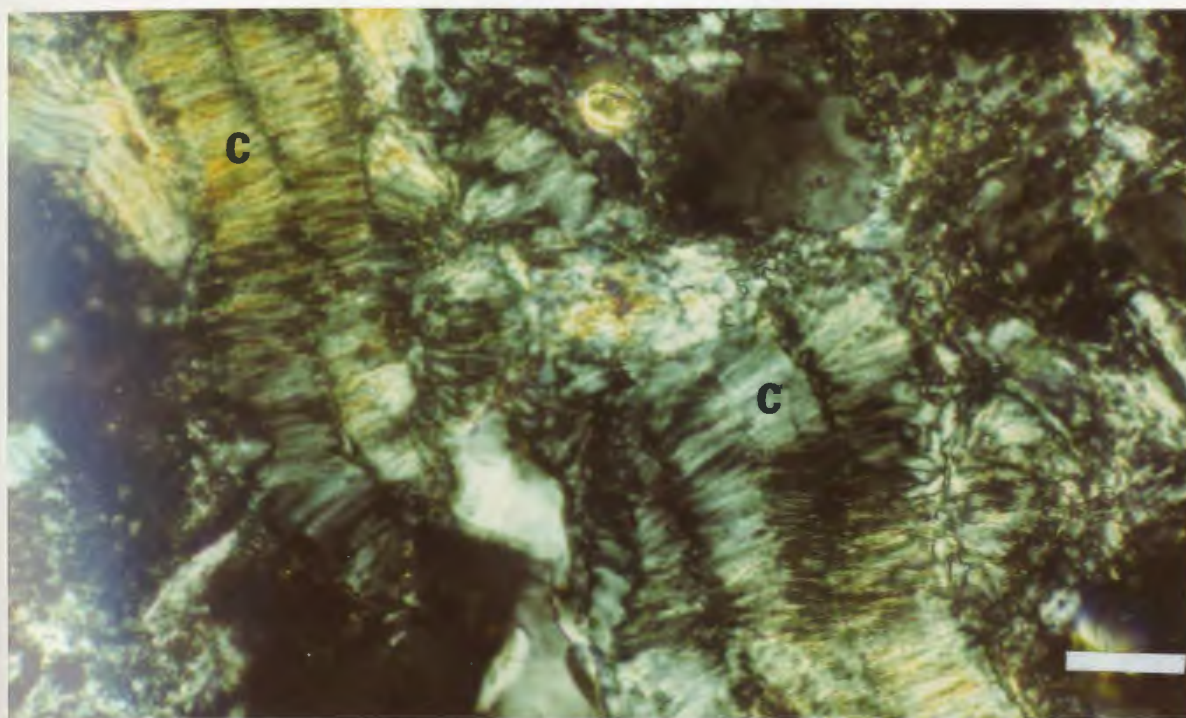


Figure 3.59. Highly birefringent chlorite rosettes appear to blend into the adjacent detrital grains (C). Bar scale 0.05 mm.

Figure 3.60. Same as figure 3.59 but in plane light. Bar scale 0.05 mm.

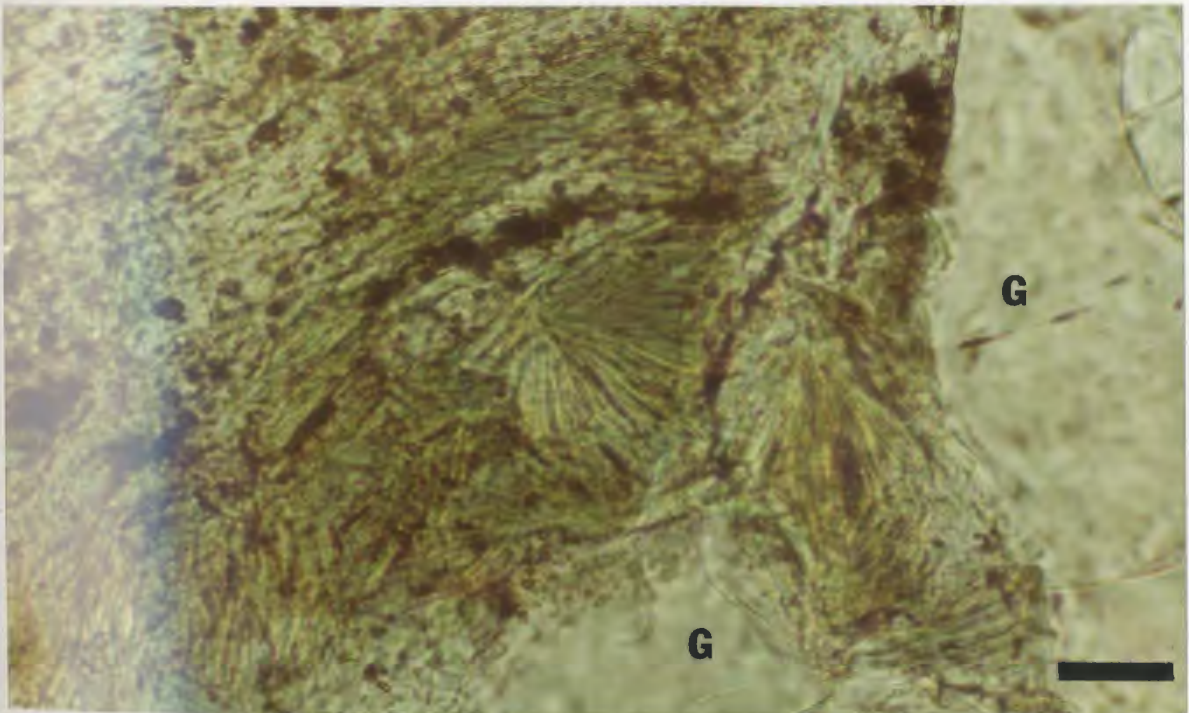
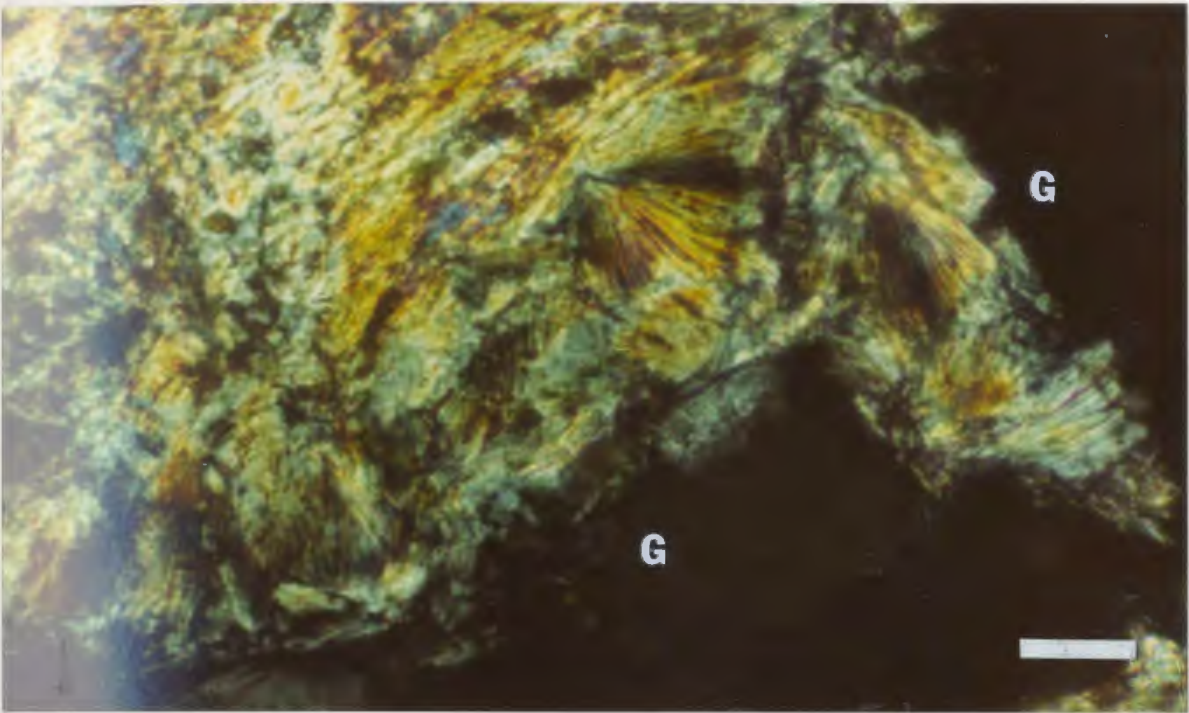
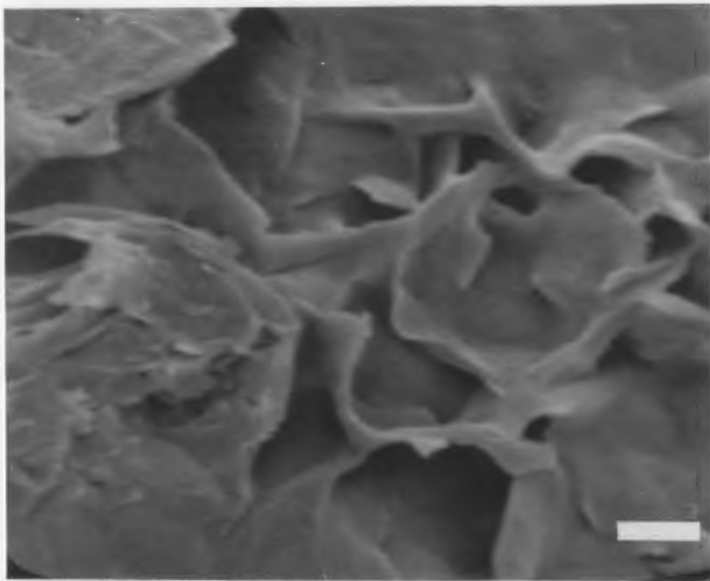
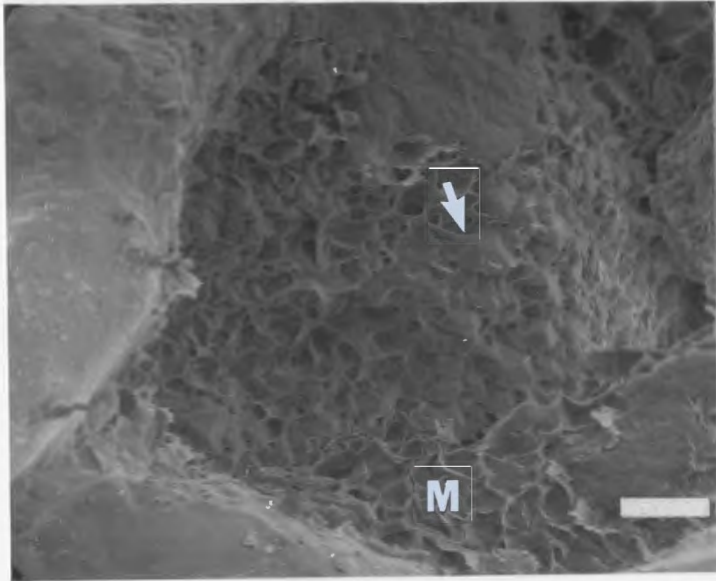


Figure 3.61. SEM photo of diagenetic montmorillonite (M) which appears to shroud earlier quartz overgrowths (arrow). Bar scale 10 μ .

Figure 3.62. SEM photo of montmorillonite showing its typical 'cornflake' morphology (c.f. Wilson and Pittman, 1979, p.64). Bar scale 2 μ .



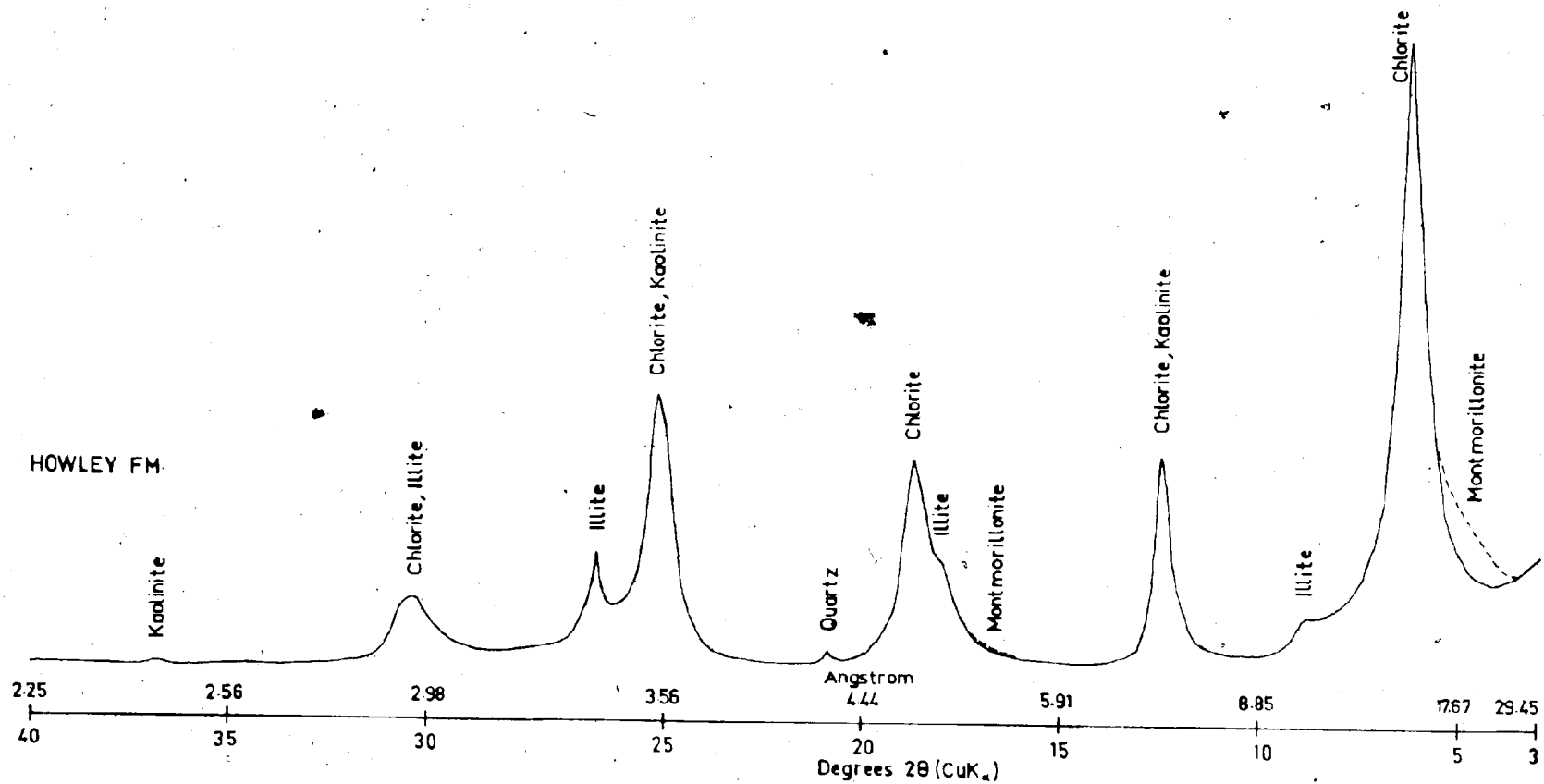


Figure 3.63 A composite clay-fraction diffractogram for the Howley Formation drill holes 79D-004 and 79D-005 (dashed line is peak position after glycolation).

Calcite cement is medium to coarsely crystalline and commonly corrodes the edges of detrital grains. Hematite cement is intergranular and relatively minor.

In thin section, secondary porosity is evident as dissolution voids left in microcline and plagioclase grains and in the interstitial diagenetic cements. The few sandstone porosity measurements that were made (Fig. 3.54) show a total porosity range of approximately 8-27 %, and also show that most of the pore space is effective. The increase in porosity with depth can not easily be correlated with any particular mineral trend, as there is a down-hole decrease in the relative amounts of montmorillonite, quartz grains, rock fragments, calcite and hematite cement, any one of which could account for such a porosity change.

3.5.3 Drill hole 79D-005 (D5)

Stratigraphy

Drill hole D5 consists of an upper section of sandstones overlain by thinner units of siltstone, and a lower section dominated by siltstones and mudstones with scattered thin units of sandstone (Fig. 3.64). Figure 3.65 shows some of the mixed sandstone-siltstone section near the top of the drill hole.

The greenish-gray to gray sandstones are arkosic in composition (Fig. 3.55), and generally medium to coarse grained and texturally immature. The intermixed siltstones and mudstones have a mottled colour due to patchy oxidation. The finer grained sediments are usually cross-laminated. Both the sandstones and finer grained sediments are poorly consolidated due to degradation before, during, and after drilling. The deteriorated state of the drill core prevented complete petrographic description.

Petrography

The detrital component of the sandstones consists dominantly of angular to subangular orthoclase and monocrystalline quartz grains, with lesser amounts of plagioclase, polycrystalline quartz, chert and plutonic rock fragments, biotite, muscovite, and accessory epidote grains (Fig. 3.64 and Appendix I). The grains have been compacted,

HOWLEY FM. 79D-005

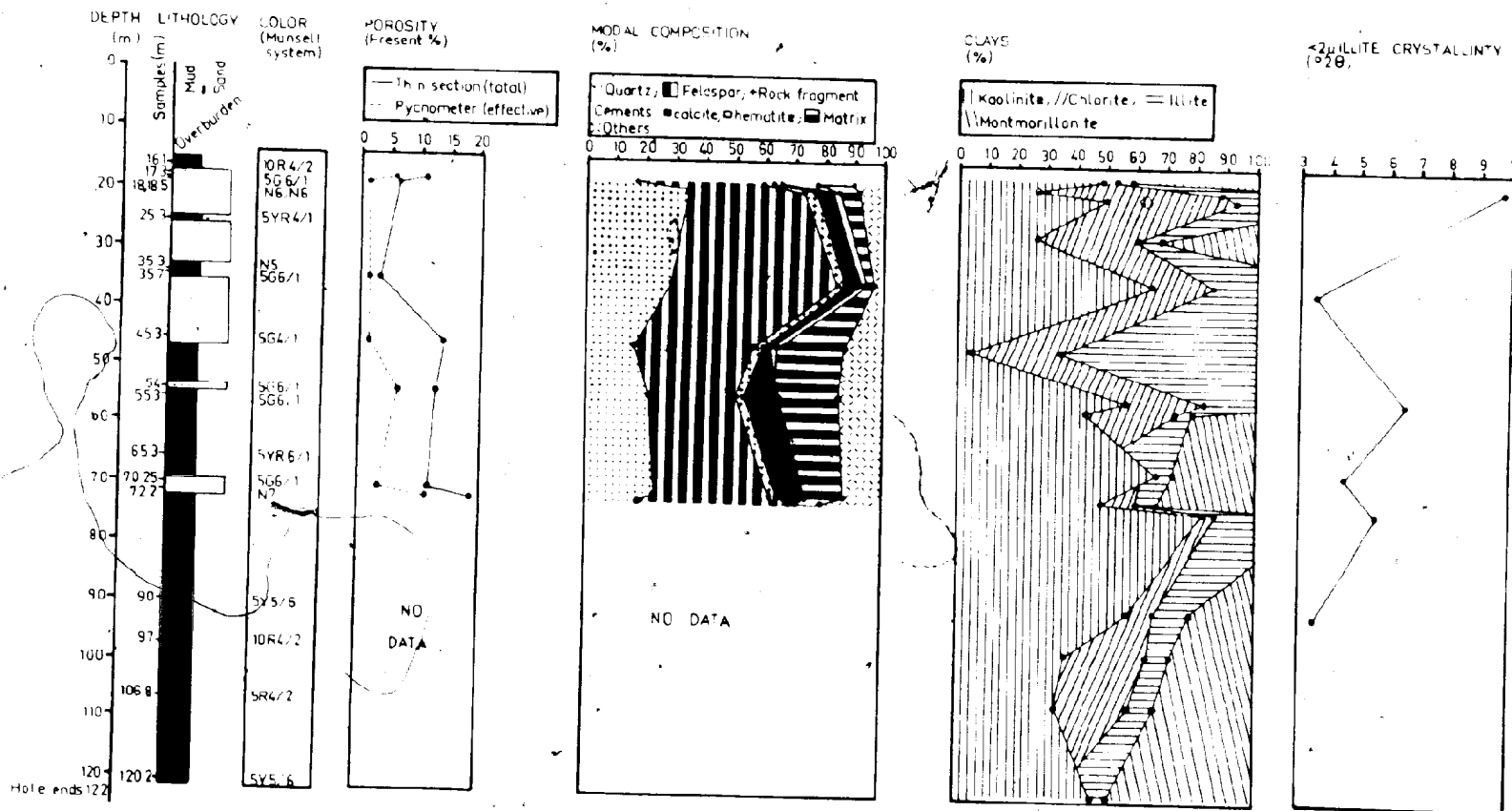


Figure 3.64 Stratigraphic and petrographic details for drill hole 79D-005.

Figure 3.65. Representative drill core from hole D5 (21-44.8 m), displaying cross-stratified, interlayered sandstones and siltstones, and the extensive recent weathering of part of the core.

Figure 3.66. Concavo-convex grain boundaries and quartz overgrowths (Q) accentuated by an oxidized dust rim (arrows). Bar scale 0.25 mm.



Figure 3.67. SEM photo of vermicular pore-filling macrokaolinite. Bar scale 20 μ .

Figure 3.68. SEM photo showing partial dissolution (arrow) of the macrokaolinite has resulted in an 'accordion' morphology. Bar scale 5.5 μ .

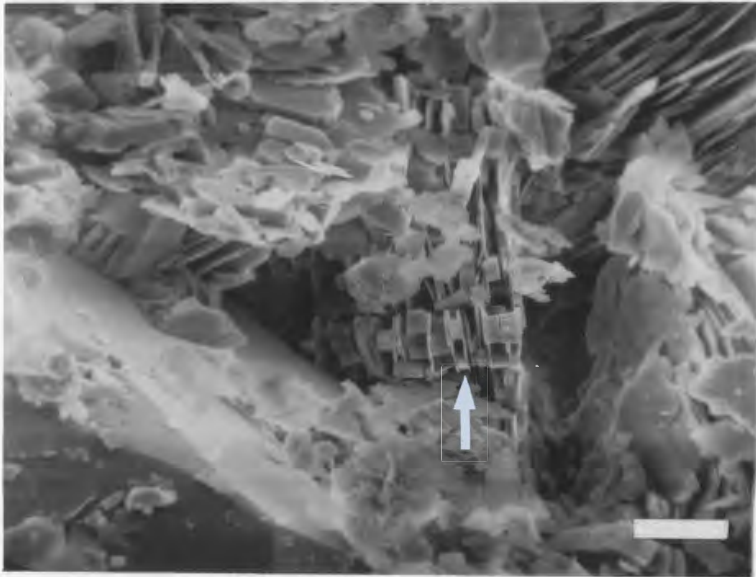
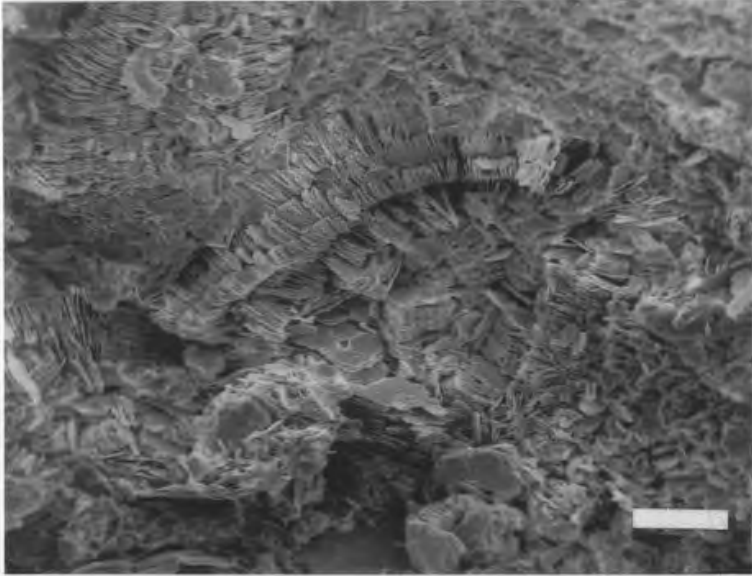
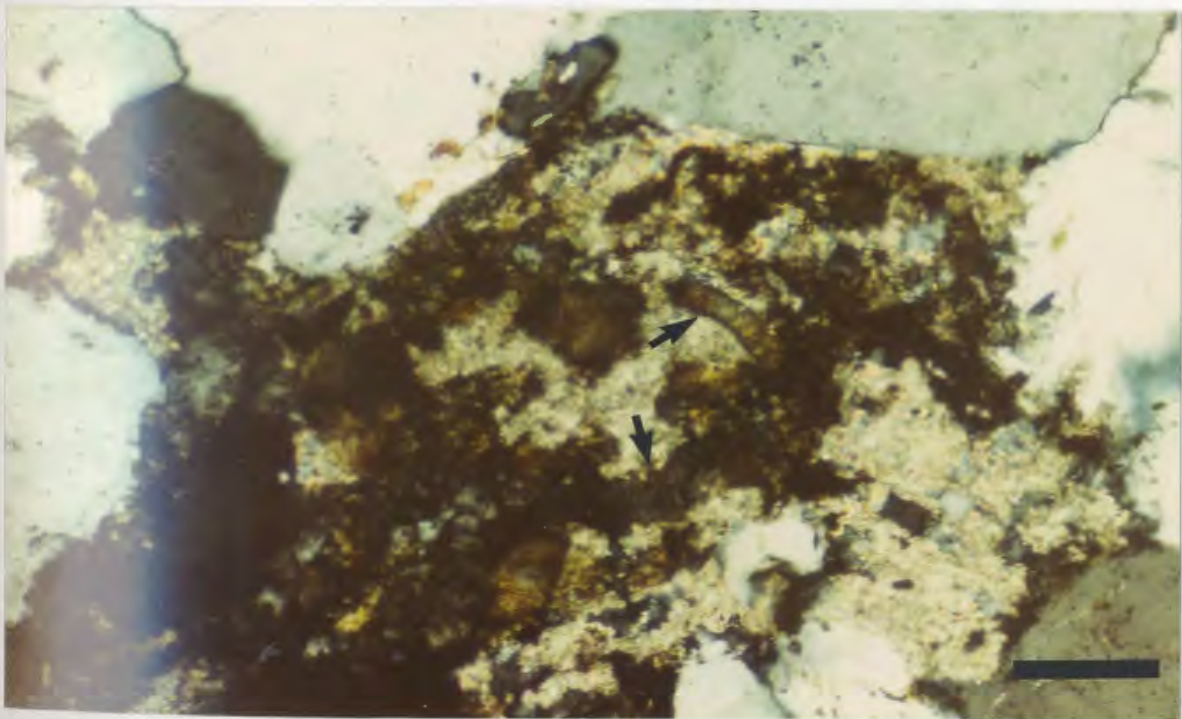
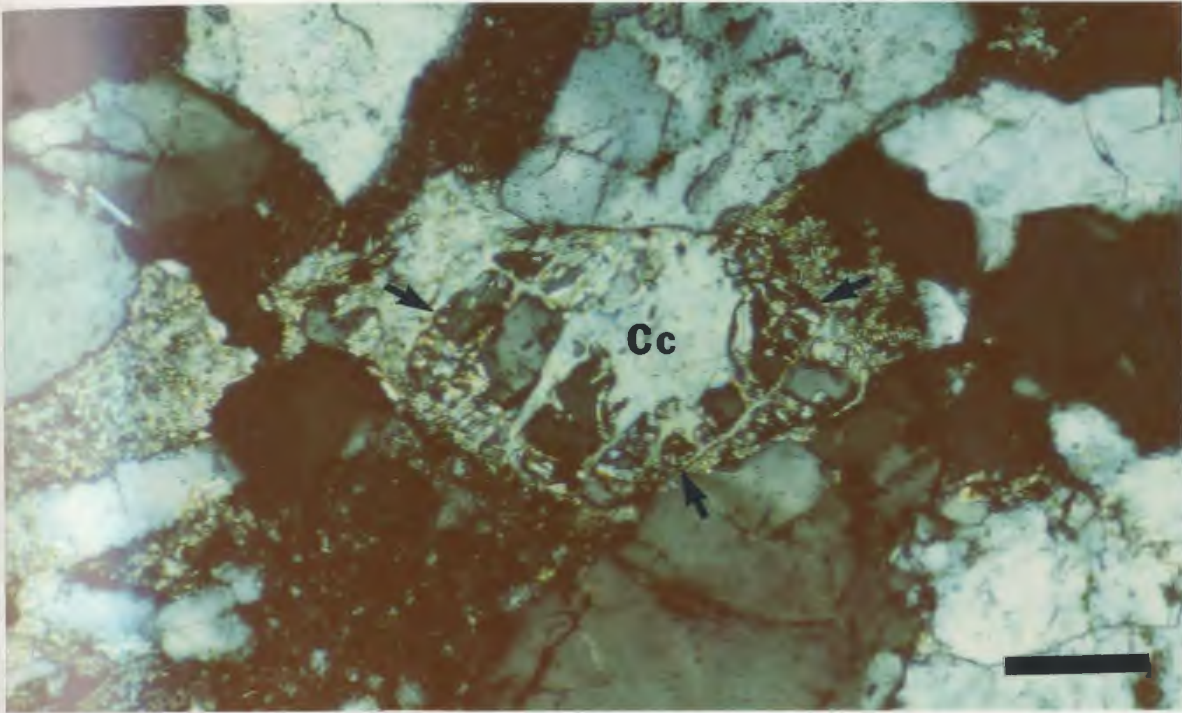


Figure 3.69. Calcite cement (Cc) has corroded a detrital silicate grain to the point where only the relic grain remains (arrows). Bar scale 0.25 mm.

Figure 3.70. Part of the paragenetic sequence is revealed here. Vermiform kaolinite (arrows) is enveloped and masked by a later stage of calcite cementation (c.f., Scholle, 1979, p.67 and 138). Bar scale 0.25 mm.



resulting in concavo-convex and sutured grain boundaries. Quartz overgrowths also occur (Fig. 3.66).

The interstitial material in the sandstones consists of a highly birefringent clay cement, kaolinite, illite, and minor silt-size quartz and feldspar grains. The highly birefringent clay cement may be finely divided illite, chlorite, or montmorillonite. Montmorillonite has only been identified by X-ray diffraction, and although it is possible some may have developed in the sandstones, Figure 3.64 indicates a strong correlation of montmorillonite with the siltstone-mudstone part of the sequence. Some of the highly birefringent clay matrix may be illite, but illite can be seen more readily as larger blades, growing on feldspars or interstitially. Therefore by elimination, a large part of the highly birefringent clay cement is inferred to be diagenetic chlorite, a conclusion supported by SEM study.

In thin section, vermicular booklets of macrokaolinite are intimately associated with potassic feldspar and quartz grains and commonly have a diffuse contact with the silicate grains. SEM photographs (Figs. 3.67 and 3.68) highlight the vermicular morphology of the kaolinite, and reveal that some of the kaolinite has been selectively leached, resulting in an 'accordion' morphology of alternating plates and pillars.

Coarsely crystalline calcite cement corrodes and disrupts the detrital grains, so that in places only relics of the original grain remain (Fig. 3.69). Development of

kaolinite and other diagenetic minerals prior to calcite cementation is suggested by the envelopment and masking of the vermiform kaolinite by calcite (Fig. 3.70), and by the corroded nature of the clay cements in general when in contact with the calcite cement. Some corrosion and staining of all the previously mentioned minerals by hematite cement is evident.

Pervasive secondary porosity appears to have been developed from the dissolution of feldspar grains, clay and calcite cements, and locally the late-stage hematite cement. Figure 3.64 shows that the total porosity ranges from 3-18 %, and that approximately half of that is effective porosity. The sandstones show slightly higher total porosities than the finer grained sediments, probably due to their coarser nature.

3.6 General discussion

The systematic analysis and description of the Carboniferous sediments from nine drill holes in the Deer Lake subbasin indicates that the sediments are generally lithologically and petrographically very similar. This is particularly true for the North Brook, Humber Falls, and Howley Formations; the shaly Rocky Brook Formation shows different characteristics. These stratigraphic and petrographic similarities allow some common traits and trends to be established. A discussion on the origin of each diagenetic mineral in the four formations is deferred until

the chapter on diagenesis.

The coarse grained North Brook, Humber Falls, and Howley Formations consist of interlayered polymict pebble conglomerates; texturally immature to submature sandstones; and siltstones, mudstones, and claystones. Grain size decreases up from the North Brook Formation (most conglomerate and least fine grained sediments) to the Howley Formation (no conglomerate and most fine grained sediments). This trend may reflect a general Late Carboniferous tectonic quiescence in the Deer Lake subbasin and the Maritimes Basin generally; or, it may be an apparent trend controlled by local facies variations and drill hole location. Patchy diagenetic reddening of these terrestrial siliciclastic sediments is due largely to diagenetic oxidation and hematite cementation, and permits them to be referred to as red-beds. An earlier stage of oxidation (dust rims) and natural mineral colouration, also played a role in the pigmentation of these sediments.

Sandstones of the North Brook, Humber Falls, and Howley Formations are composed of quartz, feldspar, rock fragments, muscovite, biotite and chlorite, and accessory amounts of epidote, sphene, zircon, and magnetite (Appendix, I).

Ternary QRF plots show that sandstones of the North Brook and Humber Falls Formations are arkoses and lithic arkoses, while the Howley Formation contains only arkoses. The majority of the rock fragments found in the sandstones and conglomerates are of granitoid intrusive, felsic volcanic, and metamorphic

origin, and can be traced to local basement lithologies. Diagenetic minerals, a quarter of the rock volume, include calcite, hematite, dolomite, quartz overgrowths, kaolinite, illite, chlorite, montmorillonite, and minor amounts of siderite, limonite and mixed-layer illite-montmorillonite. Illite-montmorillonite was only found in the North Brook and Humber Falls Formations.

The following generalities can also be made about the mineralogy of the three coarse grained formations. Detrital biotite is commonly bent, frayed, hematized or chloritized. Quartz cement consists of euhedral overgrowths on quartz grains, which grew before or during the development of the clay cement. Kaolinite occurs as large pore-filling vermicular books of attached face-to-face pseudo-hexagonal plates. It is also commonly associated with detrital quartz and potassic feldspar grains. Illite developed as blades or fibers from the alteration of feldspars or primary interstitial material. Three forms of diagenetic chlorite have been recognized: (1) individual platelets perpendicular and tangential to grain surfaces; (2) rosettes filling or lining pores; and (3) vermiform booklets within pores. Montmorillonite was only discernible as 'cornflake'-structured pore lining using SEM. Mixed-layer illite-montmorillonite was only detected by X-ray diffraction. First destructive carbonate and then hematite cementation occurred after clay cement development. Siderite and limonite are minor components. The North Brook Formation

contains more carbonate and hematite cement than the other two formations.

Unlike the coarse grained formations, the Rocky Brook Formation contains predominantly fine grained siliciclastic sediments and orthochemical and allochemical carbonate sediments. No conglomerates are present. Dominant minerals include calcite, dolomite, chlorite, illite, and montmorillonite. Dr. R. Hyde (pers. comm. 1983) has recently identified mixed-layer chlorite-montmorillonite in the Rocky Brook Formation. It is difficult to say how much of the clay minerals have been diagenetically developed. Illite crystallinity measurements (chapter five, section 5.3.4) suggest that most of the illite in the Rocky Brook Formation is diagenetic. Lesser amounts of detrital silt (quartz > feldspar > muscovite > biotite > organic material), and diagenetic "analcime", chalcedony, chert and barite are also present.

The major mineralogical differences from the three coarse grained formations are: the presence of "analcime"; and the absence, or near absence, of kaolinite in the Rocky Brook Formation.

An early and late stage of secondary porosity development can be identified in the three coarse grained formations. The early stage is due to silicate grain dissolution, especially plagioclase and microcline, whereas a later stage of pervasive dissolution has even affected the

late hematite cement. Because of late pervasive dissolution, it is not clear how much of the porosity can be attributed to each of the two stages of porosity development. Nor is it clear what controls the relationship between effective porosity and total porosity. Perhaps successive stages of cementation occluded the early pore space in the sandstones, and the present effective porosity is equal to the amount of late pervasive dissolution which followed. In the two Rocky Brook Formation drill holes a late-stage secondary intercrystal, vug and 'open' microfracture porosity is evident. Total porosity values for all four formations have a range of 5-25 %, with most of that being effectively connected.

CHAPTER FOUR
ECONOMIC GEOLOGY

4.1 Introduction

Geologic interest in the Carboniferous Deer Lake subbasin has centred around the discovery and economic assessment of coal, oil shales, uranium, and base metal potential (chapter one, section 1.3). This chapter examines the uranium-mineralized drill core and boulder samples, and coaly material found in drill core and surface trenches. Emphasis has been placed on the uranium-mineralized and coal samples for the following reasons: (1) a number of uranium anomalies were found in the two sampled Rocky Brook Formation drill holes; (2) while the geochemistry of the high grade uranium-mineralized sandstone boulders has been adequately investigated (Elias, 1981), it was felt that a more complete petrographic description of the boulder samples was needed; (3) coal was frequently found in the Humber Falls Formation drill core and in surface trenches; (4) vitrinite reflectance ranking of the coal can help determine diagenetic paleotemperatures. General discussion of the uranium mineralization and coal can be found in Fleming (1970), Hyde (1979b, 1981, in press), and Howse and Fleischmann (1982).

A recent summary of world uranium deposits by Derry (1980) demonstrates the importance of uranium mineralization in sedimentary rocks and along unconformities associated with sedimentary rocks. Uranium mineralization associated with

the Carboniferous rocks of the Maritimes Basin are examples of the Late Paleozoic to Early Tertiary 'sandstone' and 'unconformity' types of uranium deposits. The most significant deposits in the Maritimes Basin are associated with fluvial sandstones and the Horton - Windsor unconformity (Prest et al., 1969; Dunsmore, 1977a, b; Charbonneau and Ford, 1978; Kirkham, 1978; Hyde, 1981; Hyde and Ware, 1981; Knight, 1983). In the Deer Lake subbasin, Hyde (in press) has identified three types of uranium mineralization: (1) mineralization associated with the unconformity between the Deer Lake Group and Cambro-Ordovician carbonate rocks; (2) stratiform mineralization in the lacustrine Rocky Brook Formation; and (3) mineralized sandstone boulders overlying the northern body of the Humber Falls Formation. Only the last two types are discussed here.

4.2 Uranium mineralization

4.2.1 Mineralized sandstone boulders

The discovery in 1978 of high-grade uranium-mineralized sandstone boulders in basal till above the more northern body of the Humber Falls Formation at Wigwam Brook led to extensive surface exploration and drilling in that area. Minor in situ uranium mineralization has been found (Northern Miner, 1978), but because no such samples were available, only the boulder samples are described here. Figures 4.1,

4.2A and B, and 4.3 are based on thin section point counting and clay-fraction X-ray diffractograms from all the available high-grade mineralized boulder samples. Point count data are presented in Appendix I.

According to Elias (1981), all the mineralized samples reported here are high-grade samples collected from the Birchy, Wigwam, and Goose anomalies above the northern body of the Humber Falls Formation. Due to their close petrographic similarities, the following hand sample and thin section descriptions can be used to describe uranium-mineralized boulder samples from all three anomalies.

All the samples are coarse to fine grained sandstones. The majority of the samples are grayish- or blackish-red in colour due to a late stage of hematite cementation around and within the opaque mineralization. The samples commonly show a paler, light gray or red weathered surface. Accompanying the surface weathering is a visible increase in porosity. In hand sample the most noticeable feature of the boulder samples is their very high degree of induration. This is due to extensive cementation by uraninite and hematite. No primary or secondary structures were seen in the hand samples.

In thin section the detrital grains, in order of abundance, are as follows: feldspars (orthoclase > plagioclase > microcline > perthites), quartz (monocrystalline > polycrystalline), rock fragments (plutonic

MINERALIZED SAMPLES

ANOMALY*	SAMPLE	LITHOLOGY*	COLOUR (Munsell system)	MODAL COMPOSITION†					CLAYS*					POROSITY (Present total %)	URANIUM (ppm)	<2μ ILLITE CRYSTALLINITY (°2θ)
				0%	20	40	60	80	100	0%	20	40	60			
Birchy	40523		5R4/2	[Modal Composition Diagram]					[Clays Diagram]					0.8	30,441	5
	40524		5R2/2	[Modal Composition Diagram]					[Clays Diagram]					2.4	101,057	
	40525		5R2/2	[Modal Composition Diagram]					[Clays Diagram]					1.6	35,037	
	40526		5R4/2	[Modal Composition Diagram]					[Clays Diagram]					0.0	39,604	6
	40527		5R4/2	[Modal Composition Diagram]					[Clays Diagram]					0.0	18,837	
Wigwam	40518		10YR5/4	[Modal Composition Diagram]					[Clays Diagram]					10.9	10,461	75
	40519		10R5/4	[Modal Composition Diagram]					[Clays Diagram]					10.0	150	35
	40522		10R5/4	[Modal Composition Diagram]					[Clays Diagram]					4.4	875	55
	40471		10R3/4	[Modal Composition Diagram]					[Clays Diagram]					7.2	23,272	
Goose	40513		10YR5/4	[Modal Composition Diagram]					[Clays Diagram]					13.6	754	
	40514		10YR6/2	[Modal Composition Diagram]					[Clays Diagram]					15.6	272	
	40515		10YR6/6	[Modal Composition Diagram]					[Clays Diagram]					0.0	130	
	40516		5YR4/4	[Modal Composition Diagram]					[Clays Diagram]					12.8	210	
	40517		N6	[Modal Composition Diagram]					[Clays Diagram]					18.4	74	
	5261		10R4/2	[Modal Composition Diagram]					[Clays Diagram]					13.3	213	
	5263		10YR5/4	[Modal Composition Diagram]					[Clays Diagram]					10	292	

* Elias, P. 1981. Private report for Westfield Minerals

† Sandstone: [] coarse, [] medium, [] fine

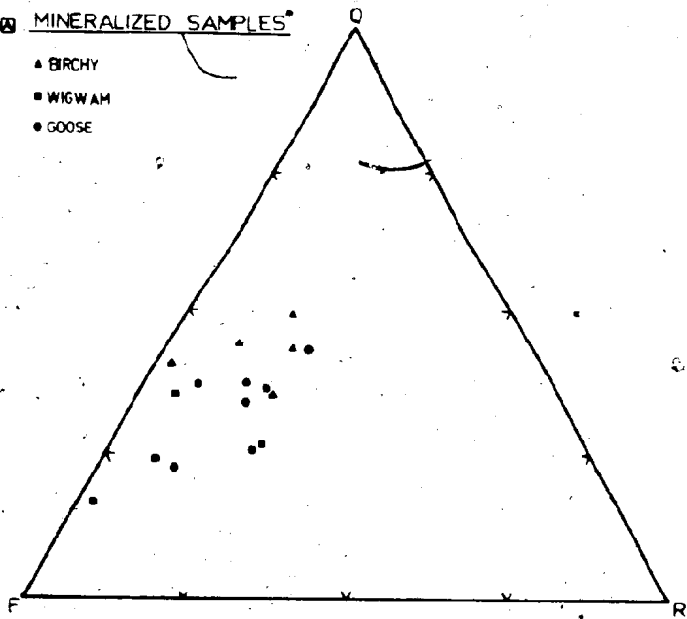
‡ Quartz [], Feldspar [], Rock fragment [], Cements: calcite [], hematite [], uraninite [], Matrix []; Others []

§ Kaolinite [], Chlorite [], Illite [], Montmorillonite []

Figure 4.1 Petrographic details for the uranium mineralized boulder samples.

MINERALIZED SAMPLES

- ▲ BIRCHY
- WIGWAM
- GOOSE



• Names after Elias 1981

COMPARATIVE PLOT

- ◆ MINERALIZED SAMPLES
- ◆ HOWLEY FM.
- ◆ HUMBER FALLS FM.
- ◆ NORTH BROOK FM.

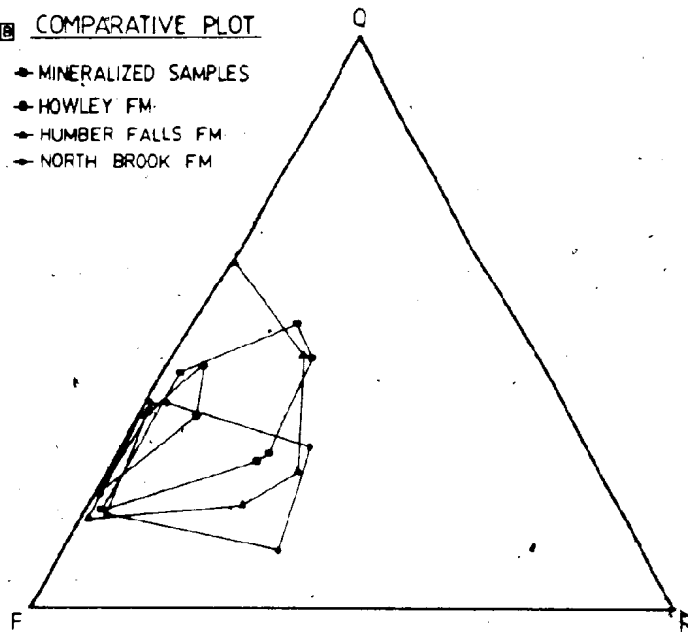


Figure 4.2 QRF classification diagrams showing:
(A) the arkosic composition of all the mineralized boulder samples;
(B) a comparative plot delineating the compositional fields for all the groups of sandstone samples which were studied.

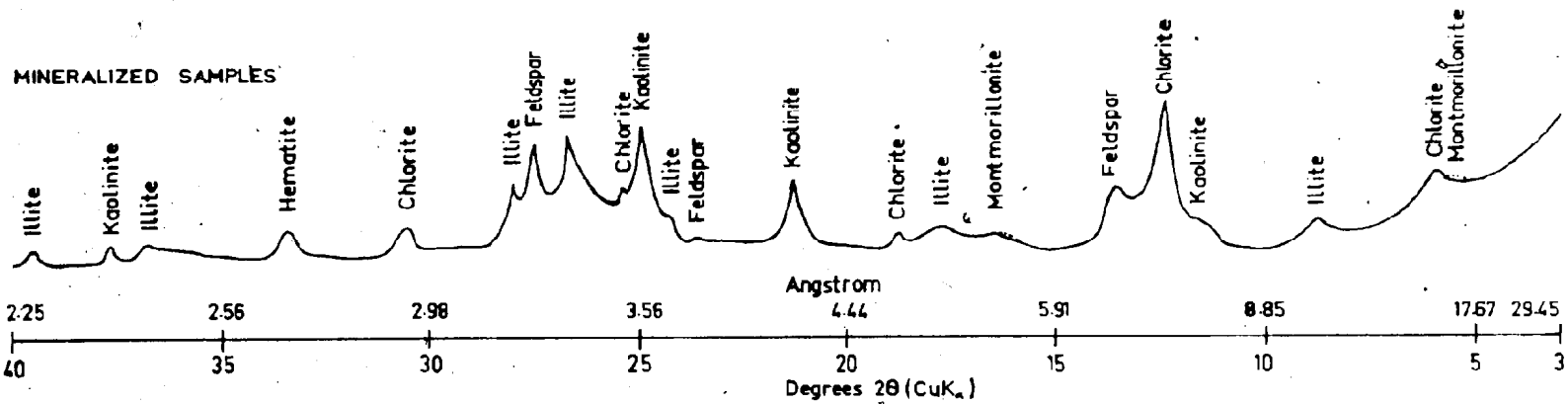


Figure 4.3 A composite clay-fraction diffractogram for the mineralized boulder samples.

> metamorphic > chert), minor muscovite and biotite, and accessory amounts of epidote and zircon (Fig. 4.1). These detrital grains are subangular and subrounded sand-sized grains. The Wigwam anomaly samples show better sorting on the whole than the samples from the other anomalies. The sandstones are texturally submature to immature (Folk, 1980). As shown in Figure 4.2A, the mineralized samples consist of arkoses and lithic arkoses, with the Wigwam anomaly samples being generally more feldspathic. Plagioclase and orthoclase grains are typically illitized and kaolinitized and show the most extensive development of intragranular dissolution porosity. Detrital mica grains have been crushed and bent by compaction around the larger grains.

The interstitial material is composed of clay minerals and minor amounts of silt-size detrital quartz and feldspar grains. Medium crystalline calcite was only observed in the Birchy anomaly samples. Kaolinite, illite, chlorite, and montmorillonite are present in varying amounts (Figs. 4.1 and 4.3). In many samples, diagenetic vermiform kaolinite is developed adjacent to the larger detrital grains, and is most abundant in the Goose anomaly samples. Illite appears as very small fibres in degraded plagioclase and microcline grains, or within the interstitial cement. Kaolinite commonly intervenes between the illite and detrital framework grains. This relationship suggests that the diagenetic illite formed just after the kaolinite. Some of the illite depicted in Figures 4.1 and 4.3 represents detrital micas.

Very fine fibres of chlorite were also identified within the matrix material; no larger flakes of chlorite were seen in the thin sections. Montmorillonite was only identified by X-ray diffraction (Fig. 4.3).

A yellow mineral, possibly uranophane, was associated with the uraninite in many of the thin sections (Fig. 4.4). It appeared to disrupt some of the detrital framework grains and stained some of the other interstitial minerals yellow. The uraninite, analysed and identified by Elias (1981), commonly fills all the interstitial space, disrupts and fractures the detrital grains (Fig. 4.5), and corrodes previously developed interstitial material, including the calcite cement. An article in the Northern Miner (1978) reports that four boulder samples were assayed at 7.6, 28, 34.2, and 230 lb U_3O_8 per ton. Assays up to 890 oz per ton Ag, in the form of acanthite, have also been noted in some of the boulders (Vanderveer and Tuach, 1982).

Locally, pyrite has developed interstitially, where it partly replaces previously developed interstitial material. Many of the pyrite cubes are rimmed by hematite which in turn has stained the matrix material red. The uraninite is also rimmed by hematite (Fig. 4.6). Elias (1981) states that "The uraninite appears to be intimately intergrown with hematite, suggesting co-precipitation". Instead, it appears that hematite cementation occurred after the mineralization and not during mineralization as proposed by Elias (1981). No organic material was seen in thin section, although some

Figure 4.4. Uranophane (yellow) has fractured and corroded the silicate grain (G) and has in turn been rimmed by hematite cement (arrow). Bar scale 0.25 mm.

Figure 4.5. Opaque uraninite filling pore space and fractures in detrital silicate grains. Bar scale 0.25 mm.

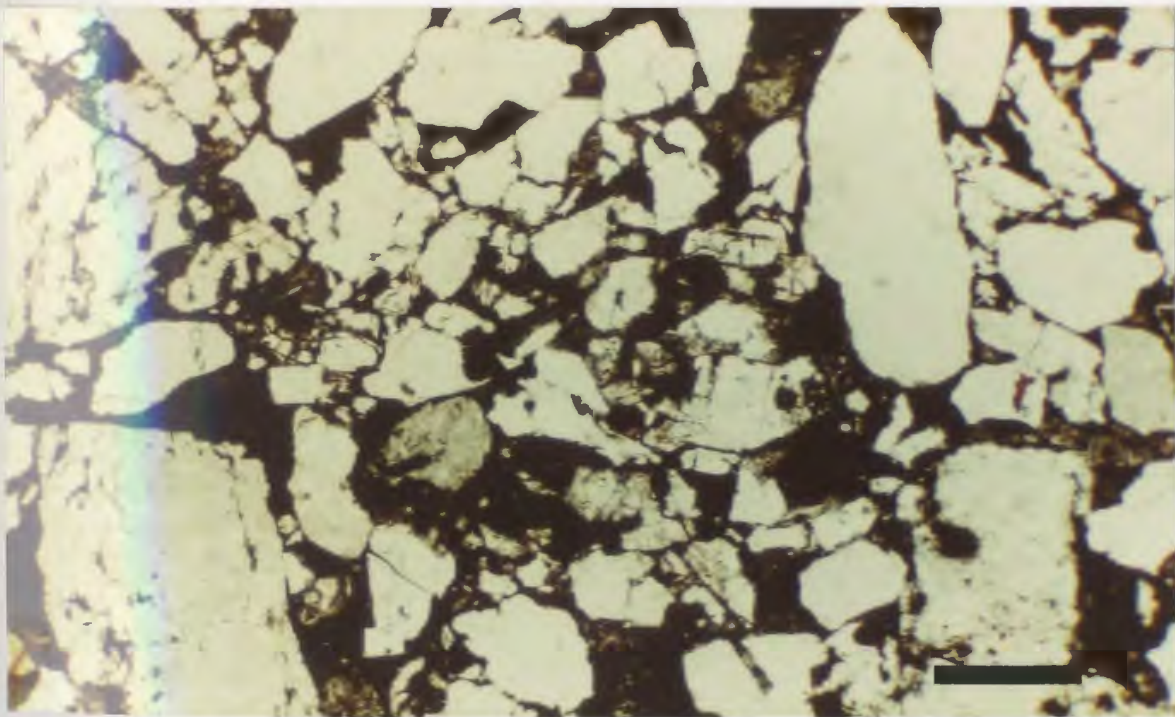
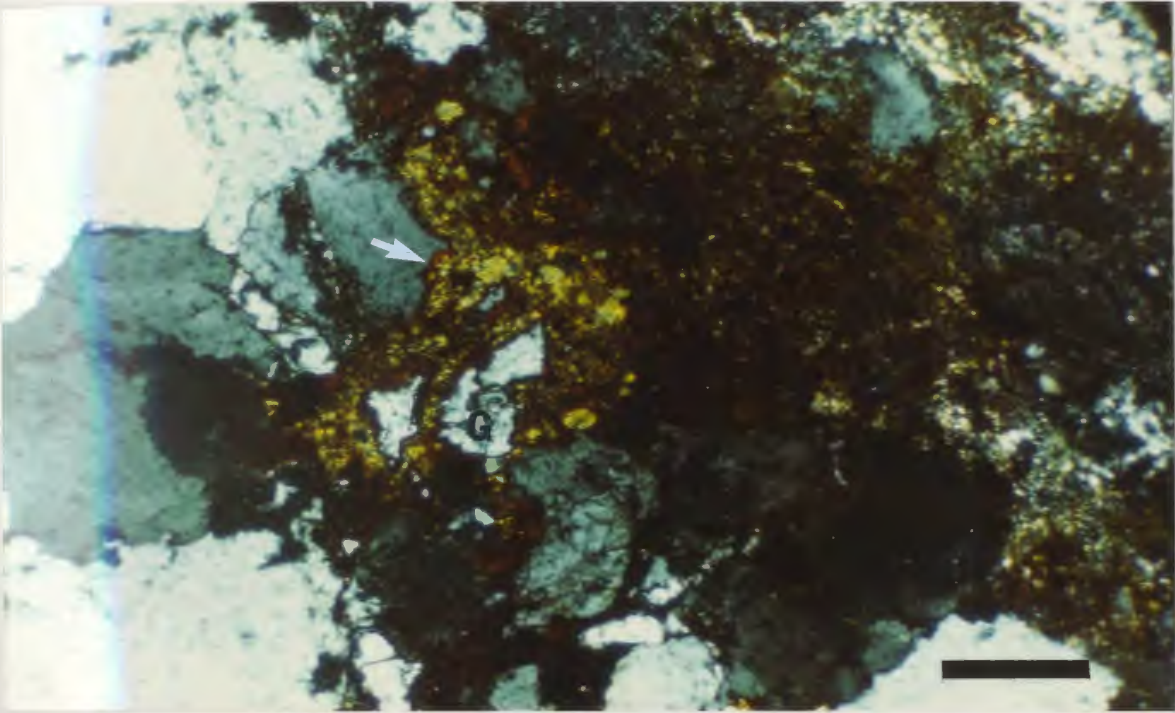
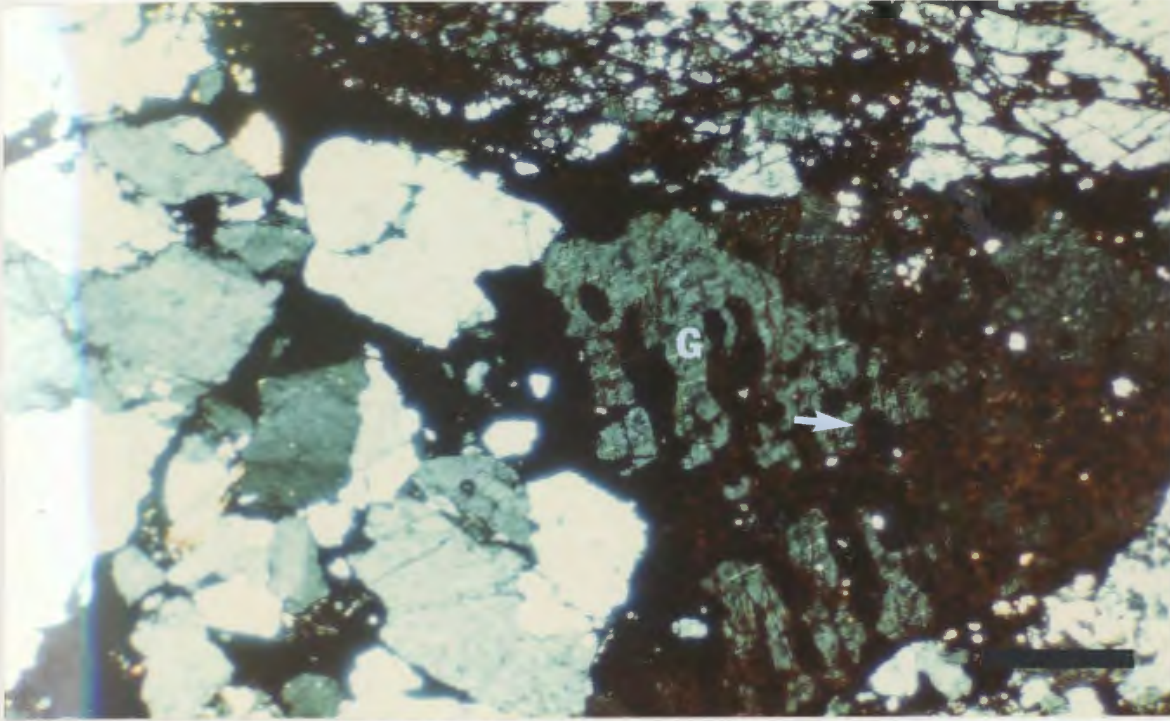


Figure 4.6. Opaque uraninite has corroded a feldspar grain (G) and has in turn been rimmed by a later stage of dark red hematite cement (arrow). Bar scale 0.25 mm.



has been found in the boulders (J. Tuach, pers. comm. 1983).

Total porosity ranges from approximately 0-18.4 % in the mineralized boulder samples (Fig. 4.1). From thin section inspection, the majority of the porosity appears to be due to extensive feldspar dissolution. In some feldspar grains the dissolution has been extensive enough to give the grain a delicate cobweb appearance. Effective porosity was not recorded as only some high-grade hand samples were available, and those that were available were in poor physical condition. It is worth noting how similar in composition and texture the mineralized boulder samples are to the sandstone samples from the Deer Lake Group and Howley Formation that were described in chapter three (Figs. 4.1 and 4.2).

4.2.2 Uranium-mineralized drill core

Both Rocky Brook Formation drill holes (A3 and A5) contain thin radioactive horizons less than five centimetres thick. These horizons occur in laminated gray to greenish-gray calcareous claystones, calcareous mudstones, and argillaceous limestone. In thin section, the radioactive samples consist of crystals of pyrite and flakes of organic material disseminated throughout the mottled, fine grained clay and carbonate minerals. These samples have essentially the same petrographic properties as the unmineralized Rocky Brook Formation samples. Consequently, the petrographic description in chapter three for the fine grained sediments

in drill holes A3 and A5 can also be used to describe the uranium-mineralized samples in the Rocky Brook Formation. Uranium mineralization is not visible in these fine grained sediments. A few trace element analyses (Appendix II) of mineralized and unmineralized samples from the two drill holes indicate that the radioactivity is largely due to uranium with some contribution from its daughter products.

Similar radioactive stratiform horizons have been described by Hyde (1979a, b) from the Spillway and Squires Park Members of the Rocky Brook Formation. He has identified five or six low-grade zones up to 1.3 m thick. Mineralization was again too fine grained to be discerned. A feature seen by Hyde, but not seen in the drill hole anomalies, was uraniferous solid hydrocarbon nodules.

4.2.3 Discussion

The uraniferous fine grained siliciclastic and carbonate sediments of the Rocky Brook Formation have a disseminated stratiform distribution. The uranium mineralization has not been found within fractures. This suggests to Hyde (in press) and the writer that the uranium mineralization in the Rocky Brook Formation is syngenetic or very early diagenetic.

In discussing the type and origin of the uranium in the lacustrine sediments, it is constructive to include the most plausible source, and mode of transport and deposition. During the time of development of the Rocky Brook Formation

lake, both external and internal sources for the uranium may have existed. Externally, Siluro-Devonian felsic volcanic and granitic rocks to the north and east of the Deer Lake subbasin most likely contained many possible uranium-bearing minerals that could have released uranium or uranyl complexes upon leaching (Stuckless and Ferreira, 1976; Rich et al., 1977; Komarov et al., 1982; Ford and Ballantyne, 1983). Uranium may also have come from granitoid rocks of the Long Range inlier, where uraniferous pegmatites have been reported (Fritts, 1953). Leaching of uranium by ground waters moving through the underlying North Brook Formation may have constituted an important internal source for the uranium. An early stage of silicate dissolution in the North Brook Formation sediments supports this possibility.

It is difficult to state in what chemical form the uranium was transported and then deposited in. The presence of uraniferous carbonates in the Rocky Brook Formation suggests transportation in di- or tri-carbonate complexes under basic conditions, perhaps with the aid of evaporitic pumping (Rich et al., 1977; Langmuir, 1978). The association of mineralization with organic-bearing and clay-rich siliciclastic sediments raises the additional possibility that transportation of uranyl complexes may have taken place through leaching and chelation by organic acids (Huang and Keller, 1972; Fitch, 1980), or by adsorption onto detrital clays, especially montmorillonite (Davey and Scott, 1956; Tsunashima et al., 1981).

Uranyl ions are typically taken out of solution at reduced sites in the sediment or at the sediment-water interface. In the dark coloured siliciclastic sediments of the Rocky Brook Formation, organic material, pyrite, hydrocarbons, and H_2S could have acted as reducing agents. The presence of uraniferous bitumen nodules indicates that hydrocarbons were an influence in fixing uranium (c.f., Curiale et al., 1983). Apparently, fluctuations in pH may influence uranium solubility and precipitation as much as Eh (Langmuir, 1978). Thus it is apparent that several mechanisms could have led to the disseminated, stratiform distribution of uranium mineralization in the Rocky Brook Formation.

The uranium-mineralized boulders, and few exposures of in situ mineralized Humber Falls Formation, show many similarities to sandstone-type uranium deposits as described by Garrels and Larsen (1959), Harshman (1970), Fischer (1974), and Adams et al. (1973). The following are some of the more direct similarities between the mineralized sandstones in the Deer Lake subbasin and sandstone-type deposits: (1) on a regional scale, the deposits are located in tectonically active intermontane continental basins; (2) the deposits are flanked by felsic volcanic and granitic highlands, likely sources for the uranium; (3) the uranium mineralization is in fluvial arkoses; (4) these sediments are interlayered with finer grained sediment forming a red-bed sequence, in which the sandstone may act as a permeable conduit for mineralizing fluids; (5) as in many of

the Colorado Plateau deposits, pore-filling uraninite is a major uranium-bearing mineral, and is commonly associated with organic material and pyrite.

A study of glacial till in the Deer Lake subbasin by Rogerson (1981) showed that ice transport was from the northeast or the southwest along the subbasin axis, and that the till was immature and had not travelled more than ten kilometres. Therefore, in an attempt to determine a local source for the boulders, a comparative QRF diagram was made (Fig. 4.2B), including the compositional fields for arkosic sandstones of the Deer Lake Group and Howley Formation and the mineralized boulder samples. The mineralized samples are most similar to the Humber Falls Formation sandstones. Magnetic susceptibility measurements from the mineralized boulders also show greatest similarity to sandstone samples from the Humber Falls Formation (Dr. H. Miller, pers. comm. 1983). Both of these independent results, and discovery of the mineralized boulders in till above the northern body of the Humber Falls Formation, strongly suggest that the boulders were locally eroded from the Humber Falls Formation by glacial ice. The mineralized bedrock may, however, have been an isolated occurrence, and may have been entirely removed by glacial erosion.

There are two possible sources for the uranium found in the mineralized sandstone boulders and in the in situ mineralized strata in the northern body of the Humber Falls Formation. Externally, there are the same source terranes

proposed for the Rocky Brook Formation mineralization. A second, internal, source for the uranium has been proposed by Hyde (in press), who contends that the Wigwam Fault, which delimits the eastern margin of the northern body of the Humber Falls Formation, may penetrate the underlying Rocky Brook Formation. If this is so then reductants in the Rocky Brook Formation (e.g., H_2S gas) may have migrated up along the fault and then out into the overlying porous Humber Falls Formation sandstones. A later upwelling of uranium-bearing fluids from the Rocky Brook Formation along the faults may have brought about uranium precipitation within the tongue of reduced sandstones in the overlying Humber Falls Formation. This situation would be similar to the stacking of uranium ore bodies along faults as described by Fitch (1980). This hypothesis is supported by the presence of a reduced tongue of sediment within the Humber Falls Formation that extends westward away from the Wigwam Fault (Hiscott, 1980). As well, there are pores and fractures filled by pyrite in the sediments adjacent to the fault, which may have been developed with the aid of reductants escaping from the Wigwam Fault. Uraniferous coalified tree fragments have also been found by surface trenching within the same area. The tongue of unoxidized sediment also correlates with a magnetic tongue (Dalley, 1982), and some U-Cu-Mo anomalies (Furey, 1982).

The silver in one of the sandstone boulders is also of economic interest. Silver will undergo dissolution-transportation-precipitation in much the same way

as uranium (Boyle, 1968; Rich et al., 1977). That is, silver can be mobilized and transported in an oxygenated state by acidic and alkaline solutions and then precipitated by decomplexing in relatively reduced areas (e.g., by carbonaceous material). Most U-Ag mineral deposits have been classified as hydrogenic (McMillan, 1979). Generally these deposits are associated with veins, unconformities, or the minerals are disseminated in dark, fine grained sediments (McMillan, 1979; Rich et al., 1977). In the Carboniferous sediments of the Maritimes Basin, the writer is only aware of one other occurrence of acanthite, but there is no uranium associated with this deposit. The Ba-Pb-Zn-Cu-Ag mineralization within the Wilton Formation in Nova Scotia is found in lenses of reduced sandstone and brecciated sediments, respectively, adjacent to and within a fault zone (Boyle, 1963). Boyle (1963) believes that the silver migrated along the faults after being mobilized from underlying Carboniferous sediments, and/or was leached from overlying mafic intrusives. The silver in the uraniferous boulders in the Deer Lake subbasin may have been derived from similar sources. Internally the silver may have been mobilized from the argillaceous lacustrine sediments of the Rocky Brook Formation along faults, such as the Wigwam Fault; the silver may also have been leached from felsic volcanic or plutonic rocks by meteoric waters or by solutions within faults where the faults cut both the Carboniferous sediments and underlying felsic igneous country rocks. Both fine grained sediments and felsic igneous rocks are known to

contain higher than normal silver values (Boyle, 1968).

The general diagenetic sequence does not instill optimism that significant amounts of uranium ore will be found in the Humber Falls Formation. Late-stage oxidation and hematite cementation in the mineralized and unmineralized sandstones suggests that some of the uranium that was present may have been remobilized by the oxygenated fluids. Some of the uranium flushed out of the sediments by the oxygenated fluids may have been deposited along the unconformity between the Deer Lake Group and Cambro-Ordovician carbonate basement rocks, where minor mineralization now exists (i.e., Hyde's type I deposit, in press). It is probable that only isolated pods of uranium mineralization still exist in the northern body of the Humber Falls Formation, particularly around organic matter. These could only be detected by closely spaced drill holes, especially along the down-dip side of redox fronts once they are established. In my opinion, however, prospects for economic ore bodies are slim.

4.3 Coal

4.3.1 Coal petrology

In the Deer Lake subbasin, coal has been found as thin in situ coal seams and partings within a strip of the Howley Formation along the northeast shore of Grand Lake, and as coaly plant trash and thin laminations in the older Carboniferous formations. In this section, coaly material found during the systematic sampling of the nine representative drill holes, and similar material collected from trench sampling in the northern body of the Humber Falls Formation, is examined. A summary of the in situ coal from the Howley Formation is given first.

Coal seams and partings in the Howley Formation are, of Westphalian A age and thus correlate with the Barachois Group coal in the Bay St. George subbasin, and with late Cansoan - early Riversdalian coals of the Maritime Provinces. Howse and Fleischmann (1982) described the seams as occurring in interbedded greenish-gray and red sandstones and siltstones with intimately associated ironstone nodules. Based on criteria outlined by Collinson (1978) (e.g., sediment mottling, ferruginous nodules, carbon films and rootlets), they interpret these deposits as part of a paleosol. The seams, which are up to two centimetres thick, have been ranked as high-volatile bituminous B coal by Hayes (1949) with the following properties: 54.03 % fixed carbon, 8.66 % ash, 1.04 % sulphur. Hacquebard and Donaldson (1970) results

differ from Hayes (1949) in that they rank the Howley Formation coal as high-volatile bituminous A with 61-64 % fixed carbon. The same coal-bearing strata also yield two to three times background radioactivity (Howse and Fleischmann, 1982).

Coincidentally, all seven samples of coaly material found in drill core came from three drill holes (80-70, 79-29, and 79-69) within the northern body of the Viséan Humber Falls Formation, the same area in which the four available trench samples were collected by Dr. D. Strong. Coaly material was noticed in drill hole DDH 79-28 (abbr. 79-28) during a quick reconnaissance of some of the available drill core, and was sampled for comparison.

All four trench samples were collected along Wigwan Brook (Table 4.1). Three of them are unmistakably coalified wood fragments exhibiting a fibrous 'woody' surface. These samples are dark brown in colour with lighter reddish-brown patches of surface oxidation. Their very high induration is probably due to disseminated pyrite in the samples, and possibly some uranium mineralization (Table 4.1). Polished grain mounts of these three samples yield structured (telinite) and structureless vitrinite group macerals, and inertinite group macerals. The structureless vitrinite group maceral can not easily be categorized using the three-fold vitrinite maceral classification of Stach et al. (1975) (i.e., telinite, collinite, and vitrodetrinite). Apart from its structureless appearance, it looks most similar to

Table 4.1 Summary of trench and drill core sample properties.

Sample	\bar{R}_{oil}^{max} *	δ	Macerals**	Radioactivity(cps)
Trench				
DFS 81-30	0.99	0.09	Fusinite(I) Semifusinite(I) Structureless(V)	50
DFS 81-31	0.61	0.07	Structureless(V) Telinite(V)	--
DFS 81-34	0.62	0.06	Structureless(V) Semifusinite(I)	--
DFS 81-35	--	--	Fusinite(I) Semifusinite(I) Macrinite(I)	150
Drill core				
80-70 12	0.68	0.04	Structureless(V)	--
80-70 18.8	0.74	0.05	Structureless(V) Telinite(V)	--
80-70 27.8	0.63	0.04	Structureless(V) Telinite(V)	--
80-70 49.4	0.68	0.06	Telinite(V)	--
80-70 68.3	0.65	0.04	Structureless(V)	--
79-29 34.4	0.97	0.11	Telinite(V) Fusinite(I) Sclerotinite(I)	--
79-28 35.4	0.81	0.11	Telinite(V) Semifusinite(I)	--

* $n_{oil} = 1.518$, $n_{glass\ standard} = 0.940$

** (V) from vitrinite maceral group
(I) from inertinite maceral group

Figure 4.7. Cellular vitrinite maceral. Bar scale 0.25 mm.

Figure 4.8. Cellular inertinite maceral. Bar scale 0.25 mm.

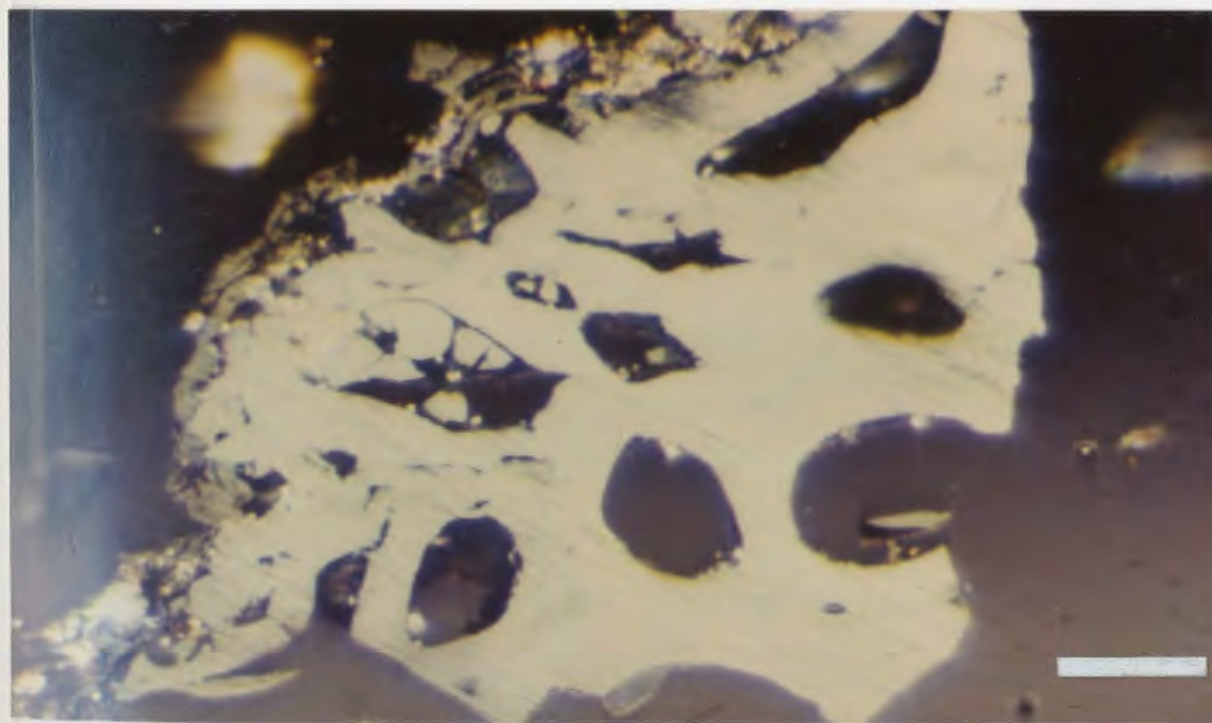
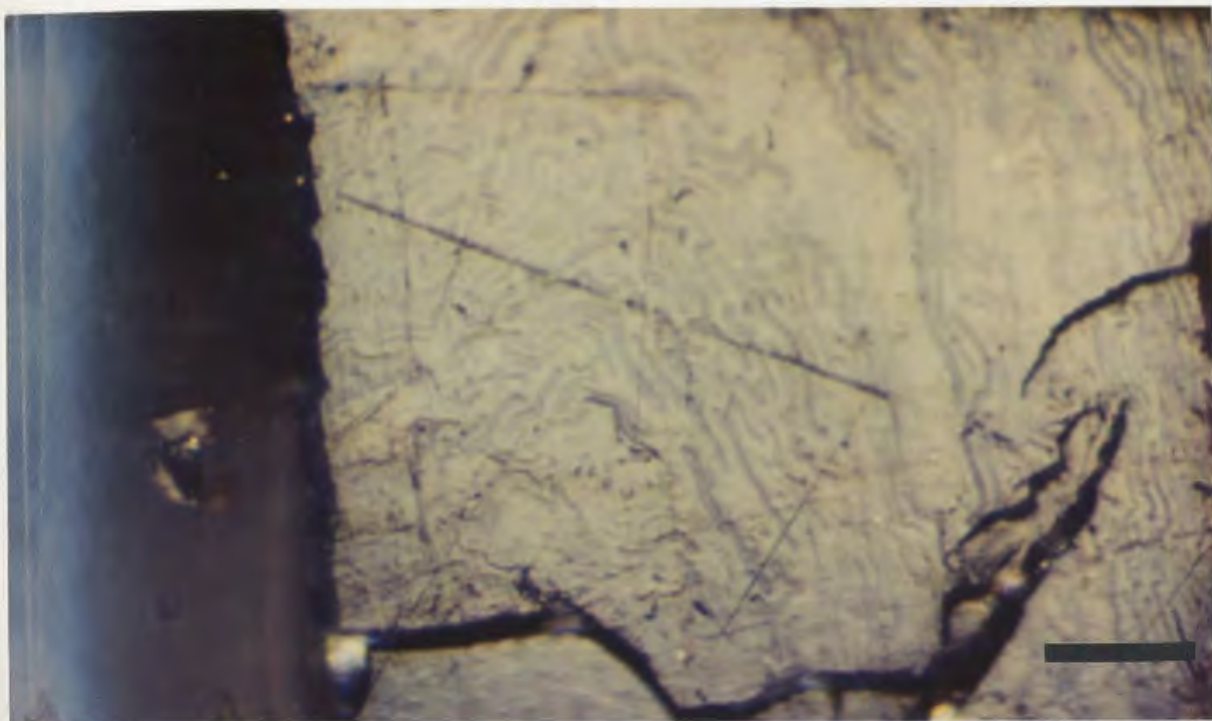
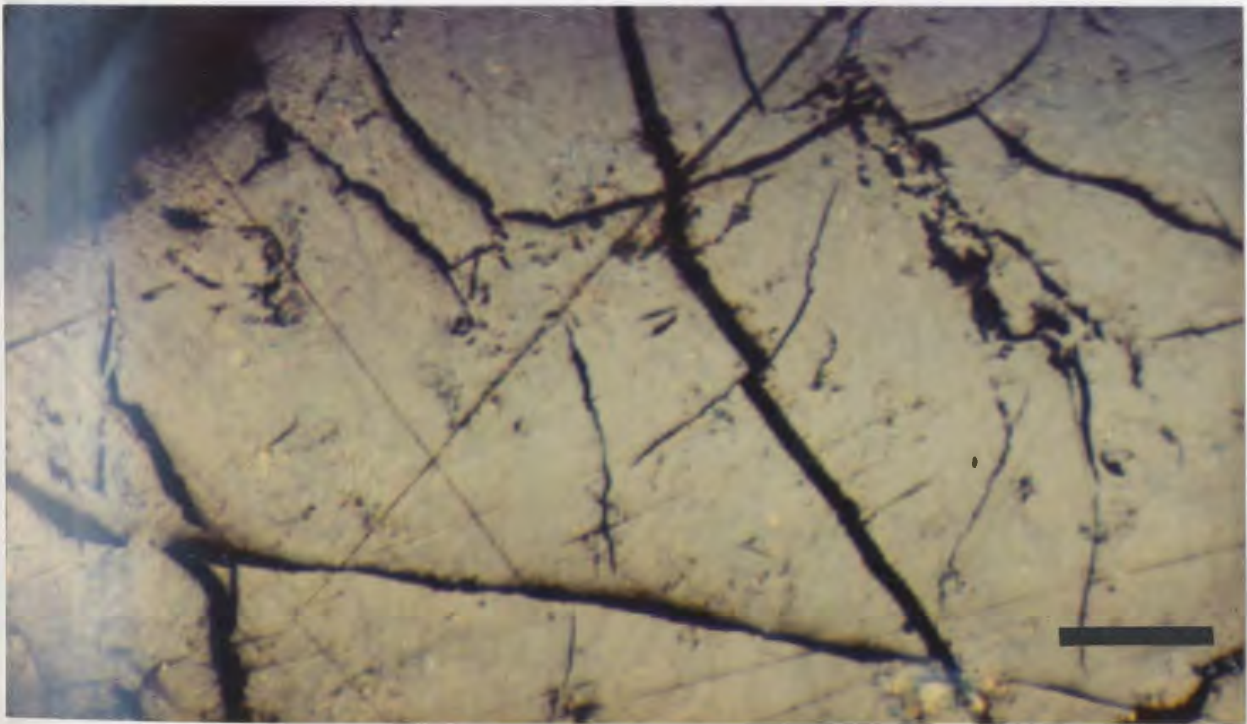
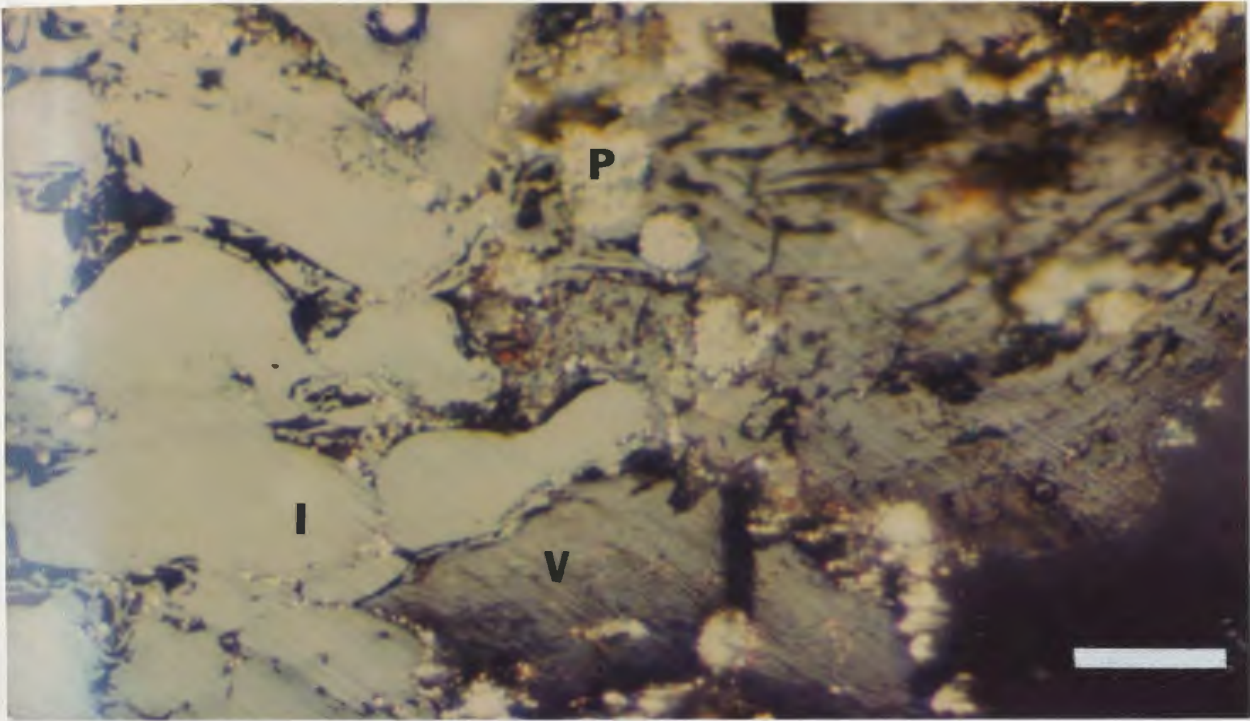


Figure 4.9. Pyrite (P) intimately associated with cellular inertinite (I) and vitrinite (V) macerals. Bar scale 0.25 mm.

Figure 4.10. Gray, structureless vitrinite maceral. Bar scale 0.25 mm.



telinite. The fourth trench sample (81-30) consists of a black coal with a light surface oxidation and a vitreous lustre. It is a much smaller, brittle sample consisting of the inertinite group macerals fusinite and semifusinite and some structureless vitrinite macerals.

Five coal samples were collected from drill hole 80-70 (Table 4.1). The coal was found in granular to medium grained sandstone. The gray sandstones are arkosic in composition with local cross-stratification. Pyrite and kaolinitized feldspars are readily visible in these drill core samples. The presence of these two minerals probably reflects the relatively reduced, acidic microenvironment developed during coalification. Pyrite commonly shows red to yellow hematite-limonite halos. The coal occurs as very thin to medium laminae and thin wisps of organic material. The macerals extracted from the five samples were mostly lower reflecting gray telinite and a structureless vitrinite group maceral. Many of the grain mounts made from these samples show cellular plant material (Figs. 4.7 and 4.8).

The coal sample from drill hole 79-29 was found in a coarse grained arkosic sandstone. The sandstone is highly indurated and red in colour due to extensive hematite cementation. The laminae of coal consist of telinite, bogen structured (collapsed cell walls) fusinite, and sclerotinite (Table 4.1). The last drill core sample, from drill hole 79-28, contained thin fragments and laminae of coaly material within a pinkish, medium grained, micaceous arkose.

Feldspars were again extensively kaolinitized. Telinite and semifusinite are the major maceral types (Table 4.1). Again, in both these samples, euhedral crystals and framboidal aggregates of pyrite are intimately associated with the coal macerals (Fig. 4.9).

4.3.2 Vitrinite reflectance

Reflectance measurements were made on ten of the eleven coal samples described in the previous section. The samples were prepared following the method prescribed by Dr. P. Hacquebard (Dr. R. Hyde, pers. comm. 1982) and partly described in Hacquebard and Donaldson (1970). The general stages in the preparation of the polished grain mounts were as follows: (1) the dark organic material was picked from the crushed sample and washed with distilled water; (2) carbonate minerals were removed using hydrochloric acid; (3) the samples were then macerated in hydrofluoric acid; (4) the organic residue was then dried and mounted in cold-curing epoxy on glass slides; (5) the grain mounts were ground and polished using a levelling technique developed by Baskin (1979).

The prepared polished grain mounts were viewed through oil with a Zeiss 03 photometer. Maximum reflectance values were recorded on medium to dark gray macerals (Fig. 4.10) while rotating them 360° beneath the incident beam. The maximum reflectance values for fifty grains in each grain mount were recorded as percentages and averaged ($\bar{R}_{0.1}^{\max}$). The

average reflectance values for ten of the eleven coal samples collected and their standard deviations are listed in Table 4.1, together with available scintillometer radioactivity readings and the types of macerals found in each sample. Macerals were identified using criteria and photomicrographs contained in Stach et al. (1975). It should be mentioned here for future considerations that, due to slight differences in measurement technique, the measurements (in percent) recorded here are on the average 0.04 higher than those measured by Dr. R. Hyde.

A reflectogram showing the modal distribution of the averaged reflectance measurements for the ten coal samples is presented in Figure 4.11. The histogram defines two groups of reflectance measurements: one group of seven between 0.63 % and 0.74 %, and a second group of two samples (0.97 % and 0.99 %), with an intervening sample yielding 0.81 % reflectance.

It is not immediately obvious why there are two groupings. The bimodality of the reflectance measurements may be due to the influence of coal which had been eroded from coal-bearing strata within the Anguille Group thus yielding different reflectance measurements from the coal which underwent coalification within the Humber Falls Formation. This may be the case as fossil trees have been identified within the Anguille Group (Popper, 1970). Unfortunately this hypothesis could not be tested as no samples of the fossil trees were available for reflectance

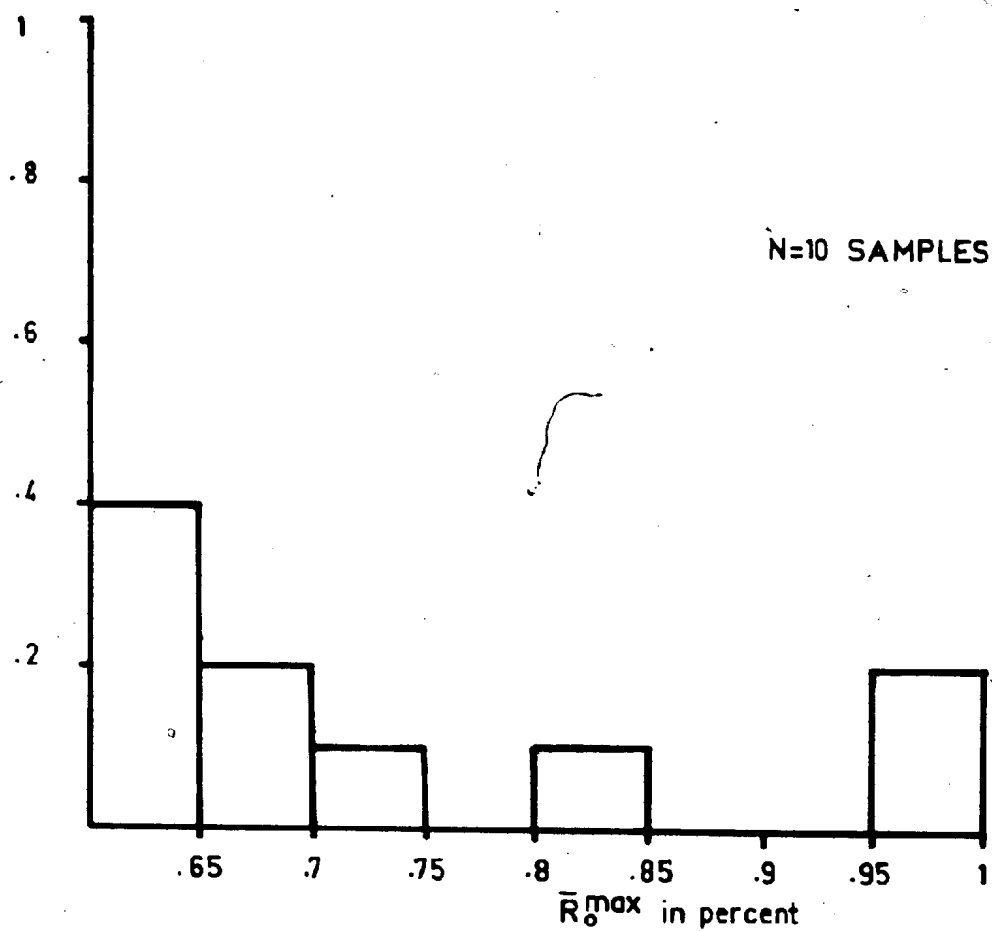


Figure 4.11 Reflectogram of mean reflectance maxima, in oil, for ten trench and drill core coal samples.

measurements. Preliminary vitrinite reflectance measurements by Dr. R. Hyde (pers. comm. 1984) on coaly material from the Anguille Group show reflectance values that are generally greater than 1.0 %. A second possible reason for the bimodality is that due to similarities in appearance, some higher reflecting inertinite group macerals were misidentified as vitrinite group macerals (e.g., semifusinite and pseudovitrinite are similar in appearance), thus increasing the averaged reflectance of a sample.

It is interesting to note that as well as playing an important role in trapping uranium, the coaly material might itself have been irradiated by its adsorbed uranium, causing an increase in reflectivity (Breger, 1974). Unfortunately, there is not enough data (Table 4.1) to determine if such a relationship applies here. Finally, if it is assumed that the vitrinite reflectance measurements from the larger group of coal samples (0.63-0.74 %) is representative of the coaly material, then the coal associated with the Humber Falls Formation can be ranked as high-volatile bituminous B or C. This ranking correlates well with the high-volatile bituminous B rank of the in situ coals in the Howley Formation as determined by Hayes (1949); but show a lower rank than that determined by Hacquebard and Donaldson (1970) for the in situ Howley Formation coal.

4.3.3 Discussion

Whereas the coal described by Howse and Fleischmann (1982) and Hayes (1949) from the Howley Formation on the northeast shore of Grand Lake are considered to be in situ coal, the coaly samples collected from drill core and trenches in and above the northern body of the Humber Falls Formation is considered to be detrital in origin. A detrital, or transported, origin for the precursor woody material is suggested by the association of many of the samples with cross-stratified fluviatile sandstones, the parallel alignment of small wisps of coaly fragments, and the fragmental nature of some of the coaly material. This is a different scenario from the paralic environment envisaged for some Maritime coal deposits (Duff et al., 1982). Nor can these occurrences be related to paleosol development as is suggested for the in situ Howley Formation coal (Howse and Fleischmann, 1982). Due to its fragmental nature and its association with fluviatile sediments the coaly material associated with the northern body of the Humber Falls Formation is more easily related to coalification of transported woody material after it was deposited in a fluviatile regime within a semi-arid to humid environment, as has been proposed for other coal occurrences within the Maritime Provinces (Macquebard and Donaldson, 1969; Legun and Rust, 1982; Mason and Rust, 1983).

Stach et al. (1975) claim that bituminous coal formation is possible between 100°C and 150°C. If, as suggested, the lower reflecting group does have a coal rank of high-volatile bituminous B or C then it seems feasible that these coals have been subjected to temperatures in the range of 100°C to 150°C during coalification. An interesting consequence of the vitrinite reflectance data is that the Humber Falls Formation, even though older than the Howley Formation, shows a slightly lower coal rank (high-volatile bituminous B or C) than the Howley Formation (high-volatile bituminous A or B). This suggests: (1) that the Humber Falls Formation coal was not buried as deeply as the Howley Formation coal seams and therefore experienced lower geothermal temperatures; and (2) that the Howley Formation never covered the Humber Falls Formation. If the Howley Formation had covered the Humber Falls Formation the rank of coal in the two formations would suggest a decrease in burial temperature with depth, which is unlikely.

CHAPTER FIVE

DIAGENESIS

5.1 General introduction

The complexities involved in sedimentary diagenesis are reflected in the plethora of definitions which have been proposed for the term diagenesis. Here, the term diagenesis refers to all the physical and chemical changes which have taken place in the sediments between the time of deposition and the onset of low-grade metamorphism. In siliciclastic rocks containing diagenetic clay minerals, as is the situation in the Deer Lake subbasin, the transition from diagenesis to metamorphism is specified using changes in the diagenetic clay minerals such as illites (Kubler, 1966; Dunoyer De Segonzac, 1970; Frey, 1970; Winkler, 1979).

The processes involved in the diagenesis of sediments are many and it would be a monumental task to decipher all the physicochemical interactions which have taken place in the Deer Lake subbasin sediments. Important interrelated factors which may influence sediment diagenesis, particularly in sandstones, include the following: temperature, pressure (lithologic and fluid), burial rate, detrital mineralogy, pore-fluid composition, sedimentary facies, tectonic setting, and time (Packham and Crook, 1960; Hurst and Irwin, 1982; Hutcheon, 1983).

The following sections deal with two paragenetic sequences which have developed in sediments of the Deer Lake Group, their correlation, their geochemical trends, and their duration. As well, the degree to which the sediments have been heated during diagenesis is estimated by considering organic and mineral thermal maturation indicators within the sediments.

5.2 Paragenetic sequences in the Deer Lake Group and Howley Formation

5.2.1 Introduction

Two paragenetic sequences are proposed for the Deer Lake Group and Howley Formation sediments (Fig. 5.1A and B). All samples from the North Brook, Humber Falls and Howley Formations, and the uranium-mineralized sandstone boulders display the same paragenetic sequence (Fig. 5.1A). The second paragenetic sequence holds for the Rocky Brook Formation sediments (Fig. 5.1B). For brevity these two paragenetic sequences are referred to as the "sandstone" and "shale" sequences respectively. In Figures 5.1A and B, "time" does not imply that the sequence of diagenetic events in the formations were time correlative in an absolute sense; this may or may not have been the case. What "time" does imply is simply that for all the samples concerned the events were superimposed on each other in the order specified by the sequence. This is a relative time sequence of events. In

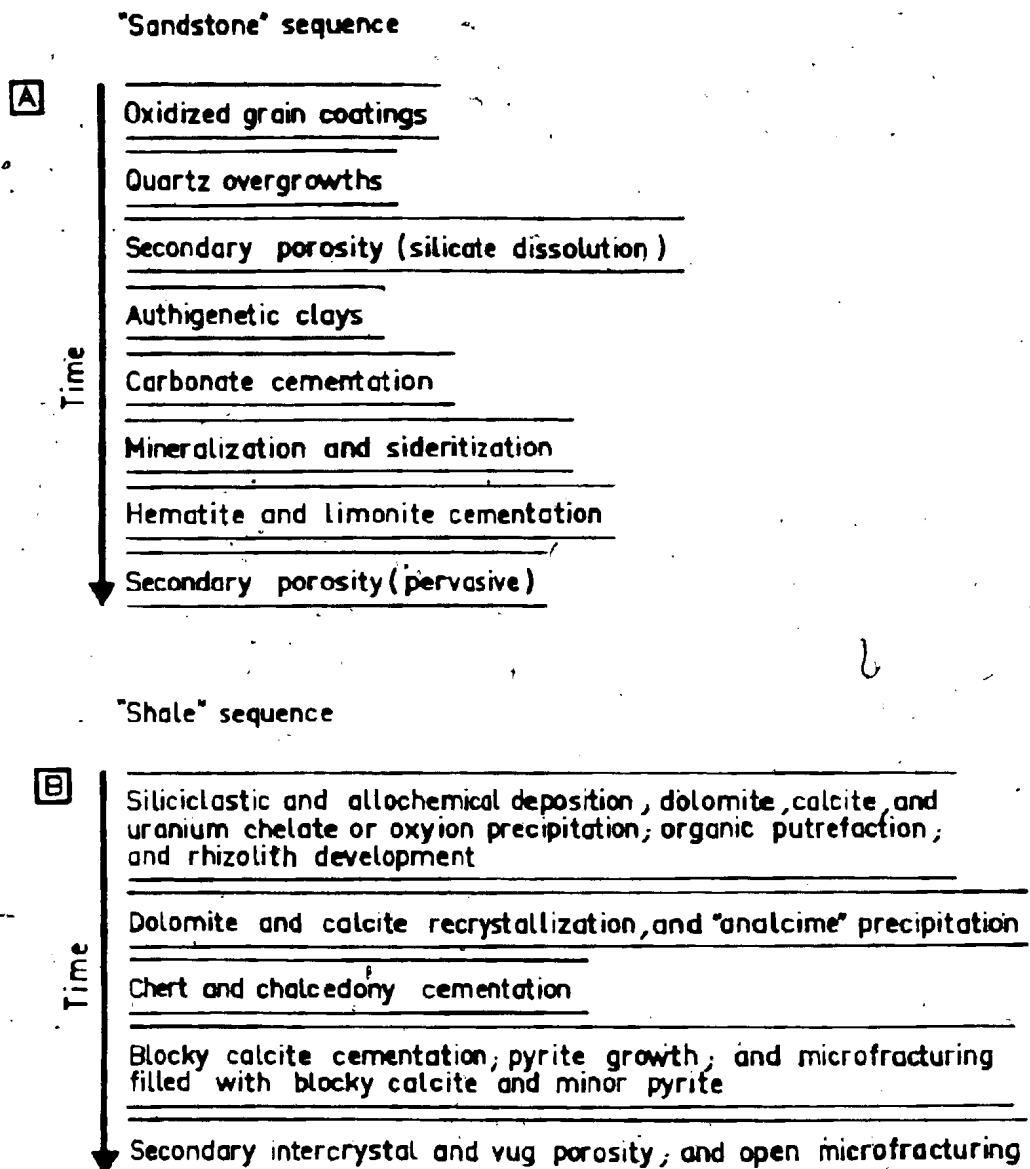


Figure 5.1 (A) The "sandstone" paragenetic sequence
 (B) The "shale" paragenetic sequence
 "Time" implies a relative, superimposed sequence of events.

the following three sections the two paragenetic sequences will be described stage by stage and then discussed.

5.2.2 The "sandstone" sequence

The first stage in this paragenetic sequence (Fig. 5.1A) involved the development of dust rims just prior to the formation of quartz overgrowths (Fig. 3.66). These coatings are referred to as dust rims due to their appearance as faint rims of finely crystalline oxidized material around grain boundaries. The dust rims were probably formed after deposition as the oxidized material would have been abraded during grain transport. Some of the finely crystalline oxidized material may well be infiltrated detrital material which was oxidized before quartz overgrowth development.

The quartz overgrowths were developed before growth of authigenic clays. For example, in Figures 3.12 and 3.56, montmorillonite and chlorite, respectively, formed on previously developed quartz overgrowths. This fits with the general observation that quartz precipitation is apparently minimal on grain surfaces which are covered by clay minerals (Heald and Larese, 1974; Taylor, 1978). Possible sources for the silica are: (1) pressure solution of compacting detrital silicate grains (supported by the presence of sutured and concavo-convex grain boundaries); (2) detrital clay mineral reactions (Sibley and Blatt, 1979; Blatt, 1979).

Secondary porosity was also developed early in the "sandstone" paragenetic sequence through the dissolution of detrital feldspar grains, feldspathic rock fragments and, locally, quartz grains (Fig. 5.1A). Plagioclase and microcline underwent the most extensive dissolution, a fairly typical feature in sandstones, which invariably depends on the bonding strength between oxygen and cations in the silicate grains (Keller, 1957) and is in keeping with the mineral stability series predicted by Goldich (1938). The voids which developed in the grains were not formed before deposition as some of them extend to the margins of the grains and it is likely that grains with such voids would have been broken during transport. An early porosity development is corroborated by the development of authigenic clay minerals and carbonate cement within this intergranular and intragranular pore space (Figs. 3.37 and 3.38).

The next stage in the "sandstone" sequence (Fig. 5.1A) was the development of authigenic kaolinite, illite, montmorillonite, chlorite, and mixed-layer illite-montmorillonite, all of which are typically developed within or adjacent to the detrital grains, and are partly or completely covered by later diagenetic mineral phases such as the carbonate and hematite cements. Both of these features suggest an early development for the authigenic clay minerals. These minerals probably developed through the dissolution of detritus and the in situ replacement by clay, a mechanism which is fairly common in sandstones (Hayes,

1970; Walker et al., 1978; Blatt et al., 1980; Hurst and Irwin, 1982; Eslinger and Sellars, 1981; Curtis, 1983).

Although physical evidence is lacking, it is possible that some of the authigenic clays may have developed through the transformation of other authigenic clays, e.g., montmorillonite from kaolinite plus quartz (Hutcheon, 1983), illite-montmorillonite from montmorillonite (Dunoyer De Segonzac, 1970), and chlorite from montmorillonite (Hoffman and Hower, 1979).

The next stage in the "sandstone" paragenetic sequence was the influx of carbonate cement, particularly calcite, into the sediments. The carbonate cement typically corrodes and partly masks both the detrital grains and the authigenic clays (Figs. 3.14, 3.35, 3.36, 3.69, 3.70). The two pulses of calcite cementation detected in some North Brook Formation samples, which reflect a decrease in iron content (Figs. 3.15 and 3.16), show no intervening mineral development. The coarsely crystalline, blocky and zoned nature of most of the carbonate cement, suggests that it was precipitated within the phreatic zone (Flügel, 1982). Also, the rupturing and corrosion of detrital silicate grains, especially quartz, indicates that the carbonate cement was destructive and cementation occurred slowly enough to enable silicate grain dissolution (Dapples, 1971). Carbonate cementation of recent alluvial fans has been attributed to leaching of the appropriate ions from the local detritus, especially basic igneous rock fragments (Lattman, 1973; Stadler, 1975). It

is evident that some of the calcium was derived from the leaching of calcium from plagioclase grains (Fig. 3.11), but this source cannot account for all the carbonate cement present. Most of the ions needed for calcite and dolomite cementation could have been picked up by groundwaters moving through the calcite- and dolomite-bearing carbonates which form part of the basement terrane along the west side of the subbasin (Fig. 2.3).

Next was a stage of more localized pyrite, uraninite, and siderite cementation. All three minerals cut into, engulf, or are superimposed on the detrital grains and diagenetic minerals discussed so far (Figs. 3.49, 3.51, 3.52, 4.5). It is fairly well established that precipitation of pyrite and uraninite in sediments is most likely to take place by sulphate, iron, or uranium reduction in the presence of organic or inorganic reductants (Garrels and Christ, 1965; Curtis and Spears, 1968; Blatt et al., 1980). Furthermore, Berner (1970) believes that in the absence of sea water, the sulphur for pyrite formation comes mainly from organic matter. In the northern body of the Humber Falls Formation, the pyrite and uraninite mineralization may have received some sulphur, iron, and uranium from solutions percolating up faults (e.g., the Wigwam Fault) from the organic-rich, partly uraniferous sediments of the Rocky Brook Formation. The occurrence of pyrite around radioactive coal suggests that the coal acted locally as a reductant for the uranium and as both reductant and sulphur donor for the pyrite. The

development of siderite, on the other hand, is not closely associated with organic material. A likely origin for siderite is that described by Castaño and Garrels (1950) and Blatt et al. (1980), in which aqueous solutions carrying reduced iron cause calcite dissolution and the subsequent precipitation of siderite. The close association between calcite, siderite, and chlorite (a further iron contributor) is consistent with this mechanism for siderite formation.

A stage of hematite cementation followed. The hematite corroded and masked both detrital grains and all the previously formed diagenetic minerals, including the carbonate cement and uranium mineralization (Figs. 3.6, 3.7, 3.39, 3.43, 4.6). The leaching of iron from iron-bearing minerals by oxygenated fluids and the subsequent development of hematite cement has been used to explain the pigmentation of many red-bed sequences (Walker, 1967; Hubert and Reed, 1978; Turner, 1980). Some of the iron which went into the formation of hematite in the sediments was leached from iron-bearing detritus. There seem to be too few iron-bearing minerals in the sandstones themselves (Appendix I), however, to produce all the hematite cement which is present. The oxygenated fluids must have already been carrying dissolved iron leached from surrounding basement rocks and from the fine grained clay-rich sediments interlayered with the sandstones and conglomerates.

The last change to take place in the sandstones was an episode of pervasive secondary porosity development. This can be distinguished from the early stage of secondary porosity development, as the late stage of dissolution affected all the detrital framework grains and diagenetic mineral phases, including the hematite cement (Fig. 3.44).

5.2.3 The "shale" sequence

The first stage of the "shale" paragenetic sequence (Fig. 5.1B) involves the deposition of shallow-water lacustrine or lake-margin siliciclastic and allochemical carbonate sediments accompanied by calcite and dolomite precipitation in the epilimnion and the upper layer of the profundal sediment (Eugster and Surdam, 1973; Hardie et al., 1978; Dean and Fouch, 1983). During early sediment deposition and carbonate precipitation, living or decaying plant roots contributed to the development of rhizolith zones 1 (outer micrite-cemented envelope) and 2 (clay- and organic-rich ring), while within the Rocky Brook Formation lake, uranium was deposited through a variety of mechanisms (chapter four, section 4.2.3) and organic putrefaction was leading to the formation of oil shales.

The next stage in the second sequence involved some recrystallization and growth of the finely crystalline calcite and dolomite cement to medium size crystals (0.62-0.25 mm, Folk, 1962). Although the evidence for this stage is not ubiquitous, the presence of medium size

subhedral crystals in an otherwise finely crystalline calcilutite (Fig. 3.28) suggests that some recrystallization did take place.

"Analcime" also precipitated from solution during the second stage. The "analcime" is found associated with the coarsely crystalline calcite patches (which clearly postdate the material developed during the first stage); it forms a mineral phase which typically develops along the margins of the patches and shows corroded edges when in contact with the coarsely crystalline calcite (Fig. 3.20). "Analcime" is similarly associated with the coarsely crystalline calcite in rhizolith cores (Figs. 3.22 and 3.24). These relationships show that the "analcime" formed after the initial stage of sediment diagenesis but slightly before the influx of the coarsely crystalline calcite (stage four). Traditionally, the presence of "analcime" in lacustrine sediments has been linked to the degradation of volcanoclastic material in the immediate vicinity (Deffeyes, 1959; High and Picard, 1965; Coombs and Whetten, 1967). There is not enough volcanoclastic material in the Rocky Brook Formation, or in the adjacent formations, to account for all the "analcime". Microprobe analyses (Appendix II) show a composition between stoichiometric analcime and albite for the crystals. No intergrowths of albite were seen in the "analcime" crystals, and there does not seem to be enough albite in the sediments to account for "analcime" development entirely through albite hydrolysis. The "analcime" probably precipitated from highly

alkaline waters within the sediments (Hay and Mofiola, 1963; Hay, 1966; Coombs and Whetten, 1967). The sodium necessary for "analcime" development could have been leached from sodium-bearing detritus (e.g., plagioclase feldspars, paragonite) within the Rocky Brook or North Brook Formations. The necessary ions for "analcime" development may also have been derived from the breakdown of sodium-bearing clay minerals such as montmorillonite (Hay, 1966; Helgeson et al., 1969). Some authors believe that sodium can combine with kaolinite to form "analcime" (Foster and Feicht, 1946; Smith, 1982). The paucity of kaolinite in the Rocky Brook Formation sediments is negative evidence supporting this mechanism of "analcime" development. A small amount of sodium released from decaying plant material may have led to the precipitation of "analcime" in the centre of the rhizoliths.

Minor amounts of silica cementation in the form of chert and chalcedony was also developed in the Rocky Brook Formation about halfway through the "shale" paragenetic sequence (Fig. 5.1B). The silica cement occurs as subrounded patches which penetrate and disrupt the first stage carbonate and siliciclastic sediments. The length-fast chalcedony typically occurs in the centre of the silica patches, suggesting that the chalcedony was the last of the two void-filling quartz phases to form. Frondel (1982) believes the development of chalcedony is favoured by silica supersaturation and high growth rates. This may have been

the case during the closing stage of the episode of minor silica precipitation within the Rocky Brook Formation and would therefore account for the chert-chalcedony zonation.

The relative timing of (1) carbonate recrystallization and "analcime" precipitation, and (2) silica cementation could not be determined as the minerals were never seen together in the same thin section. In Figure 5.1B the stage of silica cementation was not included with the stage of carbonate recrystallization and "analcime" precipitation, as quartz and carbonates will usually develop under different chemical conditions (Blatt et al., 1980, p.348). It is possible that silica cementation only occurred in very localized areas within the sediment while carbonate recrystallization and "analcime" precipitation were taking place elsewhere.

The fourth stage in the "shale" sequence involves the development of irregular patches of coarsely crystalline calcite and anastomosing microfractures, which are also filled by coarsely crystalline calcite (Fig. 3.29). Based on the reasoning in chapter three, section 3.3.2, the patches and stockwork appear to have developed at the same time. Both the patches and the stockwork cut the siliciclastic and carbonate material and silica cement developed during the first three stages, and corrode the edges of the "analcime" crystals. Minor pyrite is also locally developed in the stockwork (Fig. 3.29). In places within the sediment, authigenic pyrite crystals appear to have aggregated and

encroached on neighbouring minerals (Fig. 3.28). These two features suggest that the pyrite developed in part during the fourth stage, possibly due to the movement of sulphur along the microfractures (cf., Curtis and Spears, 1968).

The last feature to be developed in the lacustrine Rocky Brook Formation sediments was secondary, microintercrystal, mesovug and 'open' microfracture porosity. This late porosity cuts all material developed earlier in the "shale" sequence. Figure 3.21 shows an 'open' microfracture clearly cross-cutting the calcite stockwork developed during the previous paragenetic stage.

5.2.4 Discussion

Unfortunately, the two paragenetic sequences which were developed for the Deer Lake Group and Howley Formation sediments (Figs. 5.1A and B) do not show many similarities. The only two similar events found in both sequences are: (1) the carbonate cementation stage of the "sandstone" sequence and the blocky calcite cementation stage in the "shale" sequence; and (2) the late-stage pervasive secondary porosity of the "sandstone" sequence and the late-stage secondary intercrystal, vug, and 'open' microfracture porosity of the "shale" sequence. The main reason why the two sequences do not correlate better is the fact that they represent rocks from different sedimentary facies which inherently possess, for example, different bulk primary mineralogies, porosities, permeabilities.

There do not appear to have been any major geochemical changes during the development of the "shale" paragenetic sequence (Fig. 5.1B). The abundance of carbonate minerals and "analcime", and the absence of kaolinite, indicate that, apart from the relatively minor silica cement, the paragenetic sequence which developed in the Rocky Brook Formation evolved under alkaline conditions. The "sandstone" paragenetic sequence, however, does show a change in geochemical environment during its development. The oxidized nature of the dust rims suggests that they were formed in an oxygenated environment. The quartz overgrowths and authigenic kaolinite that developed early in the "sandstone" sequence were probably formed under relatively acidic conditions. The leaching effect of acidic meteoric water in sandstones and the consequent production of kaolinite and quartz is well documented (Bucke and Mankin, 1971; Davies et al., 1979; Curtis, 1983). An increase in cation activity possibly suppressed the continued growth of kaolinite (Curtis, 1983), and allowed montmorillonite, illite-montmorillonite, and chlorite to develop. The eventual influx of calcite cement suggests that the geochemical environment had slowly become alkaline. The coarse blocky nature of the carbonate cement also suggests that carbonate cementation took place below the water table. The pyrite and uraninite mineralization probably developed in more localized areas where anoxic and acidic conditions prevailed.

A general idea of the absolute time involved in diagenesis is provided by a paleomagnetic study by Irving and Strong (in press) on some of the same drill core which was used to derive the "sandstone" paragenetic sequence. The Deer Lake Group red-beds have a Kiaman (Late Carboniferous to Early Permian) paleomagnetic overprint, apparently related in time to hematite cementation. If this is true, and given that the sediments were deposited during the Viséan, then it must have taken between 40 Ma and 80 Ma for the "sandstone" paragenetic sequence to reach the stage of hematite cementation. If the late stage of hematite cementation did develop between the Late Carboniferous and Early Permian, then one may conclude that oxygenated solutions flushed through the entire Deer Lake Group and Howley Formation sequence late in the development of the paragenetic sequence.

5.3 Thermal maturation indicators

5.3.1 Introduction

Diagenetic clay mineral assemblages and organic matter are the two most widely used thermal maturation indicators in unmetamorphosed sedimentary rocks (Héroux et al., 1979). Most authors agree that temperature, time, and type of organic matter or mineral composition are the most important factors controlling the degree of thermal maturation (Teichmüller and Teichmüller, 1967; Castaño and Sparks, 1974; Stach et al., 1975; Héroux et al., 1979; Hoffman and Hower, 1979). No single indicator is self-sufficient in estimating the degree of thermal maturation, as any single indicator may give spurious or inconsistent results for a variety of reasons; e.g., sediment reworking, analytical error, variable sample treatment and therefore uncertain correlation between research laboratories. Therefore, it is best to use a few indicators, from the same sediment samples if possible, and then to try and correlate the indicators based on their physical or chemical changes with temperature increase.

In this section, three thermal maturation indicators within the Deer Lake Group and Howley Formation sediments are tested. The three are: (1) vitrinite reflectance ranking of coaly material; (2) diagenetic clay mineral assemblages; and (3) illite crystallinity measurements.

5.3.2 Vitrinite reflectance

The use of vitrinite reflectance to rank coal has been used successfully by many researchers (e.g., Hacquebard and Donaldson, 1970; Stach et al., 1975; Bostock, 1979). Based on the vitrinite reflectance results and discussion in chapter four, section 4.3.2, the coal found in the Humber Falls Formation drill core and the surface trenches is ranked as high-volatile bituminous B and C. According to Stach et al. (1975) bituminous coal may develop between 100°C and 150°C. Bostock (1979) has constructed a table comparing minimum burial paleotemperatures needed to attain various levels of vitrinite reflectance. Using Bostock's table and the vitrinite reflectance measurements listed in Table 4.1 for the lower reflecting group of coal (Fig. 4.11), the minimum paleotemperature range needed for this group of samples is bracketed between approximately 128°C (lower limit of group, 0.61 % \bar{R}_{oil}^{max}) and 150°C (upper limit of group, 0.74 % \bar{R}_{oil}^{max}).

5.3.3 Diagenetic clay mineral assemblages

The diagenetic clay mineral assemblages in sediments, like coal, have been used by many researchers as diagenetic geothermometers (e.g., Dunoyer De Segonzac, 1970; Zen and Thompson, 1974; Hoffman and Hower, 1979; Winkler, 1979). Two diagenetic clay mineral assemblages have been identified, one for the North Brook, Humber Falls, and Howley Formations, and one for the finer grained lacustrine sediments of the Rocky Brook Formation.

The diagenetic clay mineral assemblage for the North Brook, Humber Falls, and Howley Formations consists of: kaolinite, chlorite, montmorillonite, illite, and, in the North Brook and Humber Falls Formations, disordered illite-montmorillonite. Although the confirmation of the diagenetic clay minerals in the Rocky Brook Formation by SEM is precluded by the fine grain size of the shaly sediments, it is felt that some diagenetic chlorite, illite, and montmorillonite are present, together with "analcime". Dr. R. Hyde (pers. comm. 1983) has recently identified a mixed-layer clay mineral in the Rocky Brook sediments that appears to be mixed-layer chlorite-montmorillonite.

A review of the literature on diagenetic clay mineral stabilities revealed the following geothermic information:

(1) A study by Dunoyer De Segonzac (1970) demonstrated that diagenetic kaolinite has a maximum stability between 80°C and 190°C with an average maximum stability of approximately 136°C.

(2) Only a few studies have been able to monitor the stability of montmorillonite with changing temperatures. In the southwest Texas Wilcox Formation the upper stability limit for montmorillonite is approximately 70°C (Boles and Franks, 1979) while in various locations along the Gulf Coast montmorillonite is stable up to 95°C (Burst, 1959).

(3) It is generally accepted that illite-montmorillonite forms through the aggradation or degradation of pre-existing clay minerals (Weaver, 1956; Dunoyer De Segonzac, 1970). The development of disordered illite-montmorillonite in the Deer Lake subbasin may have followed either course. The degradation processes can take place during early weathering (Stoch and Sikora, 1976). With aggradational processes, Dunoyer De Segonzac (1970) has reported that the transition of montmorillonite to disordered illite-montmorillonite generally takes place between 70°C and 95°C. The same transition is reported to take place at 70°C in the Rhine Graben and 100°C along the Gulf Coast (Heling and Teichmüller, 1974). Perry and Hower (1970) show that in the Gulf Coast region, with 35 % expandible layers in the illite-montmorillonite minerals (as is the situation in the North Brook and Humber Falls Formations) there is a corresponding formation temperature of approximately 95°C.

(4) The writer does not believe that the discrete diagenetic illite was formed by illitization of precursor diagenetic clay minerals (i.e., through a mixed-layer phase (Dunoyer De Segonzac, 1970)). The temperature for discrete illite formation via mixed-layer mineral transformations appears to be too high, e.g., 200°C (Dunoyer De Segonzac, 1970) or 375°C (Austin and Leininger, 1976), if illite indeed coexists with the other diagenetic clay minerals. Physical evidence shows that most of the illite is associated with detrital feldspar grains. Therefore the hydrolysis of feldspars, particularly potassic feldspars (Helgeson et al., 1969), at lower temperatures (~ 65°C, Garrels and Howard (1959) or 100°C, Zen and Thompson (1974)) is considered to be the cause of illite development.

It is concluded from the above that the assemblage of diagenetic clay minerals in the four studied formations could coexist at temperatures between approximately 80°C and 135°C. This paleotemperature range should only be applied to the stage of authigenic clay development in the "sandstone" paragenetic sequence for two reasons: (1) the mineral phases which developed after the formation of the authigenic clays (carbonates, mineralization, hematite) quite likely formed at different paleotemperatures (possibly only obtainable through isotope or fluid inclusion studies); (2) since a stage of authigenic clay development cannot be readily recognized in the "shale" paragenetic sequence, it is difficult and unwise to try and apply the paleotemperature range estimation to any

particular stage in the second sequence.

5.3.4 Illite crystallinity

The crystallinity of illite as defined by Kubler (1966) increases as the prevailing postdepositional conditions change from the diagenetic zone to the anchizone (zone of transition between diagenesis and metamorphism) and finally to the epizone of metamorphism (Dunoyer De Segonzac, 1970). An illite crystallinity measurement is obtained from a clay fraction diffractogram by measuring in millimetres the peak-width (H_b) of the 10 Å illite reflection, at half the height above a determined base line (Kubler, 1966; Dunoyer De Segonzac, 1970; Weber, 1972). The narrowing of the 10 Å peak (increase in illite crystallinity) is dependent on temperature and the chemical composition of the illite (Kubler, 1966, 1967; Dunoyer De Segonzac, 1970). To allow comparison, measurements must be made on diffractograms obtained with the same chart speed.

Many studies have used illite crystallinity measurements to determine whether the illites in different sedimentary sequences are diagenetic, transitional anchizonal, or metamorphic epizonal (e.g., Dunoyer De Segonzac et al., 1968; Frey, 1970; Foscolos and Stott, 1975; Frey et al., 1980; Ogunyomi et al., 1980; Fieremans and Bosmans, 1982). Unfortunately many researchers either do not document their precise experimental procedures or fail to use standardized procedures, thus making the correlation of results between

laboratories difficult. In this study the illite crystallinity measurements were carried out on diffractograms from the $<2 \mu$ fraction of material separated from a sampling of sandstones and finer grained sediments from each of the nine drill hole. The following diffractometer operating conditions were used: Cu $K\alpha$ radiation, 1° 2 θ per minute goniometer rate, 2 cm per minute chart speed, rate meter of 2000 cps, time constant of 4, 1° divergent slit, 1° receiving slit. These operating conditions are almost identical to those used by Fieremans and Bosmans (1982) who in turn compared their data to that of Dunoyer De Segonzac (1970) by using illite crystallinity standards supplied by him. Fieremans and Bosmans (1982) used cobalt radiation and a time constant of 1, neither of which should affect the outcome of the illite crystallinity measurements. According to Fieremans and Bosmans (1982), their diagenesis/anchizone boundary at 8.5 mm (Hb) and anchizone/epizone boundary at 5.2 mm (Hb) correspond to similar zonal boundary changes at 5.5 mm (Hb) and 3.5 mm (Hb) respectively as originally defined by Dunoyer De Segonzac (1970).

In Figures 5.2A to D, the illite crystallinity measurements obtained for the North Brook, Rocky Brook, Humber Falls, and Howley Formations are plotted against sample depth. The zone boundaries are delineated according to the correlations made by Fieremans and Bosmans (1982) between their work and that of Dunoyer De Segonzac (1970). In Figures 3.1, 3.8, 3.17 for example the illite

crystallinity measurements were reported using the change in 2θ to record the 10 \AA peak-width at half height. This was done because it reduces the effects that variations in scanning rate and chart speed have on measuring the peak width, thus allowing some comparison to be made between this study and studies that may have used slightly different scanning rates and chart speeds. However, as stated by Ogunyomi et al. (1980) this method of recording illite crystallinity measurements does not eliminate the effects that varying other operating conditions (e.g., slit widths, humidity, ion saturation) will have on the illite crystallinity results.

In Figures 5.2A, C, and D the illites show a scattering of crystallinity measurements between the diagenetic and anchimetamorphic zones. The finer grained Rocky Brook Formation samples appear to only contain diagenetic illites (Fig. 5.2B). The scattering of measurements in Figures 5.2A B and C does not mean that certain sections in the drill holes have been subjected to higher temperatures than others. The scattering of illite crystallinity measurements between the diagenetic, transitional anchizone, and metamorphic epizone likely reflects the relative abundance of diagenetic and detrital illite in the samples. This conclusion is based on the assumption that the detrital illites, supposedly eroded from metamorphic and igneous terranes where illites tend to be more highly crystallized 2M polymorphs, would yield higher illite crystallinity measurements (epizone and

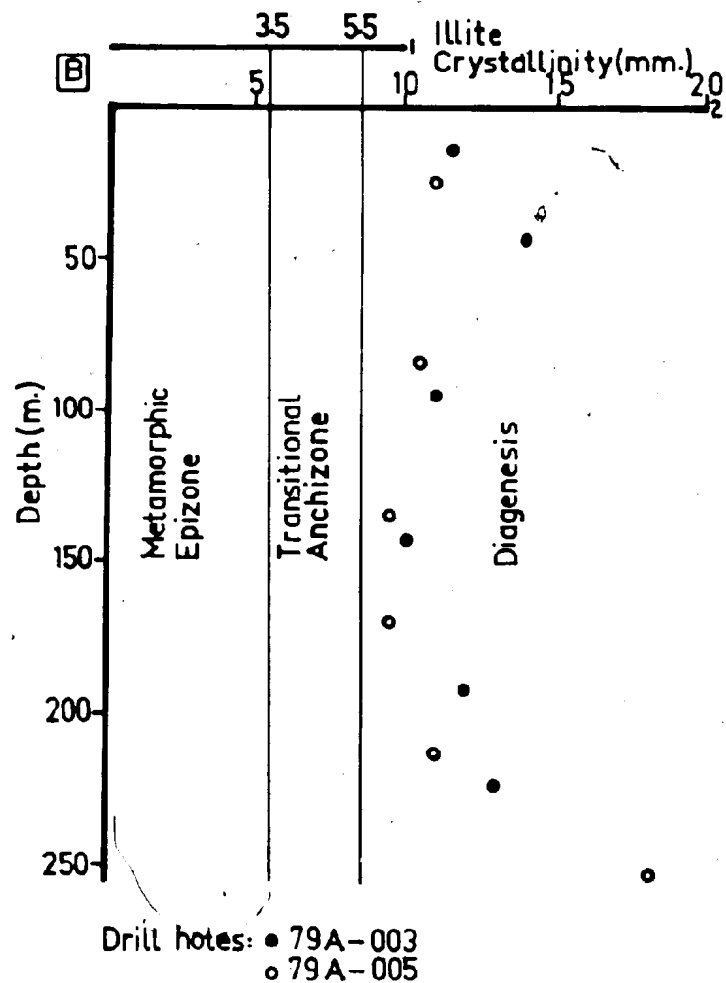
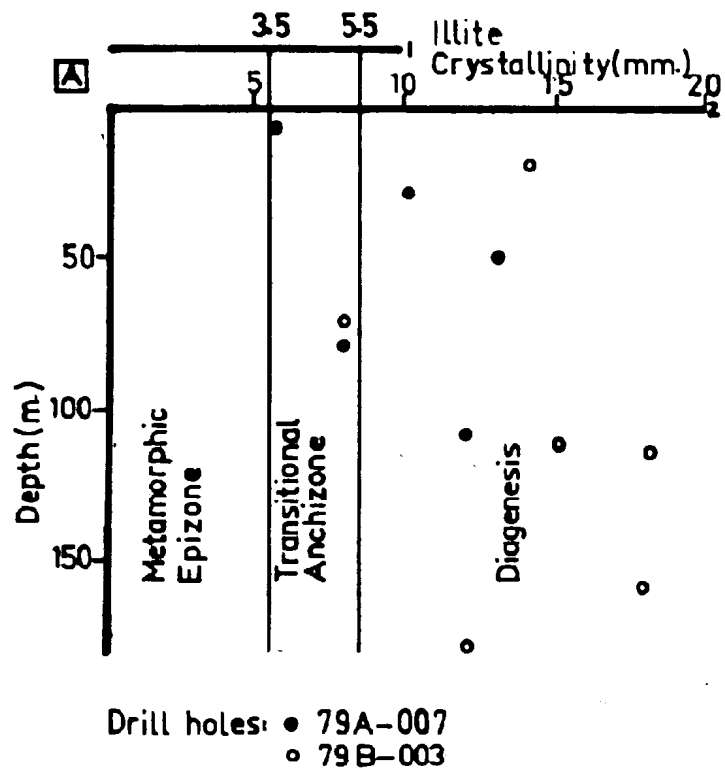
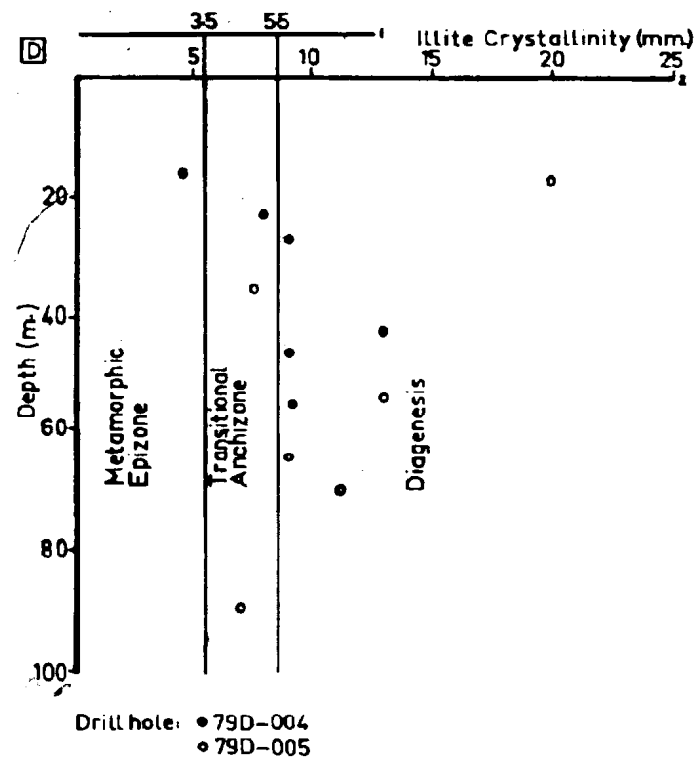
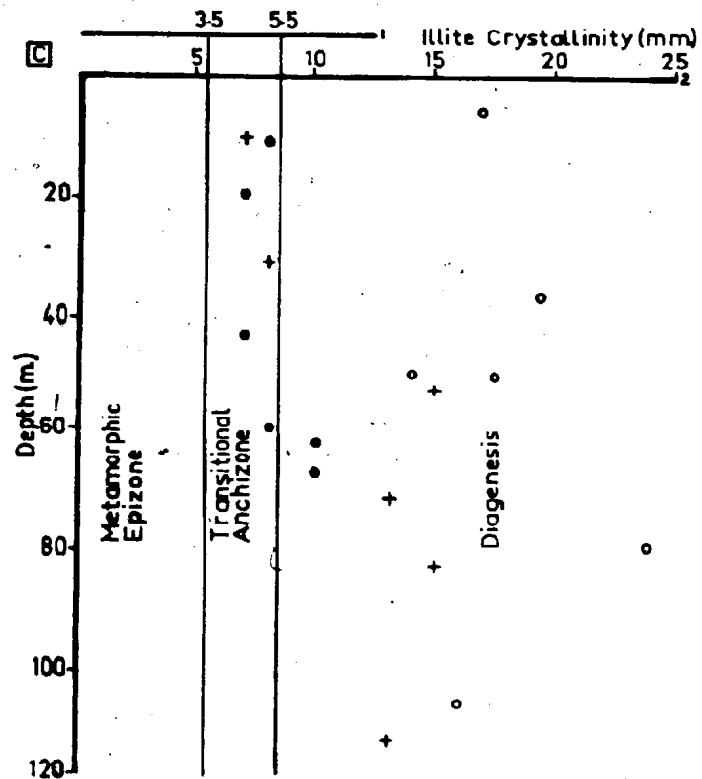


Figure 5.2 $\langle 2\mu$ illite crystallinity measurements for selected samples from the: (A) North Brook Formation, (B) Rocky Brook Formation. The scales, in millimetres, of Dunoyer De Segonzac (1970)= 1, and Fieremans and Bosmans (1982)= 2, are used to delimit the zones of diagenesis the anchizone and the epizone.



Drill holes: + DDH 79-29
 o DDH 79-69
 • DDH 80-70

Figure 5.2 $\langle 2\mu$ illite crystallinity measurements for selected samples from the:
 (C) Humber Falls Formation, (D) Howley Formation.

anchizone) rather than poorly crystallized diagenetic IM or IMd illite polymorphs (Yoder and Eugster, 1955; Kubler, 1966, 1967; Maxwell and Hoyer, 1967; Dunoyer De Segonzac, 1970). Also, according to Dunoyer De Segonzac (1970) and Weber (1972), the crystallinity of detrital illite is generally higher (narrower peak-width) than diagenetic illite since the particles are larger. It is possible that some of the poorly crystallized illite (diagenetic zone) could be the result of progressed degradation of detrital illites which were originally of higher crystallinity (Hutcheon et al., 1980).

For the samples which were measured, the illite crystallinity results are only semi-quantitative measurements defining the 'state' of illite in the sediments (i.e., epizonal, anchizonal, diagenetic). Illite crystallinity measurements can therefore best be used in tandem with other thermal maturation indicators to determine the paleotemperatures responsible for their formation.

5.3.5 Discussion

Two thermal maturation indicators help determine the range in temperature to which the sediments were subjected during diagenesis. The indicators revealed the following information: vitrinite reflectance- 100°C to 150°C (Stach et al., 1975) and 128°C to 150°C (Bostock, 1979); diagenetic clay mineral assemblages- 80°C to 135°C (from compiled mineral stability data). Using the temperatures from these

results the paleotemperature maximum was probably between about 125°C and 135°C for the formation of the authigenic clays and coalification. Illite crystallinity measurements confirm the existence of diagenetic illite (IC > 5.5 nm, Dunoyer De Segonzac (1970)).

It can be concluded from examining the available coexisting thermal maturation indicators from the Deer Lake Group and Howley Formation sediments that these sediments have stayed within the diagenetic realm after deposition.

CHAPTER SIX

SUMMARY AND CONCLUSIONS

Starting in the Late Devonian, the Alleghanian disturbance developed a large northeast-trending depression, the Maritimes Basin, which extended across all the northern Appalachian lithotectonic zones. Within the Maritimes Basin, intrabasinal horsts and grabens developed a host of fault-controlled subbasins, including the Deer Lake subbasin of western Newfoundland. The eastern half of the subbasin is extensively dissected by northeast-trending high angle faults. It can be demonstrated that fault movements were contemporaneous with sedimentation in the Deer Lake subbasin, and furthermore that the oldest most highly deformed sediments in the subbasin, the Anguille Group (Tournasian), were deposited during an episode of strike-slip faulting while the overlying, essentially undeformed sediments (Wigwan Brook - Wetstone Point Formations, the Deer Lake Group, and the Howley Formation respectively) were deposited during an episode of normal or reverse faulting. The terrestrial siliciclastic sediments in this sedimentary sequence were derived from various proximal Humber Zone, Baie Verte - Brompton Line, and Dunnage Zone basement lithologies. The Deer Lake Group (Viséan) and Howley Formation (Westphalian A) sediments, the focus of this thesis, consist of alluvial fan, fluvial, and lacustrine sediments unconformably overlying the Anguille Group and basement rocks. Together the Deer

Lake Group and Howley Formation form an approximately 6.8 km-thick red-bed sequence.

The petrographic and diagenetic data for this thesis study were obtained by systematically sampling nine representative drill holes from the North Brook, Rocky Brook, Humber Falls and Howley Formations and carrying out various microscopic and analytical techniques on these samples. Samples of high-grade uranium-mineralized sandstone boulders were similarly analyzed. It was found that the petrographic and diagenetic characteristics of the North Brook Formation, Humber Falls Formation, and Howley Formation sediments, and the mineralized sandstone boulders, were essentially the same. The sediments sampled from the two Rocky Brook Formation drill holes displayed different petrographic and diagenetic characteristics from the other three formations. The reason for this difference probably lies in the fact that the data for the three sandy formations were derived from alluvial fan and fluvial siltstones, sandstones, and conglomerates, while the Rocky Brook Formation data came from finer grained siliciclastic and carbonate lacustrine sediments, which inherently possess different physical and chemical characteristics. This thesis not only provides the first complete petrographic and diagenetic study of the Deer Lake Group and Howley Formation sediments, but is also an example of how sedimentary facies can control diagenesis.

The samples from the North Brook, Humber Falls, and Howley Formations and the mineralized sandstone boulders show the following characteristics:

(1) The drill holes contained polymict conglomerates, cross-stratified sandstones, siltstones and some mudstones. The North Brook Formation drill core contains the most conglomerates and fewer fines, while the Howley Formation drill core contains the most fines and no conglomerates. This apparent fining-upward trend may either be a function of proximity of drill holes to the contemporary basin margin or it may reflect a general decrease in fault activity during the development of the sedimentary sequence.

(2) The detrital composition of the sandstones from the three sandy formations and mineralized samples consists of quartz (monocrystalline and polycrystalline) and feldspars (orthoclase, plagioclase, and microcline) with lesser amounts of rock fragments (mostly granitic intrusive, felsic volcanic, and metamorphic) micas and chlorite. QRF plots show that the sandstones are either arkoses or lithic arkoses. Comparative QRF plots also show that the mineralized sandstones have a modal composition most similar to the Humber Falls Formation sandstone samples.

(3) Coarsely crystalline calcite and dolomite and finely crystalline hematite cement dominate the diagenetic mineralogy except in the mineralized samples where uraninite cement is far more prevalent. Diagenetic clay minerals,

quartz overgrowths, siderite, and limonite also developed in the sediments and boulder samples. The constituents necessary for the development of the diagenetic minerals in the sandstones were derived from the in situ degradation of the sandstone detritus and from solutions which had leached elements from the interlayered fines and surrounding basement lithologies.

(4) The diagenetic clay mineral assemblage reveals the following features: (a) pore-filling vermicular kaolinite is commonly closely associated with detrital silicate grains; (b) illite displays a variety of crystal sizes from poorly defined fibres to euhedral laths, and is typically developed on or adjacent to feldspar grains; (c) chlorite has grown on quartz overgrowths, detrital grain surfaces, and interstitially as individual discs, rosettes, or rarely with a vermiform morphology; (d) montmorillonite has grown on quartz overgrowths and grain surfaces and typically displays a 'cornflake' morphology; (e) mixed-layer disordered illite-montmorillonite was only identified in the North Brook Formation and Humber Falls Formation sandstones.

(5) Total porosity for both mineralized and unmineralized sandstone samples has a range between 5 % and 20 %, with most of that being effectively interconnected. The porosity is secondary, developed by an early stage of detrital silicate grain dissolution and a later stage of pervasive detrital and diagenetic mineral dissolution. It is difficult to say what controls the effective porosity, but

perhaps it is the late-stage pervasive dissolution which created the effective pore space after the carbonate cement had occluded earlier porosity.

(6) The mineralized and unmineralized sandstone samples display the same paragenetic sequence. The sequence is as follows: (a) an early stage of oxidation and quartz overgrowth development; (b) early silicate grain dissolution; (c) authigenic clay mineral development; (d) carbonate cementation; (e) uranium mineralization and sideritization; (f) hematite cementation and limonitization; (g) late-stage pervasive dissolution. This paragenetic sequence began to develop within an acidic environment which became basic with time. The late stages of hematization suggest that there was an influx of iron-bearing oxygenated and leaching solutions throughout the sedimentary sequence which was studied. The postmineralization hematizing fluids may have caused extensive remobilization of the uranium so that now only small concentrations of highly reduced, organic-bearing subsurface mineralization remain. Paleomagnetic data indicate that it may have taken between 40 Ma and 80 Ma for this paragenetic sequence to develop to the stage of hematization.

The samples from the two Rocky Brook Formation drill holes show the following features:

(1) The sediments consist of interlayered claystones, mudstones, siltstones, and various allochemical and orthochemical calcareous rocks. There are a few thin layers of sandstone in these holes but no conglomerate.

(2) Although difficult to identify in these finer grained sediments, there are probably some diagenetic clay minerals in the samples. Illite crystallinity measurements indicate that diagenetic illite is present.

(3) Diagenetic minerals include calcite, "analcime", chert, chalcedony, pyrite, and minor barite. Generally there is no diagenetic kaolinite or mixed-layer illite-montmorillonite within the Rocky Brook Formation.

(4) "Analcime" occurs as a marginal mineral phase in rhizolith cores and in patches of coarsely crystalline calcite. In both situations the "analcime" crystals are partly corroded by the coarsely crystalline calcite (stage 4 calcite of the "shale" paragenetic sequence, Fig. 5.1B). Microprobe analyses give an anomalous, but consistent, composition between analcime and albite for these crystals. Due to the lack of albitic or volcanoclastic detritus in the sediment, the sodium in the "analcime" is considered to have come primarily from the breakdown of sodic clay minerals, and/or from sodium-bearing detritus and possibly from plant root decay in the rhizolith occurrences.

(5) The sediments have an effective porosity range between 0 % and 18 %, which is due to secondary intercrystal, vug, and 'open' microfracture porosity development.

(6) A paragenetic sequence for the Rocky Brook Formation, which incorporates information from all the fine grained samples, is as follows: (a) sedimentation (carbonate and siliciclastic) within a lake or lake margin environment, syngenetic pyrite and uranium mineralization, carbonate development (rhizolith zone 1) around plant roots (rhizolith zone 2) and the beginning of rhizolith development, and organic putrefaction; (b) carbonate recrystallization, and "analcime" precipitation within calcareous sediments and rhizolith cores (rhizolith zone 3); (c) silica cementation; (d) blocky calcite cementation in irregular patches and within rhizolith cores (rhizolith zone 3), development of calcite stockwork, and pyritization; (e) late-stage secondary microintercrystal, mesovug, and 'open' microfracture porosity development. Minor hematization accompanies the late-stage 'open' microfracturing. The relative timing of carbonate recrystallization, and "analcime" and quartz cementation is not fixed but they all developed between the (a) and (d) stages of this paragenetic sequence. Unlike the paragenetic sequence for the sandy units, the minerals which developed within the Rocky Brook Formation formed within an alkaline environment, except where localized silica cement suggests a brief or local decline in pH. There are two events in each of the two paragenetic

sequences which can be tentatively correlated. The first is the development of coarsely crystalline carbonate cement in the North Brook, Humber Falls and Howley Formations and blocky calcite cementation and stockwork development in the finer grained Rocky Brook Formation sediments. The second is a common final stage of secondary porosity development.

Detrital coal material from trenches and drill holes within the northern body of the Humber Falls Formation are considered to have undergone coalification after being deposited as wood debris in fluvial channel sediments. The coal consists of a number of inertinite- and vitrinite-group macerals with intimately associated pyrite. Some of the samples are radioactive. Vitrinite reflectance measurements reveal a high-volatile bituminous B and C rank for the coal.

The vitrinite reflectance ranking of the coal samples, diagenetic clay mineral assemblages, and illite crystallinity measurements were used as thermal maturation indicators. The high-volatile bituminous B and C coal rank, and the diagenetic clay mineral assemblage of kaolinite, montmorillonite, and disordered illite-montmorillonite bracket the maximum temperature for coalification and diagenetic clay-mineral development between about 125°C and 135°C. More refined paleotemperature analyses on other mineral phases may be possible through fluid inclusion and isotope studies. Illite crystallinity measurements confirmed the suspicion that the 10 Å illite peaks represent both diagenetic and detrital illite, and also indicate that the

sediments have remained within the diagenetic realm after deposition and have not entered the transitional anchimetamorphic realm which heralds metamorphism.

Only one stratigraphic trend was revealed by these thermal maturation indicators, namely the appearance of mixed-layer illite-montmorillonite in the North Brook and Humber Falls Formations. This trend could be explained if the Howley Formation covered the Deer Lake Group at one time, then the greater depth of burial, and therefore higher temperatures with increased depth, experienced by the Deer Lake Group may have caused the mixed-layer illite-montmorillonite to develop. However, if the Howley Formation did overly the Deer Lake Group at one time, then the persistence of mixed-layer illite-montmorillonite to a burial depth of approximately 6.8 km is much deeper than other occurrences of mixed-layer illite-montmorillonite (e.g., chapter five, section 5.3.3). Therefore one may conclude that the Howley Formation did not overly the Deer Lake Group in the past, and that other factors, such as cation availability and activity and lithologic and fluid pressures, may have been responsible for mixed-layer clay development in the North Brook and Humber Falls Formations. The conclusion that the Howley Formation did not cover the Deer Lake Group in the past is also supported by the difference in coal rank between the Humber Falls Formation (high-volatile bituminous B or C) and Howley Formation (high-volatile bituminous A or B).

Magnetic susceptibility measurements and compositional comparisons with sandstones from the North Brook, Humber Falls and Howley Formations (Fig. 4.2B) suggest that the uranium-mineralized boulders are most similar to the Humber Falls Formation sandstones. Coincidentally, the mineralized boulders were found in till overlying the northern body of the Humber Falls Formation. Unfortunately, the general diagenetic sequence for the mineralized and unmineralized sandstones which were studied (Fig. 5.1A) does not instill optimism that significant amounts of uranium (or silver) mineralization will be found in the sandstones of the Deer Lake subbasin. A postmineralization stage of hematite cementation in both mineralized and unmineralized sandstones quite likely remobilized much of the mineralization. Probably only isolated pods of mineralization remains concentrated around organic matter in the subsurface. The thin horizons of disseminated uranium mineralization in the fine grained Rocky Brook Formation sediments are also not economically encouraging. Extensive in situ mineralization has yet to be found. On a more optimistic note, these conclusions on the sediment-hosted mineralization in the Deer Lake subbasin do not preclude the possibility of finding uranium or silver mineralization within pre-Upper Devonian igneous rocks adjacent to the subbasin, which may have acted as sedimentary and hydrographic source terranes during the Carboniferous.

REFERENCES

- ADAMS, S.S., CURTIS, H.S., HAFEN, P.L., and SALEK-NEJAD, H. 1973. Interpretation of postdepositional processes related to the formation and destruction of the Jackpile - Paguate uranium deposit, northwest New Mexico. *Economic Geology*, 79, pp. 1635-1654.
- ARNOTT, R.J. 1983. Sedimentology of Upper Ordovician-Silurian sequences on New World Island, Newfoundland: separate fault-controlled basins? *Canadian Journal of Earth Sciences*, 20, pp. 345-354.
- AUSTIN, G.S., and LEININGER, R.K. 1976. The effect of heat-treating sedimented mixed-layer illite-smectite as related to quantitative clay mineral determinations. *Journal of Sedimentary Petrology*, 46, pp. 206-215.
- AYDIN, A., and NUR, A. 1982. Evolution of pull-apart basins and their scale of independence. *Tectonics*, 1, pp. 91-105.
- BAIRD, D.M. 1950. Oil shales of the Deer Lake region. Unpublished report, Geological Survey of Newfoundland. 23 p.
- 1959. Geology, Sandy Lake (west half), Newfoundland. Geological Survey of Canada, Map 47.
- 1966. Carboniferous rocks of the Conche-Groais Island area, Newfoundland. *Canadian Journal of Earth Sciences*, 3, pp. 247-257.
- BAIRD, D.M., and COTE, P.R. 1964. Lower Carboniferous sedimentary rocks in southwestern Newfoundland and their relations to similar strata in western Cape Breton Island. *Bulletin Canadian Institute of Mining and Metallurgy*, 57, pp. 509-520.
- BASKIN, D. 1979. A method of preparing phytoclasts for vitrinite reflectance analysis. *Journal of Sedimentary Petrology*, 49, pp. 633-635.
- BAYLISS, P., BERRY, L.G., MROSE, M.E., and SMITH, D.K. 1980. Mineral powder diffraction file: data book. JCPDS International Centre for Diffraction Data, Pennsylvania, 1168 p.
- BELL, K., and BLENKINSOP, J. 1977. Geochronological evidence of Hercynian activity in Newfoundland. *Nature*, 265, pp. 616-618.
- BELT, E.S. 1968a. Carboniferous continental sedimentation, Atlantic Provinces, Canada. In: *Late Paleozoic Mesozoic continental sedimentation, northeastern North America*. Edited by: G. De V. Klein. Geological Society of America, Special Paper 106, pp. 127-176.
- 1968b. Post-Acadian rifts and related facies, eastern Canada. In: *Studies of Appalachian geology, northern and maritime*. Edited by: E-an Zen, W.S. White, J.B. Hadley, and J.B. Thompson. Interscience Publications, pp. 95-113.
- 1969. Newfoundland Carboniferous stratigraphy and its relation to the Maritimes and Ireland. In: *North Atlantic geology and continental drift*. Edited by: M. Kay. American Association of Petroleum Geologists, Memoir

- 12, pp. 734-753.
- BERNER, R. 1970. Sedimentary pyrite formation. *American Journal of Science*, 268, pp. 1-23.
- BISCAYE, P.E. 1965. Mineralogy and sedimentation of Recent deep-sea clay in the Atlantic Ocean and adjacent seas and oceans. *Geological Society of America Bulletin*, 76, pp. 803-832.
- BLATT, H. 1979. Diagenetic processes in sandstones. In: *Aspects of diagenesis*. Edited by: P.A. Scholle and P.R. Schluger. Society of Economic Paleontologists and Mineralogists, Special Publication 26, pp. 141-157.
- BLATT, H., MIDDLETON, G., and MURRAY, R. 1980. Origin of sedimentary rocks. Prentice Hall Inc., 782 p.
- BOLES, J.R., and FRANKS, S.G. 1979. Clay diagenesis in Wilcox sandstones of southwest Texas: implications of smectite diagenesis on sandstone cementation. *Journal of Sedimentary Petrology*, 49, pp. 55-70.
- BOSTOCK, N.H. 1979. Microscopic measurement of the level of catagenesis of solid organic matter in sedimentary rocks to aid exploration for petroleum and to determine former burial temperatures: a review. In: *Aspects of diagenesis*. Edited by: P.A. Scholle and P.R. Schluger. Society of Economic Paleontologists and Mineralogists, Special Publication 26, pp. 17-44.
- BOYLE, R.W. 1963. Geology of the barite, gypsum, manganese, and lead-zinc-copper-silver deposits of the Walton-Cheverie area, Nova Scotia. Geological Survey of Canada, Paper 62-25, 36 p.
- 1968. The geochemistry of silver and its deposits. Geological Survey of Canada, Bulletin 160, 264 p.
- BRADLEY, D.C. 1982. Subsidence in Late Paleozoic basins in the northern Appalachians. *Tectonics*, 1, pp. 107-123.
- BRINDLEY, G.W., and BROWN, G. 1980. Crystal structure of clay minerals and their X-ray identification. Mineralogical Society, Monograph 5, 544 p.
- BROWN, G. 1955. The effects of isomorphous substitutions on the intensities of (001) reflections of mica- and chlorite-type structures. *Mineralogical Magazine*, 30, pp. 657-665.
- BREGER, I.A. 1974. The role of organic matter in the accumulation of uranium. In: *Formation of uranium ore deposits*. International Atomic Energy Agency, pp. 1775-1785.
- BUGKE, D., and MANKIN, C. 1971. Clay-mineral diagenesis within interlaminated shales and sandstones. *Journal of Sedimentary Petrology*, 41, pp. 971-981.
- BURCHFIEL, B.C., and STEWART, J.H. 1966. 'Pull-apart' origin of the central segment of Death Valley, California. *Geological Society of America Bulletin*, 77, pp. 439-442.
- BURST, J.F. 1959. Postdiagenetic clay-mineral environmental relationship in the Gulf Coast Eocene. *Proceeding of the 6th National Conference on Clays and Clay Minerals*, pp. 327-341.

- CARROLL, D. 1970. Clay minerals: a guide to their X-ray identification. Geological Society of America, Special Paper 126, 80 p.
- CASTANO, J.R., and GARRELS, R.M. 1950. Experiments on the deposition of iron with special reference to the Clinton iron ore deposits. *Economic Geology*, 45, pp. 755-770.
- CASTANO, J.R., and SPARKS, D.M. 1974. Interpretation of vitrinite reflectance measurements in sedimentary rocks and determination of burial history using vitrinite reflectance and authigenic minerals. In: *Carbonaceous materials as indicators of metamorphism*. Edited by: D.R. Dutcher, P.A. Hacquebard, J.M. Schopf and J.A. Simon. Geological Society of America, Special Paper 153, pp. 31-52.
- CHANDLER, F.W. 1982. Sedimentology of the two Middle Paleozoic terrestrial sequences, King George IV Lake area, Newfoundland, and some comments on regional paleoclimate. In: *Current research, part A. Geological Survey of Canada, Paper 82-1A*, pp. 213-219.
- CHARBONNEAU, B., and FORD, R. 1978. Uranium mineralization at the base of the Windsor Group, South Maitland, Nova Scotia. In: *Current research, part A. Geological Survey of Canada, Paper 78-1A*, pp. 419-425.
- CHOQUETTE, P.W., and PRAY, L.C. 1970. Geologic nomenclature and classification of porosity in sedimentary carbonates. *American Association of Petroleum Geologists Bulletin*, 54, pp. 207-250.
- CHURCH, W.R., and STEVENS, R.K. 1971. Early Paleozoic ophiolite complexes of the Newfoundland Appalachians as mantle-oceanic crust sequences. *Journal of Geophysical Research*, 76, pp. 1460-1466.
- CLARKE, D.F., BARR, S.M., and DONOHUE, H.V. 1980. Granitoid and other plutonic rocks of Nova Scotia. In: *Proceedings "the Caledonides in the U.S.A." International Geological Correlation Programme project 27: Caledonide Orogen. 1979 meeting, Blacksburg, Vermont*. Edited by: D.R. Wones. Virginia Polytechnic Institute and State University, Memoir 2, pp. 107-116.
- CLIFFORD, P.M., and BAIRD, D.M. 1962. Great Northern Peninsula of Newfoundland-Grenville inlier. *Bulletin Canadian Institute of Mining and Metallurgy*, 599, pp. 150-157.
- CLOOS, E. 1955. Experimental analysis of fracture patterns. *Geological Society of America Bulletin*, 66, pp. 241-256.
- COLLINSON, J.D. 1978. Alluvial sediments. In: *Sedimentary environments and facies*. Edited by: H.G. Reading. Elsevier, pp. 15-60.
- COOMBS, D.S., and WHETTEN, J.T. 1967. Composition of analcime from sedimentary and burial metamorphic rocks. *Geological Society of America Bulletin*, 78, pp. 269-282.
- CROWELL, J.C. 1974. Origin of Late Cenozoic basins in southern California. In: *Tectonics and sedimentation*. Edited by: W.R. Dickinson. Society of Economic Paleontologists and Mineralogists, Special Publication 22, pp. 190-204.

- 1975. The San Andreas Fault in southern California. In: San Andreas Fault in southern California. Edited by: J.C. Crowell. California Division of Mines, Special Report 118, pp. 7-27.
- CURIALE, J., BLOCH, S., RAFALASK-BLOCH, J., and HARRISON, W. 1983. Petroleum-related origin for uraniferous organic-rich nodules of southwestern Oklahoma. American Association of Petroleum Geologists Bulletin, 67, pp. 588-608.
- CURTIS, C.D. 1983. Link between aluminum mobility and destruction of secondary porosity. American Association of Petroleum Geologists Bulletin, 67, pp. 380-393.
- CURTIS, C.D., and SPEARS, D.A. 1968. The formation of sedimentary iron material. Economic Geology, 63, pp. 257-270.
- DALLEY, D. 1982. The relationship between magnetic minerals and uranium mineralization in the Deer Lake Basin in western Newfoundland. B.Sc. thesis, Memorial University of Newfoundland.
- DAPPLES, E.C. 1971. Physical classification of carbonate cement in quartzose sandstones. Journal of Sedimentary Petrology, 41, pp. 196-204.
- DAVEY, P.T., and SCOTT, T.R. 1956. Adsorption of uranium on clay minerals. Nature, 178, p. 1195.
- DAVIES, D.K., ALMON, W.R., BONIS, S.B., and HUNTER, B.E. 1979. Deposition and diagenesis of Tertiary-Holocene volcaniclastics, Guatemala. In: Aspects of diagenesis. Edited by: P.A. Scholle and P.R. Schluger. Society of Economic Paleontologists and Mineralogists, Special Publication 26, pp. 281-306.
- DEAN, W.E., and FOUCH, T.D. 1983. Lacustrine environment. In: Carbonate Depositional environments. Edited by: P.A. Debout and C.H. Moore. American Association of Petroleum Geologists, Memoir 33, pp. 97-130.
- DEER, W.A., HOWIE, R.A., and ZUSSMAN, J. 1966. An introduction to the rock forming minerals. Longman Group Ltd., 528 p.
- DEFREYES, K.S. 1959. Zeolites in sedimentary rocks. Journal of Sedimentary Petrology, 29, pp. 602-609.
- DERRY, D.R. 1980. Uranium deposits through time. In: The continental crust and its mineral deposits. Edited by: D.W. Strangway. Geological Association of Canada, Special Paper 20, pp. 625-632.
- DEWEY, J.F. 1969. Evolution of the Appalachian-Caledonian orogen. Nature, 222, pp. 124-129.
- DIEHL, J.F., and SHIVE, P.N. 1981. Paleomagnetic results from the Late Carboniferous/Early Permian Casper Formation: implications for northern Appalachian tectonics. Earth and Planetary Science Letters, 54, pp. 281-292.
- DUFF, P.M.C.L.D., FORGERÓN, S., and VAN DE POLL, H.W. 1982. Upper Pennsylvanian sediment dispersal and paleochannel orientation in the western part of the Sydney coalfield, Cape Breton, Nova Scotia. Maritimes Sediments and Atlantic Geology, 18, pp. 83-90.

- DUNOYER DE SEGONZAC, G. 1970. The transformation of clay minerals during diagenesis and low-grade metamorphism: a review. *Sedimentology*, 15, pp. 281-346.
- DUNOYER DE SEGONZAC, G., FERRERO, J., and KUBLER, B. 1968. Sur la cristallinité de l'illite dans la diagenèse et l'anchimétamorphisme. *Sedimentology*, 10, pp. 137-143.
- DUNSMORE, H. 1977a. A new genetic model for uranium-copper mineralization, Permo-Carboniferous basin, northern Nova Scotia. In: Report of activities, part B. Geological Survey of Canada, Paper 77-1B, pp. 247-253.
- 1977b. Uranium resources of the Permo-Carboniferous basin, Atlantic Canada. In: Report of activities, part B. Geological Survey of Canada, Paper 77-1B, pp. 341-348.
- ELIAS, P. 1981. Deer Lake Basin project petrographic and chemical analyses. Private Report for Westfield Minerals Limited, 26 p.
- ESLINGER, E., and SELLARS, B. 1981. Evidence for the formation of illite from smectite during burial metamorphism in the Belt Supergroup, Clark Fork, Idaho. *Journal of Sedimentary Petrology*, 51, pp. 203-216.
- EUGSTER, H.P., and SURDAM, R.C. 1973. Depositional environment of the Green River Formation of Wyoming: a preliminary report. *Geological Society of America Bulletin*, 84, pp. 1115-1120.
- FIJEREMANS, M., and BOSMANS, H. 1982. Colour zones and the transition from diagenesis to low-grade metamorphism of the Gedinnian shales around the Stavelot massif (Ardennes, Belgium). *Schweizische Mineralogische und Petrographische Mitteilungen*, 62, pp. 99-112.
- FISCHER, R.P. 1974. Exploration guides to new uranium districts and belts. *Economic Geology*, 69, pp. 362-376.
- FITCH, D. 1980. Exploitation for uranium deposits, Grants mineral belt. In: *Geology and mineral technology of the Grants uranium region 1979*. New Mexico Bureau of Mines and Mineral Resources, Memoir 38, pp. 40-51.
- FLEMING, J.M. 1970. Petroleum exploration in Newfoundland and Labrador. Department of Mines, Agriculture, and Resources, Mineral Resources Report 3, 118 p.
- FLUGEL, E. 1982. *Microfacies analysis of limestones*. Springer-Verlag, 633 p.
- FOLK, R.L. 1962. Spectral subdivision of limestone types. In: *Classification of carbonate rocks*. Edited by: W.E. Ham. American Association of Petroleum Geologists, Memoir 1, pp. 62-84.
- 1965. Some aspects of recrystallization in ancient limestones. In: *Dolomitization and limestone diagenesis, a symposium*. Edited by: L.C. Pray and R.C. Murray. Society of Economic Paleontologists and Mineralogists, Special Publication 13, pp. 14-48.
- 1976. Reddening of desert sands: Simpson Desert, N.T., Australia. *Journal of Sedimentary Petrology*, 46, pp. 604-615.

- 1980. Petrology of sedimentary rocks. Hemphill Publishing Company, 184 p.
- FONG, C.K. 1976. Geological mapping- Deer Lake - White Bay Carboniferous basin. In: Report of activities. Newfoundland Department of Mines and Energy, pp. 19-24.
- FORD, K.L., and BALLANTYNE, S.B. 1983. Uranium and thorium distribution patterns and lithogeochemistry of Devonian granites in the Chedabucto Bay area, Nova Scotia. In: Current research, part A. Geological Survey of Canada, Paper 83-1A, pp. 109-119.
- FOSCOLOS, A.E., and STOTT, D.F. 1975. Degree of diagenesis, stratigraphic correlations and potential sediment sources of Lower Cretaceous shale of northeastern British Columbia. Geological Survey of Canada, Bulletin 250, 46 p.
- FOSTER, W.D., and FEICHT, F.L. 1946. Mineralogy of concretions from Pittsburg coal seam, with special reference to analcime. American Mineralogist, 31, pp. 357-364.
- FRALICH, P.W., and SCHENK, P.E. 1981. Mollase deposition and basin evolution in a wrench tectonic setting: the Late Paleozoic, Eastern Cumberland Basin, Maritime Canada. In: Sedimentation and tectonics in alluvial basins. Edited by: A.D. Miall. Geological Association of Canada, Special Paper 23, pp. 77-98.
- FREY, M. 1970. The step from diagenesis, to metamorphism in pelitic rocks during Alpine orogenesis. Sedimentology, 15, pp. 261-279.
- FREY, M., TEICHMULLER, M., TEICHMULLER, R., MULLIS, J., KUNZI, B., BREITSCHMID, A., GRUNER, U., and SCHWIZER, B. 1980. Very low-grade metamorphism in external parts of the Central Alps: illite crystallinity, coal rank and fluid inclusion data. Eclogae Geologicae Helvetiae, 73, pp. 173-203.
- FRIEDMAN, G.M. 1971. Staining. In: Procedures in sedimentary petrology. Edited by: R.E. Carver. Wiley Interscience, pp. 511-530.
- FRITTS, C.E. 1953. Geological reconnaissance across the Great Northern Peninsula, Newfoundland. Geological Survey of Newfoundland, Report 4, 37 p.
- FRONDEL, C. 1982. Structural hydroxyl in chalcedony (type B quartz). American Mineralogist, 67, pp. 1248-1257.
- FUREY, D. 1982. Bouguer gravity anomaly and geochemical till sample trends in the Carboniferous Deer Lake Basin in western Newfoundland. B.Sc. thesis, Memorial University of Newfoundland.
- GARRELS, R.M., and CHRIST, C.L. 1965. Solutions, minerals, and equilibria. Harpers Geoscience Series, 450 p.
- GARRELS, R.M., and HOWARD, P. 1959. Reactions of feldspar and mica with water at low temperature and pressure. Clays and Clay Minerals, 6, pp. 68-88.
- GARRELS, R.M., and LARSEN, E.S. 1959. Geochemistry and mineralogy of the Colorado Plateau uranium ores. United States Geological Survey, Professional Paper 320, 236 p.

- GELDSETZER, H. 1977. The Windsor Group of Cape Breton Island, Nova Scotia. In: Report of activities, part A. Geological Survey of Canada, Paper 77-1A, pp. 425-428.
- 1978. The Windsor Group of Atlantic Canada-an update. In: Current research, part C. Geological Survey of Canada, Paper 78-1C, pp. 43-48.
- GIBBS, R.J. 1968. Clay mineral mounting techniques for X-ray diffraction analysis: a discussion. *Journal of Sedimentary Petrology*, 38, pp. 242-244.
- GILES, P.S., BOEHNER, R.C., and RYAN, R.J. 1979. Carbonate banks of the Gays River Formation in central Nova Scotia. Nova Scotia Department of Mines, Paper, 79-7, 57 p.
- GLENNIE, K.W. 1970. Desert sedimentary environments. *Developments in Sedimentology* 14. Elsevier, 222 p.
- GOLDICH, S.S. 1938. A study in rock-weathering. *Journal of Geology*, 46, pp. 17-58.
- GRAY, T.R., and WILLIAMS, S.T. 1971. Soil micro-organisms. Oliver and Boyd, Edinburgh, 240 p.
- GRIM, R.E., BRAY, R.H., and BRADLEY, W.F. 1937. The mica in argillaceous sediments. *American Mineralogist*, 22, pp. 813-829.
- HACQUEBARD, P.A., BARSS, M.S., and DONALDSON, J.R. 1960. Distribution and stratigraphic significance of small spore genera in the Upper Carboniferous of the maritime provinces of Canada. 4th International Carboniferous Stratigraphy and Geology Congress, Heerlen, 1, pp. 237-245.
- HACQUEBARD, P.A., and DONALDSON, J.R. 1969. Carboniferous coal deposition associated with flood-plain and limnic environment in Nova Scotia. In: *Environments of coal deposition*. Edited by: E.C. Dapples and M.E. Hopkins. Geological Society of America, Special Paper 14, pp. 143-191.
- 1970. Coal metamorphism and hydrocarbon potential in the Upper Paleozoic of the Atlantic Provinces, Canada. *Canadian Journal of Earth Sciences*, 7, pp. 1139-1163.
- HARDIE, L.A., SMOOT, T.P., and EUGSTER, H.P. 1978. Saline lakes and their deposits: a sedimentological approach. In: *Modern and ancient lacustrine environments*. Edited by: A. Matter and M.E. Tucker. International Association of Sedimentologists, Special Publication 2, pp. 7-42.
- HARSHMAN, E.N. 1970. Uranium ore rolls in the United States. In: *Uranium exploration geology*. International Atomic Energy Agency, pp. 219-231.
- HATCH, H.B. 1919. Deer Lake, Humber River and Grand Lake shales area. Unpublished report, Reid Newfoundland Company, 11 p.
- HAWORTH, R.T., POOLE, W.H., GRANT, A.C., and SANFORD, B.V. 1976. Marine geoscience survey northeast of Newfoundland. In: Report of activities, part A. Geological Survey of Canada, Paper 76-1A, pp. 7-15.
- HAY, R.L. 1966. Zeolites and zeolitic reactions in sedimentary rocks. Geological Society of America, Special Paper 85, 130 p.

- HAY, R.L., and MOIOLA, R.J. 1963. Authigenic silicate minerals in Searles Lake, California. *Sedimentology*, 2, pp. 312-332.
- HAYES, A.O. 1949. Coal possibilities of Newfoundland. Geological Survey of Newfoundland, Information Circular 6, 31 p.
- HAYES, A.O., and JOHNSON, H. 1938. Geology of the Bay St. George Carboniferous area. Newfoundland Geological Survey, Bulletin 12, 62 p.
- HAYES, J. 1970. Polytypism of chlorite in sedimentary rocks. *Clays and Clay Minerals*, 18, pp. 285-306.
- HEALD, M.T., and LARESE, R.E. 1974. Influence of coatings on quartz cementation. *Journal of Sedimentary Petrology*, 44, pp. 1269-1274.
- HEATH, G.R., and PISIAS, N.G. 1979. A method for the quantitative estimation in North Pacific deep-sea sediments. *Clays and Clay Minerals*, 27, pp. 175-184.
- HELGESON, H.C., GARRELS, R.M., and MACKENZIE, F.T. 1969. Evaluation of irreversible reactions in geochemical processes involving minerals and aqueous solutions-II. Applications. *Geochimica et Cosmochimica Acta*, 33, pp. 455-481.
- HELING, D., and TEICHMULLER, M. 1974. Die grenze montmorillonit/mixed layer-minerale und ihre beziehung zur inkohlung in der Graven Schichten-folge des Oligozans in Oberrheingraben. *Fortschritte in der Geologie von Rheinland Westfalen*, 24, pp. 113-127.
- HEROUX, Y., CHAGNON, A., and BERTHAND, R. 1979. Compilation and correlation of major thermal maturation indicators. *American Association of Petroleum Geologists Bulletin*, 63, pp. 2128-2144.
- HEYL, G.R. 1937. The geology of the Sops Arm area White Bay, Newfoundland. Newfoundland Department of Natural Resources, Geological Section, Bulletin 8, 42 p.
- HIBBARD, J., and WILLIAMS, H. 1979. Regional setting of the Dunnage Melange in the Newfoundland Appalachians. *American Journal of Science*, 279, pp. 993-1021.
- HICKS, R.T., LOWRY, R.M., DELLA VALLE, R.S., and BROOKINS, D.G. 1980. Petrology of Westwater Canyon Member, Morrison Formation, East Chaco Canyon drilling project, New Mexico- comparison with Grants mineral belt. In: *Geology and mineral technology of the Grants uranium region 1979*. Edited by: C.A. Rautman. New Mexico Bureau of Mines and Mineral Resources, Memoir 38, pp. 208-214.
- HIGH, L.R., and PICARD, M.D. 1965. Sedimentary petrology and origin of analcime-rich Popo Agie Member, Chugwater (Triassic) Formation, west-central Wyoming. *Journal of Sedimentary Petrology*, 35, pp. 49-70.
- HISCOTT, R.N. 1979. Sedimentology of Humber Falls Formation Wigwam Brook- RL 218 drill core study. Private Report for Westfield Minerals Limited, 20 p.
- 1980. Some impressions concerning regional trends in Humber Falls Formation, northern lobe. Private Report for Westfield Minerals Ltd., 5 p.

- HISCOTT, R., JAMES, N.P., and PEMBERTON, S.G. In press. Sedimentology and ichnology of the Lower Cambrian Bradore Formation: fluvial to shallow-marine transgressive sequence, coastal Labrador. Bulletin of Canadian Petroleum Geology.
- HOFFMAN, J., and HOWER, J. 1979. Clay mineral assemblages as low grade metamorphic geothermometers: application to the thrust faulted, disturbed belt of Montana, U.S.A.. In: Aspects of diagenesis. Edited by: P.A. Scholle and P.R. Schluger. Society of Economic Paleontologists and Mineralogists, Special Publication 26, pp. 55-79.
- HOWER, J., and MOWATT, T.C. 1966. The mineralogy of illites and mixed-layer illite/montmorillonites. American Mineralogist, 51, pp. 825-854.
- HOWIE, R.D. 1979. Carboniferous evaporites in Atlantic Canada. 9th International Congress on Carboniferous Stratigraphy and Geology, Illinois, pp. 93-94.
- HOWIE, R.D., and BARSS, M.S. 1974. Upper Paleozoic rocks of the Atlantic Provinces, Gulf of St. Lawrence, and adjacent continental shelf. Geological Survey of Canada, Paper 74-30, pp. 35-50.
- HOWSE, A., and FLEISCHMANN, J. 1982. Coal assessment in the Deer Lake Carboniferous basin. In: Current research. Department of Mines and Energy Government of Newfoundland and Labrador, Report 82-1, pp. 208-213.
- HUANG, W.H., and KELLER, W.D. 1972. Organic acids as agents of chemical weathering of silicate minerals. Nature, 239, pp. 149-151.
- HUBERT, J.F., and REED, A.A. 1978. Red-bed diagenesis in the East Berlin Formation, Newark Group, Connecticut Valley. Journal of Sedimentary Petrology, 48, pp. 175-184.
- HURST, A., and IRWIN, H. 1982. Geological modelling of clay diagenesis in sandstones. Clay Minerals, 17, pp. 5-22.
- HUTCHEON, I. 1983. Aspects of the diagenesis of coarse-grained siliciclastic rocks. Geoscience Canada, 10, pp. 4-14.
- HUTCHEON, I., OLDERSHAW, A., and GHENT, E. 1980. Diagenesis of Cretaceous sandstones of the Kootney Formation at Elk Valley (southeastern British Columbia) and Mt. Allan (southwestern Alberta). Geochimica et Cosmochimica Acta, 44, pp. 1425-1435.
- HYDE, R.S. 1978. Stratigraphic subdivisions and mapping of the Lower Mississippian Anguille Group, Deer Lake - White Bay area, Newfoundland. In: Report of activities for 1977. Newfoundland Department of Mines and Energy, Mineral Development Division, Report 78-1, pp. 116-123.
- 1979a. Geology of portions of the Carboniferous Deer Lake Basin, western Newfoundland. In: Report of activities for 1978. Department of Mines and Energy Government of Newfoundland and Labrador, Report 79-1, pp. 11-17.
- 1979b. Geology of Carboniferous strata in portions of the Deer Lake Basin, western Newfoundland. Geological Survey of Newfoundland, Report 79-6, 43 p.

- 1981. Geology and mineral resources of the Carboniferous Deer Lake Basin. In: Preliminary project reports for 1981. Department of Mines and Energy Government of Newfoundland and Labrador, pp. 6-P2.
- 1983. Map 28-7 Geology of the Carboniferous Deer Lake Basin. Department of Mines and Energy, Government of Newfoundland and Labrador.
- In press. Geological setting and aspects of uranium mineralization in the Carboniferous Deer Lake Basin, western Newfoundland. Economic Geology.
- HYDE, R.S., and WARE, M.J. 1980. Geological map with marginal notes, Cormack - Silver Mountain area. In: Current research. Mineral Development Division Department of Mines and Energy, Newfoundland, Report 80-1, pp. 29-36.
- 1981. Geology of Carboniferous strata in the Deer Lake and Rainy Lake map areas, Newfoundland. In: Current Research. Mineral Development Division Department of Mines and Energy, Newfoundland, Report 81-1, pp. 17-31.
- IRVING, E. 1977. Drift of the major continental blocks since the Devonian. Nature, 270, pp. 304-309.
- 1979. Paleopoles and paleolatitudes of North America and speculations about displaced terrains. Canadian Journal of Earth Sciences, 16, pp. 669-694.
- IRVING, E., and STRONG, D.F. In press. Paleomagnetism of the Viséan Deer Lake Group, western Newfoundland: no evidence for Carboniferous displacement of "Acadia". Earth and Planetary Science Letters.
- ISPHORDING, W., and LODDING, W. 1973. Geochemistry and diagenesis of macrokaolinite. Geological Society of America Bulletin, 84, pp. 2319-2326.
- JAMES, N.P. 1981. Megablocks of calcified algae in the Cow Head Breccia, western Newfoundland: vestiges of a Cambro-Ordovician platform margin. Geological Society of America Bulletin, 92, pp. 799-811.
- JENNESS, S.E. 1958. Geology of the Gander River Ultrabasic Belt, Newfoundland. Geological Survey of Newfoundland, Report 11, 58 p.
- JOHNS, W.D., GRIM, R.E., and BRADLEY, W.F. 1954. Quantitative estimations of clay minerals by diffraction methods. Journal of Sedimentary Petrology, 24, pp. 242-251.
- JOHNSON, D.L. 1967. Caliche on the Channel Islands. Mineral Information California Division of Mines and Geology, 20, pp. 151-158.
- KARLSTROM, K.E. 1983. Reinterpretation of Newfoundland gravity data and arguments for an allochthonous Dunnage Zone. Geology, 11, pp. 263-266.
- KEAN, B.F., and STRONG, D.F. 1975. Geochemical evolution of an Ordovician island arc of the central Newfoundland Appalachians. American Journal of Science, 275, pp. 97-118.
- KELLER, W.D. 1957. The principles of chemical weathering. Lucas Brothers Montana, 111 p.

- 1978. Classification of kaolins exemplified by their textures in scanning electron micrographs. *Clays and Clay minerals*, 26, pp. 1-20.
- KENT, D.V. 1982. Paleomagnetic evidence for post-Devonian displacement of the Avalon Platform (Newfoundland). *Journal of Geophysical Research*, 87, pp. 8709-8716.
- KENT, D.V., and OPDYKE, N.D. 1979. The Early Carboniferous paleomagnetic field of North America and its bearing on tectonics of the northern Appalachians. *Earth and Planetary Science Letters*, 44, pp. 365-372.
- KEPPIE, J.D., GILES, P.S., and BOEHNER, R.C. 1978. Some Middle Devonian to Lower Carboniferous rocks of Cape George, Nova Scotia: Nova Scotia Department of Mines, Paper 78-4, 37 p.
- KIRKHAM, R. 1978. Base metal and uranium distribution along the Windsor-Horton contact, central Cape Breton Island, Nova Scotia. In: *Current research, part B. Geological Survey of Canada, Paper 78-1B*, pp. 121-135.
- KLAPPA, C.F. 1980. Rhizoliths in terrestrial carbonates: classification, recognition, genesis and significance. *Sedimentology*, 27, pp. 613-629.
- KLAPPA, C.F., OPALINSKI, P.R., and JAMES, N.P. 1980. Middle Ordovician Table Head Group of western Newfoundland: a revised stratigraphy. *Canadian Journal of Earth Sciences*, 17, pp. 1007-1019.
- KNIGHT, I. 1983. Geology of the Carboniferous Bay St. George Subbasin, western Newfoundland. Department of Mines and Energy, Government of Newfoundland and Labrador, Memoir 1, 385 p.
- KODAMA, H., SCOTT, G., and MILES, N. 1977. X-ray quantitative analysis of minerals in soils. Soil Research Institute publication, Agriculture Canada, 49 p.
- KOMAROV, A., SERGEYEV, S., VARZELASHVILI, N., and PAVSHUKOV, V. 1982. Quantitative radiographic analysis of the uranium distribution in a granite. *Geochemistry International*, 19, pp. 157-170.
- KRYNINE, P.D. 1950. Petrology, stratigraphy and origin of the Triassic sedimentary rocks of Connecticut. Connecticut State Geology and Natural History Survey, Bulletin 73, 239 p.
- KUBLER, B. 1966. La cristallinité de l'illite et les zones tout a fait supérieures du métamorphisme. In: *Etages tectoniques. Colloque De Neuchatel 18-21 Avril 1966*, pp. 105-122.
- 1967. Anchimétamorphisme et schistosité. *Bulletin Centre de Recherches de Pau, Société Nationale des Pétroles D'Aquitaine*, 1, pp. 259-278.
- LANDELL-MILLS, T. 1922. The Carboniferous rocks of the Deer Lake district of Newfoundland. *Geological Society of London, Abstracts of Proceedings* 1083, pp. 53-54.
- 1954. Report on the Oxley oil and oil shale concession in the Deer Lake district Newfoundland. Private report for Claybar Uranium and Oil, 7 p.

- LANGMUIR, D. 1978. Uranium solution-mineral equilibria at low temperatures with applications to sedimentary ore deposits. *Geochimica et Cosmochimica Acta*, 42, pp. 547-569.
- LARACY, P.J., and HISCOTT, R.N. 1982. Carboniferous rebeds of alluvial origin, Spanish Room Formation, Avalon Zone, southeastern Newfoundland. *Bulletin of Canadian Petroleum Geology*, 30, pp. 264-273.
- LATTMAN, L.H. 1973. Calcium carbonate cementation of alluvial fans in southern Nevada. *Geological Society of America Bulletin*, 84, pp. 3013-3028.
- LEEDER, M.R. 1975. Pedogenic carbonates and flood sediment accretion rates: a quantitative model for alluvial arid-zone lithofacies. *Geological Magazine*, 112, pp. 257-270.
- LEFORT, J.P., and VAN DER VOO, R. 1981. A kinematic model for the collision and complete suturing between Gondwanaland and Laurasia in the Carboniferous. *Journal of Geology*, 89, pp. 537-550.
- LEGGETT, J.K. 1978. Eustacy and pelagic regimes in the Iapetus Ocean during the Ordovician and Silurian. *Earth and Planetary Science Letters*, 41, pp. 163-169.
- LEGUN, A., and RUST, B. 1982. The Upper Carboniferous Clifton Formation of northern New Brunswick: coal-bearing deposits of semi-arid alluvial plain. *Canadian Journal of Earth Sciences*, 19, pp. 1775-1785.
- LOCK, B.E. 1969. Paleozoic wrench faults in the Canadian Appalachians: discussion. *American Association of Petroleum Geologists, Memoir 12*, pp. 789-790.
- MASON, A.G., and RUST, B. 1983. Lacustrine stromatolites and algal laminites in a Pennsylvanian coal-bearing succession near Sydney, Nova Scotia, Canada. *Canadian Journal of Earth Sciences*, 20, pp. 1111-1118.
- MAXWELL, D.T., and HOWER, J. 1967. High-grade diagenesis and low-grade metamorphism of illite in the Precambrian Belt series. *American Mineralogist*, 52, pp. 843-857.
- MCCABE, P.J., MCCARTHY, K.L., and PLUIM, S.B. 1980. Terrestrial sedimentation associated with strike-slip fault movement in middle Carboniferous of Nova Scotia, Canada. *American Association of Petroleum Geologists Bulletin*, 64, pp. 747-748.
- MCMASTER, R.L., DE BOER, J., and COLLINS, B.P. 1980. Tectonic development of southern Narragansett Bay and offshore Rhode Island. *Geology*, 8, pp. 496-500.
- MCMILLAN, R.H. 1979. Genetic aspects and classification of important Canadian uranium deposits. In: *Uranium deposits: their mineralogy and origin*. Edited by: M.M. Kimberley. *Mineralogical Association of Canada Short Course*, pp. 187-204.
- MEHRA, O.P., and JACKSON, M.L. 1960. Iron removal from soils and clays by a dithionite-citrate system buffered with sodium bicarbonate. *Clays and Clay Minerals*, 7, pp. 317-327.

- MILLER, H.G., and WRIGHT, J.A., 1984. Gravity and magnetic interpretation of the Deer Lake basin, Newfoundland. *Canadian Journal of Earth Sciences*, 21, pp. 10-18.
- MOODY, J.D., and HILL, M.J. 1956. Wrench-fault tectonics. *Geological Society of America Bulletin*, 67, pp. 1207-1246.
- NORTHERN MINER November 30 1978. Westfield Minerals 'U' find holds important connotations.
- OGUNYOMI, O., HESSE, R., and HEROUX, Y. 1980. Pre-orogenic and synorogenic diagenesis and anchimetamorphism in Lower Paleozoic continental margin sequences of the northern Appalachians in and around Quebec city, Canada. *Bulletin of Canadian Petroleum Geology*, 28, pp. 559-577.
- PACKHAM, G., and CROOK, K. 1960. The principle of diagenetic facies and some of its applications. *Journal of Geology*, 68, pp. 392-407.
- PAJARI, G.E., and CURRIE, K.L. 1978. The Gander Lake and Davidsville Groups of northern Newfoundland: a re-examination. *Canadian Journal of Earth Sciences*, 15, pp. 708-714.
- PALMER, A.R., and JAMES, N.P. 1980. The Hawke Bay Event: a circum-Iapetus regression near the Lower-Middle Cambrian boundary. In: *Proceedings "the Caledonides in the U.S.A." International Geological Correlation Programme project 27: Caledonide Orogen. 1979 meeting, Blacksburg, Vermont. Edited by: D.R. Wones. Virginia Polytechnic Institute and State University, Memoir 2, p. A3.*
- PERRY, E., and HOWER, J. 1970. Burial diagenesis in Gulf Coast pelitic sediments. *Clays and Clay Minerals*, 18, pp. 165-177.
- PHAIR, G. 1949. *Geology of the southwestern part of the Long Range, Newfoundland. Ph.D. thesis, Princeton University.*
- PICARD, M.D. 1971. Classification of fine-grained sedimentary rocks. *Journal of Sedimentary Petrology*, 41, pp. 179-195.
- PIERCE, J.W., and SIEGEL, F.R. 1969. Quantification in clay mineral studies of sediments and sedimentary rocks. *Journal of Sedimentary Petrology*, 39, pp. 187-193.
- POPPER, G.H.P. 1970. Paleobasin analysis and structure of the Anguille Group, west-central Newfoundland. Ph.D thesis, Lehigh University.
- PRATT, B.R., and JAMES, N.P. 1982. Cryptalgal-metazoan bioherms of early Ordovician age in the St. George Group, western Newfoundland. *Sedimentology*, 29, pp. 543-569.
- PREST, V.K., STEACY, H.R., and BOTTRILL, T.J. 1969. Occurrences of uranium and vanadium in Prince Edward Island. *Geological Survey of Canada, Paper 68-74, 13 p.*
- RAISWELL, R. 1971. The growth of Cambrian and Liassic concretions. *Sedimentology*, 17, pp. 147-171.
- RAST, N., GRANT, R.H., PARKER, J.S.D., and TENG, H.C. In press. The Carboniferous succession in southern New Brunswick and its state of deformation. 9th International Congress on Carboniferous Stratigraphy and Geology, Illinois.

- RICH, R.A., HEINRICH, H.D., and PETERSEN, U. 1977. Hydrothermal uranium deposits. *Developments in Economic Geology* 6. Elsevier, 264 p.
- RODGERS, J. 1968. The eastern edge of the North American continent during the Cambrian and Early Ordovician. In: *Studies of Appalachian geology- northern and Maritime*. Edited by: E-an Zen, J.B. Hadley and J.B. Thompson Jr. Wiley Interscience, pp. 141-149.
- ROGERSON, R.J. 1981. Drift prospecting in the Deer Lake lowland. Private Report for Westfield Minerals Limited, 12 p.
- RUST, B.R. 1981. Alluvial deposits and tectonic style: Devonian and Carboniferous successions in Eastern Gaspe. In: *Sedimentation and tectonics in alluvial basins*. Edited by: A.D. Miall. Geological Association of Canada, Special Paper 23, pp. 49-77.
- SANDFORD, B.V., GRANT, A.C., WADE, J.A., and BARSS, M.S. 1979. Map 1401A: Geology of eastern Canada and adjacent regions. Geological Survey of Canada, Paper Series.
- SCAFE, D.W., and KUNZE, G.W. 1971. A clay mineral investigation of six cores from the Gulf of Mexico. *Marine Geology*, 10, pp. 69-85.
- SCHENK, P.E. 1969. Carbonate-sulfate-redbed facies and cyclic sedimentation of the Windsorian Stage (Middle Carboniferous), Maritime Provinces. *Canadian Journal of Earth Sciences*, 6, pp. 1037-1066.
- 1975. Carbonate-sulfate intertidalities of the Windsor Group (Middle Carboniferous), Maritime Provinces, Canada. In: *Tidal deposits. A casebook of Recent examples and fossil counterparts*. Edited by: R.N. Ginsburg. Springer-Verlag, pp. 373-380.
- SCHILLEREFF, S., and WILLIAMS, H. 1979. Geology of Stephenville map area, Newfoundland. In: *Current research, part A*. Geological Survey of Canada, Paper 79-1A, pp. 327-332.
- SCHMIDT, V., MCDONALD, D.A., and PLATT, R.L. 1977. Pore geometry and reservoir aspects of secondary porosity in sandstones. *Bulletin Canadian Petroleum Geology*, 25, pp. 271-290.
- SCHOLLE, P.A. 1979. A color illustrated guide to constituents, textures, cements, and porosities of sandstones and associated rocks. *American Association of Petroleum Geologists, Memoir* 28, 201 p.
- SCHUCHERT, C., and DUNBAR, C.O. 1934. Stratigraphy of western Newfoundland. *Geological Society of America, Memoir* 1, 123 p.
- SIBLEY, D.F., and BLATT, H. 1979. Intergranular pressure solution and cementation of the Tuscarora orthoquartzite. In: *Diagenesis of sandstones: cement-porosity relationships*. Edited by: E. McBride. *Society of Economic Paleontologists and Mineralogists, Reprint Series* 9, pp. 123-139.
- SIPPEL, R., and GLOVER, E.D. 1965. Structures in carbonate rocks made visible by luminescence petrography. *Science*, 150, pp. 1283-1287.

- SMITH, P.R. 1982. Sedimentology and diagenesis of the Miocene Peace Valley Formation, Ridge Basin, southern California. In: Geologic history of Ridge Basin, southern California. Edited by: J.C. Crowell and M.H. Link. Pacific Section, Society of Economic Paleontologists and Mineralogists, pp. 151-158.
- ST-JULIEN, P., HUBERT, C., and WILLIAMS, H. 1976. The Baie Verte - Brompton Line and its possible tectonic significance in the northern Appalachians. Geological Association of America, Abstracts with Programs, 8, pp. 259-260.
- STACH, E., MACKOWSKY, M.-TH., TEICHMULLER, M., TAYLOR, G.H., CHANDRA, D., and TEICHMULLER, R. 1975. Stach's textbook of coal petrology. Gebruder Borntraeger, 428 p.
- STADLER, P.J. 1975. Cementation of Pliocene-Quaternary fluviatile clastic deposits in and along the Oman Mountains. Geologie en Mijnbouw, 54, pp. 148-156.
- STEEL, R.J., and AASHEIM, S.M. 1978. Alluvial sand deposition in a rapidly subsiding basin (Devonian, Norway). In: Fluvial sedimentology. Edited by: A.D. Miall. Canadian Society of Petroleum Geologists, Memoir 5, pp. 385-412.
- STEEL, R.J., and GLOPPEN, T.G. 1980. Late Caledonian (Devonian) basin formation, western Norway: signs of strike-slip tectonics during infilling. In: Sedimentation in oblique-slip mobile zones. Edited by: P.F. Ballance and H.G. Reading. International Association of Sedimentologists, Special Publication 4, pp. 79-103.
- STOCH, L., and SIKORA, W. 1976. Transformations of micas in the process of kaolinitization of granites and gneisses. Clays and Clay Minerals, 24, pp. 156-162.
- STOKKE, P.R., and CARSON, B. 1973. Variation in clay mineral X-ray diffraction results with the quantity of sample mounted. Journal of Sedimentary Petrology, 43, pp. 957-964.
- STRONG, D.F. 1975. Plateau lavas and diabase dykes of northwestern Newfoundland. Geological Magazine, 111, pp. 501-514.
- 1977. Volcanic regimes of the Newfoundland Appalachians. In: Volcanic regimes in Canada. Edited by: W.R.A. Baragar, L.C. Coleman and J.M. Hall. Geological Association of Canada, Special Paper 16, pp. 61-90.
- 1980. Granitoid rocks and associated mineral deposits of Eastern Canada and Western Europe. In: The continental crust and its mineral deposits. Edited by: D.W. Strangway. Geological Association of Canada, Special Paper 20, pp. 741-769.
- STRONG, D.F., O'BRIEN, S.J., TAYLOR, S.W., STRONG, P.G., and WILTON, D.H. 1978. Aborted Proterozoic rifting in eastern Newfoundland. Canadian Journal of Earth Sciences, 15, pp. 117-131.

- STUCKLESS, J.S., and FERRIRA, C.P. 1976. Labile uranium in granitic rocks. International Atomic Energy Agency, SM-208/17, pp. 717-730.
- SWETT, K., and SMIT, D.E. 1972. Paleogeography and depositional environments of the Cambro-Ordovician shallow-marine facies of the North Atlantic. Geological Society of America Bulletin, 83, pp. 3223-3248.
- TAYLOR, J.C.M. 1978. Control of diagenesis by depositional environment within a fluvial sandstone sequence in the northern North Sea Basin. Journal of the Geological Society, 135, pp. 83-91.
- TEICHMULLER, M., and TEICHMULLER, R. 1967. Diagenesis of coal (coalification). In: Diagenesis in sediments. Edited by: G. Larsen and G. Chilinger. Elsevier, pp. 391-413.
- TILLMAN, R.W., and ALMON, D.K. 1979. Diagenesis of Frontier Formation offshore bar sandstones, Spearhead Ranch field, Wyoming. In: Aspects of diagenesis. Edited by: P.A. Scholle and P.R. Schluger. Society of Economic Paleontologists and Mineralogists, Special Publication 26, pp. 337-378.
- TSUNASHIMA, A., BRINDLEY, G.W., and BASTOVANOV, M. 1981. Adsorption of uranium from solutions by montmorillonite, compositions and properties of uranyl montmorillonites. Clays and Clay Minerals, 29, pp. 10-16.
- TURNER, P. 1980. Continental red beds. Developments in sedimentology 29. Elsevier, 562 p.
- UPADHYAY, H.D., DEWEY, J.F., and NEALE, E.W. 1971. The Betts Cove ophiolite complex, Newfoundland: Appalachian oceanic crust and mantle. Geological Association of Canada, Proceedings, 24, pp. 27-34.
- VAN HOUTEN, F.B. 1961. Climatic significance of red beds. In: Descriptive paleoclimatology. Edited by: A.E. Nairn. Interscience, pp. 89-139.
- VANDERVEER, D.G., and TUACH, J. 1982. Field trip guide Deer Lake basin area. Prospecting in glaciated terrain. Canadian Institute of Mining and Metallurgy, field trip guide, 17 p.
- WALKER, T.R. 1967. Formation of red beds in modern and ancient deserts. Geological Society of America Bulletin, 78, pp. 353-368.
- 1974. Formation of red beds in moist tropical climates: hypothesis. Geological Society of America Bulletin, 85, pp. 633-638.
- WALKER, T.R., WAUGH, B., and GRONE, A.J. 1978. Diagenesis in first-cycle desert alluvium of Cenozoic age, southern United States and northwestern Mexico. Geological Society of America Bulletin, 89, pp. 19-32.
- WEAVER, C.E. 1956. The distribution and identification of mixed-layer clays in sedimentary rocks. American Mineralogist, 41, pp. 202-221.
- WEBB, G.W. 1969. Paleozoic wrench faults in Canadian Appalachians. In: North Atlantic- geology and continental drift. Edited by: M. Kay. American Association of Petroleum Geologists, Memoir 12, pp.

754-786.

- WEBER, K. 1972. Notes on determination of illite crystallinity. *Neues Jahrbuch Für Mineralogie Monatshefte*, 6, pp. 267-276.
- WERNER, H.J. 1955. The geology of Humber Valley, Newfoundland. Private Report for Newkirk Mining Company, 116 p.
- 1956. The geology of Humber Valley, Newfoundland. Ph.D thesis, Syracuse University.
- WILCOX, R.E., HARDING, T.P., and SEELY, D.R. 1973. Basic wrench tectonics. *American Association of Petroleum Geologists Bulletin*, 57, pp. 74-96.
- WILLIAMS, E.P. 1974. Geology and petroleum possibilities in and around Gulf of St. Lawrence. *American Association of Petroleum Geologists Bulletin*, 58, pp. 1137-1155.
- WILLIAMS, H. 1964. The Appalachians in northeastern Newfoundland. A two-sided symmetrical system. *American Journal of Science*, 262, pp. 1137-1158.
- 1971. Mafic-ultramafic complexes of western Newfoundland Appalachians and the evidence for their transportation: a review and interim report. *Geological Association of Canada, Proceedings*, 24, pp. 9-25.
- 1975. Structural succession, nomenclature, and interpretation of transported rocks in western Newfoundland. *Canadian Journal of Earth Sciences*, 12, pp. 1874-1894.
- 1976. Tectonic stratigraphic subdivision of the Appalachian Orogen. *Geological Society of America, Abstracts with Programs*, 8, p. 300.
- 1978. Tectonic-lithofacies map of the Appalachian Orogen. Memorial University of Newfoundland, Map 1.
- 1979. Appalachian orogen in Canada. *Canadian Journal of Earth Sciences*, 16, pp. 792-807.
- 1980. Structural telescoping across the Appalachian orogen and the minimum width of the Iapetus Ocean. *Geological Association of Canada, Special Paper 20*, pp. 421-440.
- WILLIAMS, H., and ST-JULIEN, P. 1982. The Baie Verte - Brompton Line: Early Paleozoic continental ocean interface in the Canadian Appalachians. In: *Major structural zones and faults of the northern Appalachians*. Edited by: P. St-Julien and J. Béland. *Geological Association of Canada, Special Paper 24*, pp. 177-208.
- WILLIAMS, H., and STEVENS, R.K. 1974. The ancient continental margin of eastern North America. In: *The geology of continental margins*. Edited by: C.A. Burk and C.L. Drake. Springer-Verlag, pp. 781-796.
- WILLIAMS, H., and TALKINGTON, R.W. 1977. Distribution and tectonic setting of ophiolites and ophiolitic melange in the Appalachian orogen. In: *North American ophiolites*. Edited by: R.G. Colman and W.P. Irwin. *Oregon Department of Geology and Mineral Industries, Bulletin 95*, pp. 1-11.

- WILSON, J.T. 1966. Did the Atlantic close and then re-open? *Nature*, 211, pp. 676-681.
- WILSON, M.D., and PITTMAN, E.D. 1977. Authigenic clays in sandstones: recognition and influence on reservoir properties and paleoenvironmental analysis. *Journal of Sedimentary Petrology*, 47, pp. 3-31.
- WILTON, D.H. 1983. The geology and structural history of the Cape Ray Fault in southwestern Newfoundland. *Canadian Journal of Earth Sciences*, 20, pp. 1119-1133.
- WINKLER, H.G.F. 1979. *Petrogenesis of metamorphic rocks*. 3rd Ed. Springer-Verlag, 348 p.
- YODER, H., and EUGSTER, H. 1955. Synthetic and natural muscovites. *Geochimica et Cosmochimica Acta*, 8, pp. 225-280.
- ZEN, E-AN., and THOMPSON, A.B. 1974. Low grade regional metamorphism: mineral equilibrium relations. *Annual Review of Earth and Planetary Sciences*, 2, pp. 179-212.

APPENDIX I

Modal composition for each drill hole described in chapter three (sample depths in metres, point counts in percentages).

	North Brook Formation 79A-007								79B-003															
	6.7	7	19	29	40.2	49	60.5	69	9.8	20.2	28	36.5	43	53	80	90	97	110.1	120	150	160			
Monocrystalline quartz	11.6	13.6	15.6	16.0	9.5	10.2	8.0	10.1	10.7	14.6	16.3	11.2	13.9	4.2	14.7	11.6	11.9	5.2	5.9	3.6	4.0			
Polycrystalline quartz	---	4.8	0.4	0.4	4.0	1.0	2.0	0.9	2.0	---	6.4	---	6.8	7.0	2.4	3.2	4.0	2.4	11.1	6.4	2.4			
Total quartz	11.6	18.4	16.0	16.0	13.5	11.0	10.0	11.0	12.7	14.6	22.7	11.2	20.7	11.2	17.1	14.8	15.9	7.6	17.0	10.0	6.4			
Plagioclase	6.8	19.2	10.8	8.0	18.3	15.3	16.4	19.7	20.2	6.3	22.7	33.7	17.1	29.6	13.9	9.5	23.9	11.6	10.4	10.4	19.2			
Orthoclase	13.8	14.0	21.6	20.8	16.3	16.2	15.6	16.4	15.9	20.0	18.4	18.7	18.7	19.7	22.3	15.9	20.9	11.9	6.7	10.4	10.0			
Microcline	0.4	0.8	---	---	6.8	7.6	6.0	3.8	7.1	0.8	6.4	5.0	7.2	8.5	9.6	6.9	7.0	17.5	6.7	13.2	8.8			
Perthites	0.4	0.8	---	---	---	1.0	1.2	0.4	4.0	---	1.4	---	0.4	---	1.2	1.1	0.5	---	0.7	---	---			
Total feldspars	20.8	36.8	34.0	30.8	41.4	40.1	39.2	40.3	47.2	27.1	48.9	57.4	43.4	57.8	47.0	33.4	52.3	41.0	24.5	34.0	38.0			
Sedimentary fragments	---	---	---	---	---	0.5	---	---	---	---	---	---	---	---	---	0.5	---	---	---	---	---			
Metamorphic fragments	---	3.2	2.4	0.8	2.8	1.5	4.8	4.8	---	---	---	---	---	---	---	---	---	---	---	---	---			
Volcanic fragments	---	0.4	---	0.4	0.4	---	---	---	---	---	---	---	---	---	---	---	---	---	---	---	---			
Plutonic fragments	1.2	4.4	2.4	0.8	6.0	2.0	10.0	0.4	1.6	---	0.8	---	---	---	0.8	---	---	0.4	1.5	1.2	4.3			
Chert	---	---	---	---	---	---	---	---	6.7	0.4	3.5	2.5	2.8	1.4	4.4	11.6	5.5	19.6	13.3	18.0	18.4			
Total rock fragments	1.2	8.0	4.8	2.0	9.2	4.0	16.4	5.2	8.3	0.4	4.2	2.5	3.2	2.8	5.6	15.3	6.5	21.1	18.5	20.8	22.4			
Biotite	0.8	0.4	---	0.4	---	---	0.8	0.4	0.4	0.8	---	1.3	---	---	---	---	---	---	---	0.4	---			
Muscovite	0.4	0.8	0.8	0.8	1.6	1.0	0.4	---	0.4	0.8	---	---	---	1.4	---	---	---	0.4	---	0.4	1.6			
Chlorite	0.4	---	0.4	0.4	---	---	---	---	---	0.4	---	---	---	---	---	---	---	0.4	---	0.4	0.4			
Opaque	1.6	4.4	1.6	7.2	5.2	8.6	4.0	7.2	2.0	8.3	2.1	1.3	4.8	4.2	4.8	1.1	---	0.8	---	1.2	---			
Organic material	---	---	---	---	---	---	---	---	---	---	---	---	---	---	---	---	---	---	---	---	---			
Accessory minerals	---	---	---	---	---	---	---	---	---	---	---	---	---	---	---	---	---	---	---	---	---			
Clay cement	---	1.2	1.2	1.2	4.8	1.5	2.0	0.9	---	---	---	---	0.4	---	0.4	---	---	---	---	---	---			
Carbonate cement	34.8	15.6	2.4	15.6	2.0	12.2	16.0	10.6	2.0	0.8	0.8	2.5	---	2.8	5.2	9.0	0.5	---	---	---	---			
Hematite cement	18.4	8.8	21.6	12.8	6.0	11.2	2.4	13.4	---	23.3	0.8	13.7	9.6	4.0	3.2	12.7	0.5	15.9	33.4	20.4	16.0			
Total cement	53.2	25.6	25.2	29.6	12.8	24.9	20.4	24.9	11.5	4.6	8.4	1.3	0.8	1.4	0.4	0.5	12.4	2.0	---	0.8	1.2			
Total porosity	10.0	5.6	17.0	12.8	16.3	10.2	8.8	11.0	13.5	28.7	10.0	17.5	10.4	8.4	8.8	22.2	13.4	17.9	34.1	21.2	20.0			
Effective porosity	---	---	15.1	12.8	16.3	10.2	8.8	11.0	15.5	18.9	12.1	8.8	17.1	14.2	16.3	13.2	11.9	11.2	5.9	8.4	10.0			
						7.2						4.6			8.2		6.5	9.8	1.5		9.6			

Rocky Brook Formation										
79A-003										
	56	86	95.9	106	126	196	216	226	236	246
Clays	48.0	57.0	63.0	55.0	31.0	43.0	31.0	37.0	26.0	6.0
Carbonates	39.0	41.0	37.0	33.0	30.0	57.0	36.0	27.0	41.0	2.0
Silt	---	2.0	---	12.0	33.0	---	33.0	28.0	33.0	84.0
Opauques	6.0	---	---	---	2.0	---	---	8.0	---	8.0
Organic material	7.0	---	---	---	4.0	---	---	---	---	---
Effective porosity	7.9	9.6	13.6	---	---	---	6.0	5.8	0.4	17.1

79A-005										
	7.4	27	47	57	77	97	107	137	267	
Clays	71.0	66.0	62.0	72.0	69.0	62.0	34.0	66.0	55.0	
Carbonates	22.0	31.0	31.0	26.0	27.0	31.0	40.0	16.0	44.0	
Silt	---	3.0	1.0	1.0	3.0	1.0	16.0	18.0	---	
Opauques	2.0	---	4.0	1.0	1.0	---	8.0	---	---	
Organic material	5.0	---	2.0	---	---	6.0	2.0	---	---	
Effective porosity	2.3	---	1.0	0.3	0.4	4.1	4.4	7.8	---	

Humber Falls Formation DQH 79-69										
	2.3	28.7	34.4	37	39.3	49.8	51.2	82.9	89	106.1
Monocrystalline quartz	15.6	12.6	10.8	17.5	11.6	15.5	7.4	25.2	9.1	24.4
Polycrystalline quartz	2.0	11.7	4.0	1.4	14.4	10.0	5.5	---	8.4	---
Total quartz	17.6	24.3	14.8	24.3	26.0	25.5	12.9	25.2	17.5	24.4
Plagioclase	22.4	10.3	14.4	0.4	7.2	9.1	13.5	12.4	11.9	6.8
Orthoclase	29.6	24.3	34.0	27.5	24.0	28.7	15.3	26.8	20.6	24.0
Microcline	1.6	6.7	15.2	19.9	6.8	7.2	13.5	6.4	7.9	2.8
Perthite	---	0.8	---	---	2.0	---	0.6	---	---	---
Total feldspars	53.6	42.6	63.6	47.8	40.0	45.0	42.9	45.6	40.4	33.6
Sedimentary fragments	---	---	---	---	---	---	---	---	---	---
Metamorphic fragments	---	---	---	---	---	---	---	---	---	---
Volcanic fragments	0.4	---	---	0.4	---	0.4	---	---	---	---
Plutonic fragments	2.0	8.4	3.2	5.6	3.6	8.4	17.2	---	15.9	---
Chert	0.4	---	---	---	---	0.8	---	---	---	---
Total rock fragments	2.8	8.4	3.2	6.0	3.6	9.6	17.2	---	16.3	---
Biotite	1.2	---	---	---	---	---	---	---	---	---
Muscovite	1.2	---	---	---	---	---	1.2	---	0.4	---
Chlorite	---	---	1.6	---	---	---	4.0	0.4	1.2	---
Opaque	3.2	0.4	---	---	0.4	---	8.0	---	---	16.0
Organic material	---	---	---	---	---	---	1.2	---	---	---
Accessory minerals	---	---	---	---	---	---	0.4	0.8	---	---
Clay cement	4.4	7.1	4.0	3.6	0.4	0.8	12.0	4.0	4.4	---
Carbonate cement	---	---	1.2	5.7	9.2	---	1.7	2.0	5.9	4.0
Hematite cement	---	---	---	15.6	---	---	---	0.4	0.4	8.4
Total cement	4.4	7.1	5.2	10.3	25.2	0.8	2.3	14.4	10.3	16.8
Total porosity	16.0	17.2	11.2	11.6	4.4	19.1	34.5	---	19.3	7.6
Effective porosity	12.7	8.8	---	---	3.9	16.7	20.3	8.6	---	3.2

DQH 79-29															
	3.4	10.7	25.9	31.4	33	34.4	43	45.4	53	63	72.9	80.5	87.3	103	
Monocrystalline quartz	28.4	26.7	23.5	11.5	18.2	24.0	18.8	8.9	5.0	14.6	15.6	12.0	10.8	8.2	
Polycrystalline quartz	3.2	---	3.2	2.3	9.6	11.9	6.4	19.4	4.0	12.8	1.6	0.8	10.8	11.2	
Total quartz	31.6	26.7	26.8	14.4	27.8	34.9	25.2	27.3	10.0	28.4	20.6	18.8	21.6	19.4	
Plagioclase	14.2	3.0	12.4	18.0	6.7	5.5	22.8	20.4	25.2	16.0	13.8	19.2	4.0	11.1	
Orthoclase	22.0	13.3	26.0	37.2	25.3	18.7	22.0	17.3	20.2	26.8	21.7	34.0	26.0	31.5	
Microcline	0.4	---	---	0.8	---	---	0.8	7.3	2.4	6.0	0.4	4.0	17.6	4.0	
Perthite	0.8	---	---	---	---	---	---	1.0	---	0.8	---	0.8	0.4	---	
Total feldspars	39.4	16.8	38.4	58.4	32.8	26.2	45.6	46.0	56.8	49.5	35.9	52.0	48.0	45.8	
Sedimentary fragments	---	---	0.4	---	---	---	---	---	---	---	---	---	---	---	
Metamorphic fragments	---	---	---	---	---	---	---	---	---	---	---	---	---	---	
Volcanic fragments	2.4	---	---	0.8	---	---	0.4	---	---	---	---	---	0.4	1.0	
Plutonic fragments	0.4	---	---	0.4	0.8	0.4	---	---	---	0.4	---	---	---	---	
Chert	0.4	---	---	2.0	14.0	2.0	2.0	7.9	0.8	4.0	0.4	0.8	3.6	9.2	
Total rock fragments	3.2	---	0.4	2.4	15.6	2.4	2.4	7.9	0.8	4.4	0.4	0.8	4.0	16.1	
Biotite	---	0.5	---	---	---	---	---	---	---	---	---	---	---	---	
Muscovite	1.2	1.0	1.6	0.8	0.8	---	---	---	0.8	0.8	1.2	0.8	1.2	---	
Chlorite	---	---	1.6	---	---	---	---	---	---	---	---	---	---	---	
Opaque	2.4	3.5	0.8	1.2	2.1	---	1.6	0.5	3.2	---	19.4	2.8	5.2	4.9	
Organic material	---	---	---	---	---	---	---	---	---	---	---	---	---	---	
Accessory minerals	---	---	---	---	---	---	---	---	---	---	---	0.8	---	---	
Clay cement	4.8	1.5	11.2	4.4	4.6	---	---	---	---	---	---	---	---	---	
Carbonate cement	0.4	23.3	5.0	1.2	0.8	---	6.4	4.2	10.0	0.8	13.0	4.8	2.0	4.0	
Hematite cement	---	---	---	---	---	---	---	---	---	0.8	---	---	---	6.5	
Total cement	4.4	7.1	5.2	10.3	25.2	0.8	2.3	14.4	10.3	16.8	---	---	---	---	
Total porosity	16.0	17.2	11.2	11.6	4.4	19.1	34.5	---	19.3	7.6	---	---	---	---	
Effective porosity	11.8	5.4	10.3	10.5	---	17.9	11.9	18.2	---	---	---	8.1	4.4	---	

Humber Falls Formation								
DDH 80-70								
	14	20	30.4	35.7	43.6	50	62.5	70
Monocrystalline quartz	6.8	16.7	10.4	14.0	12.0	22.7	24.4	23.2
Polycrystalline quartz	10.8	6.4	21.2	17.6	9.6	10.0	0.8	10.8
Total quartz	17.6	23.3	31.6	31.6	21.6	32.7	25.2	34.0
Plagioclase	4.4	6.4	10.0	9.6	11.2	7.2	3.6	12.4
Orthoclase	25.8	25.5	17.2	18.0	31.8	21.1	31.6	26.8
Microcline	3.2	4.4	6.0	3.6	4.4	4.7	1.2	4.0
Perthites	1.6	1.9	2.4	1.2	2.4	2.8	0.8	1.2
Total feldspars	35.0	38.4	35.6	32.4	49.8	35.8	37.2	44.4
Sedimentary fragments	---	---	---	---	---	0.4	---	---
Metamorphic fragments	5.2	0.8	0.4	---	---	---	---	---
Volcanic fragments	---	---	---	---	---	---	---	---
Plutonic fragments	16.7	17.9	12.0	10.0	2.4	4.4	---	0.4
Chert	---	---	---	---	0.4	0.4	---	1.6
Total rock fragments	21.9	18.7	12.4	10.0	2.8	5.2	---	0.4
Biotite	---	---	---	---	---	---	0.4	---
Muscovite	---	0.4	0.8	---	0.4	0.4	2.8	0.8
Chlorite	---	---	---	---	---	---	2.4	---
Opagues	1.6	2.0	0.8	6.4	0.8	2.4	0.8	2.4
Organic material	---	---	---	---	---	---	---	---
Accessory minerals	---	---	---	---	---	---	---	---
Clay cement	3.6	4.0	4.0	4.0	4.4	2.0	12.8	4.0
Carbonate cement	2.0	3.6	0.8	0.4	2.4	4.4	---	4.0
Hematite cement	---	2.0	---	0.4	---	---	---	---
Total cement	5.6	9.6	4.8	4.8	6.8	6.4	12.8	8.0
Total porosity	18.3	9.6	14.0	14.8	17.8	17.1	18.4	8.0
Effective porosity	7.3	---	12.9	13.8	9.3	12.3	11.1	---

	Howley Formation							79D-004		
	79D-005	18	35.7	45.3	54	70.3	72.2	16.3	22.7	26.8
Monocrystalline quartz	11.8	25.9	22.6	15.2	19.6	16.7	18.4	19.5	16.1	8.3
Polycrystalline quartz	4.8	8.0	4.9	0.8	1.2	2.4	0.4	2.8	---	---
Total quartz	16.6	33.9	27.5	16.0	20.8	19.1	18.8	22.3	16.1	8.3
Plagioclase	2.0	0.4	---	---	1.6	---	---	2.4	6.4	10.7
Orthoclase	40.6	38.2	56.0	40.8	27.6	42.2	45.6	32.5	23.7	22.6
Microcline	---	---	---	---	---	---	---	3.2	1.6	1.6
Perthites	---	---	---	---	---	---	---	---	---	---
Total feldspars	42.6	38.6	56.0	40.8	29.2	42.2	45.6	38.1	31.7	34.9
Sedimentary fragments	---	0.8	---	---	---	---	---	0.4	---	---
Metamorphic fragments	---	1.3	0.4	---	1.2	1.2	0.8	1.6	---	---
Volcanic fragments	0.8	---	---	---	0.4	---	---	0.8	---	---
Plutonic fragments	1.2	0.4	1.2	1.2	---	0.4	1.2	2.0	---	---
Chert	0.4	1.7	1.2	1.2	0.8	1.6	1.6	1.2	0.8	---
Total rock fragments	2.4	4.2	2.8	2.4	2.4	3.2	3.6	6.0	0.8	---
Biotite	---	---	---	0.4	---	---	1.2	2.8	6.0	4.0
Muscovite	0.8	---	0.4	---	1.2	---	---	---	3.6	2.0
Chlorite	---	---	---	---	---	---	---	---	---	---
Opaques	0.8	3.7	0.4	---	0.8	0.8	0.8	0.4	---	0.4
Organic material	---	---	---	---	---	---	---	---	0.4	0.4
Accessory minerals	---	---	---	---	---	---	---	---	0.4	0.4
Clay cement	11.5	8.2	1.6	24.0	20.4	12.0	10.7	12.0	24.9	23.0
Carbonate cement	2.8	4.4	6.9	1.6	12.0	9.6	0.8	8.4	---	---
Hematite cement	11.9	1.3	1.2	0.8	---	---	---	1.2	1.6	---
Total cement	26.2	13.9	9.7	26.4	32.4	21.6	11.5	21.6	26.5	23.0
Total porosity	10.6	5.7	3.2	14.0	13.2	12.7	18.4	8.4	14.5	26.6
Effective porosity	5.6	1.3	1.4	1.6	6.7	3.2	12.5	7.3	12.0	19.0

Modal composition of the uranium mineralized sandstone boulders described in chapter four (point counts in percentages)

	Birchy anomaly					Wigwam anomaly				Goose anomaly							
	40523	40524	40525	40526	40527	40518	40519	40522	40471	40513	40514	40515	40516	40517	526I	526J	
Monocrystalline quartz	19.2	15.6	21.2	17.2	23.2	15.9	8.8	10.8	8.3	10.0	7.2	19.0	14.0	14.4	10.9	13.2	
Polycrystalline quartz	8.2	3.2	8.0	7.6	10.8	3.1	8.4	3.2	---	14.8	11.2	14.7	8.8	16.4	6.8	14.8	
Total quartz	27.2	18.8	29.2	24.8	34.0	19.0	17.2	14.0	8.3	24.8	18.4	33.7	22.8	30.8	17.7	28.0	
Plagioclase	10.0	8.0	5.2	10.0	8.0	14.6	16.8	18.8	23.2	12.4	13.2	8.6	9.6	12.4	14.1	10.4	
Orthoclase	17.2	19.6	18.8	20.0	14.8	17.4	11.2	19.2	16.1	16.4	20.8	31.9	21.2	12.4	29.3	24.8	
Microcline	0.8	---	1.2	0.4	0.8	1.2	3.2	1.6	2.0	2.0	4.0	3.7	1.6	0.4	8.0	6.4	
Perthites	---	---	0.4	1.2	0.4	---	---	---	---	0.4	---	---	1.2	0.4	1.2	0.8	
Total feldspars	28.0	27.6	25.6	31.6	24.0	33.2	33.2	39.6	41.3	31.2	38.0	44.2	33.6	25.6	52.6	42.4	
Sedimentary fragments	---	---	---	---	---	---	---	---	---	---	---	---	---	---	---	---	
Metamorphic fragments	---	0.4	0.4	0.4	---	---	---	---	---	---	---	---	---	---	---	---	
Volcanic fragments	---	---	---	0.4	---	---	---	---	---	---	---	---	0.8	---	0.4	---	
Plutonic fragments	6.8	1.2	12.8	14.0	11.2	---	---	---	---	---	---	---	---	---	---	---	
Chert	---	---	---	0.4	---	3.5	15.2	4.8	0.8	13.2	16.4	14.8	10.8	16.4	9.2	4.8	
Total rock fragments	6.8	1.6	13.2	14.8	11.2	3.5	15.2	4.8	1.2	13.2	16.4	14.8	11.6	16.4	9.6	6.4	
Biotite	---	---	---	---	---	---	---	0.4	---	---	---	---	---	---	0.4	---	
Muscovite	0.8	0.4	0.4	0.4	0.8	0.8	---	0.8	2.0	0.4	0.4	0.6	0.4	0.8	---	0.8	
Chlorite	---	---	---	---	---	---	---	---	0.8	---	---	---	---	---	---	---	
Opques	22.4	39.6	16.4	16.4	17.6	1.2	20.8	2.4	22.0	4.4	0.4	1.2	6.8	0.4	---	0.4	
Organic material	---	---	---	---	---	---	---	---	---	---	---	---	---	---	---	---	
Accessory minerals	---	---	---	---	---	---	---	---	---	---	---	---	---	---	---	---	
Clay cement	---	3.6	4.4	0.8	0.8	---	---	---	0.4	---	---	---	---	---	---	---	
Carbonate cement	8.8	2.4	5.6	5.2	8.4	22.5	0.4	16.8	2.8	9.6	8.8	3.7	5.2	4.8	4.0	11.2	
Hematite cement	5.2	3.6	3.6	6.0	3.2	---	---	---	---	---	---	---	0.4	---	---	---	
Total cement	14.0	9.6	13.6	12.0	12.4	8.9	3.2	16.8	14.0	2.8	2.0	1.8	6.4	2.8	2.4	0.8	
Total porosity	0.8	2.4	1.6	---	---	10.9	10.0	4.4	7.2	12.4	10.8	5.5	12.0	7.6	6.4	12.0	
										13.6	15.6	---	12.8	18.4	13.3	10.0	

APPENDIX II

Microprobe analyses of Rocky Brook Formation analcime.

	1	2
Na ₂ O	5.63	5.41
MgO	0.00	0.00
Al ₂ O ₃	22.30	22.50
SiO ₂	63.80	63.20
K ₂ O	0.01	0.01
CaO	0.05	0.08
TiO ₂	0.00	0.00
Cr ₂ O ₃	0.00	0.00
MnO	0.01	0.01
FeO	0.01	0.02
NiO	0.01	0.02
Total	91.82	91.25

- 1 79A-003, average of 9 single crystal analyses from a rhizolith core
- 2 79A-003, average of 6 single crystal analyses from a rhizolith core

Trace element analyses of mineralized and unmineralized Rocky Brook Formation samples (ppm).

	1	2	3	4	5	6
Pb	7	0	9	23	8	7
Th	89	8	6	3	7	4
U	266	33	2	19	17	2
Rb	37	107	82	63	66	92
Sr	2319	1401	839	831	1134	1267
Y	221	44	31	14	23	24
Zr	73	94	130	98	85	114
Nb	7	12	13	12	10	11
Zn	35	49	92	64	107	79
Cu	410	32	26	63	31	32
Ni	28	66	50	105	36	57
La	36	23	22	22	25	22
Ba	218	393	581	397	442	491
Ti	.22	.52	.61	.70	.50	.58
V	41	91	110	173	134	123
Ce	47	38	38	29	33	33
Cr	4	59	50	91	41	58
Ga	5	21	16	15	15	19

- 1 Drill hole A3, 52m, mineralized
- 2 Drill hole A3, 86m, mineralized
- 3 Drill hole A3 background average (n= 25 samples)
- 4 Drill hole A5, 149.5m, mineralized
- 5 Drill hole A5, 167m, mineralized
- 6 Drill hole A5 background average (n= 23 samples)

0203

CENTRE FOR NFLD. STUDIES
NOV 8 1986
MEMORIAL UNIVERSITY
OF NEWFOUNDLAND

MEMORIAL UNIVERSITY
PERIODICALS
NOV 6 1986
DIVISION
OF NEWFOUNDLAND

032

CENTRE FOR NFLD. STUDIES
NOV 8 1986
MEMORIAL UNIVERSITY
OF NEWFOUNDLAND

MEMORIAL UNIVERSITY
PERIODICALS
NOV 6 1986
DIVISION
OF NEWFOUNDLAND

